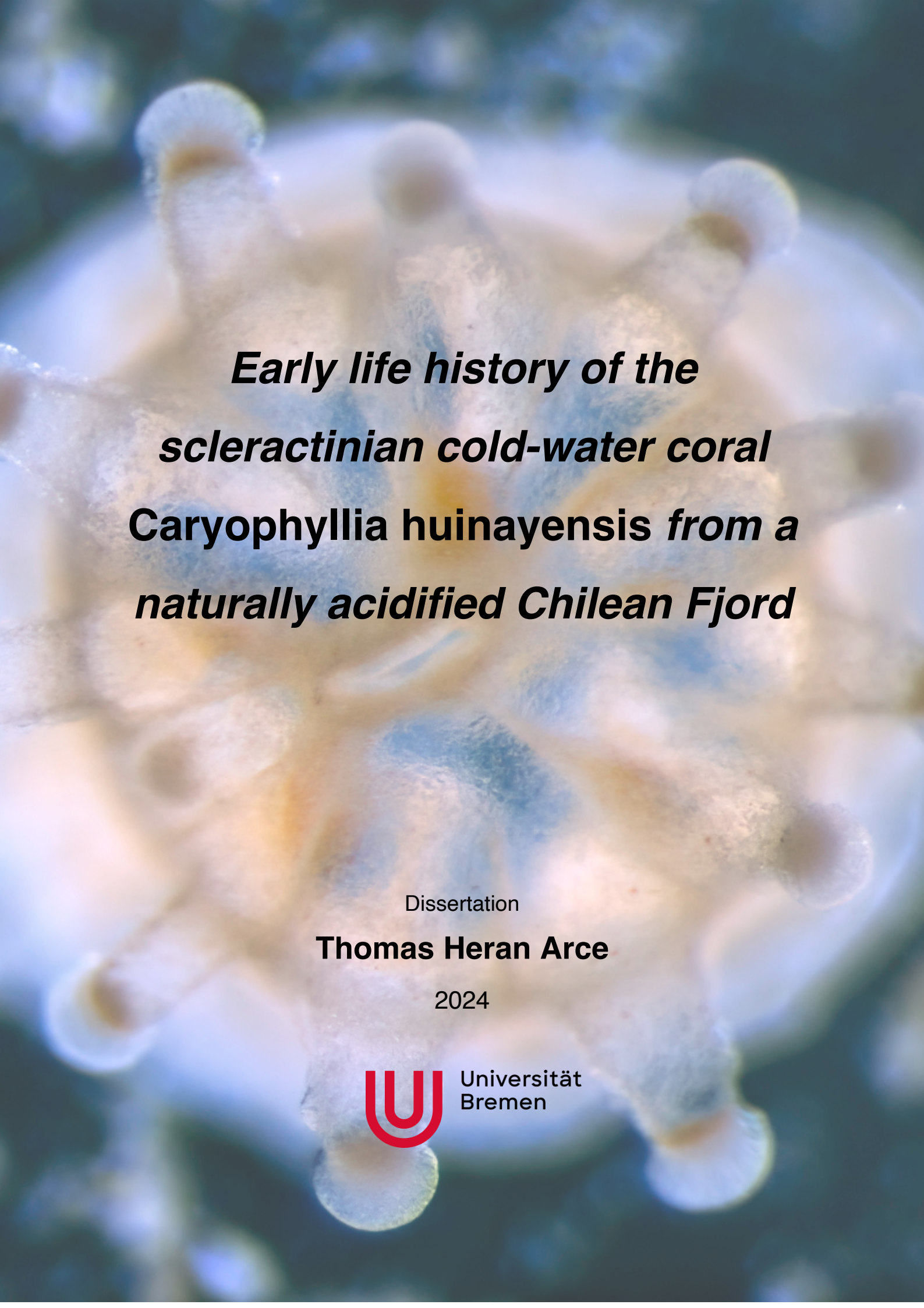

Early life history of the scleractinian cold-water coral Caryophyllia huinayensis *from a naturally acidified Chilean Fjord*

Dissertation

Thomas Heran Arce

2024

Universität Bremen

Universität Bremen

Early life history of the scleractinian cold-water coral *Caryophyllia huinayensis* from a naturally acidified Chilean Fjord

Dissertation

In partial fulfilment of the requirements for the degree of

Doctor of natural sciences

–Dr. rer. nat. –

Faculty of Biology / Chemistry

University of Bremen

Submitted by

Thomas Heran Arce

December - 2024

Front and back cover:

Images of the first scleractinian cold-water coral recruit reared in an aquarium: *Caryophyllia huinayensis*

The present study was carried out from January 2018 to August 2024 at the Alfred-Wegener-Institut, Helmholtz-Zentrum für Polar- und Meeresforschung (AWI), Bremerhaven, Germany. It was financed by the AWI, ANID (Agencia Nacional de Investigación y Desarrollo, Chile), DAAD (Deutscher Akademischer Austaushdienst), including DAAD/BECAS Chile and STIBET Doktoranden (Stipendien- und Betreuungsmaßnahmen für internationale Studierende), and NGS (National Geographic Society).

Date of the doctoral colloquium: 18 December 2024

Supervisor:

Dr. Jürgen Laudien
Alfred-Wegener-Institut, Helmholtz-Zentrum für Polar- und Meeresforschung, Bremerhaven, Germany

Examination committee:

Committee Chair:

Prof. Dr. Tilmann Harder
Alfred-Wegener-Institut, Helmholtz-Zentrum für Polar- und Meeresforschung, Bremerhaven, Germany
University of Bremen, Bremen, Germany

1st Examiner:

Prof. Dr. Claudio Richter
Alfred-Wegener-Institut, Helmholtz-Zentrum für Polar- und Meeresforschung, Bremerhaven, Germany
University of Bremen, Bremen, Germany

2nd Examiner:

Dr. Covadonga Orejas Saco del Valle
Instituto Español de Oceanografía, Gijón, Spain

3rd Examiner:

Prof. Dr. Iliana Baums
Helmholtz-Institut für Funktionelle Marine Biodiversität an der Universität Oldenburg (HIFMB)

1st Student member:

M. Sc. Marie Kaufmann
PhD candidate
University of Bremen, Bremen, Germany

2nd Student member

B.Sc. Patrik Beggel
Marine Biology student,
University of Bremen, Bremen, Germany

Dedicado a mis grandes inspiradores: *“La gran decisión”*

Table of contents

Summary

Scleractinian cold-water corals (CWCs) are a diverse group of the phylum Cnidaria. As structuring species, they sustainably change the abiotic and biotic environment and thus maintain a self-organized habitat that supports a diverse associated fauna. Furthermore, they play a key role in regional carbon cycles by coupling benthic and pelagic ecosystems. Their reproduction can follow two different modes, brooding of larvae and broadcast spawning of gametes. Additionally, the reproduction of unisexual polyps (gonochorism) and hermaphroditism results in two sexual strategies, and two known asexual reproductive mechanisms (fragmentation and fission). Scleractinian CWC ecosystems are present globally and predominantly occur in deep waters. Hence, their accessibility is limited, which has hampered a comprehensive understanding of certain aspects of their life cycle, including gametogenesis, dispersal, metamorphosis from larva to polyp and early skeletogenesis. Consequently, the potential impact of the predicted ocean acidification (OA) on the early life cycle of scleractinian CWCs remains elusive.

The aim of this thesis is therefore to describe the reproductive biology of the scleractinian CWC *Caryophyllia (Caryophyllia) huinayensis* and to predict the possible impacts of OA on its early life history based on observational and experimental evidence. Both *in vitro* and *in situ* investigations were carried out to determine the reproductive mode and strategy, gametogenesis, potential dispersal mechanism, and the effect of aragonite undersaturation of seawater ($\Omega_{arag} < 1$) and low seawater pH on early skeletogenesis and oogenesis of this scleractinian CWC, respectively.

Observations revealed that *C. huinayensis* broods larvae, which are released throughout the year. At the end of a one-week planktonic stage, larvae settle and initiate metamorphosis, developing their first set of tentacles within two days. Skeletal formation and the development of the second set of tentacles started *ca*. 5 days after settlement. Zooplankton feeding, and the development of the third and fourth set of tentacles started *ca*. 21, 153 and 895 days after settlement, respectively (**Chapter 2**). During a three-year *in vitro* maintenance period, we documented reverse development in adult polyps through an ontogenetic reversal process, occurring spontaneously and without environmental stressors, as corroborated by *in situ* evidence. Termed “polyp

dropout", this phenomenon entails tissue retraction and tissue detachment from the skeleton. The detached polyps can survive for several weeks, but we never observed re-settlement (**Chapter 3**). Should re-settlement occur *in situ*, polyp dropout would mark a potential new mechanism, aligning with Stanley´s "naked coral" hypothesis, which explains how corals may have endured the Permian-Triassic mass extinction.

The early skeletogenesis of this scleractinian CWC was described using both real-time *in vivo* polarized light microscopy (PLM) and scanning electron microscopy (SEM) (**Chapter 4**). Remarkably, early skeletogenesis in this species follows a similar temporal and sequential development pattern to that of warm-water scleractinian corals. This suggests the presence of a genetically encoded body plan in scleractinian CWC, orchestrating a precisely timed biomineralization processes from the micro to macroscale during the early stages of development.

Additionally, I revealed that aragonite undersaturation of seawater ($\Omega_{arag} < 1$) has no effect on skeletal formation during early skeletogenesis, as *C huinayensis* recruits are still able to build integral micro- and macrostructural crystal morphologies (**Chapter 4**). Although the precise mechanism enabling scleractinian CWCs recruits to compensate for $\Omega_{arag} < 1$ remains elusive, it seems that the early life stages of *C. huinayensis* are equipped to cope with the projected alteration in seawater Ω_{arag} by the end of the century. However, it should be noted that compensating for changes in seawater pH and its resultant alteration in seawater Ω_{arag} is known to require higher energy expenditure, potentially leading to imbalances in energy utilization.

In a naturally acidified fjord in Chile, I utilized histological methods to investigate the effect of low seawater pH, and its interaction with temperature and oxygen on the reproductive biology of *C. huinayensis* across all seasons (**Chapter 5**). My findings indicate that the seawater pH effect varies depending on the interaction with environmental parameters. This suggests that *C. huinayensis* reproduction is influenced by a mixture of environmental and endogenous factors.

Overall, this thesis contributes to the understanding of the reproductive biology, potential dispersal mechanisms, and early life cycle of scleractinian CWCs, using *C. huinayensis* as a model species. It emphasises the importance of understanding a species' reproductive strategy and mode, and dispersal mechanism, which in all provide insights into its potential phylogeography, distribution, and habitat colonization

ability. In this study, I present the first documentation from the larval stage up to three years post-settlement of a scleractinian CWC. The findings demonstrate that, with their heterotrophic feeding, CWCs develop at a rate similar to that of scleractinian warm-water corals, despite significant environmental differences. Moreover, the opportunity to rear newly settled polyps allowed the first assessment of the effect of $\Omega_{arag} < 1$ on early skeletogenesis, revealing an integral formation of skeletal structures. Moreover, we observed that seawater pH an its interaction with temperature and oxygen showed inconsistent effects on reproduction, suggesting that other environmental and endogenous factors also play a significant role in reproductive processes.

Based on these results, I suggest that future studies should consider reproduction as a critical factor in assessing the overall effect of ocean acidification. A pressing question remains as to whether the combination of rising ocean temperatures and OA will affect the early life stages of these corals. The foundational knowledge of reproductive biology and its interaction with OA, along with the tools developed during this study, provide a way to address this question and shed light on the response of scleractinian CWCs to our changing planet.

Zusammenfassung

Kaltwassersteinkorallen (engl. cold-water corals, CWCs) sind eine vielfältige Gruppe innerhalb des Stamms der Nesseltiere (Cnidaria). Als strukturierende Arten verändern sie nachhaltig die abiotische und biotische Umwelt und schaffen so einen selbstorganisierten Lebensraum, der eine vielfältige Begleitfauna unterstützt. Darüber hinaus spielen sie eine Schlüsselrolle im regionalen Kohlenstoffkreislauf, indem sie benthische und pelagische Ökosysteme miteinander verbinden. Ihre Fortpflanzung kann auf zwei verschiedene Arten erfolgen: durch das Ausbrüten von Larven und durch das Ablaichen von Gameten. Zusätzlich gibt es mit der Fortpflanzung eingeschlechtlicher Polypen (Gonochorismus) und Hermaphroditismus zwei sexuelle Strategien und zwei bekannte asexuelle Fortpflanzungsmechanismen (Fragmentierung und Spaltung). Von Kaltwassersteinkorallen gebildete Ökosysteme sind weltweit verbreitet und kommen überwiegend in tiefen Gewässern vor. Daher sind sie nur begrenzt zugänglich, was ein umfassendes Verständnis bestimmter Aspekte ihres Lebenszyklus, einschließlich ihrer Gametogenese, der Ausbreitung, der Metamorphose von der Larve zum Polypen und der frühen Skelettogenese, erschwert. Folglich sind die potenziellen Auswirkungen der prognostizierten Ozeanversauerung auf den frühen Lebenszyklus der Kaltwassersteinkorallen nach wie vor schwer zu erfassen.

Ziel dieser Dissertation ist es daher, die Fortpflanzungsbiologie der Kaltwassersteinkoralle *Caryophyllia (Caryophyllia) huinayensis* zu beschreiben und auf der Grundlage von Beobachtungen und Erkenntnissen aus Experimenten die möglichen Auswirkungen der Ozeanversauerung auf ihre frühe Lebensgeschichte vorherzusagen. Es wurden sowohl *in-vitro-* als auch *in-situ*-Untersuchungen durchgeführt, um den Fortpflanzungsmodus und die Fortpflanzungsstrategie, die Gametogenese, den potenziellen Ausbreitungsmechanismus sowie die Auswirkungen einer Aragonit-Untersättigung des Meerwassers ($\Omega_{arag} < 1$) und eines niedrigen Meerwasser-pH-Werts auf die frühe Skelettogenese und die Oogenese dieser Kaltwassersteinkoralle zu bestimmen.

Beobachtungen zeigten, dass *C. huinayensis* Larven ausbrütet, die das ganze Jahr über freigesetzt werden. Am Ende einer einwöchigen planktonischen Phase

siedeln sich die Larven an und beginnen die Metamorphose, wobei sie innerhalb von zwei Tagen ihren ersten Satz Tentakel entwickeln. Die Skelettbildung und die Entwicklung des zweiten Tentakelsatztes beginnen etwa 5 Tage nach der Ansiedlung. Das Fressen von Zooplankton sowie die Entwicklung des dritten und vierten Tentakelsatzes beginnen etwa 21, 153 bzw. 895 Tage nach der Ansiedlung (**Kapitel 2**). Während einer dreijährigen *in-vitro* Hälterungsperiode dokumentierten wir eine umgekehrte Entwicklung adulter Polypen durch einen ontogenetischen Rückentwicklungsprozess, der spontan und ohne Umweltstressoren auftrat, was durch *in-situ*-Nachweise bestätigt wurde. Dieses Phänomen, das als „Polyp dropout" („dropout" engl. für Aussteiger) bezeichnet wird, beschreibt ein Zurückziehen und Ablösen des Gewebes vom Skelett. Die abgelösten Polypen können mehrere Wochen lang überleben, wir haben jedoch keine Neuansiedlung beobachtet (**Kapitel 3**). Sollte die Wiederansiedlung erfolgen, wäre Polyp dropout ein potenzieller, bisher unbekannten Verbreitungsmechanismus hin, der mit Stanleys „naked coral"-Hypothese übereinstimmt, welche erklärt, wie Korallen das Perm-Trias-Massenaussterben überlebt haben könnten.

Die frühe Skelettogenese dieser Kaltwassersteinkoralle wurde sowohl durch Echtzeit-*in-vivo*-Polarisationslichtmikroskopie als auch Rasterelektronenmikroskopie beschrieben (**Kapitel 4**). Bemerkenswerterweise folgt die frühe Skelettogenese bei dieser Art einem ähnlichen zeitlichen und sequenziellen Entwicklungsverlauf wie bei Warmwassersteinkorallen. Dies deutet auf einen genetisch kodierten Körperplan von Kaltwassersteinkorallen hin, der während der frühen Entwicklungsstadien einen präzise zeitgesteuerte Biomineralisierungsprozesse von der Mikro- bis zur Makroebene vorgibt.

Darüber hinaus zeigte ich, dass die Untersättigung des Meerwassers mit Aragonit ($\Omega_{arag} < 1$) keinen Einfluss auf die Skelettbildung während der frühen Skelettogenese hat, da *C. huinayensis*-Rekruten weiterhin in der Lage sind, vollständige mikro- und makrostrukturelle Kristallstrukturen zu bilden (**Kapitel 4**). Obwohl der genaue Mechanismus, der es den Rekruten der Kaltwassersteinkoralle ermöglicht, $\Omega_{arag} < 1$ zu kompensieren, noch nicht klar ist, scheint es, dass die frühen Lebensstadien von *C. huinayensis* in der Lage sind, mit der bis zum Ende des Jahrhunderts prognostizierten Veränderung der Ω_{arag} des Meerwassers fertig zu

werden. Es ist jedoch zu anzumerken, dass die Kompensation von Änderungen des Meerwasser-pH-Wertes und der daraus resultierenden Änderung des Ω_{arag}-Werts des Meerwassers bekanntermaßen einen höheren Energieaufwand erfordert, was möglicherweise zu Ungleichgewichten in der Energienutzung führt.

In einem natürlich versauerten Fjord in Chile untersuchte ich mit histologischen Methoden die Auswirkungen eines niedrigen Meerwasser-pH-Wertes und dessen Wechselwirkung mit Temperatur und Sauerstoff auf die Fortpflanzungsbiologie von *C. huinayensis* über alle Jahreszeiten hinweg (**Kapitel 5**). Meine Ergebnisse zeigen, dass der Effekt durch den Meerwasser-pH-Wert je nach Wechselwirkung mit den Umweltparametern variiert. Dies deutet darauf hin, dass die Fortpflanzung von *C. huinayensis* aus einer Mischung von umweltbedingten und endogenen Faktoren beeinflusst wird.

Insgesamt trägt diese Dissertation zum Verständnis der Fortpflanzungsbiologie, potenzieller Ausbreitungsmechanismen und des frühen Lebenszyklus von Kaltwassersteinkorallen bei, wobei *C. huinayensis* als Modellart dient. Sie unterstreicht, wie wichtig es ist, die Fortpflanzungsstrategie und -weise sowie die Ausbreitungsmechanismen einer Art zu verstehen, die insgesamt Aufschluss über ihre potenzielle Phylogeographie, Verbreitung und Fähigkeit zur Besiedlung von Lebensräumen geben. In dieser Studie präsentiere ich die erste Dokumentation vom Larvenstadium bis zu drei Jahre nach der Ansiedlung einer Kaltwassersteinkoralle. Die Ergebnisse zeigen, dass sich Kaltwassersteinkorallen mit ihrer heterotrophen Ernährung und trotz erheblicher Umweltunterschiede ähnlich schnell wie Warmwassersteinkorallen entwickeln. Darüber hinaus ermöglichte die Aufzucht neu angesiedelter Polypen die erste Bewertung der Auswirkungen von Aragonituntersättigung des Meerwassers auf die frühe Skelettogenese, was eine intakte Bildung der Skelettstrukturen offenbarte. Darüber hinaus haben wir festgestellt, dass der Meerwasser-pH-Wert und seine Wechselwirkung mit der Temperatur und dem Sauerstoffgehalt uneinheitliche Auswirkungen auf die Fortpflanzung haben, was darauf hindeutet, dass auch andere umweltbedingte und endogene Faktoren eine wichtige Rolle bei den Fortpflanzungsprozessen spielen.

Auf der Grundlage dieser Ergebnisse schlage ich vor, dass künftige Studien die Fortpflanzung als kritischen Faktor bei der Bewertung der Gesamtauswirkung der

Ozeanversauerung berücksichtigen sollten. Es bleibt die dringende Frage, ob die Kombination aus steigenden Meerestemperaturen und Ozeanversauerung die frühen Lebensstadien dieser Korallen beeinflussen wird. Das grundlegende Wissen über die Fortpflanzungsbiologie und deren Wechselwirkung mit der Ozeanversauerung sowie die im Rahmen dieser Studie entwickelten Instrumente bieten eine Möglichkeit, diese Frage zu klären und die Reaktion von Kaltwassersteinkorallen auf die sich verändernde Umwelt zu erhellen.

Resumen

Los corales escleractineos de aguas frías (inglés, cold-water corals, CWCs) son un grupo diverso del filo Cnidaria. Como especies estructurantes, cambian de manera sostenible el entorno abiótico y biótico, manteniendo así un hábitat autoorganizado que sostiene una fauna asociada diversa. Además, juegan un papel clave en los ciclos de carbono regionales al acoplar los ecosistemas bentónicos y pelágicos. Su reproducción puede seguir dos modos diferentes: la incubación de las larvas (inglés, brooding) y la liberación masiva de gametos (inglés broadcast spawning). Además, la reproducción de pólipos unisexuales (gonocorismo) y el hermafroditismo dan lugar a dos estrategias sexuales, y se conocen dos mecanismos de reproducción asexual (fragmentación y fisión). Los ecosistemas de escleractineos CWCs están presentes globalmente y se encontran predominantemente en aguas profundas, lo que limita su accesibilidad y ha dificultado la comprensión integral de ciertos aspectos de su ciclo de vida, como la gametogénesis, medios de dispersión, la metamorfosis de larva a pólipo y la esqueletogénesis temprana. Como resultado, el impacto potencial de la acidificación oceánica (inglés, ocean acidification, OA) prevista en las primeras etapas del ciclo de vida de los escleractineos CWCs sigue siendo incierto.

El objetivo de esta tesis es, por lo tanto, describir la biología reproductiva del escleractineo CWC *Caryophyllia (Caryophyllia) huinayensis* y predecir los posibles impactos de la OA en sus primeras etapas de vida basándose en evidencias observacional y experimental. Se realizaron investigaciones tanto *in vitro* como *in situ* para determinar el modo y la estrategia reproductiva, la gametogénesis, el mecanismo potencial de dispersión, y el efecto de la subsaturación de aragonita en el agua de mar ($\Omega_{arag} < 1$) y el bajo pH del agua de mar sobre la esqueletogénesis temprana y la oogénesis de este CWC, respectivamente.

Las observaciones revelaron que *C. huinayensis* incuba larvas que se liberan durante todo el año. Al final de una etapa planctónica de una semana, las larvas se asientan e inician la metamorfosis, desarrollando su primer conjunto de tentáculos en dos días. La formación del esqueleto y el desarrollo del segundo conjunto de

tentáculos comenzó aproximadamente cinco días después del asentamiento. La alimentación de zooplancton y el desarrollo del tercer y cuarto conjunto de tentáculos comenzó aproximadamente 21, 153 y 895 días después del asentamiento, respectivamente (**Capítulo 2**). Durante un período de tres años de mantenimiento *in vitro*, documentamos un desarrollo inverso en pólipos adultos a través de un proceso de reversión ontogenética, que ocurre espontáneamente y sin la presencia de factores estresantes ambientales, como corroboraron evidencias *in situ*. Denominado "polyp dropout", este fenómeno implica la retracción y separación del tejido del esqueleto. Los pólipos separados del esqueleto pueden sobrevivir varias semanas, aunque nunca se observó reasentamiento (**Capítulo 3**). Si el reasentamiento ocurre *in situ*, la separación del pólipo del esqueleto podría representar un mecanismo potencial de dispersión nuevo, la cual se alínea con la hipótesis del "coral desnudo" de Stanley, que explica cómo los corales pudieron haber sobrevivido a la extinción masiva del Pérmico-Triásico.

La esqueletogénesis temprana de este escleractineo CWC fue descrita utilizando tanto microscopía de luz polarizada (inglés, polarized light microscopy, PLM) *in vivo* en tiempo real como microscopía electrónica de barrido (inglés, scanning electron microscopy, SEM) (**Capítulo 4**). Notablemente, la esqueletogénesis temprana en esta especie sigue un patrón de desarrollo temporal y secuencial similar al de los corales escleractineos de aguas cálidas. Esto sugiere la presencia de un plan corporal genéticamente codificado en los escleractineos CWCs, que orquesta procesos de biomineralización precisamente sincronizados desde la micro- a la macroescala durante las primeras etapas del desarrollo.

Además, revelé que $\Omega_{arag} < 1$ no afecta la formación esquelética durante la esclerogénesis temprana, ya que los reclutas de *C. huinayensis* son capaces de construir morfologías cristalinas micro- y macroestructurales integras (**Capítulo 4**). Aunque el mecanismo preciso que permite a los reclutas de escleractineos CWCs compensar $\Omega_{arag} < 1$ sigue siendo desconocido, parece que las etapas tempranas de vida de *C. huinayensis* están equipadas para enfrentarse a los cambios proyectados en Ω_{arag} del agua de mar hacia finales de siglo. Sin embargo, cabe destacar que compensar los cambios en el pH del agua de mar y la subsaturación resultante de

Ω_{arag} en el agua de mar requiere un mayor gasto de energía, lo que podría provocar desequilibrios en la utilización de energía.

En un fiordo naturalmente acidificado en Chile, utilicé métodos histológicos para investigar el efecto del bajo pH del agua de mar, y su interacción con la temperatura y el oxígeno, en la biología reproductiva de *C. huinayensis* en todas las estaciones (**Capítulo 5**). Mis hallazgos indican que el efecto del pH del agua de mar varía según la interacción con los parámetros ambientales. Esto sugiere que la reproducción de *C. huinayensis* está influenciada por una combinación de factores ambientales y endógenos.

En conjunto, esta tesis contribuye a la comprensión de la biología reproductiva, los posibles mecanismos de dispersión y el ciclo de vida temprano de los escleractineos CWCs, utilizando a *C. huinayensis* como especie modelo. Enfatiza la importancia de comprender la estrategia, el modo de reproducción y el mecanismo de dispersión de una especie, lo que en su conjunto proporciona información sobre su potencial filogeográfico, distribución y capacidad de colonización de hábitats. En este estudio, presento la primera documentación desde la etapa larval hasta tres años después del asentamiento de un escleractineo CWC. Los hallazgos demuestran que, con una alimentación heterotrófica, los CWCs se desarrollan a un ritmo similar a la de los corales escleractineos de aguas cálidas, a pesar de las significativas diferencias ambientales. Además, la oportunidad de criar pólipos recién asentados permitió realizar la primera evaluación del efecto de $\Omega_{arag} < 1$ en la esqueletogénesis temprana, revelando una formación integral de estructuras esqueléticas. Además, observamos que el pH del agua de mar y su interacción con la temperatura y el oxígeno mostraron efectos inconsistentes sobre la reproducción, lo que sugiere que otros factores ambientales y endógenos también juegan un papel importante en los procesos reproductivos.

Basado en estos resultados, sugiero que los futuros estudios consideren la reproducción como un factor crítico al evaluar el efecto general de la acidificación oceánica. Una pregunta clave que queda por responder es si la combinación de aumento de las temperaturas oceánicas en y OA afectará las primeras etapas de vida de estos corales. El conocimiento fundamental de la biología reproductiva y su interacción con la OA, junto con las herramientas desarrolladas en esta tesis,

proporcionan una vía para abordar esta pregunta y arrojar luz sobre la respuesta de los escleractineos CWCs frente a nuestro planeta cambiante.

1

General introduction

Scleractinian cold-water corals (CWCs), like their counterparts, the warm-water corals (WWCs), are among the most important ecosystem engineers within the world's deep oceans, as they function as keystone species (Roberts et al. 2009). CWC ecosystems are present globally and occur in fjords, along continental shelves and on submarine seamounts in tropical to polar oceans and in shallow to deep waters (Freiwald et al. 2004; Roberts et al. 2009). Their diverse reproductive modes, including sexual strategies such as gonochorism and hermaphroditism, as well as asexual mechanisms such as fragmentation and fission, provide a good basis to colonise (new) habitats (Waller et al. 2023). Understanding their spatio-temporal distribution and biological features is a key concern to determine their biodiversity patterns, their drivers, and recognize endemism (Balogh et al. 2023). Over the past thirty years, *in situ* ecological studies of CWCs have established the environmental requirements for experimental studies of adult polyps in the laboratory (Roberts and Cairns 2014). However, until recently, suitable aquarium conditions for reproduction, larval development, settlement, and metamorphosis of recruited CWC species have not been achieved. Therefore, a comprehensive description of the early life history of CWCs, including gametogenesis and subsequent larval development, as well as their features, such as the duration of the pelagic larval period until settlement, is lacking. Thus, the somatic and skeletal developmental processes that occur within their developmental timetable are still poorly understood. Consequently, the extent to which the low seawater pH and aragonite (primary building mineral of the coral skeleton) seawater concentration predicted for the end of the century may affect these early life stages, which are considered a bottleneck for survival, remains uncertain. In this thesis, the fundamental early life developmental stages of the scleractinian CWC

Caryophyllia (Caryophyllia) huinayensis Cairns, Häussermann & Försterra (2005) are outlined and the potential impact of the upcoming ocean scenario on its early life stages is revealed.

1.1 Scleractinian cold-water corals (definition, relevance and distribution)

Scleractinian CWCs are a diverse order belonging to the phylum Cnidaria. Hermatypic scleractinian CWCs perform a fundamental ecological function as they build reefs, promoting and sustaining a biological rich variety of marine life (Jones et al. 1994; Roberts et al. 2016). Scleractinian CWCs are characterized by a calcium carbonate ($CaCO_3$) skeleton, which in most cases is composed of aragonite, one naturally occurring crystal forms of $CaCO_3$. While some scleractinian species occur as solitary polyps (e.g., *C. huinayensis*), other scleractinian CWCs form colonies (e.g., *Desmophyllum pertusum*, *Madrepora oculata*) or pseudocolonies (e.g., *Desmophyllum dianthus*). Scleractinian CWCs can provide a complex habitat that can host a wide variety of associated fauna and serve as nurseries for commercial species, sessile epifauna, and skeletal and tissue endoparasites (Buhl-Mortensen et al. 2015), among others. Due to their role as structuring species that regulate the abiotic and biotic environment and maintain a self-organized habitat that supports a diverse associated fauna, scientists often refer to CWCs as “marine animal forests”, that play a similar ecological role to that of terrestrial forests (Försterra et al. 2017; Rossi et al. 2017; Häussermann et al. 2024) (Fig. 1a). Furthermore, they play a key role in the regional biogeochemical carbon cycle by coupling the benthic and pelagic ecosystems (Cathalot et al. 2015).

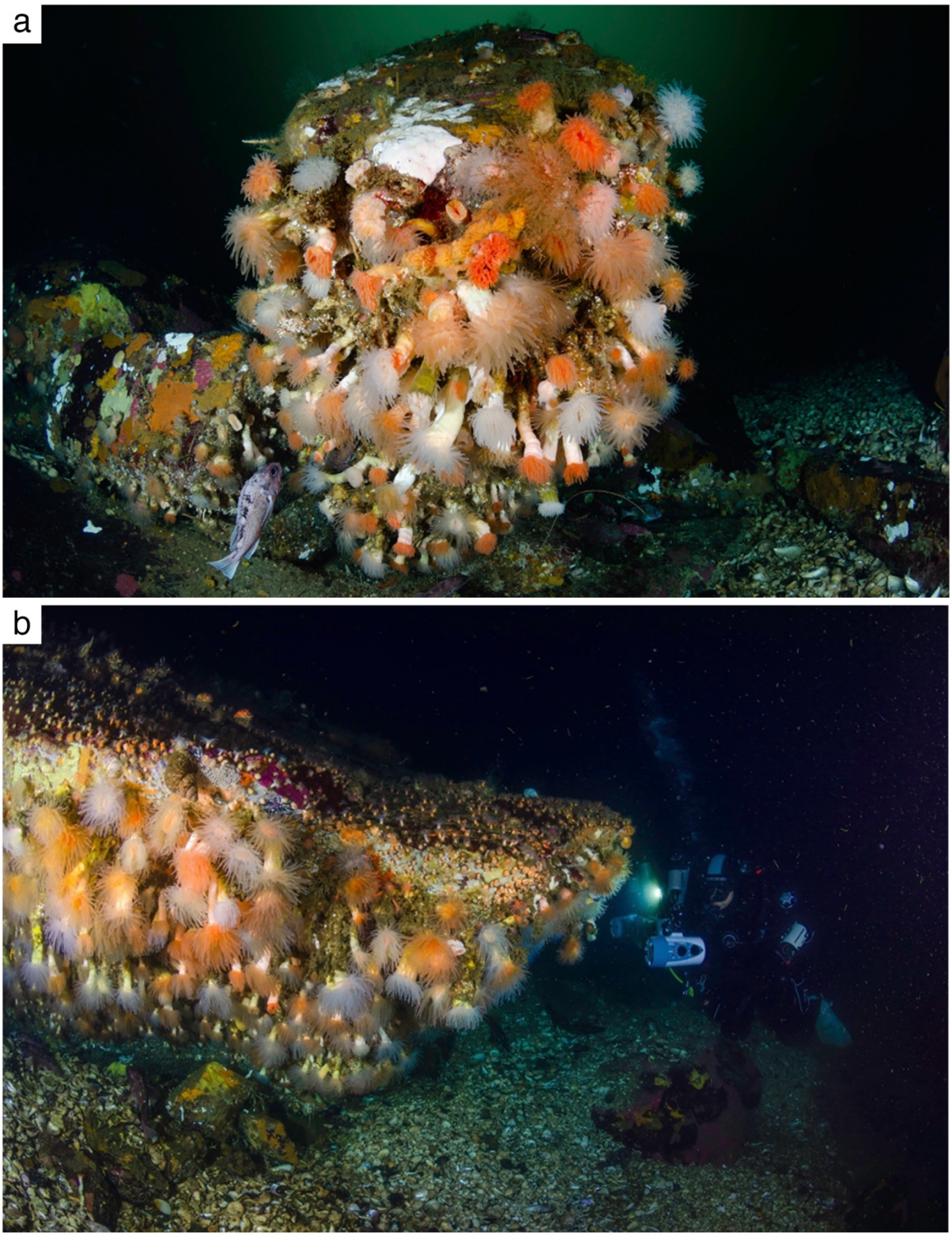

Figure 1: (a) Marine Animal Forest formed by the CWC *D. dianthus*, (b) which is normally a deep-water species, but here occurs in shallower water due to the phenomenon of "deep-water emergence". Both images obtained at 26 m water depth (Comau Fjord, Chilean Patagonia).

CWCs ecosystems are found throughout the world's oceans on continental shelves, submarine seamounts, in fjords, from the equator to the poles, and in shallow

and deep waters down to 4,000 m (Freiwald et al. 2004; Roberts et al. 2009, Fig. 2). The deep occurrence of scleractinian CWCs is possible due to their heterotrophic diet; as they have no endosymbiotic dinoflagellate algae (zooxanthellae) like scleractinian WWCs. The later are dependent on zooplankton and these symbionts to supply themselves with energy through photosynthetic products such as glucose (Falkowski et al. 1984; Dubinsky and Falkowski 2011) (mixotrophic diet), which limits their distribution to shallow waters and the mesophotic zone.

Approximately 65 % of the CWC species, including Scleractinia, Antipatharia, Octocorallia, Stylasteridae, and Milleporidae, two zoanthids, and three calcified hydractiniids, are found below 50 m water depth (Cairns 2007; Roberts et al. 2009). The highest abundances of these species are likely to occur between 200 and 1,000 m (Roberts et al. 2009).

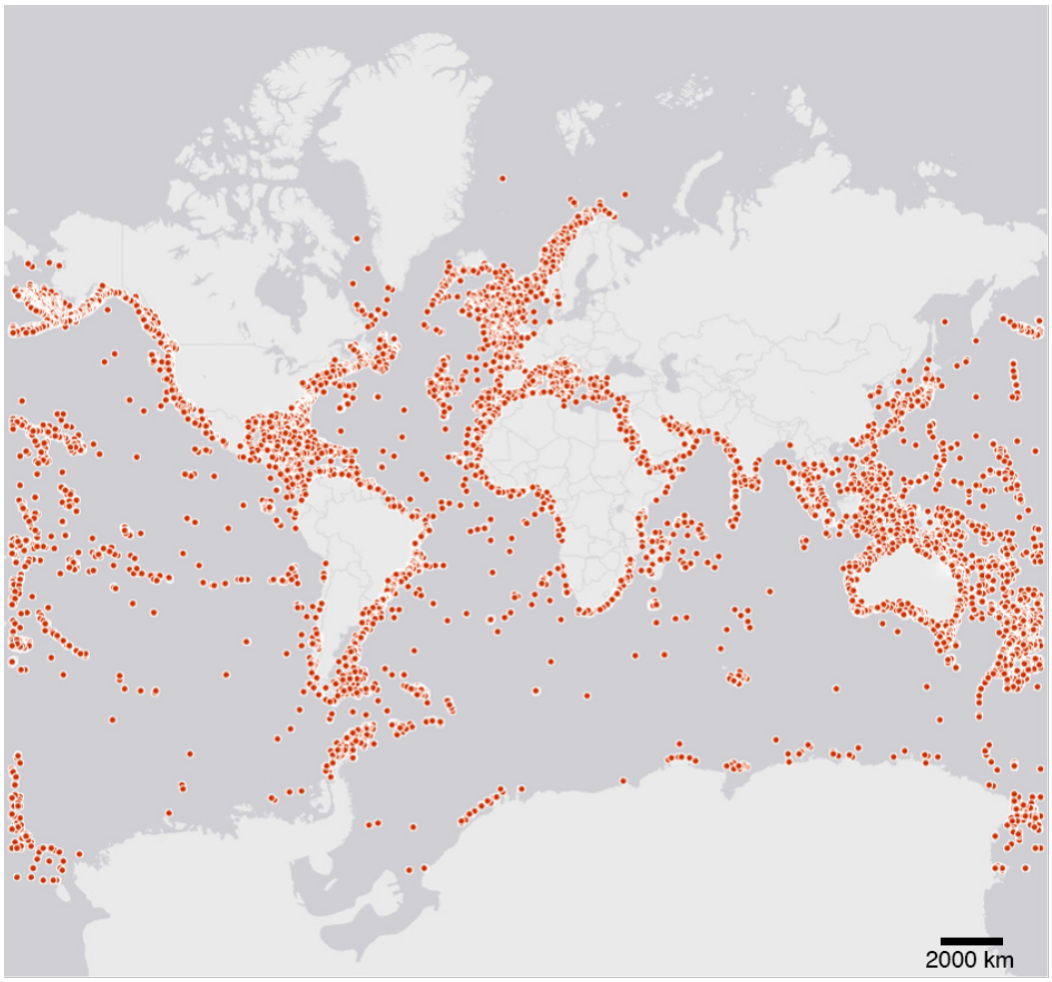

Figure 2: Global distribution of scleractinian cold-water corals. From Ocean Biodiversity Information (OBIS, access date: 02.08.2024).

In the high-latitude fjord system of Chile (e.g., Häussermann et al. 2021, 2024), North America (e.g., Stone et al. 2005), Scandinavia (e.g., Mortensen and Fosså 2006), and New Zealand (e.g., Grange 1985) scleractinian CWCs occur at depths as shallow as 7 m, a phenomenon known as “deep-water emergence” (Hessler 1970) (Fig. 1b). Although species that emerge from deep-water have been widely found in fjord regions, the ecological reasons for this remain an open scientific question (Häussermann et al. 2021).

1.2 Life cycle of scleractinian CWCs

Scleractinian CWCs are diploblastic metazoans that lack mesoderm and the ability to form organs. Their life cycle consists of a sessile benthic phase and a mobile phase with a crawling or a swimming larva (Harrison 2011). Scleractinian CWCs have two modes of sexual reproduction: “broadcast spawning”, in which female and male gametes are released into the water column where fertilization and larval development occur; and “brooding”, in which internal fertilization and larval development occur prior to the release of a mobile larva (Harrison 2011) (Fig. 3). The sexual mechanism in scleractinian CWCs can follow two reproductive strategies: “gonochoric”, in which the sexes are separate, and “hermaphroditic”, in which both sexes are present in a single polyp (Fig. 3). While most scleractinian WWC are hermaphroditic broadcast spawners, most scleractinian CWCs studied to date are gonochoric broadcast spawners. For the latter, only a few exceptions have been described, both in the genus *Caryophyllia,* which exhibits hermaphroditism (Waller et al. 2005), and in the genus *Flabellum,* where brooding has been described in three Antarctic species (Waller and Tyler 2011). The reproductive mode of brooding in these three Southern Ocean species follows the postulated patter according to Thorson’s rule (Thorson 1957; Mileikovsky 1971). Here, it is suggested that organism thriving at higher latitudes produce larger and fewer offspring due to the conditions of these regions, including lower seawater temperature and a shorter seasonal window for reproduction. Hence, these species are usually brooders.

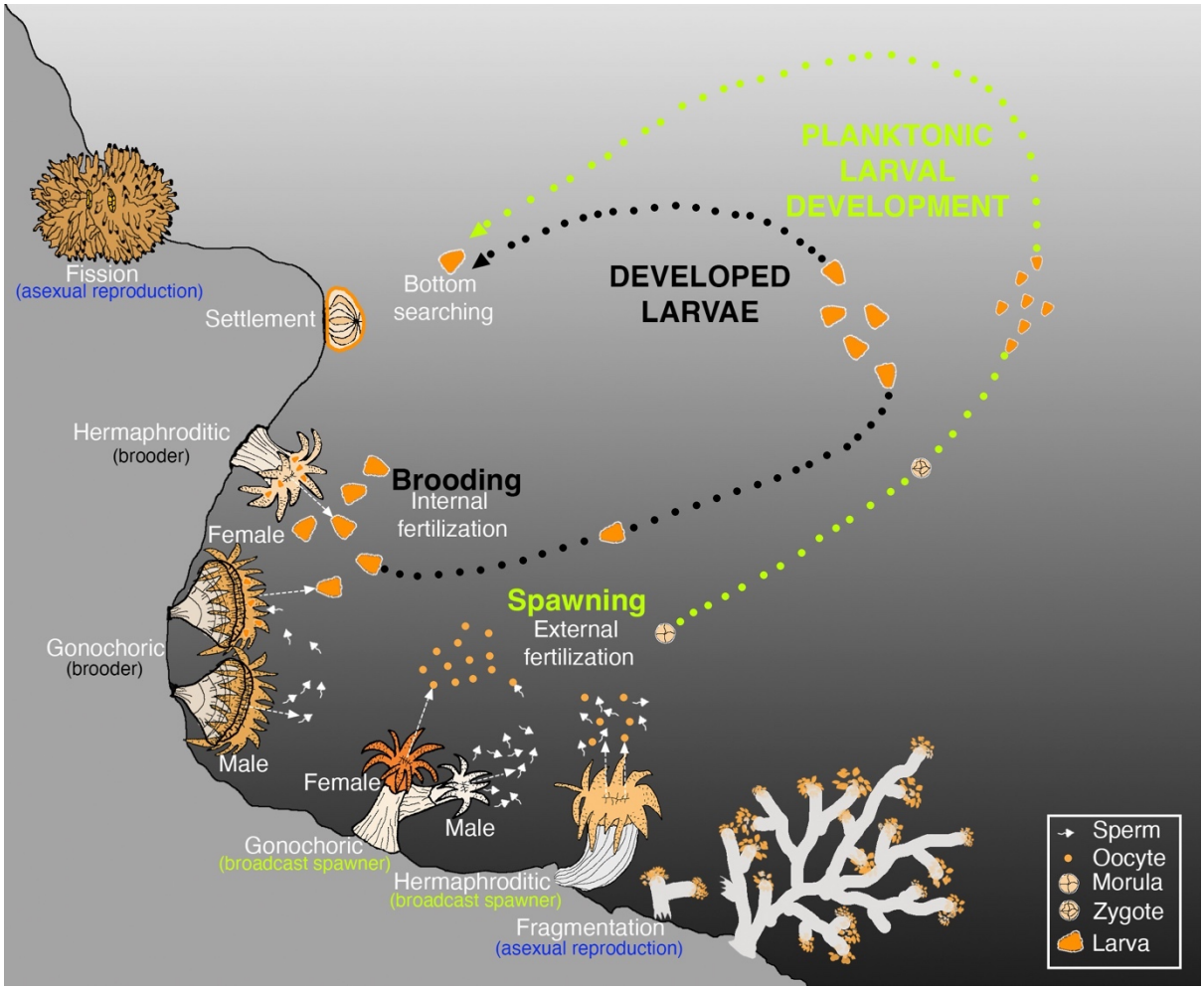

Figure 3: Life cycle of scleractinian CWCs showing the known reproductive strategies. Concept modified from Waller et al. (2023).

Current, phylogenetic studies on coral reproduction address the evolutionary patterns and relationships between reproductive strategies and modes across organisms. They suggest a transition between these reproductive strategies and modes, governed by the organism's strategy (Kerr et al. 2011). These findings emphasize that it is the interplay between the reproductive strategy and mode and not their latitudinal distribution that determines the success of a species, e.g., in a mass extinction event where the reproductive trait is affected.

Scleractinian CWCs generally live in the deep-sea, often in sparse populations. This requires significant sampling effort and expenses to obtain sufficiently sample sizes for statistically relevant results. Because funds are limited, information is so far limited. To date, information on some aspects of reproduction is available for only 3.5 % of the 1,170 known scleractinian CWC species (Balogh et al. 2023; Waller et al.

2023). In contrast, approximately 50 % of the scleractinian WWC have been studied in terms of their reproduction (Harrison 2011). Maintaining scleractinian CWCs in laboratories requires stablishing aquarium conditions that mimic their deep-sea environment. An environment characterized by low and constant temperatures (between 2 °C and 15 °C (Keller and Os' kina 2008)) and a fluctuating food supply whose composition and quantity vary with the seasons (Garcia-Herrera et al. 2022). The slow growth of scleractinian CWCs (Freiwald et al. 1997; Brooke and Young 2009; Orejas et al. 2011) results in a long-term development process to achieve maturity. When the time comes for the larvae to undergo metamorphosis, a suitable substrate for larval settlement has to be found to ensure the long-term survival of the recruits and their subsequent attainment of maturity. Consequently, despite efforts, a comprehensive understanding of the complete life cycle of scleractinian CWCs remains elusive.

1.3 Sexual and asexual reproduction and seasonality

Gonochorism is the most common sexual strategy in scleractinian CWCs (Waller et al. 2023), whereas hermaphroditism predominates in scleractinian WWC (Harrison 2011). Hermaphroditic polyps so identified in scleractinian CWCs belong to the family Caryophylliidae, including *Caryophyllia ambrosia*, *C. cornuformis*, and *C. seguenzae* (Waller et al. 2005). These species are cyclical hermaphrodites in which there is a constant sex change within a single polyp, with one sex dominating at any given time (Waller et al. 2005).

Scleractinian WWC exhibit a wide range of asexual reproductive processes, including "budding" through intratentacular and extratentacular division, "colony fission", "polyp expulsion", "bail-out" and "fragmentation" (e.g., Sammarco 1982; Cairns 1988; Harrison and Wallace 1990; Kramarsky-Winter et al. 1997). The scleractinian WWCs *Pocillopora damicornis* (Sherman et al. 2006), *Tubastrea coccinea*, and *T. diaphana* also features parthenogenetically (i.e., asexually) produce planula larvae which they brood in their gastrovascular cavity (Ayre and Resing 1986). Scleractinian CWCs polyps have so far been observed to reproduce asexually through

fission is the solitary polyp *Fungiacyathus marenzelleri* (Waller et al. 2002) and the colonial CWC *Desmophyllum pertusum*. The latter also reproduces by fragmentation (Le Goff-Vitry et al. 2004; Morrison et al. 2011) (Fig. 3). It is likely that CWC scleractinians, have more forms of asexual reproduction, similar to scleractinian WWCs, that have not been documented so far due to the limited number of studies.

Asexual and sexual reproduction follows biological and environmental stimuli, which determine the timing of their seasonal activities, i.e., phenology (sensu Walther et al. 2002). As access to scleractinian CWCs is challenging, observations of asexual reproduction and offspring release are rare, making it difficult to link reproduction to environmental cues. Currently, genetic studies remain the primary means of assessing asexual reproduction in scleractinian CWCs (Morrison et al. 2011; Combosch and Vollmer 2013; Miller and Gunasekera 2017; Oury et al. 2019). The linkage between sexual reproduction and environmental conditions is primarily established through histological analyses, which examine patterns in gametogenesis and the timing of larval production pulses across different periods. Seasonal fluctuations in seawater temperature play an important role governing gametogenesis and larval release in scleractinian WWCs (Szmant-Froelich et al. 1980; Tranter et al. 1982; Fadlallah 1985; Babcock et al. 1986; Harrison and Wallace 1990). However, in deep habitats inhabited by scleractinian CWC, where seasonal temperature variations are low (Børsheim et al. 1999; Dullo et al. 2008; Beck et al. 2022), other environmental factors may exert greater influence. In corals, the production of gametes is an energy-consuming process. Oocyte vitellogenesis, in particular, involves the assimilation of high proportions of lipids (20–50 % of egg composition) and proteins (Hoegh-Guldberg and Emlet 1997; Sewell and Manahan 2001; Moran and Manahan 2004; Byrne et al. 2008), suggesting that the timing and magnitude of food availability could be the primary determinant of reproductive seasonality in deep scleractinian CWCs (Maier et al. 2020). However, given the high number of abiotic factors affecting reproduction, including temperature, salinity, pH, and oxygen concentration (Beck et al. 2022), it remains a challenge to fully understand the reproductive seasonality of scleractinian CWCs.

The long-term persistence of a species and population depends not only on environmental factors, but also on the recruitment rate matching or exceeding the

mortality rate (Hixon et al. 2002). Mortality in the population is primarily attributed to various environmental disturbances, which can range from frequent but less intense events such as storms and heat waves (Knutson et al. 2010; Hughes et al. 2017, 2018), as well as hypoxia events (< 2 ml O_2 l^{-1}) (Breitburg 2002; Silva and Vargas 2014), to a more rare yet intense occurrences such as earthquakes (Siringoringo et al. 2021), and landslides (Sepúlveda et al. 2011).

Based on the frequency and intensity of these events, corals are thought to have survived by adapting and/or evolving their reproductive mode (Szmant-Froelich et al. 1980; Van Moorsel 1983; Szmant 1986). For instance, stable environments with occasional disturbances favour species with seasonal reproduction and low energy costs of gamete production, making broadcast spawners with their seasonal gamete release and long larval dispersal an advantageous reproductive mode (Szmant 1986). Conversely, unpredictable and frequently disturbed environments may favour species with higher reproductive efficiency, such as brooders with shorter larval dispersal and reduced larval mortality, thus ensuring higher reproductive success in unstable environments (Szmant 1986). However, the observation of these different reproductive modes coupled with different sexualities in scleractinian corals within small geographical areas suggests that factors beyond the environment have likely driven the diversity of reproductive modes and sexualities in modern scleractinian CWCs (section 1.2).

1.4 Gametogenesis

Scleractinian CWCs have no organs such as sex glands or gonads (Harrison and Wallace 1990). Consequently, it is not possible to visually distinguish male from female living polyps unless sexual reproduction take place. Therefore, dissection and/or histological analyses are required for sex determination. Coral gametes develop in the mesoglea of a mesentery lined by gastrodermal tissue (Farrant 1986; Goffredo et al. 2010) (Fig. 4). As the polyp matures, or during the reproductive period, these cells go through several developmental stages until they reach maturity (Harrison and Wallace 1990) (Fig. 4).

Oogenesis begins with yolk accumulation in the oocyte (vitellogenesis), which involves the ooplasmic storage of nutritive material (glycogen, lipids and proteins) that support embryogenesis, i.e., planula larva development (Wallace and Selman 1985; Espinel-Velasco et al. 2018). Vitellogenesis is the longest and most energy-consuming phase of oogenesis, during which the oocyte undergoes volumetric growth. As the oocyte matures, the large centrally located nucleus (germinal vesicle) migrates to the periphery of the oocyte, where meiosis takes place and the nucleus is finally degraded (Eckelbarger and Hodgson 2021) (Fig. 4). Spermatogenesis takes place in the spermatocyst, where sperm also accumulate. During spermatogenesis, both mitosis and meiosis occur to form spermatid cells. The development of the sperm leads to a decrease in cell size and an increase in number. Subsequently, they acquire a flagellum and a pointed head composed of condensed chromatin as they mature into motile spermatozoa (Johnstone et al. 2021) (Fig. 4). When mature, spermatocysts either rupture before spawning and release mature spermatozoa into the gastrovascular cavity (e.g., *D. pertusum* (Larsson et al. 2014)) or spermatocysts are expelled into the gastrovascular cavity before leaving the polyp through the mouth into the surrounding water. There they disintegrate and release mature spermatozoa (e.g., *Pennatula aculeata* (Eckelbarger et al. 1998)).

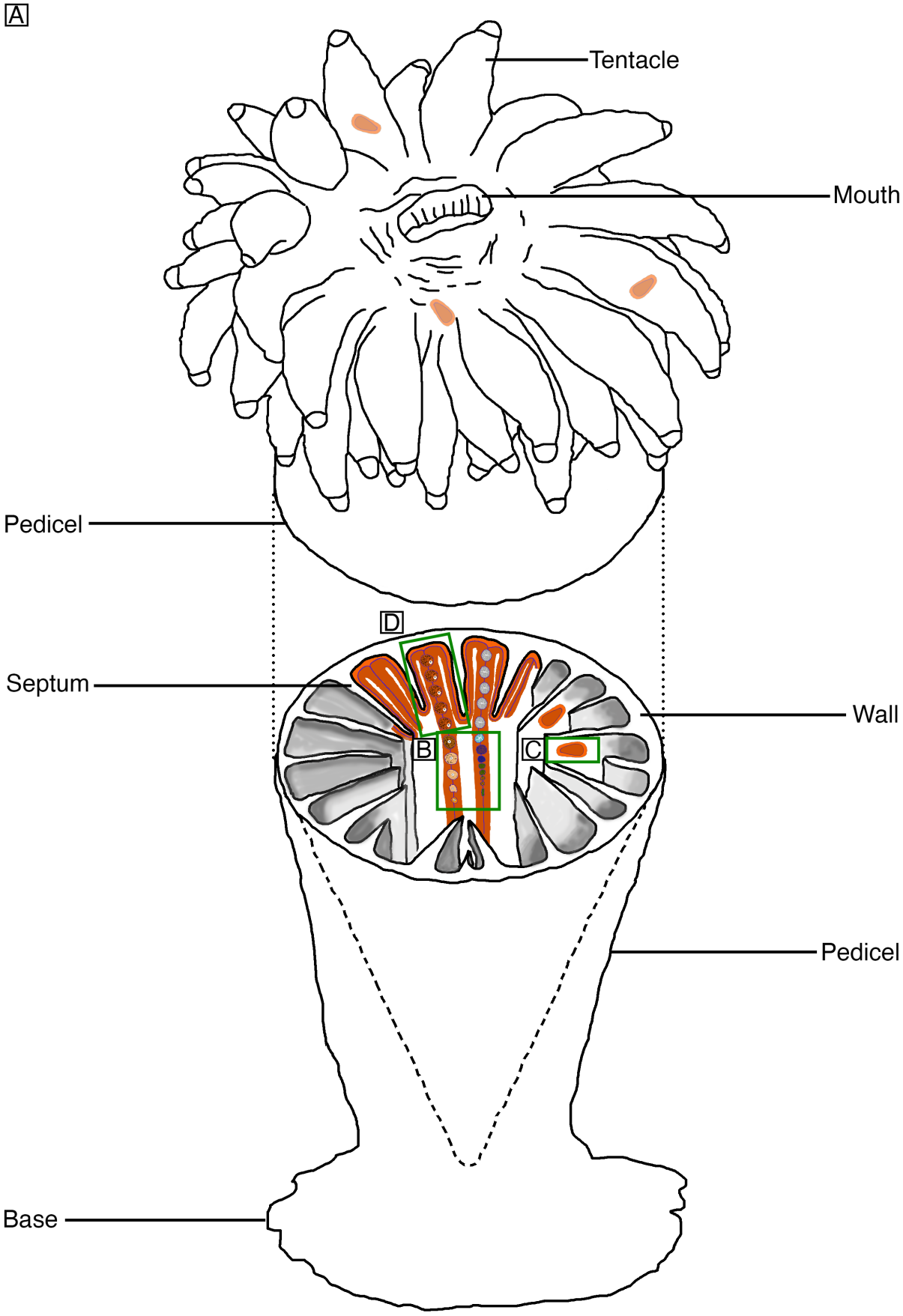
A
Tentacle
Mouth
Pedicel
D
Septum
Wall
B
C
Pedicel
Base

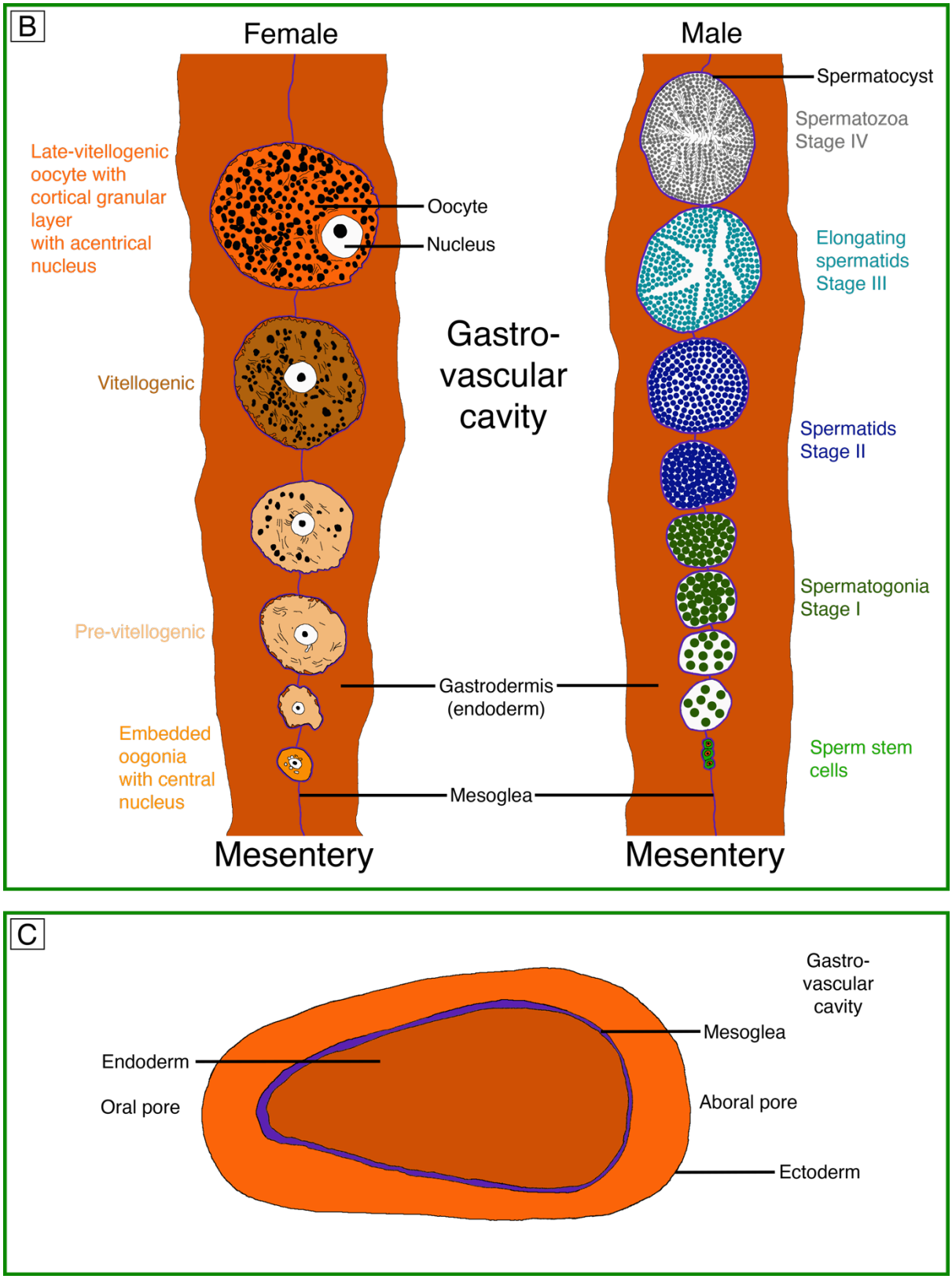

Figure 4: Schematic illustrations of the CWC *C. huinayensis* (Heran et al. 2023) exhibiting the process of gametogenesis and the features of a brooded larva. The green rectangles (B) in (A) shows a longitudinal cut of female and male gametes, detailed in Figure (B), which depicts a female mesentery undergoing oogenesis, exhibiting both pre-vitellogenic and vitellogenic oocytes (Fig. 2d, Chapter 5).

The right mesentery shows the process of spermatogenesis, displaying developmental stages I–IV within spermatocytes, starting from the putative sperm stem cells. The green rectangle (C) in (A) illustrate a longitudinal cut of a larva, detailed in Figure (C). The latter features a larva with the typical bilayered tissue, comprising a uniform ectoderm, a thin layer of mesoglea, and an endoderm. The green rectangle (D) in (A) shows a transverse cut of a female mesentery, which displays vitellogenic oocytes at the same developmental stage as illustrated in Figure 2c, Chapter 5. Both gametes develop in the mesoglea of a mesentery, while the larvae develop in the gastrovascular cavity. Notes: the dashed line within the corallum in (A) denotes the inner growth shape analogous to that of a solitary scleractinian coral, illustrated by (Cairns 1981). The colour coding of the tissue depicted within the corallum in (A) corresponds to those shown in Figure (C).

1.5 Dispersion and settlement

Knowledge about the development and behaviour of larvae from brooding or broadcast spawning scleractinian CWCs is limited. Currently, such knowledge is only available from laboratory studies on 12 scleractinian CWC species (Waller et al. 2023), representing five families: Caryophylliidae (Tranter et al. 1982; Burgess and Babcock 2005; Goffredo et al. 2012; Larsson et al. 2014; Tracey et al. 2021), Dendrophyllidae (Altieri 2003), Flabellidae (Heltzel and Babcock 2002; Waller et al. 2008; Mercier et al. 2011), Oculinidae (Brooke and Young 2003, 2005) and Rhizangiidae (Szmant-Froelich et al. 1980). The rather low number results from the difficulties of reproducing scleractinian CWC species in aquaria or capturing larvae in the natural habitat, due to their small size (e.g., *D. pertusum* larvae are only 120–270 μm long) and their potential dispersal capacities (Larsson et al. 2014). However, such information is crucial to infer population connectivity and the potential for (re)colonization.

The different reproductive modes (spawning and brooding) and the different larval behaviour (pelagic swimming and benthic crawling) may lead to differences in the pelagic larval duration and dispersal scales (Fadlallah 1983; Harrison and Wallace 1990). During the planktonic phase, larval development involves two stages. The first is the pre-competency period, during which the larva has no structural means to attach and settle to the substrate, as cnidae and/or mucus serving as anchoring structures have not yet develop (Strömberg et al. 2019). The second is the competency period, in which the larva is capable of probing the bottom and settling once it has found a

suitable substrate (Pechenik 1990; Young 1995). For spawners, fertilisation and larval development occur in the water column, whereby the timing of these processes enables the zygote to be dispersed beyond its natal habitat by currents (Harrison and Wallace 1990). Laboratory studies have shown that the pre-competency period in the broadcast spawner *D. pertusum* is on average 3 to 5 weeks (Strömberg et al. 2019), whereas models of their genetic population structure suggest a larval competency period of 8 days (Fox et al. 2016). In brooders, these processes occur within the parental polyps. Here the likelihood of larval release during the competency period is high, which potentially limits dispersal compared to spawners (Fadlallah 1983; Harrison and Wallace 1990). For example, larvae of the brooded tropical coral *Favia fragum* were observed to be in the planktonic phase for less than 24 hours (Szmant-Froelich et al. 1985). In species that release crawling larvae, the pre-competency and competence periods are of less importance, as dispersal is restricted to a few metres from the parental polyp (Gerrodette 1981; Harrison and Wallace 1990).

Settlement during the competency period in scleractinian WWCs is triggered by exogenous cues. These include algal (Tebben et al. 2015) and microbial biofilms (Webster et al. 2004). However, experiments on larval settlement cues in scleractinian CWCs have been inconclusive, as the offered settlement substrates, including coralline algae, coral skeleton, glass, and limestone, were disregarded by the larvae (Brooke and Young 2003). External chemical cues are sensed by specialised cilia located on the aboral epidermis of the larvae, known as the apical tuft (Vandermeulen 1974). While the presence of the apical tuft has been observed in *C. smithii* and *O. varicosa* (Tranter et al. 1982; Brooke and Young 2003, 2005, respectively), it is absent in *D. pertusum* (Larsson et al. 2014), indicating a possible endogenous cue for settlement. Larvae initiate probing the bottom, which may take a few seconds to hours, before swimming away and repeating the process (Larsson et al. 2014). Once final contact with the substrate is made at the aboral end or calicoblastic epithelia (Galloway et al. 2006), the larva contracts along the oral-aboral axis, resulting in a flattened disc divided by radial mesenteries (Fig. 3). On the calicoblastic epithelia, specialised stinging cell called nematocytes released organelles called nematocyst to form a sticky plug on the substrate (Kinchington 1982). This process has been well investigated in scleractinian WWCs (Atoda 1951a, b). However, settlement in scleractinian CWCs

has only been observed in *O. varicosa* without the process being described (Brooke and Young 2003).

After settlement, the process of skeletogenesis begins. In scleractinian WWCs, this process is initiated by the deposition of microscale skeletal features such as six radial lamellae, the so-called primary septa, on the substrate. In some corals, the primary septa may be connected at their edges by a circular boundary called the wall. The basal plate, a thin skeletal layer, is subsequently secreted in an eccentric growth and covers the entire substrate surface beneath the polyp. In certain polyps, the basal plate converges at the centre, where a columella develops as a central support for the skeleton, which initiates vertical extension (Gilis et al. 2014, 2015). At the microscale, various complex crystal morphologies, such as aragonitic dumbbell and semispherulitic structures, are deposited (Gilis et al. 2014, 2015). These crystal structures initiate the scaffolding of the individual skeletal features (e.g., septa) (Gilis et al. 2014, 2015), which in some corals ultimately form the corallite in which the polyp resides. The temporal and spatial deposition of these structures in scleractinian CWCs is currently unknown, raising questions regarding potential differences in skeletal structure deposition across space and time, compared to scleractinian WWCs.

Under environmental stress, the development of a polyp may be reverse. A settled and already calcified polyp can regain its body plan and transform into a mobile secondary larva through a process known as reverse metamorphosis or ontogenetic (i.e., development of an organism from the time of fertilization to adulthood) reversal. Afterwards, it can disperse with the current and resettle elsewhere (Richmond 1985). This ontogenetic reversal can also result in polyp detachment, which includes “polyp expulsion”, in which the whole polyp including their calices leave the colony (Kramarsky-Winter et al. 1997), and “bail-out”, in which the polyp is freed without calice (e.g., Sammarco 1982; Kružić 2007; Capel et al. 2014; Serrano et al. 2018). The ability of the polyp to survive without the calice may be related to the “naked corals” hypothesis proposed by Stanley Jr (2003). The key idea of this hypothesis is that different groups of soft-bodied, unrelated anemone-like anthozoans gave rise to various calcified scleractinian corals, potentially explaining the sudden appearance of a diverse and differentiated range of scleractinian skeletal types in the Permian-Triassic. Overall, these diverse escape or dispersal mechanisms have only been

described in scleractinian WWCs, raising the question of whether this process can also occur in scleractinian CWCs.

1.6 Reproduction of scleractinian CWCs in a changing ocean

Anthropogenic combustion of fossil fuels has increased the atmospheric partial pressure of carbon dioxide (pCO_2) since the industrial revolution, ending the nearly 420,000 years of relative stability (between 180–300 ppm) (Petit et al. 1999). The increasing amount of atmospheric carbon dioxide (CO_2) absorbed by the ocean affects sea water carbonate chemistry, reflected in an increased concentration of bicarbonate ions [HCO_3^-] and hydrogen ions [H^+] and a decrease in carbonate ions [CO_3^{2-}]. This process known as ocean acidification (OA), is expected to decrease the seawater pH by an average of 0.3 units by the end of the century (Caldeira and Wickett 2005; Orr et al. 2005; Gattuso et al. 2015), as predicted by the Representative Concentration Pathway (RCP) 8.5 scenario (Meinshausen et al. 2011). This leads to a reduction of the saturation state (Ω) of aragonite, one naturally occurring crystal form of calcium carbonate ($CaCO_3$) (Feely et al. 2004; Caldeira and Wickett 2005; Orr et al. 2005). The decrease in [CO_3^{2-}], reflected in aragonite undersaturation ($\Omega_{arag} < 1$) may cause the dissolution of the aragonite skeletons of scleractinian CWCs (Hennige et al. 2015, 2020). It is predicted that by 2,100, 70 % of the habitats inhabited by scleractinian CWC will be surrounded by water with $\Omega_{arag} < 1$ (Guinotte et al. 2006).

For this reason, scleractinian CWCs have long been considered vulnerable to OA (Guinotte et al. 2006; Turley et al. 2007; Guinotte and Fabry 2008), as reduced calcification has been observed in adults (Maier et al. 2009, 2016; Movilla et al. 2014a; Büscher et al. 2017; Martínez-Dios et al. 2020). However, long-term studies have indicated that scleractinian CWCs may potentially acclimate to OA, albeit in a species-specific way (Form and Riebesell 2012; Maier et al. 2013; Carreiro-Silva et al. 2014; Movilla et al. 2014a; Hennige et al. 2015; Gori et al. 2016), and it is now widely accepted that scleractinian CWCs may be more resilient to OA than previously

thought. Indeed, scleractinian CWCs have been observed to thrive in naturally acidified seawater in certain regions, including $\Omega_{arag} < 1$ (Thresher et al. 2011; Fillinger and Richter 2013; Jantzen et al. 2013b; Baco et al. 2017; Rossbach et al. 2021).

Their resilience to OA may be due to the capacity of scleractinian CWC to upregulate the pH in the extracellular calcifying medium (ECM) (McCulloch et al. 2012) present between the polyp aboral epidermal layer and the underlying skeleton (Allemand et al. 2004). Calcium ions (Ca^{+}) are actively transported into the ECM in exchange for protons (Cohen and McConnaughey 2003; Allemand et al. 2004). The resulting increase in pH alters the equilibrium composition of dissolved inorganic carbon (DIC) species, favouring higher carbonate concentrations [CO_3^{2-}] and lower bicarbonate concentrations [HCO_3^{-}], thereby increasing the aragonite saturation state (Ω_{arag}) of the ECM. Increasing the carbonate saturation state at the calcification site thorough pH up-regulation has the potential to ameliorate or buffer the effect of reduced carbonate saturation of the external surrounding seawater (Cohen and Holcomb 2009; Holcomb et al. 2009). This process may explain to some extent how scleractinian CWCs can maintain calcification beneath the $\Omega_{arag} < 1$. However, due to the expected higher energy costs (~10 % per 0.1 pH decrease of the seawater), creating a higher pH gradient between the external seawater and the calcification site may represent an additional energetic burden (McCulloch et al. 2012).

Despite the species-specific effects of OA on adult scleractinian CWCs (Movilla et al. 2014a), early life-stages of CWCs could potentially be more affected by OA, as suggested by preliminary studies (Movilla et al. 2014a; Roberts et al. 2016). Under normal environmental conditions, an organism's energy budget can be allocated to physiological processes, including somatic growth, skeletal growth and/or reproduction, as needed. Under OA conditions, a greater proportion of this energy budget may be allocated to pH upregulation to support growth (McCulloch et al. 2012). Then, the shift in energy allocation could limit the resources required for crucial processes such as gametogenesis during the reproductive period. However, this approach has never been investigated in scleractinian CWCs.

There is also a gap in understanding the effects of OA on early life stages. Recent studies have revealed that juvenile scleractinian WWCs exhibit distinct responses to OA compared to adults (Leung et al. 2022). These responses includes

reduced skeletal mass and growth, morphological alterations in the aragonite skeleton (Cohen et al. 2009; de Putron et al. 2011; Drenkard et al. 2013; Foster et al. 2015), and increased skeletal porosity (Foster et al. 2016). Therefore, it is imperative to uncover the specific and indirect effects of OA on the early life history of scleractinian CWC species.

1.7 Research questions and hypothesis

The aim of this thesis is to describe the reproductive biology of the scleractinian CWC *Caryophyllia (Caryophyllia) huinayensis* and to predict the possible impacts of OA on its early life history based on observational and experimental evidence. Both *vitro* and *in situ* investigations were used to determine the reproductive mode and strategy, gametogenesis, a potential dispersion mechanism, and the effect of $\Omega_{arag} < 1$ and low seawater pH on early skeletogenesis and oogenesis of this scleractinian CWC, respectively. Thus, this thesis addresses the following research questions and hypothesis:

Q.1 What is the reproductive mode and strategy of the scleractinian CWC *C. huinayensis*? Has its reproduction seasonal peaks?

Thorson's rule states that organisms at higher latitudes tend to produce larger and fewer offspring, and are frequently brooders. As *C. huinayensis* is not distributed at high but at mid-latitudes (36° and 48.5° S), according to the rule this species should reproduce via spawning, as do most of the scleractinian CWCs studied so far, including colonial hermatypic (Brooke and Young 2003; Burgess and Babcock 2005; Waller and Tyler 2005; Pires et al. 2014), pseudo-colonial (Feehan et al. 2019), and solitary forms (Waller et al. 2005; Mercier et al. 2011; Waller and Tyler 2011; Waller and Feehan 2013). Although scleractinian CWCs exhibit diverse combinations of reproductive strategies, including cyclical hermaphroditism, gonochorism is the most common sexual strategy among all taxa studied, with 18 of 21 species exhibiting this

reproductive strategy (Waller et al. 2023), while cyclical hermaphroditism occurs in only three species (Waller et al. 2005).

The resultant combination of a species reproductive mode and strategy is thought to depend on the interaction with environmental conditions under which the selection on these traits occurs. However, a phylogenetic study (Kerr et al. 2011) on scleractinians suggested the opposite. The reproductive traits observed in modern-day species result from the most effective combination of these traits that facilitated their survival and, thus, were passed on over *ca.* 250 Myr of scleractinians history (Kiessling et al. 2002). Also, it is suggested that the surviving reproductive traits provide the basis for a transition rate between traits, thought to be dependent on coral sexuality (Kerr et al. 2011).

The timing of larval and gamete release is highly influenced by abiotic and biotic factors, including food availability and water temperature (Waller and Tyler 2005; Mercier et al. 2011; Rossin et al. 2017; Feehan et al. 2019; Maier et al. 2020). At high latitudes, where the environment is subject to strong seasonal fluctuations, larvae and gametes are highly seasonal mature and mainly released in spring when productivity peaks (Häussermann and Försterra 2015; Rossin et al. 2017; Feehan et al. 2019).

Chapter 2 describes both, the reproductive mode and reproductive activity of the scleractinian CWC *C. huinayensis* under aquarium conditions. In **Chapter 5,** histological techniques were used to investigate the *in situ* reproductive strategy and potential reproductive activity of *C. huinayensis*. Together, **Chapter 2** and **5** provide the basis for a comprehensive understanding of the reproductive biology of this species.

Q.2 Can scleractinian CWCs undergo reverse development to disperse, similar to what has been observed in scleractinian WWCs?

Under environmental pressure, scleractinian WWCs have evolved diverse escape or dispersal mechanisms, leading to reverse development. In all cases, the settled calcified polyp can shift backwards into a mobile phase and disperse via currents. This occurs after an ontogenetic reversal and polyp detachment, expulsion,

or bail-out (Sammarco 1982; Kramarsky-Winter et al. 1997; Piraino et al. 2004; Kružić 2007; Capel et al. 2014; Serrano et al. 2018) and may be followed by re-settlement. Based on both, laboratory and field observations on the scleractinian CWC *C. huinayensis*, **Chapter 3** provides evidence of a novel form of reverse development, which is discussed within the context of the "naked coral" hypothesis (Stanley Jr 2003).

Q.3 Do the distinct developmental stages from larvae to juvenile polyps of the scleractinian CWC *C. huinayensis* arise at a similar timing to that of zooxanthellate scleractinian WWCs, despite major environmental differences?

It has been previously assumed that zooxanthellate scleractinian corals develop and calcify faster than azooxanthellate scleractinian CWCs. This was based on the high photosynthetic energy endosymbionts translocate via photosynthates to the host (Falkowski et al. 1984; Dubinsky and Falkowski 2011), in addition to heterotrophic feeding (Porter 1976). However, studies have shown that the calcification rates of azooxanthellate scleractinian CWCs are comparable to those of zooxanthellate scleractinian WWCs (Orejas et al. 2011; Jantzen et al. 2013b). The authors hypothesise that the nutritional value (calories per unit of mass) of the heterotrophic diet in scleractinian CWCs may be greater or similar to that of mixotrophic diet of zooxanthellae scleractinian WWCs. In **Chapter 2**, the early ontogenetic stages and their duration in a scleractinian CWC species until reaching a juvenile stage are shown for the first time.

Q.4 Do early-life history stages of scleractinian CWCs during ontogenetic skeletal formation exhibit similar timing and crystal deposition patterns to those of scleractinian WWCs, despite significant environmental differences?

As azooxanthellate scleractinian CWCs typically thrive in environments with seawater temperatures between 2 °C and 15 °C (Keller and Os' kina 2008), it was commonly assumed that they have lower metabolic performance than scleractinian

WWCs, which thrive in seawater temperatures between 14 °C and 36 °C (Kleypas et al. 1999; Riegl and Purkis 2012). However, studies have shown that the nutritive value (calories per unit of mass) of scleractinian CWCs on a specialised heterotrophic diet may by greater or similar to that of a mixotrophic diet (Reed 1981), as calcification rates of azooxanthellate scleractinian CWCs are comparable to those of their zooxanthellate coral counterparts (Orejas et al. 2011). In the descriptive study of the life cycle of *C. huinayensis* in **Chapter 2**, we provided a suitable substrate on which the larvae could settle and metamorphose into a juvenile polyp. We succeeded in maintaining them alive over the descriptive period of almost three years. The long-term maintenance of the young polyp provided us with the opportunity to develop a culture chamber for *in vivo* observations under a polarized light microscopy (PLM) to document for the first time the early ontogenetic development and skeleton formation in a newly recruited polyp of a scleractinian CWC. Moreover, we used scanning electron microscopy (SEM) on the bare skeleton to describe the development of micro- and macrostructural elements forming the skeleton, providing insight into three different developmental stages and their corresponding time periods. The stages and timing of the generation of skeletal structures were compared with those of scleractinian WWCs (**Chapter 4**).

Q.5 How does aragonite undersaturation of seawater affect early skeletogenesis of scleractinian CWCs?

Skeletogenesis of scleractinian WWCs in juvenile corals has been shown to be affected differently by OA than in adults corals (Leung et al. 2022). Previous studies indicated that corallites may exhibit morphological skeletal deformations (Cohen et al. 2009), increased porosity and amount of fractures (Foster et al. 2016), and a reduction in the number of septa (Carbonne et al. 2022), while adults are more resilient due to their lower calcification rate (Maier et al. 2009, 2013; Movilla et al. 2014a, b; Martínez-Dios et al. 2020) and higher energy reserves (Beck et al. 2022). Hence, it may be hypothesized that ontogenetic skeletal formation of scleractinian CWCs is affected by aragonite undersaturation of the seawater predicted for the RCP 8.5 scenario. Using

a custom-designed chamber, I was able to culture recruits of *C. huinayensis* to investigate, for the first time in a scleractinian CWC, the potential effects of seawater aragonite undersaturation predicted for the RCP 8.5 scenario (Meinshausen et al. 2011) on early-stage skeletogenesis (**Chapter 4**).

Q.6 Does the low seawater pH predicted under the "business-as-usual" scenario (Pörtner et al. 2019) affect the reproduction of scleractinian CWCs that thrive in naturally acidified waters?

Studies have suggested that low seawater pH may affect sexual reproduction in scleractinian CWCs (Roberts et al. 2016). This could potentially be attributed to the high energy cost of pH up-regulation, favouring calcification by buffering the externally low seawater pH (McCulloch et al. 2012). For instance, a study conducted in the naturally acidified Comau Fjord in Chile (Fillinger and Richter 2013) found that 70 % of the individuals were non-reproductive during the reproductive period of *D. dianthus* (Feehan et al. 2019). This suggests that reproduction may be restricted compared to growth or that both processes are downregulated under unfavourable environmental conditions.

Based on these findings, it may be hypostatize that gametogenesis of the scleractinian CWC *C. huinayensis* thriving in a naturally acidified fjord in Chile, may be affected despite the potential adaptation of these species to the low seawater pH condition. In **Chapter 5,** the potential effects of low seawater pH on seasonal oocyte development and the potential relative fecundity (PRF: vitellogenic oocytes) were investigated at three study sites with different seawater pH levels (7.7 to 8.1).

1.8 Manuscript outline and author contribution

Chapter 2: Life cycle of the cold-water coral *Caryophyllia huinayensis*

Thomas Heran, Jürgen Laudien, Rhian G. Waller, Verena Häussermann, Günter Försterra, Humberto E. González, and Claudio Richter

Published in *Scientific Reports*, 13, 2595. DOI: 10.1038/s41598-023-29620-x

Author contribution: T.H., J.L., and C.R. conceived the study. J.L., and C.R. hosted the study. G.F. contributed with materials. T.H. carried out the analyses and created the figures. T.H., J.L., and C.R. wrote the manuscript. R.G.W., V.H., G.F., and H.E.G. contributed to the writing.

Chapter 3: Polyp dropout in a solitary cold-water coral

Jürgen Laudien, Thomas Heran, Verena Häussermann, Günter Försterra, Gertraud M. Schmidt-Grieb, and Claudio Richter

Published in *Coral Reefs*, 40, 1657–1665. DOI: 10.1007/s00338-021-02148-0

Author contribution: J.L., and T.H. conceived the study. T.H. took the pictures in the laboratory and in the field and produced all figures. J.L., T.H., and C.R. interpreted the data and wrote the manuscript. V.H., G.F., and G.M.S.G. contributed to the writing. J.L and C.R. hosted the study.

Chapter 4: Real-time *in-vivo* skeletal formation shows that newly settled cold-water corals defy ocean acidification

Thomas Heran, Jürgen Laudien, Marlene Wall, Claudio Richter, and Gernot Nehrke

Manuscript prepared for *Nature Communications*

Author contribution: T.H., J.L., G.N. and C.R. had the idea for this work, planned and designed the experiment and the setup for this study. T.H. developed the flow-chamber setup, performed the experiment, collected the data, performed the data analysis and interpretation, created all figures and tables, and drafted the first version of the manuscript. All authors made genuine and relevant scientific contributions to the manuscript and approved it for publication. J.L., C.R. and G.N. hosted the study.

Chapter 5: Seasonal reproduction of a cold-water coral in a naturally acidified Chilean fjord

Thomas Heran, Rhian Waller, Claudio Richter, Verena Häussermann, Susana Simancas-Giraldo, and Jürgen Laudien

Manuscript prepared for *Coral Reefs*, Springer

Author contribution: T.H., J.L., and R.W. conceived the study. T.H. collected the samples and prepared them for histological analysis. T.H. performed the histological examination. T.H., and S.S-G performed the statistical analysis and interpreted the data. T.H. created the figures and tables with support from S.S-G and drafted the manuscript. All authors made genuine and relevant scientific contributions to the manuscript and approved it for publication. J.L. and C.R. hosted the study.

Contribution to multi-author articles/manuscripts

Declaration on the contribution of the candidate to multi-author articles/manuscripts, which are included as chapters in the submitted doctoral thesis

Chapter 2: Life cycle of the cold-water coral *Caryophyllia huinayensis*

Contribution of the candidate in % of the total work load (up to 100% for each of the following categories):

Experimental concept and design:	*ca*. 80%
Experimental work and/or acquisition of (experimental) data:	*ca*. 100%
Data analysis and interpretation:	*ca*. 80%
Preparation of figures and tables:	*ca*. 90%
Drafting of the manuscript:	*ca*. 80%

Chapter 3: Polyp dropout in a solitary cold-water coral

Contribution of the candidate in % of the total work load (up to 100% for each of the following categories):

Experimental concept and design:	*ca*. 50%
Experimental work and/or acquisition of (experimental) data:	*ca*. 70%
Data analysis and interpretation:	*ca*. 20%
Preparation of figures and tables:	*ca*. 90%
Drafting of the manuscript:	*ca*. 20%

<u>Chapter 4:</u> Real-time *in-vivo* skeletal formation shows that newly settled cold-water corals defy ocean acidification

Contribution of the candidate in % of the total work load (up to 100% for each of the following categories):

Experimental concept and design:	*ca*. 90%
Experimental work and/or acquisition of (experimental) data:	*ca*. 100%
Data analysis and interpretation:	*ca*. 80%
Preparation of figures and tables:	*ca*. 90%
Drafting of the manuscript:	*ca*. 80%

<u>Chapter 5:</u> Seasonal reproduction of a cold-water coral in a naturally varying seawater pH of Chilean Patagonia

Contribution of the candidate in % of the total work load (up to 100% for each of the following categories):

Experimental concept and design:	*ca*. 90%
Experimental work and/or acquisition of (experimental) data:	*ca*. 100%
Data analysis and interpretation:	*ca*. 80%
Preparation of figures and tables:	*ca*. 90%
Drafting of the manuscript:	*ca*. 80%

Date:

Signatures:

2

Life cycle of the cold-water coral *Caryophyllia huinayensis*

Thomas Heran[1,2,3*], Jürgen Laudien[1], Rhian G. Waller[4], Verena Häussermann[3,5], Günter Försterra[6], Humberto E. González[7,8], Claudio Richter[1,2]

[1] Alfred-Wegener-Institut Helmholtz-Zentrum für Polar- und Meeresforschung, Am Alten Hafen 26, 27568 Bremerhaven, Germany.

[2] University of Bremen, Bibliothekstraße 1, 28359 Bremen, Germany.

[3] Fundación San Ignacio del Huinay, Casilla 462, Puerto Montt, Chile.

[4] University of Gothenburg, Tjärnö Marine Laboratory, Strömstad, 452 96 Sweden.

[5] Universidad San Sebastián, Facultad de Economía y Negocios, Lago Panguipulli, 1390 Puerto Montt, Chile

[6] Facultad de Recursos Naturales, Escuela de Ciencias del Mar, Pontificia Universidad Católica de Valparaíso (PUCV), Valparaíso, Chile.

[7] Universidad Austral de Chile, Instituto de Ciencias Marinas y Limnológicas, Valdivia, Chile.

[8] Research Center: Dynamics of High Latitude Marine Ecosystems (FONDAP-IDEAL), Chile.

Keywords: cold-water coral (CWC), early life history, larval behaviour, metamorphosis, settlement, reproductive mode.

Published in ***Scientific Reports***, 13, 2595. DOI: 10.1038/s41598-023-29620-x.

2.1 Abstract

Little is known about the biology of cold-water corals (CWCs), let alone the reproduction and early life stages of these important deep-sea foundation species. Through a three-year aquarium experiment, we described the reproductive mode, larval release periodicity, planktonic stage, larval histology, metamorphosis and post-larval development of the solitary scleractinian CWC *Caryophyllia (Caryophyllia) huinayensis* collected in Comau Fjord, Chilean Patagonia. We found that *C. huinayensis* is a brooder releasing 78.4 ± 65.9 (mean ± standard deviation [SD]) planula larvae throughout the year, a possible adaptation to low seasonality. Planulae had a length of 905 ± 114 *µ*m and showed a well-developed gastrovascular system. After 8 ± 9.3 days (d), the larvae settled, underwent metamorphosis and developed the first set of tentacles after 2 ± 1.5 d. Skeletogenesis, zooplankton feeding and initiation of the fourth set of tentacles started 5 ± 2.1 d later, 21 ± 12.9 d, and 895 ± 45.9 d after settlement, respectively. Our study shows that the ontogenetic timing of *C. huinayensis* is comparable to that of some tropical corals, despite lacking zooxanthellae.

2.2 Introduction

Cold-water corals (CWCs) are widespread across the oceans and provide important habitats for a rich associated fauna (Cairns and Stanley 1982; Mortensen and Buhl-Mortensen 2005; Roberts et al. 2009). They exhibit a great diversity of life cycles and developmental stages. Most information on coral life cycles of CWCs is available for octocorals (Sun et al. 2010), while only little is known about cold-water scleractinians (Strömberg and Larsson 2017). The difficulty to observe CWCs *in situ* and the challenge to rear corals in aquaria systems with suitable conditions for reproduction has hampered the study of the early life cycles of CWCs.

The life cycle of scleractinian corals includes a sessile benthic phase and a mobile phase with either a benthic crawling or pelagic swimming planula (Harrison 2011). The larva undergoes settlement when a permanent contact with the substrate is stablish and metamorphosis to the primary polyp (Rodriguez et al. 1993) where physiological and morphological transformation take place, with the formation of the basal plate initiating the calcium carbonate skeleton. Subsequently the primary polyp grows to an adult reproductive coral, thus completing the life cycle.

To date, two modes of sexual reproduction are known in adult CWC polyps: broadcast spawning and brooding. Broadcast spawners release gametes into the water column for external fertilization and development of free-swimming planula. In brooders, fertilization occurs internally and subsequent larval development takes place within the gastrovascular cavity of the polyp resulting in the release of developed planulae. Most scleractinian CWCs studied to date are broadcast spawners, including colonial hermatypic (Brooke and Young 2003; Burgess and Babcock 2005; Waller and Tyler 2005; Pires et al. 2014), pseudo-colonial (Feehan et al. 2019), and solitary forms (Waller et al. 2005; Mercier et al. 2011; Waller and Tyler 2011; Waller and Feehan 2013), while brooding has been observed in three Antarctic solitary scleractinians, i.e., *Flabellum thouarsii, F. curvatum* and *F. impensum* (Waller et al. 2008), and in the sub-Antarctic *Balanophyllia malouinensis* from the Drake Passage (Pendleton et al. 2021).

Previously it was hypothesized that coral sexual reproduction is related to the life history, morphology, and habitat selection in several ways (Szmant-Froelich et al. 1980; Van Moorsel 1983; Szmant 1986). First, it has been noted that small polyps

appear to produce small eggs and brood larvae, whereas massive or large-polyps spawn with subsequent external fertilization (Rinkevich and Loya 1979). Second, polyps with large inter-septa spaces allow brooding, suggesting that the inter-septa spacing would be a proxy for the reproductive mode (Fadlallah and Pearse 1982). Third, brooding may have evolved in corals as an adaptation to increase recruitment success in unstable habitats, i.e., frequent physical disturbances such as storms or substrate slumping, or infrequent but catastrophic disturbances such as extreme low tides, sea warming events, and sea level changes (Szmant 1986). Short larval dispersal could be beneficial for infrequent disturbances, and long larval dispersal would be beneficial for frequently disturbed habitats.

The contrasting modes of reproduction (spawning and brooding) could lead to differences in the pelagic larval duration (PLD), and consequently to different scales of larval dispersal. PLD correlates with both the duration of the pre-competency period, (i.e., the time during which larvae have no means to settle) and the competency window (i.e., when the larva is searching for a suitable substrate while being able to settle when it finds it). In broadcast spawners, the larval period is spent primarily in the water column, whereas in brooders, the planulae remain within the parent polyp (after internal fertilization) before leaving the parent and settling. If a larva takes too long to find a substrate, however it may not be able to settle and metamorphose (Treml et al. 2015). The competency period may also depend on the feeding ability/disability of the larvae, i.e., it may be longer for planktotrophic (feeding) larvae that have a mouth and gastrovascular cavity and shorter for lecithotrophic (non-feeding) larvae. The larval period is the most vulnerable part of the life cycle due to the presence of pelagic predators as well as environmental threats. Laboratory studies on *Desmophyllum pertusum* found a pre-competency period averaging 3–5 weeks (Strömberg et al. 2019). While the PLD has not yet been determined, it has been assumed to range from 99 d to one year (Strömberg and Larsson 2017). The long PLD is considered to be the result of the planktotrophy of *D. pertusum* larvae (Strömberg and Larsson 2017). Instead, in the facultatively photosymbiotic *O. varicosa*, the pre-competency period and PLD are shorter, lasting between 1–2 weeks and between 21–27 d (Brooke and Young 2003), respectively. Although the feeding behaviour of *O. varicosa* larvae

is still undetermined, laboratory observations suggest a lecithotrophic larva (Brooke and Young 2005).

Larval settlement in scleractinians is triggered by endo- and/or exogenous cues (Tebben et al. 2015). Exogenous chemical cues from algae (Tebben et al. 2015) and microbial biofilms (Webster et al. 2004) are detected by specialized cilia or flagella at the aboral epidermis (Vandermeulen 1974), i.e., the apical organ or apical tuft. After apical contact with the substrate, nematocysts discharge and mucus of the epidermis forms an adhesive plug (Kinchington 1982).This is followed by contraction of the oral-aboral plane, resulting in a flattened disc subdivided by radial mesenteries. In tropical corals, this process has been well studied (Atoda 1951b, a); however, in CWCs, there are few descriptions of the early life cycle (Strömberg and Larsson 2017).

Caryophyllia (Caryophyllia) huinayensis Cairns, Häussermann & Försterra, 2005 (Cairns et al. 2005) is a small (20 mm high, 10 mm ø) (Cairns et al. 2005) solitary azooxanthellate scleractinian recorded in Chilean waters between 36° and 48.5° S (Cairns et al. 2005). In Comau Fjord, Chile, it is found between 11 and at least 265 m depth (Wurz 2014; Försterra et al. 2017) (revealed from a remotely operative vehicle (ROV) until half way down in Comau Fjord), while on the continental slope it occurs between 740 and 870 m water depth (Sellanes et al. 2008). Despite being an important representative of the benthic biodiversity of the Patagonian fjords, reaching densities of up to 2,211 ± 180 ind. m^{-2} at 25 meters water depth on steep and overhanging walls (Wurz 2014), its reproductive biology and life cycle are so far unknown.

The objectives of this study were to describe (i) reproductive mode and periodicity, (ii) larval behaviour and features, and (iii) metamorphosis and post-larval development of the scleractinian CWC *C. huinayensis*. For this purpose, reproductive polyps were reared in a holding tank over three years, where released larvae were collected periodically to determine the production rate. Brooded larvae were characterized through histological cuts of the polyps. Collected larvae were introduced into flow-through glass cubes where the early life cycle was monitored from the planktonic phase through settlement, metamorphosis and growth to a young polyp.

2.3 Results

2.3.1 Reproductive mode and periodicity

For this study, seven reproductive polyps of *C. huinayensis* (Fig. 1a) were extensively monitored for 3.1 years, recording the number of released larvae twice per day. Although no sperm release was observed throughout the entire study, larvae could be observed across the translucent oral tissue of the polyps swimming in the coelenteron beneath the oral disk and tentacles. A total of 1,647 planulae were released from the polyps into the surrounding water, from which 19 larvae that settled and metamorphosised into young polyps were monitored.

It is likely that only part of the larvae in the coelenteron were counted as planulae swimming at a distance from the tissue surface may have remained undetected. Periods with no visible larvae (Fig. 1b) were generally followed by the sudden appearance of 2–3 larvae swimming from one tentacle to another. Subsequently, the number of larvae increased in the gastrovascular cavity below the oral disc and in the tentacles, reaching up to 17 planulae per polyp (Fig. 1c). As brooding progressed, polyps changed shape: the oral disc bulged outward until assuming a dome shape lasting 1–2 d which was ended by a ~10-seconds contraction causing the gastrovascular fluid containing the larvae to exit through the mouth (Fig. 1d). Occasionally, we observed larvae released at time when corals were feeding on krill.

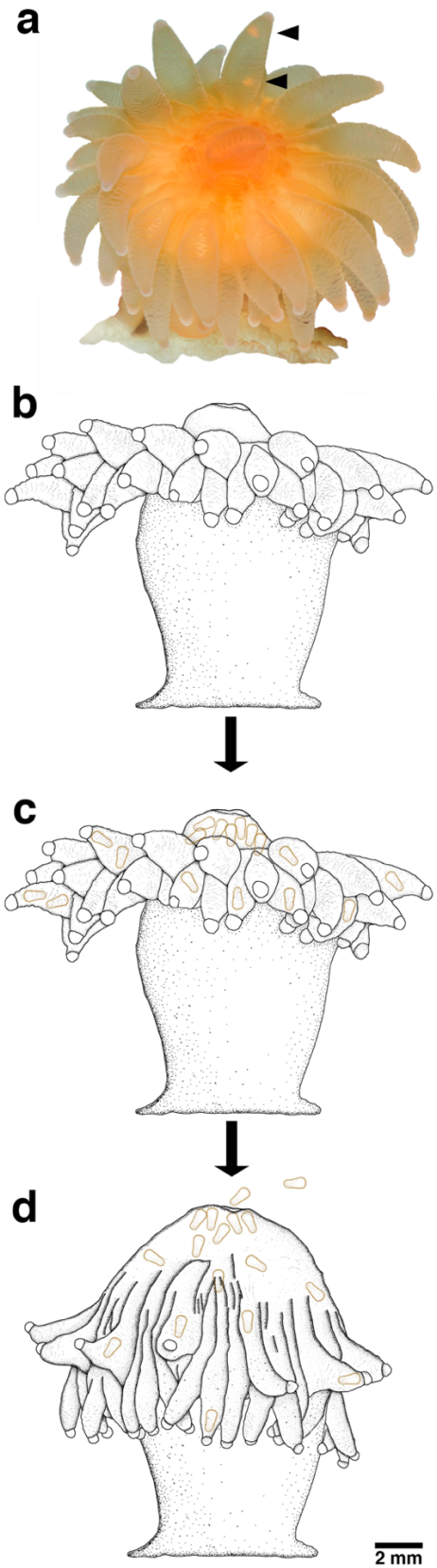

Figure 1: Temporal sequence of larval release of *Caryophyllia huinayensis.* (**a**) reproductive polyp with two larvae (black arrowheads) in a tentacle. Schematic drawing of (**b**) a polyp with larvae not visible or absent, (**c**) polyp with larvae in the gastrovascular cavity and tentacles, and (**d**) forming the dome shape before releasing larvae (in orange) through the mouth.

Caryophyllia huinayensis individuals released 78.4 ± 65.9 (mean ± SD) larvae per year, with the exception of April 2021 (Fig. 2 a–c). Synchronous spawning of all 7 polyps was observed from August 2018 to January 2019 (Fig. 2b). Thereafter, the reproductive activity showed a bi-modal distribution: where 70–80 % of the polyps released planulae in austral fall and winter (March–August 2019), and austral winter and spring (June–October 2020), in contrast to austral summer (December 2019–January 2020) and spring (March–May 2021), where only 0–13 % of the polyps released larvae (Fig. 2a).

The proportion of corals engaged in the production and release of larvae was reflected in larval numbers (Fig. 2c). We observed three peaks of released larvae: one in austral spring (October 2018) with > 40 larvae polyp^{-1} month^{-1}, and two broader ones in austral winter (June–July 2019) and spring (September–December 2020), both with < 15 larvae polyp^{-1} month^{-1} (Fig 2c). The maximum number of released larvae was observed during October 2018, with a total of 43 larvae polyp^{-1} month^{-1} (Fig. 3b), with a maximum of 14 released larvae by one polyp in one day (Fig. 3a). In November 2020, a single polyp released 21 larvae in one day. Monthly larval release differed temporally, with some polyps pausing planulation for 6.1 ± 5.9 consecutive months, with a maximum of 17 months. Compared to polyps that continuously planulated for 11.7 ± 3.4 months, with a maximum of 16 months (Fig. 2b).

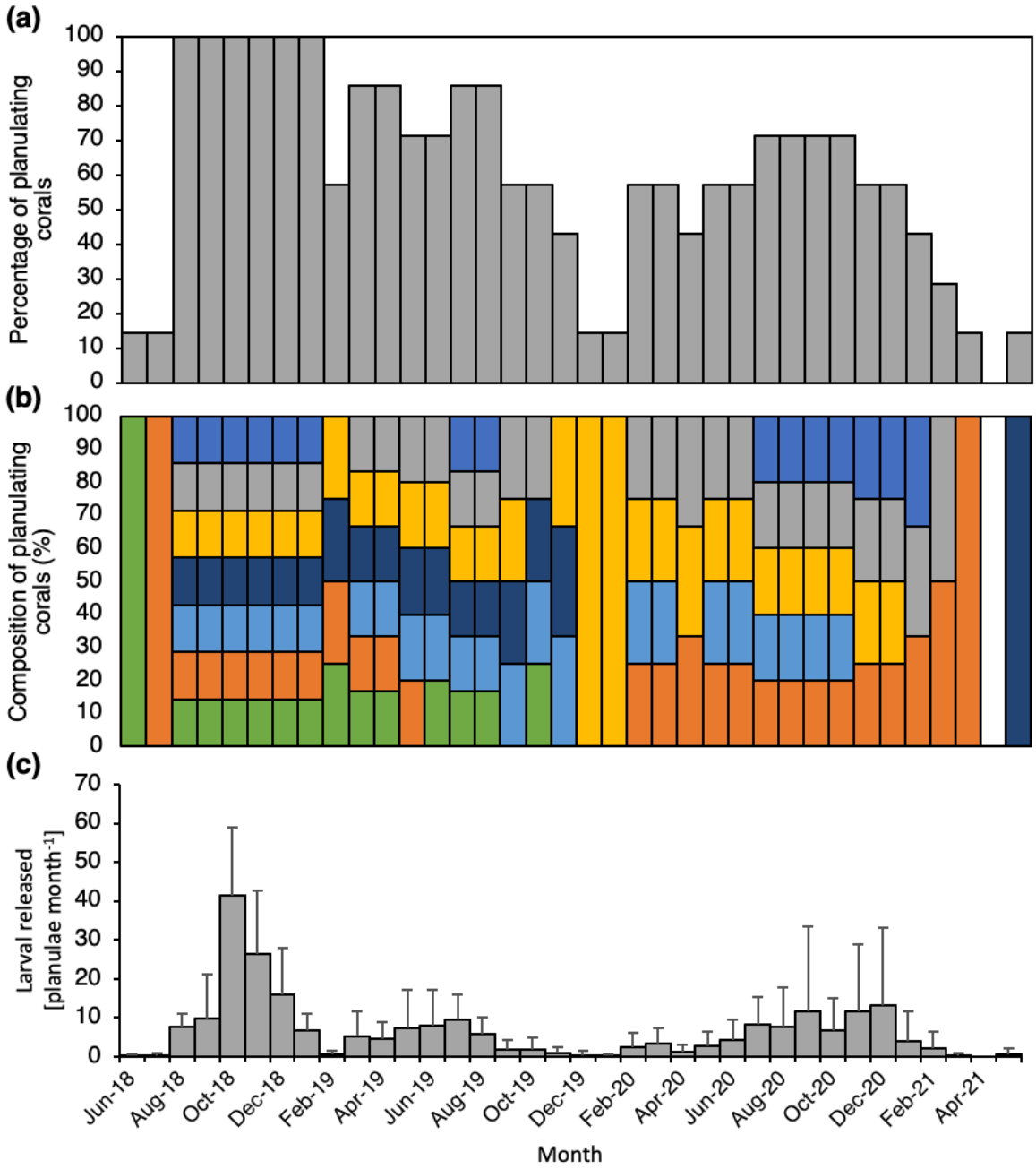

Figure 2: Seasonal and interannual variability of the planulation activity of *Caryophyllia huinayensis*. (**a**) Percentage of larval release, (**b**) composition of planulating corals, with color-coded bars representing each of the seven parental polyps included in the study. (**c**) Larval release rate (mean ± SD) per month among all parental polyps. Note: No larvae were released in April 2021.

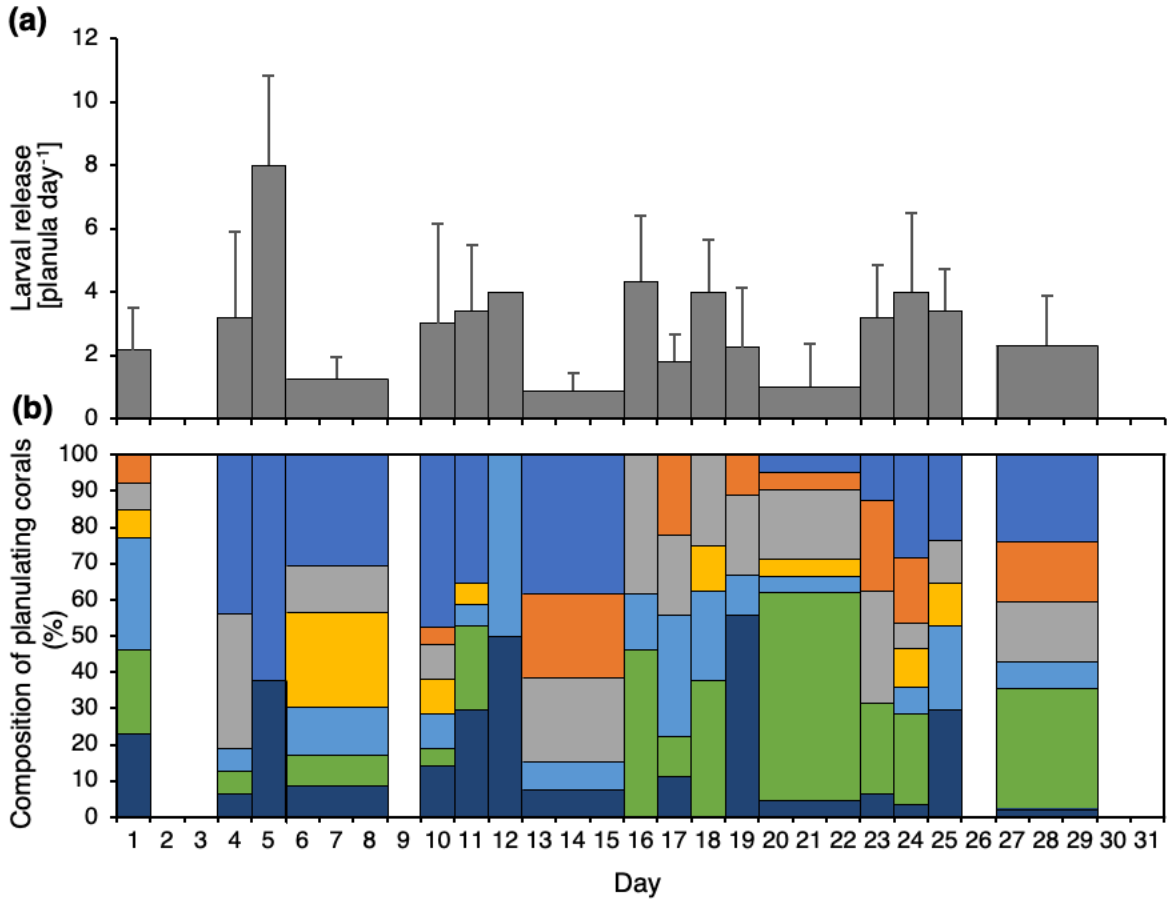

Figure 3: Daily larval release among the seven *Caryophyllia huinayensis* polyps during the most active month (October 2018). (**a**) Planula per coral and daily release rate (mean ± SD), and (**b**) composition of planulating corals, with the color-coded bars representing each of the seven parental polyps included in the study. Note: Broad bars indicate values averaged over the weekend, as larvae were monitored from Monday to Friday; no larvae were released on 2nd, 3rd, 9th, 26th, 30th, 31st of October 2018.

2.3.2 Larval features and behaviour

Larvae were 905 ± 114 μm in length, 371 ± 48 μm in width (n = 12), with a body shape that varied between cylindrical, elongated and curved within minutes when swimming. A teardrop-shaped form was acquired when the apical side was in contact with the substrate.

Histologically, the larvae featured the typical bilayered tissue with a uniformly ciliated (ci) epidermis (ep), a thin layer of mesoglea (m), and an endodermis (en) with mesenterial filaments (me) which attach to the pharynx (ph), i.e., the muscular throat

region (Fig. 4a, b). Like other cnidarian larvae, the aboral end likely holds the sensory organ (or the apical organ), being a pseudo-stratified epidermis (pse) with sensory cells that detect the exogenous chemical cues for settlement (Fig. 4a). On a total of 25 larvae, the pharynx at the oral end connected the blastopore/oral pore (*) (Fig. 4b) with the gastrovascular cavity opening (gco) (Fig. 4c).

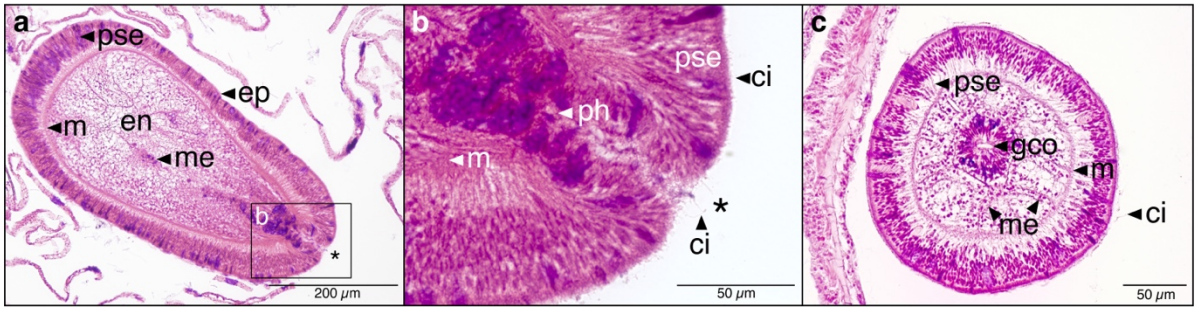

Figure 4: Haematoxylin-eosin-stained longitudinal (**a**, **b**) and transverse (**c**) histological sections of two larvae inside a polyp of *Caryophyllia huinayensis*. (**a**) Planula showing the epidermis (ep), the pseudo-stratified epidermis (pse), a thin layer of mesoglea (m), and the endodermis (en). Note that the mesenterial filaments (me) are attached to the pharynx (ph), which in turn is connected to the blastopore/oral pore (*), shown in detain in (**b**). (**b**) Detail from (**a**) showing a ciliated (ci) oral pore connected to the pharynx. (**c**) The gastrovascular cavity opening (gco) and the uniform ciliated epidermis are visible.

During the first two days after release, most larvae swam near the water surface, but for the remainder of the larval period they swam mainly near the bottom, where no benthic crawling was observed. Swimming occurred in the apical direction with a superimposed counterclockwise rotation, so that the planula moved forward in a corkscrew-like manner with a swimming velocity of 1.18 ± 0.4 mm s^{-1} (n = 12). Attachment was sometimes followed by detachment until successful settlement and subsequent metamorphosis. If temporary attachment occurred, the planula detached after a maximum of 24 h and started its searching behaviour again. The planktonic stage lasted 8 ± 9.3 d (Stage 1, Fig. 5a) when settlement surfaces were preconditioned. However, larvae exposed to non-preconditioned surfaces had a longer PLD, 26.7 ± 2.1 d (n = 4). Three of four of these eventually settled, and one died after 29 d without settling. Larvae attached on coverslips near microscale topographic features, such as silicon ridges or cracks in the coverslip glass. In all cases, settlement was limited to the overhanging surfaces, although larvae released into the holding tank settled on both the floor and walls.

2.3.3 Metamorphosis and post larval development

The time of each metamorphic stage was calculated based on the number of days since larval attachment. After attachment to the substrate, larvae flattened (Stage 2, Fig. 5b), whereupon the blastopore/oral pore (op) became visible as an oval opening (Stage 3, Fig. 5c). Stage 3 revealed the six body divisions (mesenteries), characteristic of the sixfold symmetry in the body plan of Hexacorallia. Six pairs of primary proto-mesenteries, the protocnemes (*sensu* Duerden (Duerden 1904)), divided the polyp radially in the longitudinal plane, extending from the aboral base to the oral pore and pharynx (Fig. 5d; I–VI). Of these protocnemes, four were incomplete, as were the corresponding divisions (Fig. 5d; V, VI in red). In Stage 4, the divisions of the protocnemes were more developed and alternately formed three pairs of entocoel (Fig. 5f; black arrowheads) and exocoel chamber (Fig. 5f; white arrowheads). At this stage, larvae settled and the ectoderm and the endoderm formed the bilayered tissue (bt) (Fig. 5f). In Stage 5 (2 ± 1.5 d), the first set of tentacles, called endotentacles (Fig. 5g; black arrowheads), appeared on the wall of the entocoel chamber as white nodular tissue formed around the oral pore. On the aboral side, the directional mesenteries (dm) were observed as four whitish branches connected to the endotentacles, which could contract (Fig. 5h). In Stage 6 (5 ± 2.1 d), the second set of tentacles, the exotentacles occurred on the wall of the exocoel chamber (Fig. 5i). The 12 tentacles (endo- and exotentacles) developed an acrosphere (acr), i.e., globular tip rich in cnidae (stinging organelles) (Fig. 5i, k, m). At this stage, the first skeletal elements of the basal plate (bp) formed along the periphery of the polyp and extended radially inwards along the six primary septa, the endosepta (eds) delimiting the entocoel chamber (Fig. 5j). At Stage 7 (21 ± 12.9 d), acrospheres were well developed and the tentacles could be extended to catch food (*A. persimilis*-nauplii (ap)) (Fig. 5k). The basal plate and primary septa thickened, resulting in a lateral fusion of the two. The second set of exosepta (exs) appeared (Fig. 5l), and the U-shaped columella (col) protruded from the centre of the basal plate (Fig. 5l). At this stage, in three of the eight recruits, the crystals grew in different directions, which created an opaque layer, impairing the observation of the columella and the primary and secondary septa (Fig. 6). Also, at this stage the bilayered tissue (bt), the endoderm and ectoderm layers, left

the base (b) uncovered (Fig. 5l), in contrast to the former stage (Fig. 5j). In Stage 8 (153 ± 30.6 d), the first and the second set of tentacles had visible nematocyst in the form of white packages surrounding the tentacles, and the third set of tentacles appeared between the exotentacles and entotentacles (Fig. 5m, black arrowheads). The bilayered tissue again covered the base (Fig. 5n). In Stage 9 (895 ± 45.9 d), the fourth set of tentacles developed, leading to a total of 24 tentacles (Fig. 5o). The basal plate thickened, the entocoelic septa and columella merged (Fig. 5p), and the bilayered tissue retracted from the base again (Fig. 5p). No post-settlement mortality was observed during the 3.1-year study.

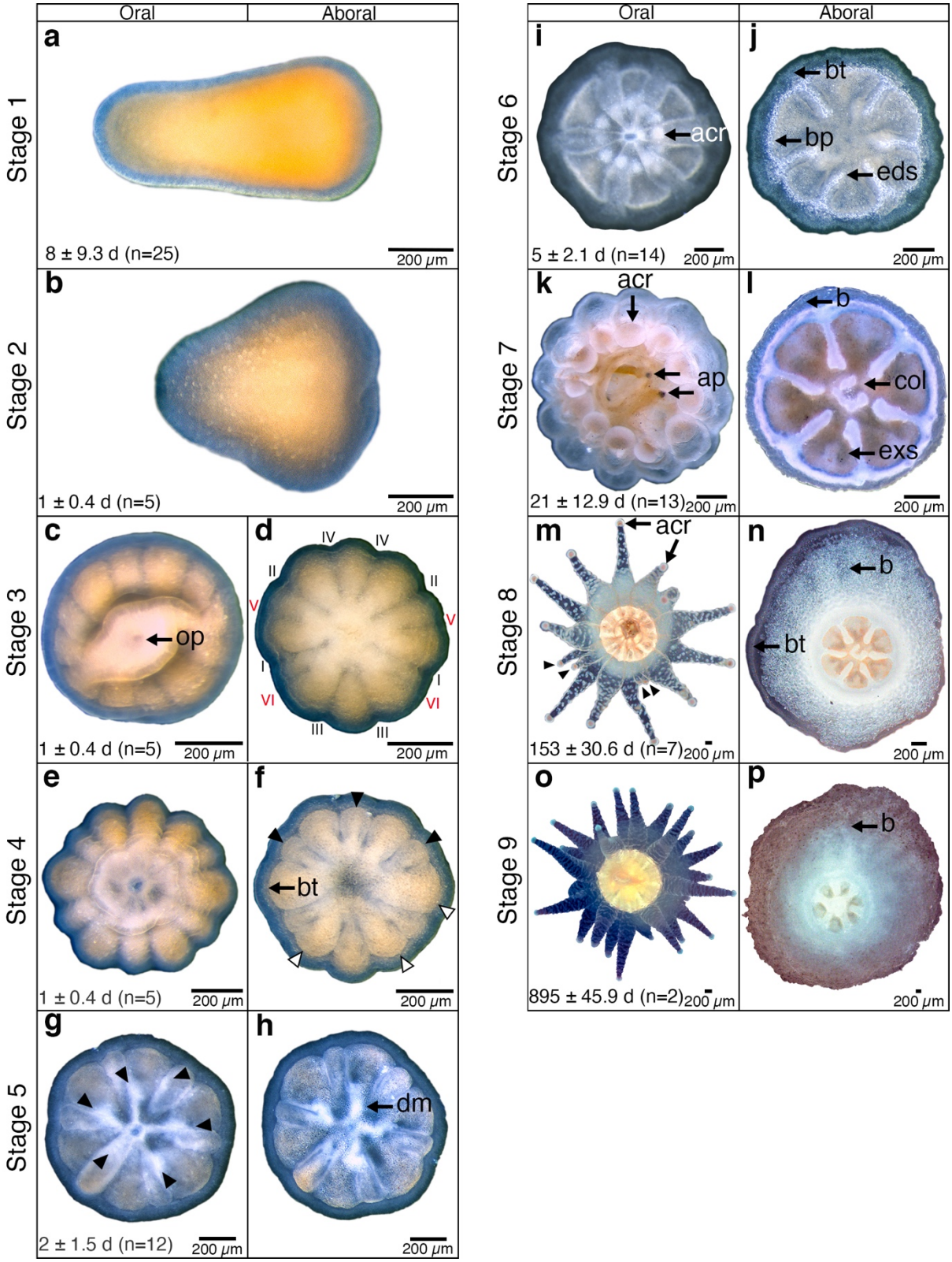

Figure 5: *Caryophyllia huinayensis* from larva to juvenile polyp (compiled from three recruits) observed under a stereomicroscope. Columns indicate the perspective (left oral/right aboral), and rows show the number of days (mean ± SD) from attachment to reach the respective stage. For description of Stages 1–9, see main text. acr: acrosphere, ap: *A. persimilis*-nauplii, b: base, bp: basal plate, bt: bilayered

tissue, col: columella, dm: directive mesenteries, eds: endosepta, exs: exosepta, op: oral pore. In all photographs, the background was replaced with white for better visualization (free-form selection).

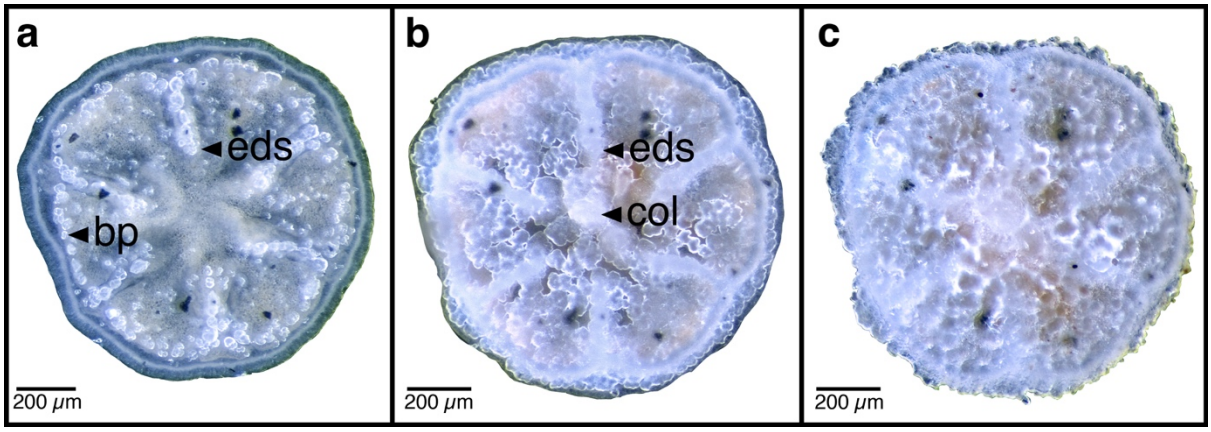

Figure 6: Aboral side of a settled *Caryophyllia huinayensis*; (**a**) 6 d, (**b**) 32 d and (**c**) 84 d after settlement. Skeletogenesis begins with the formation of a basal plate ring and the endosepta (**a**), and light scattering of the growing crystals result in an increasingly opaque appearance (**b**). Finally, the first set of endosepta is barely visible and the first set of exosepta is no longer visible, nor is the columella (**c**). All images were taken from the same coral and the background was replaced with white for better visualization (free-form selection). bp: basal plate, col: columella, eds: endosepta.

2.4 Discussion

The solitary cold-water scleractinian *C. huinayensis* is described here as a brooder. Although reproduction in scleractinian CWCs is still poorly known, no other temperate species has yet been described to brood larvae. The solitary temperate CWC *D. dianthus* (Feehan et al. 2019), as well as the temperate colonial CWC *D. pertusum* (Waller and Tyler 2005; Brooke and Järnegren 2012; Pires et al. 2014), *M. oculata* (Waller and Tyler 2005; Pires et al. 2014) and *O. varicosa* (Brooke and Young 2003) reproduce by broadcast spawning. Brooding has only been reported in subpolar and polar solitary CWCs from the Southern Ocean (Waller et al. 2008; Pendleton et al. 2021).

Although quantitative data on the number of larvae released in the four Southern Ocean brooders are lacking, a potential number of larvae released per polyp

can be inferred from their maximum fecundity (Table 1). *C. huinayensis* appears to be in the lower range of larvae production (6.5 ± 11.4 month^{-1} larvae), when compared its larval size (750–1,080 *µ*m length) with *Balanophyllia malouinensis* larvae (> 600 *µ*m, Table 1).

Thorson's rule (Thorson 1957; Mileikovsky 1971) states that organisms at higher latitudes tend to produce larger and fewer offspring and are frequently brooders. However, the brooding *C. huinayensis* appears to defy this rule, as it occurs at mid-latitudes (36° and 48.5° S (Cairns et al. 2005; Häussermann and Försterra 2007)). Though the phylogeography of *C. huinayensis* is not yet clear, six other solitary species of the genus *Caryophyllia* are endemic to Antarctica (Cairns 1982), suggesting that the genus may have originated in the Southern Ocean, with the mid-latitude distribution of *C. huinayensis* making the downstream end dispersal via the cold Humboldt Current branching off the Southern Ocean. In our case, Thorson's rule does not seem to be a good predictor of the macroevolutionary patterns and reproductive mode in *Caryophyllia*.

A better explanation can be inferred from Kerr et al. (2011). Their phylogenetic study on scleractinians revealed that the change from spawning to brooding (or *vice versa*) is based on the sexuality of the corals (i.e., gonochoric or hermaphroditic) and not on latitudinal distribution. The main pathway is from gonochoric spawners to gonochoric brooders, then to hermaphroditic brooders, and finally hermaphroditic spawning, which is the dominant reproductive mode in shallow-water corals.

The results of our study indicate that *C. huinayensis* reproduces throughout the year, albeit with large temporal variations in the number of larvae released. However, the fluctuations were not seasonal. This may be due to the fact that the aquarium for this experiment lacked external timing signals (zeitgebers) usually found in the field, i.e., there were no fluctuations e.g., in water temperature, food frequency, food quality, or salinity, which might otherwise have synchronized the corals' internal clock. Although, it is not yet known if the local *C. huinayensis* population exhibits seasonality in their larval release, the lack of larvae in April 2021 could also be due to poor internal fertilisation success based on the quality and/or quantity of sperm released (which was never observed).

If there is no seasonal release of larvae from the natural coral population, this may indicate that rapid recolonisation is possible throughout the year following a disturbance. Substrate alterations are usually observed in the Patagonian fjord region, where strong physical disturbances such as landslides occur (Sepúlveda et al. 2011), due to precipitation and earthquakes (Försterra 2009). Also, hypoxia events (< 2 ml l^{-1}) caused by pulses and subsequent degradation of terrestrial and marine organic matter (e.g., phytoplankton blooms) (Breitburg 2002; Silva and Vargas 2014) are common in the fjords (Silva and Vargas 2014), negatively impacting the benthic life, but promoting new available space for settlement. These events may be exacerbated in time and space by salmon farming activities, as bacterial respiration during the degrading of uneaten food pellets or salmon faeces (Burt et al. 2012), decreasing the oxygen concentration and thus reduces the likelihood that recolonisation can take place at a natural rate after hypoxic events.

On the one hand, brooding in *C. huinayensis* with subsequent release of well-developed larvae throughout the year has the advantage of rapid settlement, reducing the likelihood of drift to unfavourable locations and die-off (Szmant 1986). On the other hand, a high dispersal potential has a positive effect, as larvae can spread to new habitats with better conditions. Therefore, stable and suitable environmental conditions at a site, with occasional disturbances that expose substrates are favourable for brooder with short larval dispersal, as has been shown for *C. huinayensis*. However, if environmental conditions vary, longer-dispersed larvae may have an advantage. Different reproductive approaches were observed in two brooding tropical *Agarcia*-species from a reef off Curaçao, where *A. humilis*—which occurs in shallow waters subject to physical and biological disturbance—has many small larvae throughout the year. In contrast, *A. agaricites* that thrives in deeper and less disturbed areas, has few but large larvae, which are released only in spring/summer (Van Moorsel 1983). While the low fecundity and narrow time window for reproduction limit the species' capacity to colonise new available substrate, the disadvantage is compensated by the larger size and, hence, long-lasting energy reserves of the larvae, promoting higher dispersal.

As access to natural CWC populations is difficult and the release of offspring can rarely be observed, it is difficult to establish a link between reproduction and

environmental cues. However, Maier et al. (2020) conducted a transplantation experiment with *D. pertusum* at Nakken reef, Norway, determining that gametogenesis is supported by lipids obtained during spring, profiting from increased phyto- and zooplankton abundance at this time. The coral then rebuilt the tissue reserves in autumn, probably related to the spawning season (late January to early March) (Brooke and Järnegren 2012).

Spawning during the winter season was observed for the actinia *Corynactis* sp. (Häussermann and Försterra 2015) and suggested for *D. dianthus* (Feehan et al. 2019) and the octocoral *Primnoella chilensis* (Rossin et al. 2017), all from Comau Fjord. This period coincides with the seasonal temperature minimum (Garcia-Herrera et al. 2022) at the sampling depth of *C. huinayensis*. It is thus conceivable that the change in water temperature initiates gametogenesis, while increasing food availability in early spring fosters the development and release of brooded planulae. The peak of released larvae of *in vitro*-reared *C. huinayensis* (June–December 2018, Fig. 2c) matches the reproductive season of *D. dianthus* and *P. chilensis*. Although water temperature and food supply were kept constant in our laboratory study, an endogenous clock can be suspected as a pacemaker for reproduction that the adult polyps collected in the field “remembered” but run out of phase due to the lack of an external natural stimulus, which may explain the observed variability in planulation (Fig. 2c).

The swimming behaviour of *C. huinayensis* larvae in the first days was similar to that of *O. varicosa* (Brooke and Young 2005) from an *in vitro* experiment, in which the larvae spent two to four days at the water surface and three weeks in the lower water column before metamorphosing. Likewise, *D. pertusum* larvae remained at the water surface for the first two weeks before bottom-probing 3–5 weeks after fertilization (Larsson et al. 2014). Translating the *in vitro* observations of *C. huinayensis* larvae to the field, this might indicate that the two days of swimming upwards and being pelagic do not provide much potential for dispersal. However, the strong tidal currents of the photic zone (Försterra 2009; Sobarzo 2009) could significantly increase their dispersal. It should be noted, however, that in Comau Fjord a strong halocline at around 10–15 m depth probably prevents the larvae from swimming up to the brackish surface layer (7 to 31 salinity) (Försterra and

Häussermann 2003; Cairns et al. 2005). This however needs to be verified, as larvae of *D. pertusum* are able to survive at a salinity of 25 (Strömberg and Larsson 2017).

One of the forces governing connectivity between coral populations is thought to be related to the planktonic stage, though not solely based on larvae locomotion. At 1.18 ± 0.4 mm s^{-1}, the swimming velocity of *C. huinayensis* larvae is within the range of other CWCs (Table 1). The determined swimming speed of *C. huinayensis* is, however, 1–2 orders of magnitude lower than the tidal current velocities recorded at the vicinity of coral populations in Comau Fjord (5 cm s^{-1}, maximum 15 cm s^{-1}) (Laudien et al. 2021). Hence, horizontal dispersal is likely dominated by drift, as in other planktonic larvae, and the range is largely determined by the PLD ended by settlement. Former studies found that larvae released from brooders can settle within hours or a few days (Harrison and Wallace 1990), as the larvae are released at an advanced stage of development and may therefore already be competent to settle. In contrast, the entire larval stage of broadcast spawners occurs in the water column. These contrasting reproductive modes may result in different patterns of larval dispersal. For the broadcast spawners O. varicosa, the PLD is 42 d (Brooke and Young 2003), whereas for D. pertusum (where PLD was not yet described) a PLD of eight weeks made the dispersal modelling done by Fox et al. (2016) match the genetic population structure better than other models, indicating a PLD of eight weeks plausible. Thus, the potential of local settlement of these two species can be considered low due to the relatively long planktonic phase, in contrast to the 8 ± 9.3 d for *C. huinayensis*. However, studies on both sides of the Atlantic have shown a constrained genetic connectivity in *D. pertusum* between the two sides. In an investigation near Oslofjord, Norway, Dahl et al. (2012) showed that restricted connectivity also applies to populations of *D. pertusum* at a local scale. Likewise, Morrison et al. (2011) observed significant genetic differences between populations of the Gulf of Mexico and populations of the West and East Atlantic Ocean, though there is high connectivity within the regions. Populations on the European continental margin and in isolated fjords showed moderate levels of gene flow (Le Goff-Vitry et al. 2004). A microsatellite study on populations from Comau Fjord found no vertical or horizontal genetic differences and concluded that the local population of *D. dianthus* is panmictic (Addamo et al. 2021, 2022). Based on the strong tidal current in Comau Fjord, which

may transport larvae both vertically and horizontally, and the relatively short planktonic phase of *C. huinayensis* (8 ± 9.3 d), the population of *C. huinayensis* may also be panmictic. However, genetic analyses would have to be carried out to elucidate the population structure of the species to be able to assess the degree of connectivity among the populations. Overall, the levels of connectivity between coral populations appears to be the interaction between large-scale currents, local environmental conditions and the species-specific reproductive modes.

Table 1 Larval features of scleractinian CWC species.

Species	**Larval length (μm) min. – max.**	**Swimming velocity (mm s^{-1}) min. – max.**	**Maximum fecundity Oocyte per polyp (mean ± SD)**	**Reproductive mode**	**Formation**	**Geographic distribution***	**Reference**
Balanophyllia elegans	3,000–5,000	0.004–0.006	n.d.	Brooder	Solitary	Northeast Pacific	Fadlallah and Pearse (1982); Gerrodette (1981)
Balanophyllia malouinensis	> 600	n.d.	241 ± 181	Brooder	Solitary	Sub-Antarctic	Pendleton et al. (2021)
Caryophyllia huinayensis	750–1,080	0.35–1.18	n.d.**	Brooder	Solitary	Chile	This study
Caryophyllia smithii	800–1,000	*ca.* 0.017–0.05	n.d.	Broadcast spawner	Solitary	Atlantic Ocean, Mediterranean sea, Indo-West Pacific	Tranter et al. (1982)
Desmophyllum pertusum	120–270	0.29–0.86	3,146 ± 1,688	Broadcast spawner	Colonial	Cosmopolitan	Larsson et al. 2014; Waller & Tyler 2005
Flabellum angulare	2,000–3,000	n.d.	550	Broadcast spawner	Solitary	Eastern Central Pacific, Northeast Atlantic	Mercier et al. (2011)

Flabellum curvatum	n.d.	n.d.	1,618 ± 1,071	Brooder	Solitary	Antarctic, Southwest Atlantic, Southeast Pacific	Waller et al. (2008)
Flabellum impensum	n.d.	n.d.	1,270 ± 884	Brooder	Solitary	Antarctic	Waller et al. (2008)
Flabellum thouarsii	n.d.	n.d.	2,412 ± 1,554	Brooder	Solitary	Antarctic, Southwest Atlantic	Waller et al. (2008)
Oculina varicosa	217	1.6	1,000–4,800 (cm^{-2} colony)	Broadcast spawner	Colonial	Western Central Atlantic	Brooke and Young (2005); Brooke and Young (2003)

Note: n.d. = no data. *According to Palomares and Pauly (2022) .**Publication in preparation.

When the settlement surfaces in the holding tank were allowed to grow biofilms two weeks before the start of the settlement trial, 48 % of the larvae settled within one to three days. In contrast, if the surfaces were not pre-conditioned, the PLD extended up to 28 d with an average of 26.7 ± 2.1 d (n = 4). Although the number of larvae able to extend the PLD in this study is too low to draw any robust conclusions, this could nevertheless indicate that the biofilm plays a role as a cue for settlement in *C. huinayensis* larvae. This observation is supported by Webster et al. (2004), indicating that biofilms may outstrip the importance of other settlement cues (e.g., coralline algae) in shallow-water corals from the Great Barrier Reef.

Our results may imply that *C. huinayensis* larvae are able to extend their PLD when, for example, an appropriate substrate is unavailable. Consequently, PLD extension requires either energy stores (lecithotrophic larvae) or feeding (planktotrophic larvae), as shown for *D. pertusum* larvae. Here, larvae can feed on picoplankton by ciliary feeding or scavenging on mucus strings (Strömberg and Larsson 2017). Although feeding of *C. huinayensis* larvae was not determined in this study, two lines of evidence suggest planktotrophy: the PLD may be long (26.7 ± 2.1 d), suggesting storage-independent development. More importantly, the histological

cuts of 25 larvae showed a well-developed oral pore which connects to the pharynx through the gastrovascular cavity opening (Fig. 4), which may indicate a developed gastrovascular system.

Field studies on *C. huinayensis* from Comau Fjord showed high coral abundance (2,211 ± 180 ind. m^2) at 25 m water depth on a substrate inclination between 60° and 80°, but no individuals on horizontal substrate surfaces (Wurz 2014). This pattern was attributed to sedimentation, where the horizontal seafloor is smothered by inorganic terrigenous particles derived from river run-off (Försterra and Häussermann 2003; Cairns et al. 2005) and/or by organic matter from intense salmon farming in Comau Fjord (Häussermann et al. 2013) (such as fish faeces and uneaten food pellets passing through the salmon cages) (Cubitt et al. 2008; Buschmann et al. 2009). Inclined surfaces, by contrast, are too steep for the sediment to accumulate. Based on the fact that the observations in this study were carried out in sediment-free artificial sea water, this demonstrates that settlement on horizontal surfaces can occur, supporting the assumption that the distribution pattern of *C. huinayensis* in the field is likely conditioned by sedimentation.

As opposed to most larvae of shallow-water scleractinians, the larvae of *C. huinayensis* lack photosynthetic endosymbionts, so that they depend entirely on heterotrophy and/or their energy reserves. Anyhow, we observed a similar structuring and timing of tissue and skeletal development in *C. huinayensis* as in the tropical corals *Galaxea fascicularis* and *Acropora brueggemanni* (re-described as *Isopora brueggemanni*) (Atoda 1951a, b). Within the first three days after settlement, all three coral species developed four pairs of mesenteries, which reached the stomodaeum, while two pairs did not (Fig. 5d). Moreover, the first endotentacles (2 ± 1.5 d, Fig. 5g) and the second exotentacles (4 ± 2.1 d, Fig. 5i) appeared at the same time and place in all three species. Similarly, the first crystals and crystal structures of the basal plate ring and the endosepta were precipitated (4 ± 2.1 d, Fig. 5i). These similarities suggest that early development in *C. huinayensis* is highly conserved, whether the energy costs invested during metamorphosis and juvenile growth are covered by internal energy reserves or heterotrophic feeding, or a combination of both. Although no studies have addressed the relationship between internal lipid and protein reserves with growth rate during the early growth stages in CWCs, it has been observed in the

facultatively mixotrophic *O. varicosa*, where deep azooxanthellate colonies, subsisting on both energy reserves and exogenous food, grew at a higher rate than zooxanthellate shallow-water colonies (Reed 1981). This indicates that under certain conditions a heterotrophic diet may be energetically better that a mixotrophic diet.

This study was the first to describe the metamorphosis of a temperate scleractinian cold-water coral, using *C. huinayensis* as the model species. Our results show a similar ontogenetic timing from planula to juvenile polyp in *C. huinayensis* as described for tropical corals, suggesting a highly conserved evolutionary mechanism in spite of large environmental (e.g., temperature) differences.

The CWC *C. huinayensis* showed a peak in larval release *in vitro,* that coincided with the low temperatures and increased food availability at its site of origin, Comau Fjord, in austral winter. As the released larvae had a developed gastrovascular system, this could indicate a planktotrophic or mixed mode larvae, that may benefit from the increase of phyto- and zooplankton in austral spring. On the other hand, the short PLD may have the advantage of feeding immediately after settlement by offsetting the high energy costs during metamorphosis, allowing a rapid onset of skeletogenesis.

Climate change influences seasonal environmental variability by enhancing water stratification, reducing the depth of the mixed layer and water circulation, which combined, reduces the productivity of phytoplankton and consequently of the zooplankton (Seifert et al. 2020). Overall, it can alter the phenology of organisms, i.e., timing of their seasonal activities (Walther et al. 2002). Our study showed that *C. huinayensis* displays a moderate phenology, which could be a consequence of the lack of environmental variability in the aquarium, indicating the ability of *C. huinayensis* to acclimatize to new environmental conditions. However, if the phenology of this coral is pronounced in the field, the expected changes in food availability would not match the observations in the aquarium. On the contrary, lower energy uptake could therefore affect reproductive capacities, larval survival, metamorphosis and growth, impairing the connectivity and thus population stability of this species.

2.5 Materials and Methods

2.5.1 Collection of specimens

A total of 169 adult individuals of *C. huinayensis* with a length of 8.3 ± 2.0 mm and a diameter of 7.9 ± 1.4 mm were collected in 2014, 2015, and 2019 by SCUBA diving between 20–30 m water depth in X-Huinay (42° 23.213' S; 72° 27.772' W), Comau Fjord, Chile (Fig. 7). For a detailed description of the study area see Beck et al. (2022), Rossbach et al. (2021) and Sobarzo (2009). Of these corals, 60 were preserved in 4 % buffered (sodium borate) formalin seawater solution for histological analysis. The remaining corals were transported alive in plastic bags filled with one-third with seawater and two-thirds with pure oxygen to the Alfred Wegener Institute in Bremerhaven, Germany.

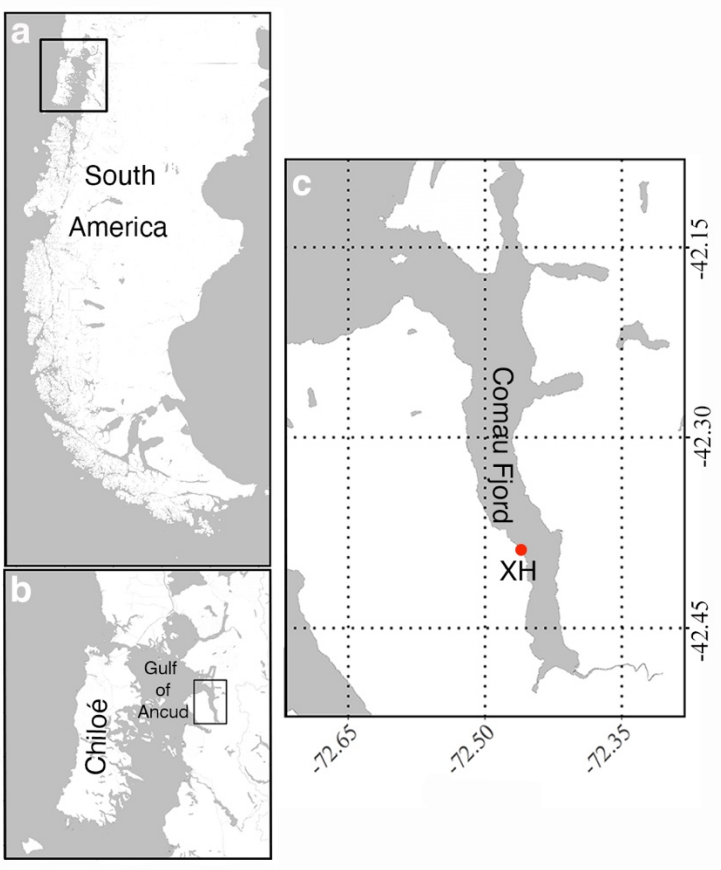

Figure 7: *Caryophyllia huinayensis* collection site. (**a**) Overview of the Patagonia. Black rectangle denotes the area in **b.** (**b**) Chiloé island and Gulf of Ancud with Comau Fjord (black rectangle). (**c**) Comau Fjord with the collection site X-Huinay (XH), where corals were sampled (red dot).

2.5.2 Maintenance specimens

After arrival, the live corals were glued to plastic screws (Fig. 8a) using Preis Easy Glue Underwater (Preis Aquaristik KG, Bayerfeld, Germany), and placed in a 285 L closed-circuit holding tank with artificial seawater (Dupla Marin Premium Reef Salt, Dohse Aquaristik, Grafschaft-Gelsdorf, Germany), which had similar characteristics to those at the sampling site and depth, analogous to the study of Laudien et al. (2021) (see their Suppl. M. 1). The aquarium was connected to a large tank (80 L) with a water flow of 5–10 L min^{-1}, in which an aquarium pump (Turbelle® stream 6105, Tunze Aquarientechnik Gmbh, Penzberg, Germany) ensured a counterclockwise current of 2.15 ± 1.03 cm s^{-1} with discrete eddies and vortices. The salinity of the UV-light treated seawater of 31.7 ± 0.6 was maintained at 11.5 ± 0.8 °C with a pH of 7.9 ± 0.1 (WTW conductivity meter, ProfiLab24 GmbH, Germany), and an oxygen concentration of 100 % saturation. The total alkalinity (TA) of the seawater was analysed once a week and measured according to Dickson et al. (2007). Aragonite saturation state (Ω_{arag}) was maintained at 1.7 ± 0.4 and calculated from pH, TA, salinity, and temperature using the program CO2SYS (Lewis et al. 1998). Immediately before the weekly water exchange, nutrient concentrations (nitrate, nitrite, phosphate, and ammonium) were determined using a photometric test (Spectroquant® test, Merck KGaA, Darmstadt, Germany).

The diet consisted of live *Artemia franciscana*-nauplii and *A. persimilis*-nauplii (*ca.* 1,200 ind. l^{-1}) three times a week and one thawed juvenile krill (*Euphausia pacifica,* Zierfischfutterhandel Norbert Erdmann e.K., Ritterhude, Germany) per polyp once a week throughout the study period. As *C. huinayensis* populations also occur in the aphotic zone (Sellanes et al. 2008), it could be inferred that a light-dark cycle is not a direct environmental factor in the reproductive cycle of this species. Hence, corals were kept in the dark to avoid fouling by cyanobacteria and macroalgae on the aquarium walls, thus decreasing coral stress by reducing regular cleanings.

2.5.3 Collection, characterization, and settlement of larvae

To investigate the reproductive mode and larval released periodicity, seven adult polyps used throughout the study were placed in individual plastic cylinders fixed on horizontal plastic holders, and immersed in the holding tank to allow retention and collection of larvae (Fig. 8a). Thanks to the translucent tissue, planulae were observed in the tentacles and gastrovascular area, which were collected at the time of release into the cylinders with a plastic pipette (3 ml) and counted twice a day from Monday to Friday to calculate the production rate of each individual polyp. A total of 27 flow-through glass cubes of 2 × 2 × 2 cm (Fig. 8b) were utilized for larval characterization and for the description of metamorphosis. The cubes consisted of four coverslips oriented parallel to the water flow and two 100 μm mesh screens intercepting the flow at the upstream and downstream face of the cube. The coverslips were glued with silicon (Silexo, Juwel Aquarium AG & Co. KG, Germany). To describe the larval behaviour, i.e., planktonic stage, 3–8 larvae were placed in two cubes and kept there until all larvae attached to the substrate. To determine the possible influence of natural biofilm on the substrate on larval settlement, seven cubes were left in the holding tank for at least 15 days before introducing 3–8 larvae, and four cubes were inserted into the tank at the same time as 3–8 larvae were introduced into them. Swimming velocities were calculated from video tracking of 12 larva inside the cubes. Video clips (3–10 seconds) recorded with a Nikon D7000 DSLR and a 60 mm lens at 24 fps were played frame by frame (spatial resolution of 1,920 × 1,080 px) and the displacement of the center of the planula between frames was recorded to the nearest 0.1 mm. A scale bar was placed next to the cube for calibration. Furthermore, a total of 12 larvae were photographed to determine their length and width using Adobe Photoshop® CC (San Jose, California, USA).

Fourteen cubes with 3–8 larvae inside were used to describe the metamorphosis and growth of juveniles. Larval attachment was considered successful if the diameter of a larva doubled in one day. Thereafter, the cube was disassembled and the settled recruit was placed in a respective glass petri dish (6 cm ø) to allow handling of the recruit without air exposure. Unsettled larvae from the cubes were released into the holding tank.

Metamorphosis and post-larval development stages were documented by inverting the coverslip in the glass Petri dish and taking photos at the oral and aboral poles of the polyps. To prevent crushing of the inverted polyp, a smaller Petri dish (0.5 cm height, 2 cm ø) holding the coverslip with the polyp facing downward was used as a spacer. Photos were taken daily for the first two weeks, then once a week for three years. The photos were taken from the same distance and angle using a Leica camera (IC80 HD; Wetzlar, Germany) connected to a stereomicroscope (Leica MZ 16, Wetzlar, Germany).

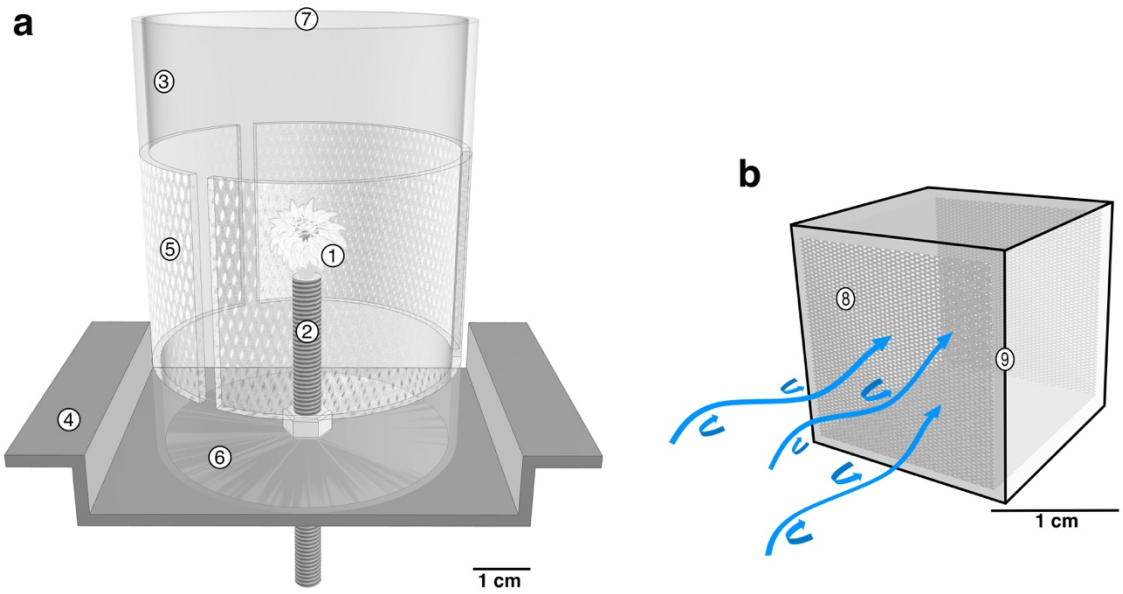

Figure 8: Schematic drawing of the (**a**) cylindrical plastic container and the (**b**) flow-through cube in the holding tank. (**a**) Reproductive polyp (1) glued onto a polyethylene screw (2), and placed in a cylindrical (7.2 cm high, 5.4 cm ø) plastic container (3), which was screwed onto a plastic holder (4). The plastic container had three side windows covered with mesh (100 μm) (5) to allow water exchange. A closed bottom (6) and an open top (7), which rose 1 cm above the water surface ensured retention of larvae. (**b**) Larvae collected from the container were placed into a cube with the upstream and downstream side covered with a 100 μm mesh (8), whereas the top, floor and walls consisted of coverslips glued with silicone (9, black line). Blue arrows indicate the direction of the water flow with eddies and vortices.

2.5.4 Histology

The 60 corals preserved in Formalin were decalcified in Rapid Bone Decalcifying solution (Thermo Scientific™ Shandon™ TBD-1™, Tudor Road, UK) for

30 minutes to dissolve the skeleton. For dehydration, the skeleton-free tissue was placed in 70–100 % ethanol, with 10 % increments every 1 h. Tissue was then immersed in Xylene twice for 1 h. The tissue was then transferred to paraffin wax (Polarit, Labortechnik Süsse, Hessen, German) in an oven at 60 °C, where it underwent four wax changes over a period of 2.6 h. After cooling, the wax blocks were cut into 3 μm thick sections, leaving a distance of 45 μm between sections, based on the mean width of the *C. huinayensis* oocyte nucleolus. The sections were then mounted on glass slides and stained with haematoxylin-eosin. Histological sections were examined under a Zeiss Axioscope microscope with an Olympus (DP70) camera mounted.

2.6 Acknowledgments

We thank Julian Bartsch, Anita Hartig, Paul Kluwer, Janis Müller and especially Esther Lüdtke and Ulrike Holtz for untiring assistance in the maintenance corals; the staff of Huinay Scientific Field Station for field support. The research is part of the Ph.D. project of T.H. at the University of Bremen, carried out at the Alfred-Wegener-Institut Helmholtz-Zentrum für Polar- und Meeresforschung (AWI). T.H., J.L. and C.R. were supported by AWI (PACES II, and 'Changing Earth – Sustaining our Future', Topic 4.2 and 6.1). T.H. received additional financial support by the National Geographic Society, Deutscher Akademischer Austauschdienst (DAAD), and Agencia Nacional de Investigación y Desarrollo (ANID), Chile. Drawings and images were created by T.H. Jonas Hagemann designed the schematic drawings in Fig. 8. Histological cuts and staining were performed by Petra Kohse-Kordes, Institut für Pathologie, Gesundheit Nord gGmbH, Klinikverbund Bremen, Germany. Specimens were exported from Chile under CITES permits 14CL000003WS, 14CL000014WS, 15CL000004WS, 19CL000015WS, and imported to Germany under permits E00154/14, E00095/15, E00725/15, and E08854/19. G.F. and V.H. gratefully acknowledge Fondecyt project No. 1201717. H.E.G. acknowledges additional support from Fondap-IDEAL 15150003.

3

Polyp dropout in a solitary cold-water coral

Jürgen Laudien[1], Thomas Heran[1,4], Vreni Häussermann[2,3], Günter Försterra[2,3], Gertraud M. Schmidt-Grieb[1], Claudio Richter[1,4]

[1] Alfred Wegener Institute Helmholtz Centre for Polar and Marine Research, 27515 Bremerhaven, Germany

[2] Huinay Scientific Field Station, Puerto Montt, Chile

[3] Pontificia Universidad Católica de Valparaíso, Facultad de Recursos Naturales, Escuela de Ciencias del Mar, Avda. Brasil 2950, Valparaíso, Chile

[4] University of Bremen, Bibliothekstraße 1, 28359 Bremen, Germany

Keywords: Cold-water scleractinia, *Caryophyllia huinayensis*, polyp detachment, polyp dropout, Chilean Fjord Region, asexual dispersal.

Published in ***Coral Reefs***, Springer, 40, 1657–1665. DOI: 10.1007/s00338-021-02148-0.

3.1 Abstract

Scleractinian corals feature both sessile and mobile stages and diverse modes of development. In some cases, development can be reverse. Examples include polyp detachment in response to environmental stress (bail-out or polyp expulsion) and reverse metamorphosis, where juveniles detach from the primary skeleton and revert to the mobile stage. Here, we provide aquaria and field evidence of a new form of reverse development: polyp dropout in the solitary cold-water coral *Caryophyllia huinayensis.* It features tissue retraction and detachment of an entire adult polyp from the skeleton in the putative absence of a stressor. The dropout polyp remains viable and continues to live for many weeks, albeit in a rather collapsed state lacking a well-developed hydroskeleton. We carried out a long-term (37 months) rearing experiment under constant aquaria conditions, and found polyp dropout in four out of 83 individuals. Detachment was accompanied by the extrusion of mesenterial filaments through perforations in the body wall. We believe this resulted in the loss of the hydroskeleton, which prevented the dropouts to subsequently resettle, or form a new skeleton. As opposed to other known forms of reverse development, the new form is not accompanied by reversible metamorphosis, abandonment of the colonial way of life, nor is it a survival or asexual reproduction strategy. We found field indications of polyp dropout in Patagonian field populations of *C. huinayensis*, where 1.4 ± 0.8 % (mean ± SD, N = 9,322) of the polyps of the natural population showed partial detachment indicative of imminent dropout in the putative absence of external impact. Polyp dropout is the first record of polyp detachment in a solitary CWC with possible repercussions for adult coral mobility, evolution and Stanley's (2003) 'naked coral' hypothesis.

3.2 Introduction

Corals are sessile animals with diverse modes of development, generally involving a mobile stage of dispersal, the planula larva, which later settles, undergoes metamorphosis and develops into the primary polyp (e.g., Richmond and Hunter 1990). Under environmental stress, development may become reverse. For example, a settled, calcified polyp may build back its radially compartmented body plan, reverse metamorphosis to become a mobile secondary larva, disperse with the currents and re-attach elsewhere (Richmond 1985). Reverse development may also affect the colony: through ontogenetic reversal, genetic programs specific to earlier stages are reactivated, leading to back-transformation to the previous morph (called "rejuvenation") resulting in resting developmental stages with inert metabolic functions (Piraino et al. 2004). Polyp detachment, including polyp expulsion and polyp bail-out, is another form of reverse development, where a sessile polyp abandons its initial structure and becomes mobile again, maintaining its biological organization. Both, polyp expulsion and polyp bail-out have been reported from shallow-water colonial scleractinians. Polyp expulsion is observed in physiologically healthy corals inhabiting chronically physically disturbed environments. Here, whole polyps, including their calices leave the colony to settle elsewhere (asexual reproduction). This process seems to be regulated by the colony (Kramarsky-Winter et al. 1997). Polyp bail-out, by contrast, refers to the escape of polyps without calices from a parent colony in response to acute environmental stress (e.g., Sammarco 1982; Kružić 2007; Capel et al. 2014; Serrano et al. 2018) and was also observed for octocoral species (Rakka et al. 2019; Wells and Tonra 2021). Thus, polyp bail-out provides a route of escape to new locations for possible resettlement. Additionally, fission (intratentacular budding), extratentacular budding (both with different modes), transverse division and asexual planula production have been reported for a number of tropical and temperate coral species as asexual reproduction modes (e.g., Cairns 1988; Tokuda et al. 2017), in some cases allowing the species to recover after external physical disturbance (Wilson 1979; Coppari et al. 2019). So far, the fragmentation of colony parts is the only reported asexual mode of dispersal in scleractinian cold-water corals (CWCs) (Wilson

1979; Le Goff-Vitry et al. 2004; Roberts et al. 2009; Dahl et al. 2012) and polyp detachment processes have not yet been described for solitary scleractinians.

Caryophylliidae are a diverse family of scleractinians with 269 species, colonizing water depths below 50 m (Roberts et al. 2009). *Caryophyllia huinayensis* Cairns et al. (2005) is a solitary, azooxanthellate member found in South Chile (36 °S to 51 °S) at water depths within the depth range 20-800 m (Fig. 1, Cairns et al. 2005; Sellanes et al. 2008). In spite of its small size (≤ 18.7 mm height and ≤ 8.7 mm calyx diameter) it is an important epibenthic component forming dense aggregations of up to 2211 ± 180 ind. m^{-2} on steep walls of fjords and channels between 16 and 265 m (Häussermann and Försterra 2007; Wurz 2014). In Comau Fjord, terrestrial runoff leads to a permanent halocline subjecting the corals at depth to hypoxic and hypercapnic conditions (Silva 2008; Fillinger and Richter 2013). As with most CWCs, very little is known about its biology and development. Here, the first field and aquaria observations of reverse development in a solitary, scleractinian CWC are reported: polyp dropout in *C. huinayensis*, where an apparently unstressed, adult, solitary polyp shows tissue retraction, autonomously detaches as a unit from its skeleton, and continues to live without calcium carbonate skeleton, with no visible fundamental modifications in its external body plan.

Fig. 1 *Caryophyllia huinayensis* at 21 m water depth (Comau Fjord, Southern Chile).

3.3 Materials and Methods

In February 2014, a total of 30 *C. huinayensis* specimens were collected by SCUBA divers from Comau Fjord (Patagonia, Chile). In March and May 2015, a second and third batch of 15 and 24 individuals were sampled, respectively. Specimens were chiselled off the substrate (~21 m water depth, photic zone) and shipped in oxygen-replete seawater to Germany. After arrival (< 35 h from dispatch), corals were visually checked for polyp activity, tentacle appearance and colour (0 % mortality) and maintained in two separate closed circuits (A and B; A: 30 individuals from 2014, B: 39 individuals from 2015) each filled with 285 litres of artificial seawater mimicking the Comau Fjord environment at the sampling site of the corals (Online supplementary material 1). Corals were reared in the dark to avoid aquaria contamination with algae/cyanobacteria and thus repetitive cleaning which may cause

stress. As populations of this species also occur in the aphotic zone (Sellanes et al. 2008) it is assumed that photoperiod is not of high importance for this species. The maintained corals were fed three times a week with live *Artemia franciscana*-nauplii and juvenile krill (one *Euphausia pacifica*/ind. × week) (Zierfischfutterhandel Norbert Erdmann e.K., Ritterhude, Germany). Each week, nutrient concentrations (nitrate, nitrite, phosphate, and ammonium) were determined photometrically (Spectroquant® test, Merck KGaA, Darmstadt, Germany) just before a third of the water in each circuit was exchanged. Deviations between the water changes were < 5 % of the respective target value.

During the study, adults of circuit A reproduced and 14 larvae settled on the aquarium glass in July 2015. The recruits (Calyx ∅ 2.3 ± 0.3 mm) were removed with razor blades without any visual damage, glued (Super Flex Glue Gel, UHU GmbH and Co KG, Bühl, Germany) on glass slides and maintained in circuit A. After this transfer they grew at a similar rate (3.4 ± 1.9 mm a^{-1}) as individuals *in situ* (Wurz 2014). This indicates good rearing conditions in the aquaria system.

Polyp appearance and activity were visually monitored on a daily basis. Based on that, polyps were classified to one of the following three stages. (1) Attached polyp–extended tissue in full contact with skeleton; (2) partially detached polyp–recession of tissue from lower to upper calyx and between septae and partial loss of contact of tissue with skeleton, with individual strands of tissue remaining; (3) fully detached polyp–complete loss of contact with skeleton, tissue sinking to the bottom. The detached polyps were kept in petri dishes (∅ 10 cm) submerged in the respective circuit and continued to be fed as specified above. Two of the detached polyps were inadvertently lost when cleaning circuit A five weeks after detachment, but one specimen (#3, circuit B) was monitored for more than seven months. Specimens were examined under a stereomicroscope biweekly to check for reattachment, skeleton precipitation and polyp activity. In order to calculate potential *in situ* dispersal by currents, the sinking rate of this specimen was determined in five runs, five weeks after the detachment by transferring it to a gridded 350 mm cylinder and estimating the time it took the specimen to sink to the bottom.

During austral winter 2019, spring 2019 and summer 2019/2020 a field study was conducted by SCUBA dives at Comau Fjord (Cross-Huinay North, 42°23’ 12.8’’

S, 72°27'46.3'' W and Liliguapi 42°9'43'' S, 72°35'55'' W) (3 seasons × 2 sites = 6 transects) to determine the proportion of *C. huinayensis* undergoing polyp detachment *in situ*. Photographs were taken with a digital camera (Nikon D7000 DSLR, 24 mm-lens, 19.5 cm × 29.6 cm frame) between 24 m and 27 m water depth along a horizontal 35 m-line transect in 1 m intervals. *C. huinayensis* individuals were counted and the polyps were classified into three stages of polyp detachment, described from the aquaria experiment: polyp attached; partially detached; fully detached.

3.4 Results and Discussion

This is the first report of reverse development in scleractinian CWC. Four out of 83 aquarium specimens (4.8 %), two in each circuit, dropped out and exposed the white skeletons of the corallites (Fig. 2d, Online supplementary material 2). Microscopic examination of the vacated skeletons indicated that no tissue remained on them. The two dropouts of circuit A were former recruits (see Materials and Methods, now adults), the two dropouts in circuit B were from wild corals. In one of the latter, the tissue began to recede twelve weeks before polyp dropout (Fig. 2, Online supplementary material 2, 3). An additional adult individual (circuit B) showed tissue recession, however, remained partially attached for ten weeks (Fig. 2b, Online supplementary material 2, 3). The other corals (A: n = 42, B: n = 36) remained attached. No unusual behaviour was observed neither before or after the event in any of the attached fellow corals, so that contamination or disease in the rearing system seems unlikely, as it would have affected more individuals.

The observed polyp dropout in the solitary *C. huinayensis* is considered to be an autonomous detachment of a previously unstressed polyp. It is preceded by tissue retraction and leads to detachment of the entire adult polyp which subsequently lives on without a calcium carbonate skeleton in an unattached state. No fundamental changes in the external body plan are apparent, the oral disc with the mouth and the tentacles as well as the mesenteries remain (Fig. 2a–c).

Polyp dropout differs from other reports of reverse development confined to stressed shallow-water colonial scleractinians in tropical, subtropical and temperate

environments in a number of ways (Table 1). In contrast to i) reversible metamorphosis (Richmond 1985) and ii) ontogeny reversal (Piraino et al. 1996; 2004), polyp dropout is not accompanied by fundamental changes in the body plan. Polyp dropout also differs from iii) polyp expulsion (Kramarsky-Winter et al. 1997) and iv) polyp bail-out (Sammarco 1982; Kružić 2007; Capel et al. 2014; Serrano et al. 2018). These are escape mechanisms of polyps from chronically physically disturbed (polyp expulsion) or acutely stressed disintegrating (polyp bail-out) colonies, resulting in dispersal and, after successful resettlement, asexual reproduction. The latter requires an adult and a reproductive product, but in the case of polyp dropout, the whole adult moves away from its skeleton and there is no reproductive product. In contrast to the polyp detachment processes described so far, polyp dropout occurs in the absence of abiotic or biotic stressors and does not appear to be related to reproduction (Table 1).

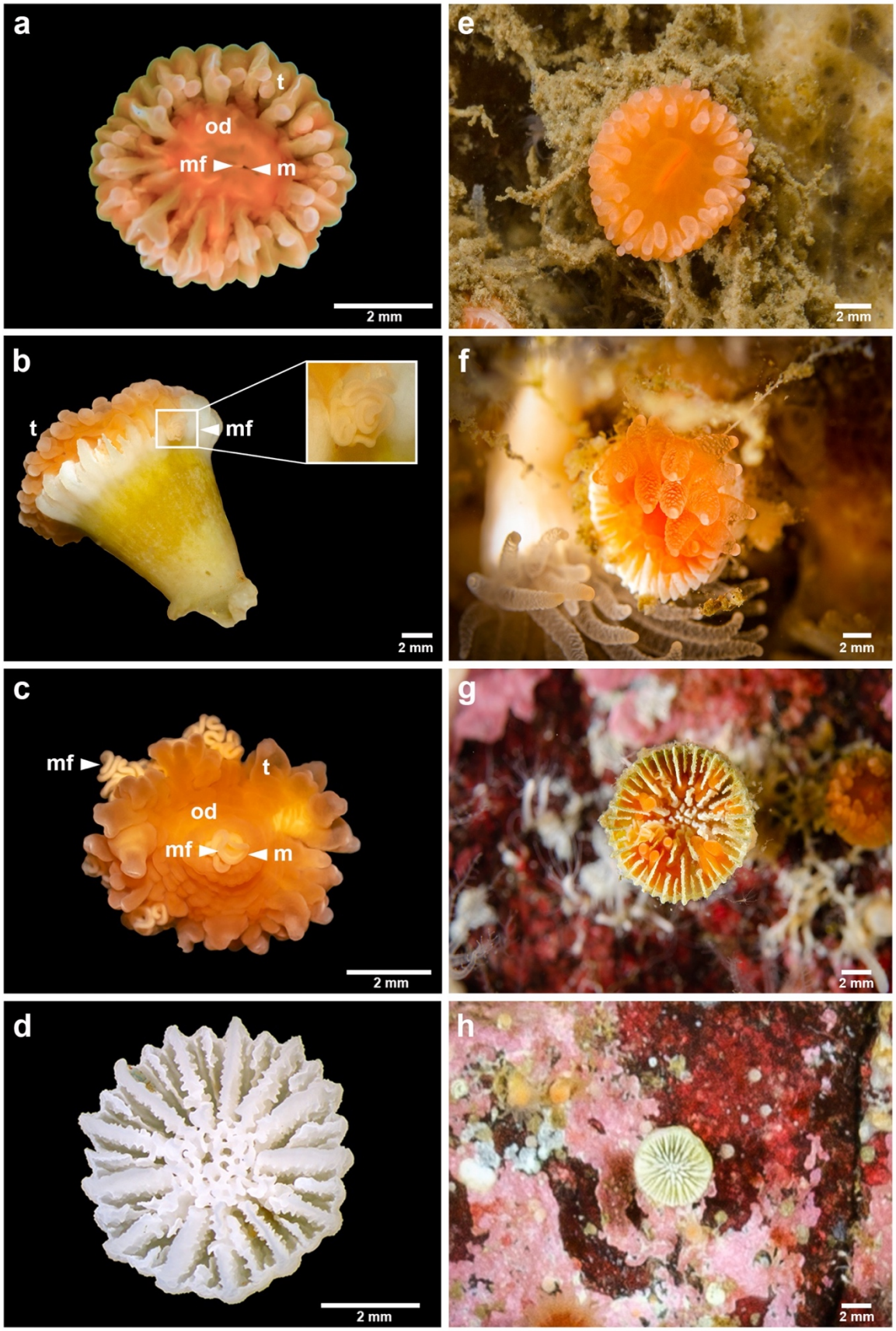

Fig. 2 *Caryophyllia huinayensis* maintained in the aquarium system before (a, b) and after (c) polyp dropout, leaving behind a denuded skeleton (d). Some mesenterial filaments are exposed (b, c).

C. huinayensis in situ (e–h) showing stages with receded tissue (f), exposed mesenterial filaments (g) and bare skeleton (h). In photographs a–d, the background was replaced with black (free-form select); for. Raw images, see Laudien et al. (2019), m: mouth, mf: mesenterial filaments, od: oral disc, t: tentacles.

The dropout polyps had a constricted appearance with mesenterial filaments protruded apically through the mouth, but also laterally through the body wall (Fig. 2c). While the apical exposure is not uncommon, the later feature is absent in attached specimens not least because of the barrier build by the calcareous skeleton. The behaviour of the mesenterial filaments (e.g., whether they can be retracted and the openings in the body wall can be closed again) cannot be described because a more detailed examination would have caused a disturbance for the polyp. Similar observations of protruded mesenterial filaments were reported for detached polyps of the tropical scleractinian *Mussa angulosa* (Goreau et al. 1971) and planula larvae of *Pocillopora damicornis*, when the formation of an organic film was prevented in an attempt to keep the larvae from settling (Richmond 1985). Also, some anemones expel filament ends (acontia) through body wall openings (cinclides) (Manuel 1988). The perforations of the coral body wall likely affected the hydroskeleton supporting the body and tentacles of attached polyps, causing the rather retracted state (Fig. 2c). It is also likely that the impaired hydroskeleton prevented the reattachment of the polyps. Accordingly, stereomicroscopical observations confirmed no signs of skeleton precipitation under the detached polyps within the four-week (circuit A) and seven-month (circuit B) observation period, respectively, similarly to the Mediterranean scleractinian *Astroides calycularis* (~ 12 weeks observation, Serrano et al. 2018). By contrast, a small portion of bailed-out polyps of the tropical coral *Seriatopora hystrix*, was able to initiate skeletogenesis as early as nine days after detachment (Sammarco 1982).

Table 1 Reported stressors causing polyp detachment in scleractinian corals and likelihood of their involvement in the observed detachment of *Caryophyllia huinayensis.*

Stressor	Species	Climatic zone	Reference	Probability for the present event	Justification
Low oxygen	*Seriatopora hystrix* *Pocillopora damicornis*	Tropics	Sammarco (1982); Richmond (1985)	Very unlikely	Minimal concentration of oxygen 8.33 mg/l, water circulated constantly, (Comau: 4–12 mg/l); 2h hypoxia did not cause detachment (A. Castrillon, pers. comm.)
High/low temperature	*Acropora tenuis* *Pocillopora damicornis* *Favia favus* *Cladocora caespitosa* *Oculina patagonica*	Tropics Subtropics Temperate region Temperate region	Yuyama et al. (2012); Fordyce et al. (2017); Kramarsky-Winter et al. (1997); Kružić (2007); Kramarsky-Winter et al. (1997)	Unlikely, unless one assumes that reduced variability induces change	Temperature was monitored constantly in a climatized cool room, measured values ranged between 12.0 and 13.3°C, without seasonal variation (Comau Fjord: 9.5–16°C)
High/low salinity	*Pocillopora damicornis*	Tropics	Shapiro et al. (2016); Liu et al. (2020)	Very unlikely	Salinity of new water introduced to the system was measured and adjusted, values of the water in the system ranged between 30.4 and 33.2 reflecting the natural salinity range in the coral's habitat (see Table SM 1). There were no abrupt changes in salinity in the aquarium system
High/low pH	*Pocillopora damicornis*	Tropics	Kvitt et al. (2015)	Very unlikely	The pH of the maintenance water and of new water introduced to the system during water exchange is controlled and ranged between 7.8 and 8.0 reflecting the natural pH range in the coral's habitat (see Table SM 1). There were no abrupt changes in pH in the aquarium system
Sedimentation	*Favia favus* *Oculina patagonica*	Subtropics Temperate region	Kramarsky-Winter et al. (1997); Kramarsky-Winter et al. (1997)	Very unlikely	Water was constantly, automatically treated, no sediment was added to the system; sediment stress experiments (sediment : water = 1 : 1,000) did not cause detachment (unbub. data.)
High nutrient concentrations	*Acropora tenuis*	Tropics	Yuyama et al. (2012)	Unlikely	Nitrate concentration (0.1–5.9 mg/l) exceeded natural values (Comau Fjord: 0.18–1.1 mg/l) 95 % of the time, however, remained stable (no sudden increases) over the entire observation period and was within the acceptable range

					for coral husbandry (Borneman 2008). As the other coral individuals remained unaffected, an effect of nitrate is unlikely. In addition, warm water scleractinians are optimally maintained at 5-10mg nitrate/l. Phosphate concentration (0.06–0.28 mg/l) was in the natural range (Comau Fjord: 0.12–0.36 mg/l)
Other allelopathic effects	*Tubastraea coccinea* *Pocillopora damicornis*	Tropics	Capel et al. (2014) ; Algae: pers. comm. K. Capel Sin et al. (2012)	Very unlikely	Autotrophs cannot grow in the system as it is permanently dark
Presence of synthetic toxins	*Pocillopora damicornis*	Tropics	Wecker et al. (2018)	Very unlikely	These substances are not used in or near the aquarium unit
High/low food	*Mussa angulosa* *Pocillopora damicornis* Not defined *Astroides calycularis*	Tropics Temperate region	Goreau et al. (1971); Richmond (1985) ; Goreau and Goreau (1959) ; Serrano et al. (2018)	Very unlikely	Fed three times a week with live *Artemia salina nauplii*, additionally each coral specimen was handfed once a week with a juvenile krill. Furthermore, it is likely that the water contained other food resources such as dissolved and particulate organic matter and micro-organisms. As the other coral individuals remained unaffected, an effect of starvation/lack of nutritional diversity is unlikely

Some of the *C. huinayensis* dropouts attached to the glass with their tentacles. However, we have no evidence for resettlement on the glass, although *C. huinayensis* larvae settle on it successfully. The swimming anemone *Stomphia coccinea* is able to routinely detach and reattach to substrate (Robson 1961) and may serve as a model for polyp detachment/reattachment. Before adhesion, its pedal disc becomes sticky due to the discharge of nematocysts (Ellis et al. 1969). The latter may be lacking in the aboral calicoblastic ectoderm of dropped out *C. huinayensis*. Indeed, after settlement of scleractinian planula larvae, the aboral ectoderm undergoes ultrastructural changes including the loss of secretory cells and nematocysts (Vandermeulen 1975). While it is uncertain if the detached *C. huinayensis* are able to restore this capacity beyond our observation period (seven months), we cannot rule

out this possibility, given that expelled polyps of the tropical *Tubastraea coccinea* have been shown to resettle after seven months (Capel et al. 2014).

If we assume that reattachment beyond our observation period might be possible, and because coral tissue is only slightly denser than seawater, we can suppose that in Comau Fjord dropouts may potentially drift with the currents, reach new habitats, resettle and reproduce. Sinking rate was 2.6 ± 0.3 cm s^{-1}. Tidally corrected current velocities of 5 cm s^{-1} (maximum 15 cm s^{-1}) were recorded in the vicinity of the coral banks (unpubl. data). Considering the steep walls and the species' distribution to at least 265 m (Häussermann and Försterra 2007), polyps dropped out at 20 m water depth may potentially drift lateral up to 3.7 km until they reach 265 m.

No direct evidence for polyp dropout was found *in situ*, but the partially detached stage, which precedes dropout over a longer period of time (twelve weeks for specimen #5 *in vitro*), provided indirect evidence for dropout in natural field populations of *C. huinayensis*. In Comau Fjord we documented partial polyp dropout in 1.4 ± 0.8 % of the polyps (six photo transects, total number of polyps analysed: 9322). Partially detached polyps were detected at both sites (1.3 ± 1.1 % of the polyps at Cross-Huinay North, 1.5 ± 0.5 % of the polyps at Liliguapi) and did not follow a common pattern in terms of frequency over the three seasons analysed. These field observations provide a strong indication that polyp dropout is a process which occurs naturally, however, under normal environmental conditions in only a few individuals. Thus, sexual dispersal apparently dominates over the asexual one (here drift of dropouts), similar to the tropical scleractinian coral *Pocillopora meandrina* (Magalon et al. 2005).

Although the respective five aquarium specimens did not show any external signs of physical stress or disease during the > 20 months maintenance period and also shortly before the polyp dropout, the possibility that some unmonitored external agent may have accounted for the observed changes cannot be excluded. It is unlikely that the removal process of the former recruits and the collection of adults had an impact 20 months after the transfer, especially as the corals grew as expected and partial detachment, indicative of imminent dropout, was also observed *in situ*. Furthermore, the lack of light during the maintenance period hardly seems to be a trigger, since only 6 % of the aquarium corals showed symptoms of dropout. Moreover,

partially detached corals were observed *in situ*, exposed to a light-dark cycle even under summer conditions. Weekly monitoring of water parameters did not reveal changes in the physico-chemical environment at the time or twelve weeks prior to the event (ANOVA $p > 0.05$, ESM_1, Laudien et al. 2018). In contrast to *Seriatopora hystrix* and *Pocillopora damicornis*, where a stress-induced dissociation of 100 % of the polyps was observed within 3 d (Sammarco 1982) and 6 d, respectively (Fordyce et al. 2017), only a small percentage of the *C. huinayensis* polyps showed symptoms of dropout (6 %) over the six years observation period. The remainder showed no sign of impairment. Potential stressors are unlikely to have triggered the polyp dropout (Online supplementary material 1), suggesting an endogenous trigger in individual *C. huinayensis*.

Analogous to some anemone species that may temporarily or permanently lift off the bottom (Riemann-Zürneck 1998; Bedgood et al. 2020) and indeed actively swim in response to abiotic or biotic cues (for review see Riemann-Zürneck 1998), polyp dropout may help *C. huinayensis* populate new regions, provided the dropout polyps are able to reattach or perform a lifestyle such as the one described as a 'straying predator' for *Korsaranthus natalensis* (Riemann-Zürneck 1998; Riemann-Zürneck and Griffiths 1999). Thus, polyp dropout allows the coral species to colonize new areas, even if the population is once unable to complete its sexual reproductive life cycle (Honnay and Bossuyt 2005) or if recruitment fails (Warner and Chesson 1985). This process may favour well-adapted genotypes even in the absence of moderate to high levels of disturbance (Miller and Ayre 2004; Foster et al. 2007). Moreover, colonizing new areas is decoupled from the reproductive season or possible unfavourable recruitment conditions (e.g., release of larva, when food is rare). Furthermore, it is well known that scleractinian corals spend a considerable amount of their energy on calcification. Corals that were experimentally not allowed to calcify diverted their energy into somatic growth (Fine and Tchernov 2007). By analogy, dropout could be the result of the coral's "decision" to divert more energy into reproduction, i.e., less into calcification – thus losing contact with its base. It would be interesting to know how "fecund" the dropouts are compared to attached polyps. Further studies should be carried out to understand, which variable(s) exert the behaviour and to confirm

C. huinayensis polyp dropout in nature. If so, are the dropouts able to survive, form new skeletons and ensure the survival of their genotype?

As a new form of reverse development, polyp dropout results in scleractinian polyps surviving without their skeleton for several weeks. Similar processes have been hypothesized to be key in the survival of 'anemone-like' ancestors of Scleractinia through periods of hostile conditions including the Permian-Triassic mass extinction according to Stanley´s "naked coral hypothesis" (Stanley 2003). Evolutionary advantage of polyp dropout, and polyp detachment in general, remains to be shown.

3.5 Acknowledgements

This study was supported by BMBF (grant-01DN13029), NatGeo (grant-EC-56391R-19), Fondecyt (grant 1201717), DAAD (grant-91608520), ANID (grant-62170011), and the Alfred-Wegener-Institut Helmholtz-Zentrum für Polar- und Meeresforschung (PACES II, DACCOR, and the programme 'Changing Earth – Sustaining our Future', Topic 4.2 and 6.1). We thank Christopher Brunner, Svantje Gottschlich and Erik Wurz for diving and sampling assistance; Julian Bartsch, Anita Hartig, Ulrike Holtz, Paul Kluwer, Esther Lüdtke, and Janis Müller for maintenance of the corals; and the staff of the Huinay Scientific Field Station for field support. We thank two anonymous reviewers for their valuable suggestions which helped to improve the paper. Specimens were exported from Chile under CITES permits 14CL000003WS, 14CL000014WS, 15CL000004WS and imported to Germany under E00154/14, E00095/15, and E00725/15. This is publication no. 178 of Huinay Scientific Field Station.

3.6 Supplementary Material

3.6.1 Supplementary Material 1:

Table SM1 Range of water parameters values of Comau Fjord compared to median, 5 and 95 percentiles, and distinct values of the water parameters of AWI's CWC rearing system (circuits A and B) for a time period and at the day, when polyp dropout occurred (see result section).

Date(s)	System	Oxygen [mg l^{-1}]	Salinity	pH	Temperature [°C]	NO^{2-} [mg l^{-1}]	NO^{3-} [mg l^{-1}]	PO_4^{3-} [mg l^{-1}]	Ω_{Ar}	Reference
18.-19.02.2014	Comau Fjord	4-12.8	30.4-32.7	7.4-8.2	9.5-16.0	n.d.	0.01-1.53	0.005-0.363	n.d.	Laudien et al. 2014; Wurz 2014
01.-03.02.2010 24.-25.02.2011 08.03.2011	Comau Fjord	8.4-9.6	32-33	7.8-7.9	11.8-12.2	n.d.	n.d.	n.d.	1.2-1.6	Jantzen et al. 2013
01.01.2017-05.11.2018	A	8.6, 8.3, 8.7	32.2, 30.4, 32.3	8.0, 7.8, 8.0	12.9, 12.0, 13.0	0.006, 0, 0.009	3.3, 0.1, 4.2	0.2, 0.1, 0.2	2.1, 1.3, 2.4	Laudien et al. 2018
20.03.17	A	8.7	31.7	7.9	12.8	0.02	4.9	0.2	1.57	Laudien et al. 2018
01.01.2017-05.11.2018	B	8.9, 8.0, 9.0	32.3, 30.6, 32.6	8.0, 7.9, 8.0	11.4, 10.8, 11.6	0.010, 0, 0.013	3.2, 0.5, 4.3	0.2, 0.1, 0.2	1.7, 1.3, 1.9	Laudien et al. 2018
10.09.18	B	8.9	32.5	7.9	11.3	0.003	4.3	0.2	1.5	Laudien et al. 2018
06.02.20	B	8.8	31.9	7.9	11.3	0.006	1.4	0.1	1.5	this study

3.6.2 Supplementary Material 2:

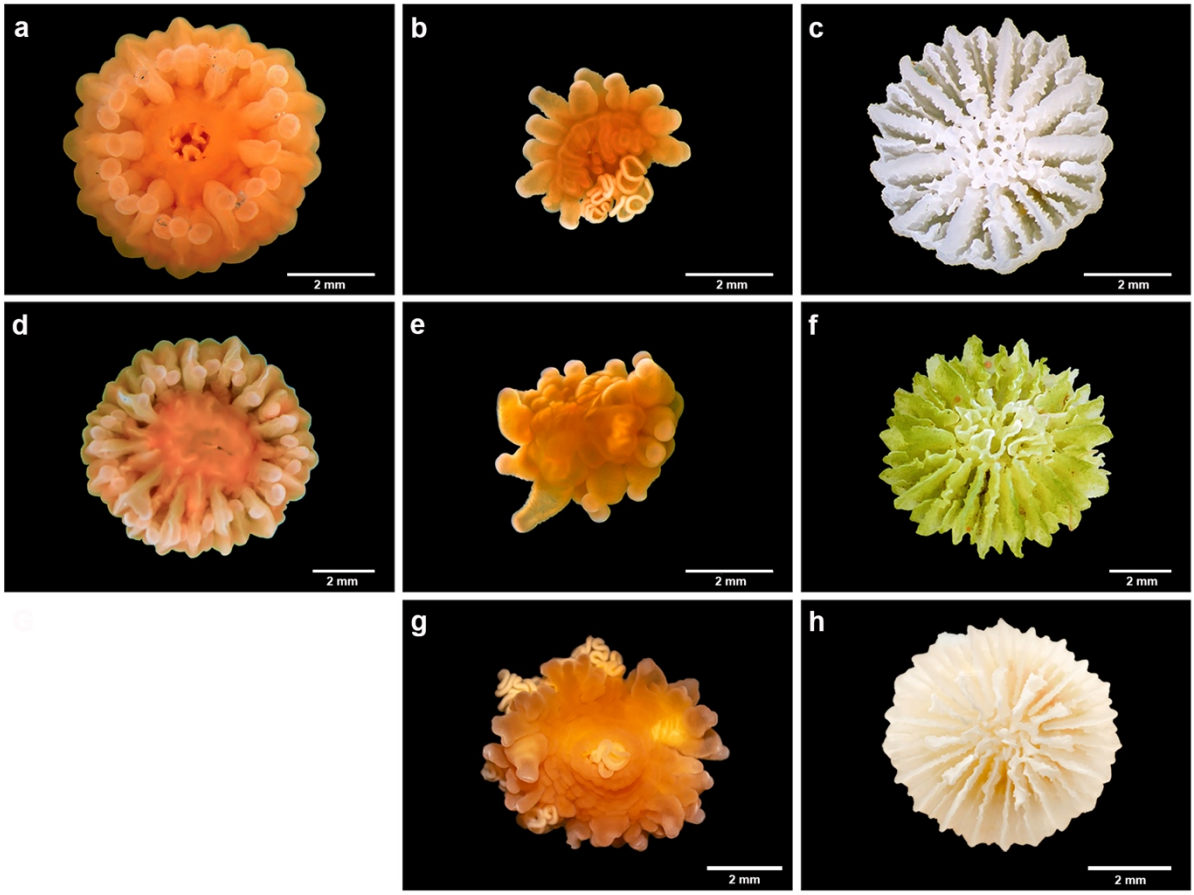

Fig. SM2: Three individuals of *Caryophyllia huinayensis* maintained in the aquarium system before (a, d) and after (b, e, g) polyp dropout and devised denuded skeletons (c, f, h), individual 1 (a-c), individual 2 (d-f), individual 3 (g, h). Note that some mesenterial filaments were exposed (b, g); Pictures c, d and g were selected for Fig. 2.

3.6.3 Supplementary Material 3:

Table SM3 listing the species number, the final phase, the state of the mesenterial filaments, the date of the event and the respective circuit.

Species No	Phase	Mesenterial filament state	Date	Circuit
#1	fully detached	Laterally exposed	20.03.2017	A
#2	fully detached	Laterally exposed	20.03.2017	A
#3	fully detached	Laterally exposed	10.09.2018	B
#4	partially detached	Laterally exposed	09.10.2018	B
#5	fully detached	Laterally exposed	06.02.2020	B

4

Real-time *in-vivo* skeletal formation shows that newly settled cold-water corals defy ocean acidification

Thomas Heran[a,b,c], Jürgen Laudien[a], Marlene Wall[a,d], Claudio Richter[a,b], Gernot Nehrke[a]

[a] Fachbereich Biowissenschaften, Alfred-Wegener-Institut Helmholtz-Zentrum für Polar- und Meeresforschung, Am Alten Hafen 26, 27568 Bremerhaven, Germany.

[b] Fachbereich Biologie/Chemie, Universität Bremen, Bibliothekstraße 1, 28359 Bremen, Germany.

[c] POETA Program (Programa de Observación de los Ecosistemas Terrestres y Acuáticos), Pontificia Universidad Católica de Valparaíso, Escuela de Ciencias del Mar, Valparaíso, Chile.

[d] GEOMAR Helmholtz-Zentrum für Ozeanforschung, Wischhofstr. 1–3, 24148 Kiel, Germany.

Keywords: scleractinian, recruit, biomineralization, crystal morphology, SEM, Raman, skeleton

Prepared to ***Nature Communications***

4.1 Abstract

The increase in atmospheric CO_2 partial pressure (pCO_2) has reduced seawater pH by 0.1 units since the pre-industrial era, with a predicted decline of 0.3 units by the end of the century. Ocean acidification (OA) decreases the aragonite saturation state (Ω_{arag}), challenging the structure and growth of the aragonite skeleton of corals, particularly in the early life stages of vulnerable deep-sea species. Using parent corals from Comau Fjord (Chile), we have for the first time achieved successful reproduction and *in vitro* culture of recruits of the scleractinian cold-water coral *Caryophyllia (Caryophyllia) huinayensis.* We used *in vivo* polarized light microscopy, scanning electron microscopy and confocal Raman microscopy to monitor and describe their skeletal development under aragonite oversaturated (Ω_{arag} = 2.4) and aragonite undersaturated (Ω_{arag} = 0.9) conditions. We found no adverse effect of OA on skeletal formation during polyp ontogeny, with no significant differences in (a) mineral composition, shape and arrangement of aragonite crystals, (b) timing and pattern of basal plate and septae formation, and (c) polyp width and height development, in both conditions. Our findings show that *C. huinayensis* recruits are able to conserve their structural integrity and skeletal developmental stage even in aragonite undersaturated waters.

4.2 Introduction

Fossil fuel combustion has increased atmospheric CO_2 partial pressure (pCO_2) from 280 parts per million (ppm) (Solomon 2007) in pre-industrial era to a current annual average of 420 (ppm) (Masson-Delmotte et al. 2021), altering the seawater chemistry of the world's oceans (Kleypas et al. 1999; Feely et al. 2004; Orr et al. 2005). As CO_2 dissolves in the seawater, carbonic acid is formed. This reduces the pH and the carbonate ion concentration of seawater, a process known as ocean acidification (OA). Scleractinian cold-water corals (CWCs) build their skeleton with aragonite, a polymorph of calcium carbonate ($CaCO_3$). Therefore the carbonate ion concentration of the seawater directly affects the formation of the skeleton (de Putron et al. 2011). The aragonite saturation state (Ω_{arag}) of seawater describes if aragonite formation (oversaturation: $\Omega_{arag} > 1$) or dissolution (undersaturation: $\Omega_{arag} < 1$) is thermodynamically possible. To date, sea-surface pH has decreased by 0.1 units since pre-industrial era (Orr et al. 2005; Jiang et al. 2019) and is predicted to decrease by 0.3 units by the end of the century under a "business-as-usual" scenario (Pörtner et al. 2019), with atmospheric pCO_2 of > 936 ppm (Representative Concentration Pathway, RCP 8.5) (Meinshausen et al. 2011) and $\Omega_{arag} < 1$ of seawater.

The majority (> 95 %) of scleractinian CWCs are found in waters that are supersaturated in respect to aragonite ($\Omega_{arag} > 1$), raising concerns about their susceptibility to OA (Guinotte et al. 2006). A meta-analysis study concluded that scleractinian corals, while sensitive to OA, may be able to acclimatize (Leung et al. 2022) by increasing their energy reserves (Büscher et al. 2017; Martínez-Dios et al. 2020) through increased food uptake or phenotypic and transgenerational plasticity (Putnam and Gates 2015). The ability to compensate for changes in seawater pH is associated with the capacity to regulate pH and dissolved organic carbon (DIC) (Venn et al. 2011) in the extracellular calcifying medium (ECM) (Allemand et al. 2004), i.e., the interface between the coral basal cell layer and the underlying skeleton, which requires higher energy expenditure (Spalding et al. 2017) and/or energy re-allocation away from energy-costly processes (e.g., reproduction (Tsounis et al. 2012; Maier et al. 2020)).

Scleractinian corals have a life cycle consisting of a mobile planula larvae phase followed by a sessile benthic phase (Harrison 2011), entailing large ontogenetic differences in size, motility, morphology and physiology. After larval attachment and polyp metamorphosis, the coral recruit begins to form the aragonitic skeleton. This is thought to be a temporally and spatially controlled microscale process, in which the chemical composition of the seawater (pH and DIC up-regulation) changes at the ECM (Venn et al. 2013; Sevilgen et al. 2019; Fietzke and Wall 2022). This process involves the transport of calcium ions and carbon species such as bicarbonate to the calcification site, while protons are removed. The increase in internal pH (Adkins et al. 2003; Gagnon et al. 2012), increases Ω_{arag}, favouring the precipitation of calcium carbonate. This precipitation results in a defined orientation of micro- and macrostructural components that are ultimately responsible for the three-dimensional orientation of the corallite.

Skeletogenesis in scleractinian corals begins with the formation of six radial lamellae, the primary septa, which generally connects at the outer periphery with a circular solid boundary, the wall. A thin skeletal layer is secreted over the entire basal area of the young polyp, called the basal plate (BP), which converges at the center of the polyp to form the columella, a central support of the skeleton (Gilis et al. 2014, 2015). On the microscale, a range of complex crystal morphologies are deposited as aragonitic dumbbell-like and semispherulitic structures that initiate the scaffolding of the septa, wall, and columella (Gilis et al. 2014, 2015).

Larval and juvenile skeletogenesis of scleractinian corals has been shown to respond differently to OA than skeletogenesis of adults (Leung et al. 2022; Beck et al. 2023), highlighting the importance of understanding the corals' response at all stages of their life cycle in order to assess and predict their performance, resistance and survival in OA environments. For instance, Cohen et al. (2009) observed changes in shape, size, orientation, and composition of aragonite crystals leading to morphological deformations of corallites in the primary polyps of the scleractinian coral *Favia fragum*. Foster et al. (2016) showed skeletal deformation and an increase in porosity in primary polyps of the coral *Acropora spicifera*, with an overall reduction in aragonite deposition. Carbonne et al. (2022) revealed that recruits of the

azooxanthellate (absence of endosymbiont) scleractinian coral *Astroides calycularis* reduced its calcified attachment area and the number of septa. Responses have mainly been studied in tropical to temperate scleractinian corals, while information on scleractinian CWC species in this context is lacking. This is mainly due to the fact that CWC settlement in the laboratory has not been achieved as suitable environmental conditions and settlement cues are lacking, with the only exception of the study of reproduction in *Oculina varicosa* (Brooke and Young 2003).

Here, we have succeeded for the first time to maintain specimens of the scleractinian CWC *Caryophyllia huinayensis* (collected from a naturally acidified location in a fjord in Chile), in aquaria on a long-term basis. The aquaria condition created were conducive to successful reproduction, larval development, survival, settlement, and metamorphosis into coral recruits. This provided a unique opportunity to study crystal formation and the effect of aragonite undersaturation of seawater on the skeletal structure from the micro- to the macroscale of newly settled scleractinian CWC recruits. Recruits were placed in a flow-through chamber and reared for 12 hours (h) to 18 days at 12.5 °C under aragonite oversaturated (Ω_{arag} = 2.4) and aragonite undersaturated (Ω_{arag} = 0.9) conditions. Our objectives were to (i) characterise growth stages of the skeleton based on their development and features, (ii) describe the skeletal microstructures at each growth stage by scanning electron microscopy (SEM), and (iii) determine the mineral composition of the skeletal microstructures by confocal Raman microscopy (CRM). Additionally, we compared across Ω_{arag} conditions (iv) the skeletal microstructures of each growth stage and (v) macrostructures including the basal plate crystals area change over time via *in vivo* polarized light microscopy (PLM), and the corallum sizes in terms of height and basal plate diameter.

4.3 Results

4.3.1 Skeletal development by growth stage

By evaluating the different micro- and macrostructural features of the recruits' primary skeleton, three growth stages were characterized. During the first growth stage (Stage 1), the outline of the corallite wall (w), the six primary septa (PS), and the basal plate (BP) periphery become visible (Fig. 1a–d), leaving a crystal-free central region (Fig. 1a–d). The second growth stage (Stage 2) is characterized by the inward extension of the BP towards the polyp centre, which is marked by the formation of conspicuous crystal clusters in the space between the primary septa. As a result, the crystal-free central region is reduced in area and the wall and primary septa thicken (Fig. 1e–h). The third growth stage (Stage 3) is defined by a closed basal plate and the formation of the columella (cl) in the centre (Fig. 1i–l).

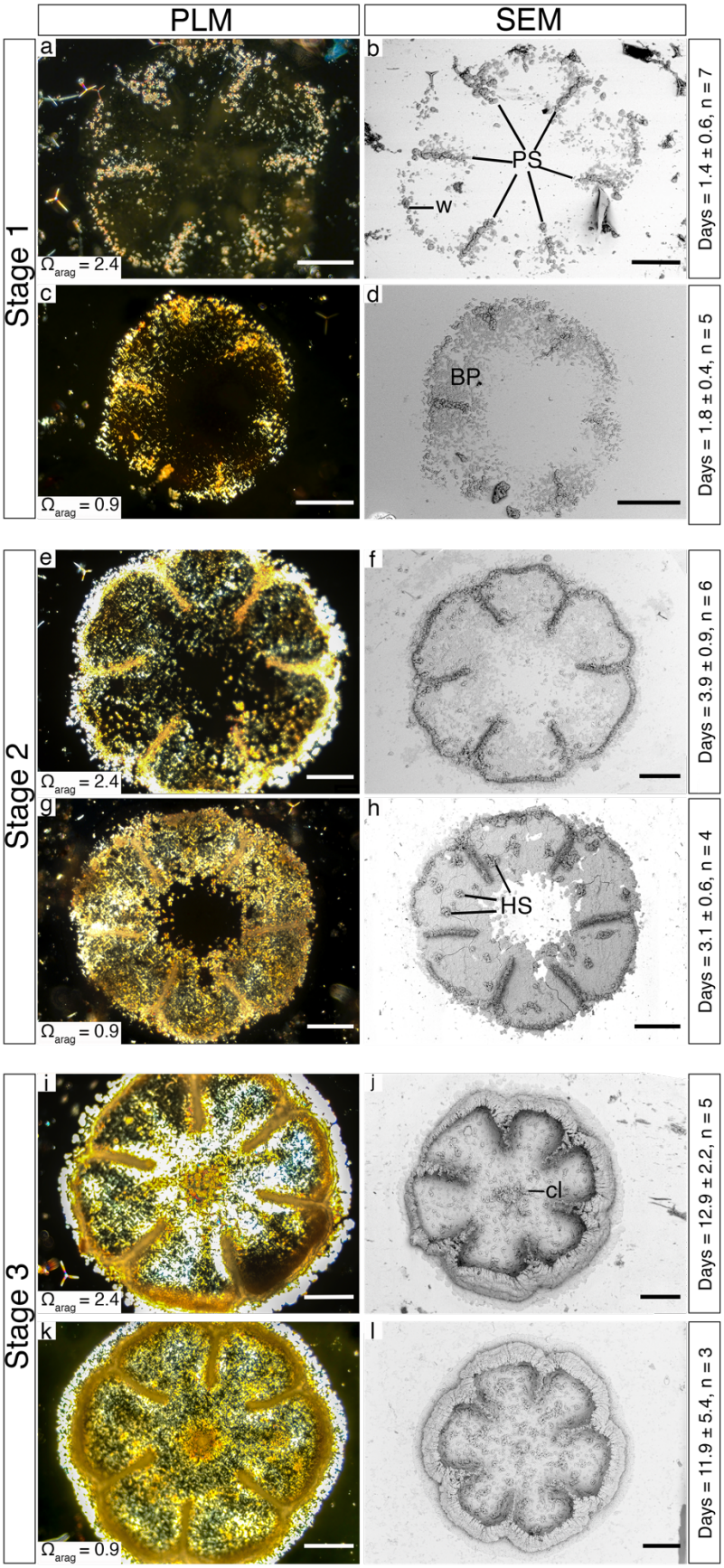

Figure 1: Growth S1–3 of *Caryophyllia huinayensis* recruits grown under Ω_{arag} = 2.4 (a, b, e, f, i, j) and Ω_{arag} = 0.9 conditions (c, d, g, h, k, l). Polarized light microscopy (PLM) view of the recruit's aboral side

(left panels: a, c, e, g, i, and k), and scanning electron microscopy (SEM) oral view of the same recruit (right panels: b, d, f, h, j, and l). Days (d, mean ± SD) represent the time from larval attachment until the BP of recruits observed through the PLM reached the corresponding growth stage. BP: basal plate, cl: columella, HS: honeycomb-like shaped, PS: primary septa, w: wall. Scale bars: 200 *μ*m.

4.3.2 Skeletal microstructures

Eight crystal morphologies during the development of *C. huinayensis* recruits were identified across growth stages (1–3) using SEM images. During the growth process, some crystal types changed their shapes, whereas others remained unchanged. The crystal types that changed include an initial fusiform-like shape (FS: Fig. 2a, f; Fig. 3e, j), which transformed into a dumbbell-like shape (DS: Fig. 2b, g; Fig. 3d, i) before ultimately becoming a semispherulitic-shape (SSS: Fig. 2c, h; Fig. 3a–c, f–h). The crystals which remained unchanged include the flat-basal shaped (FBS: Fig. 2d, e, i, j; Fig. 4c, e, h, j), circular platelet (CP: Fig. 2e, j), star-like shaped (SS: Fig. 3a–c, f–h; Fig. 4a, b, f, g), honeycomb-like shaped (HS: Fig. 3b, d, e, j; Fig. 4c, e, h, j), and platelet (P: Fig. 4d, i) types.

These crystal types differed greatly in their shape and size. For crystals that underwent structural changes, the FS started as an oval shape of 2.9 ± 1.7 *μ*m length (mean ± SD, n = 50) and grew to DS with a final length of 20.6 ± 4.5 *μ*m (n = 48). DS crystals showed needle-like fibres that began to form at both ends, creating a rough microstructural surface owing to the fibre tips. Both ends were connected by an elongated central region free of fibres (Fig. 2b, g; Fig. 3d, i). The fibres at both ends continued to grow, covering the central region forming SSS (Fig. 2c, h; Fig. 3a–c, f–h). As for the crystals that maintain their shape, FSB were 19.0 ± 4.9 *μ*m long (n = 48) with serrated edges and in some cases an oval-like structure in the centre. The FBS were translucent, as could be seen by imperfections in the coral glass holder shining through the FBS crystals (Fig. 2d, e, i, j). CP crystals of 7.5 ± 3.9 *μ*m ø (n = 50) also showed an oval-like structure on top (Fig. 2e, j). SS crystals (Fig. 3a–c, f–h; Fig. 4a, b, f, g) exhibited conical bundles of aligned fibres projected in both lateral (Fig. 3a, f) and upright orientation (Fig. 3b, c, g, h). The HS were nodular, irregularly shaped, and highly porous voids which formed on both the surface of FBS (Fig. 3b, j; Fig. 4c, h)

and the glass substrate (Fig. 3d, e). The P crystals were also irregular in shape, forming sub-platelets on the surface with angular edges.

Temporally, specific crystal types characterized the different macroscopic skeletal structures at each growth stage. During Stage 1, skeletal formation started with five crystal morphologies. The transformation of the crystals FS, DS, and SSS, initiated the formation of the wall and the six primary septa in a discontinuous fashion (Fig. 2b, c, g, h; Fig. 3a–d, f–i), which further developed and merged in Stage 2 to form a continuous structure between the wall and the primary septa. CP and FBS crystals were commonly found between the primary septa and close to the wall in a patchy distribution (Fig. 2a, d, e, f, i, j). They were also involved in the formation of the BP. In Stage 2, HS and SS crystals were formed. HS were deposited between the primary septa in a random distribution compared to DS and SSS crystals, where they continued to form in Stage 3 over the surface of the BP (Fig. 4c, e, h, j). SS crystals were formed on SSS, with an upright orientation mainly on the primary septa (Fig 3b, g, c, h) and some with lateral growth on the wall (Fig. 3a, f). In Stage 3, the SS crystals continued to develop on the primary septa and the wall to form the calyx (Fig. 4b, g; Suppl. Fig. 1). P crystals formed along the outer side of the polyp wall, initially interconnected between them and to the wall. However, as the tissue extended further away the wall, the spaces between the crystals increased, causing them to become isolated from each other (Fig. 4d, i). The crystals CP and FBS grew from the periphery to the centre of the polyp whilst merging together, thus closing the BP. The closing of the BP initiated the formation of the columella (cl) at the centre of the polyp (Fig. 4e, j; Suppl. Fig. 1).

Although the deposition of the diverse crystals varied both temporally and spatially, the mineral composition for all was pure aragonite as revealed by the characteristic aragonite Raman spectra with the diagnostic peaks at wavenumbers 155 cm^{-1} (translational mode), 208 cm^{-1} (librational mode), 710 cm^{-1} (in-plane bend), and 1,085 cm^{-1} (symmetric stretch) (Suppl. Fig. 2). We found no evidence for other precursor phases of aragonite or other minerals or organic matter (suppl. Fig. 2).

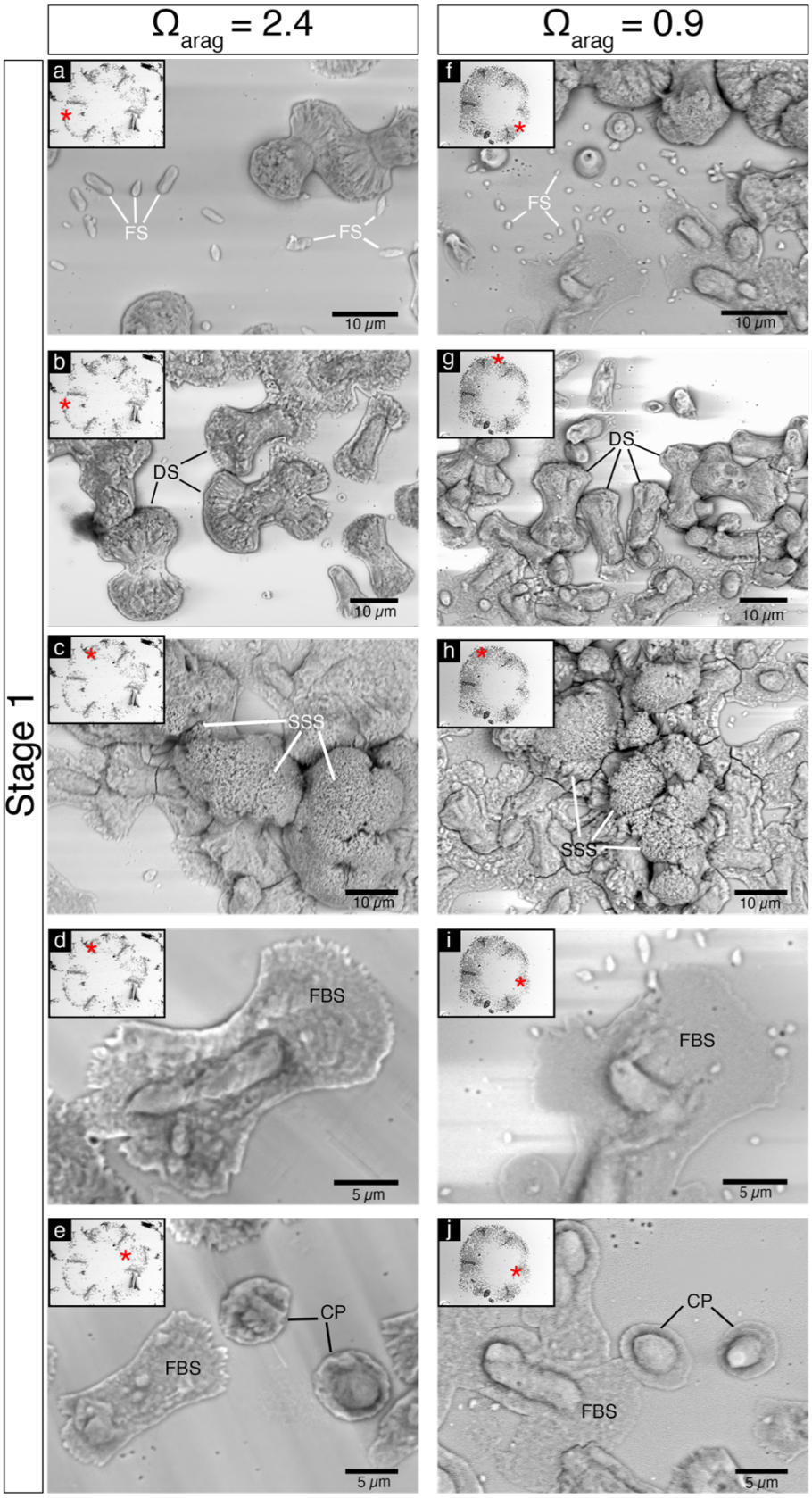

Figure 2: SEM images of five crystal morphologies of *Caryophyllia huinayensis* deposited in Stage 1 under Ω_{arag} = 2.4 (a–e) and Ω_{arag} = 0.9 conditions (f–j). Images: periphery of the BP (a, f, e, and j),

primary septa (b, g, c, and h) and interseptal zones (d, i). The five images in each column correspond to a single representative individual from each condition. Red asterisk in the upper left image in the overall view CP: circular platelet, DS: dumbbell-like shaped, FBS: flat-basal shaped, FS: fusiform-like shaped, SSS: semispherulitic-like shaped. Note: submicrometric black dots in the images are artefacts of the glass substrate.

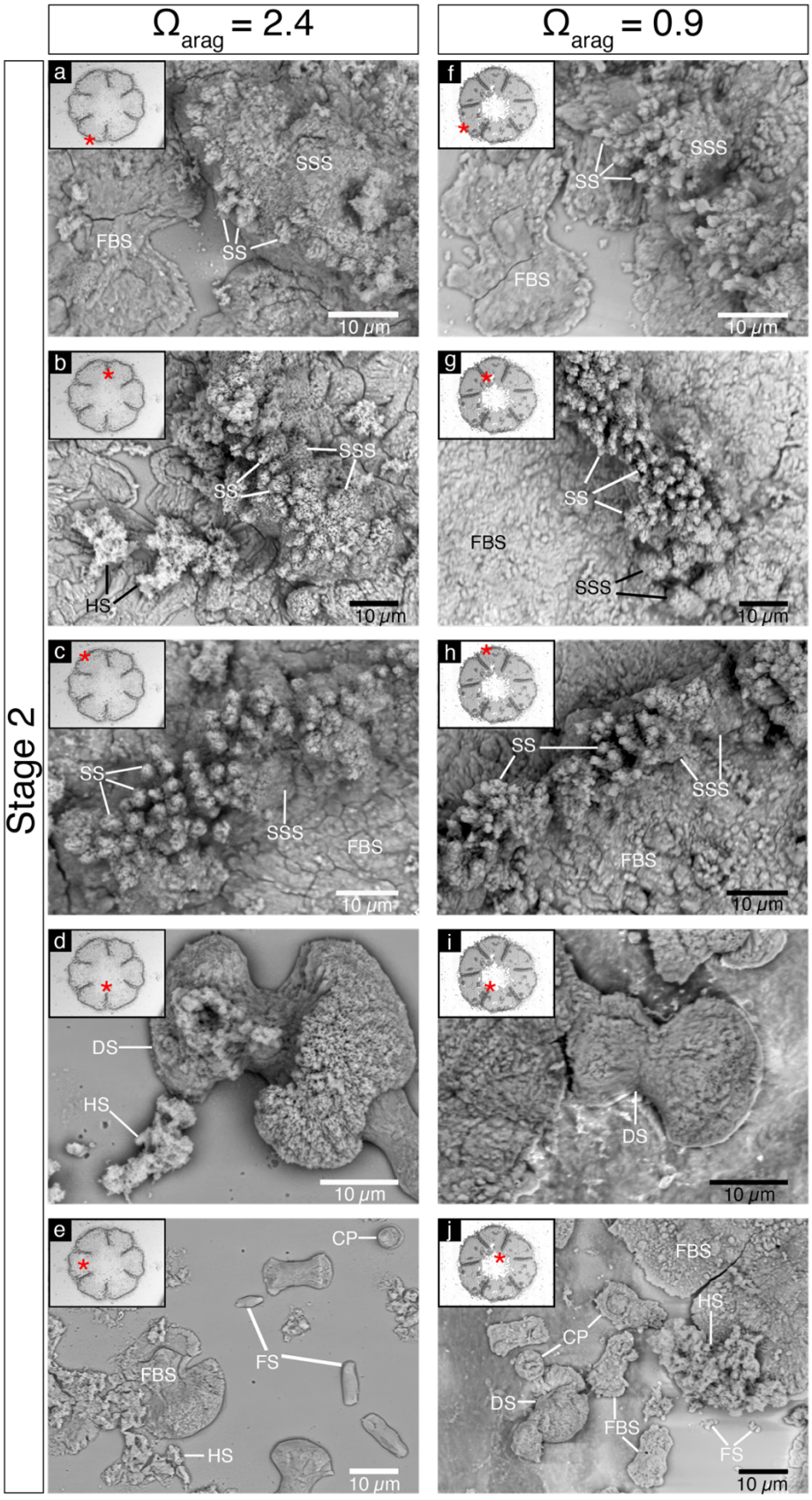

Figure 3: SEM images of seven crystal morphologies of *Caryophyllia huinayensis* deposited during growth Stage 2 under Ω_{arag} = 2.4 (a–e) and Ω_{arag} = 0.9 (f–j) conditions. Images: periphery of the BP (a,

f, c, and h), primary septa (b, g, d, and i) and interseptal zones (e, j). The five images in each column correspond to a single representative individual from each condition. CP: circular platelet, DS: dumbbell-like shaped, FBS: flat-basal shaped, FS: fusiform-like shaped, HS: honeycomb-like shaped, SS: star-like shaped, SSS: semispherulitic-like shaped. Note: submicrometric black dots in the images are artefacts of the glass substrate.

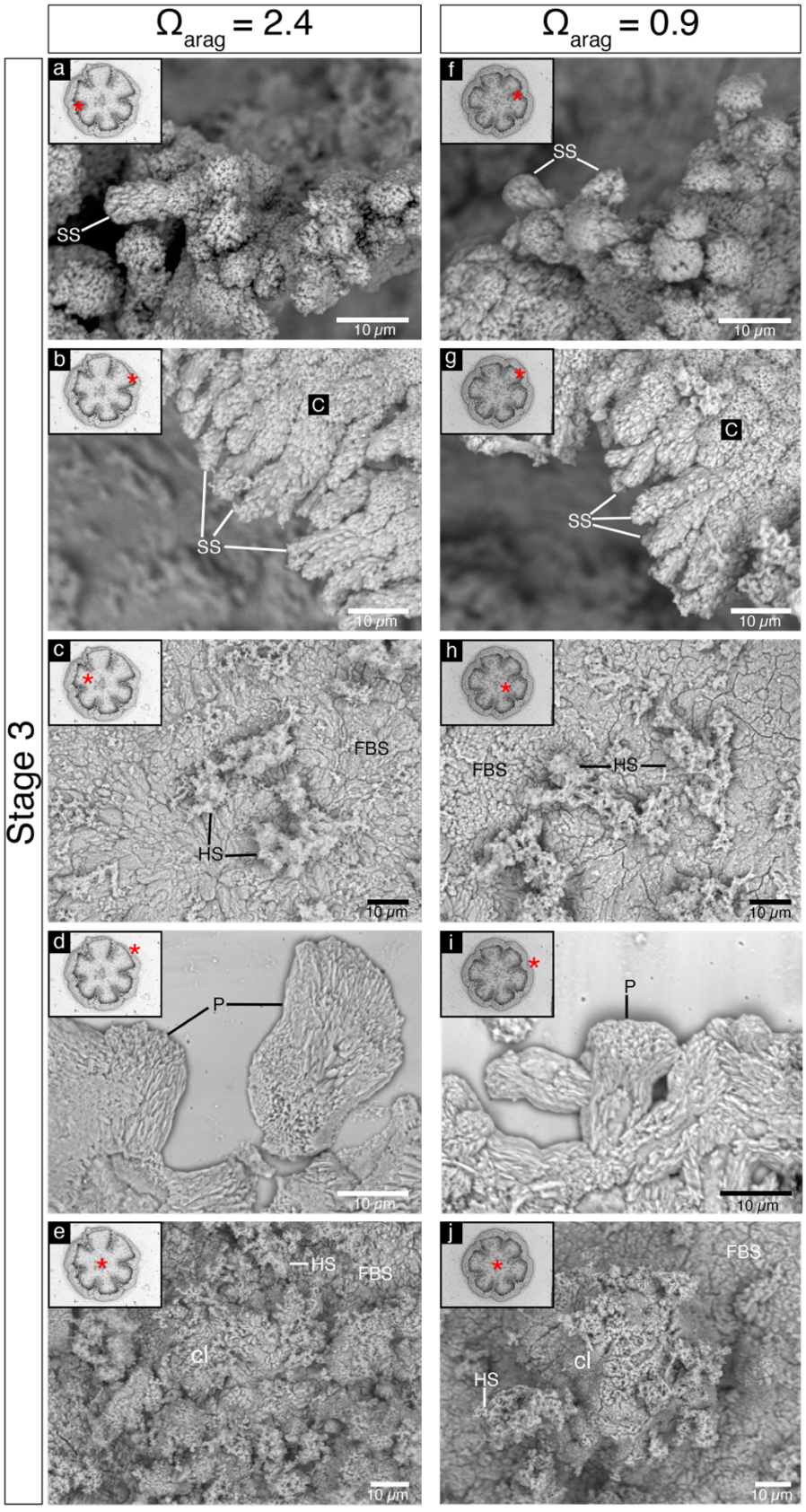

Figure 4: SEM images of four crystal morphologies and the formation of the columella of *Caryophyllia huinayensis* deposited during Stage 3 under Ω_{arag} = 2.4 (a–e) and Ω_{arag} = 0.9 (f–j)

conditions. Images: primary septa (a, f), corallite calyx (b, g), interseptal zone (c, h), periphery of the BP protruding from the wall (d, i), and columella (e, j). The five images in each column correspond to a single representative individual from each condition, cl: columella, FBS: flat-basal shaped, HS: honeycomb-like shaped, P: platelet, SS: star-like shaped. Note: submicrometric black dots in the images are artefacts of the glass substrate.

4.3.3 Crystal and basal plate changes between Ω_{arag} conditions

Four of the five crystals identified (CP, DS, FBS, and FS) showed no differences in shape between the high and low aragonite saturation treatments in any of the growth Stages (1–3) ($p > 0.05$, Suppl. Table 1, Suppl. Table 2). The only difference between aragonite saturation treatments was observed with the HS crystal: Only two polyps out of seven (one at Stage 2 and one at Stage 3) formed HS crystals in Ω_{arag} = 2.4, compared to six out of seven polyps (one at Stage 2 and five at Stage 3) in the Ω_{arag} = 0.9 treatment (Fig. 1h and Suppl. Fig. 1).

We found no differences in the growth of the basal plate between aragonite saturation treatments (Fig. 5). About 90 % of the basal plate was closed after one week in both cases and growth rates calculated from the asymptotic regression were similar (GAMs; $p > 0.05$, Suppl. Table 1, 2).

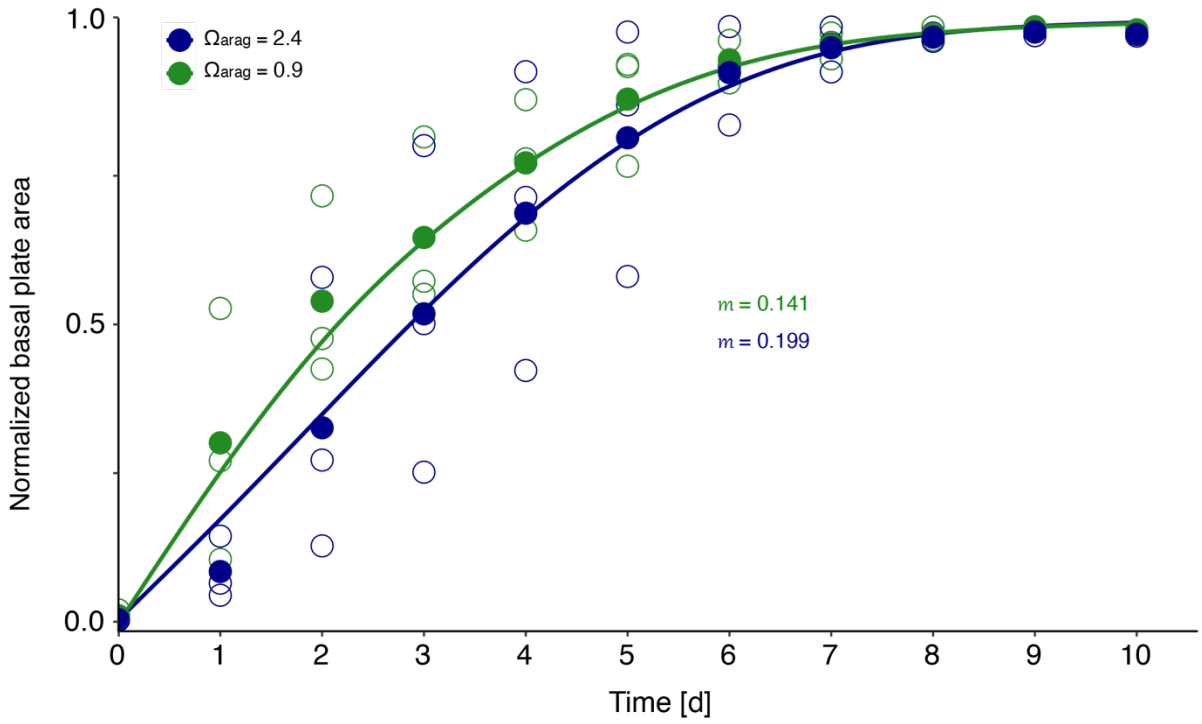

Figure 5: Normalized basal plate area of *Caryophyllia huinayensis* recruits over time (d) under Ω_{arag} = 0.9 (n = 3, green) and Ω_{arag} = 2.4 (n = 3, blue) conditions. The asymptotic regression curves show the fitted means. The curve slopes (*m*) are presented per each condition.

When comparing polyp sizes reared between conditions at Stage 3, neither the corallum height (Fig. 6a) nor the BP diameter (Fig. 6b) showed significant differences (LM; F = 0.86; p = 0.39; Suppl. Table 2, and LM; F = 2.48; p = 0.19; Suppl. Table 2, respectively).

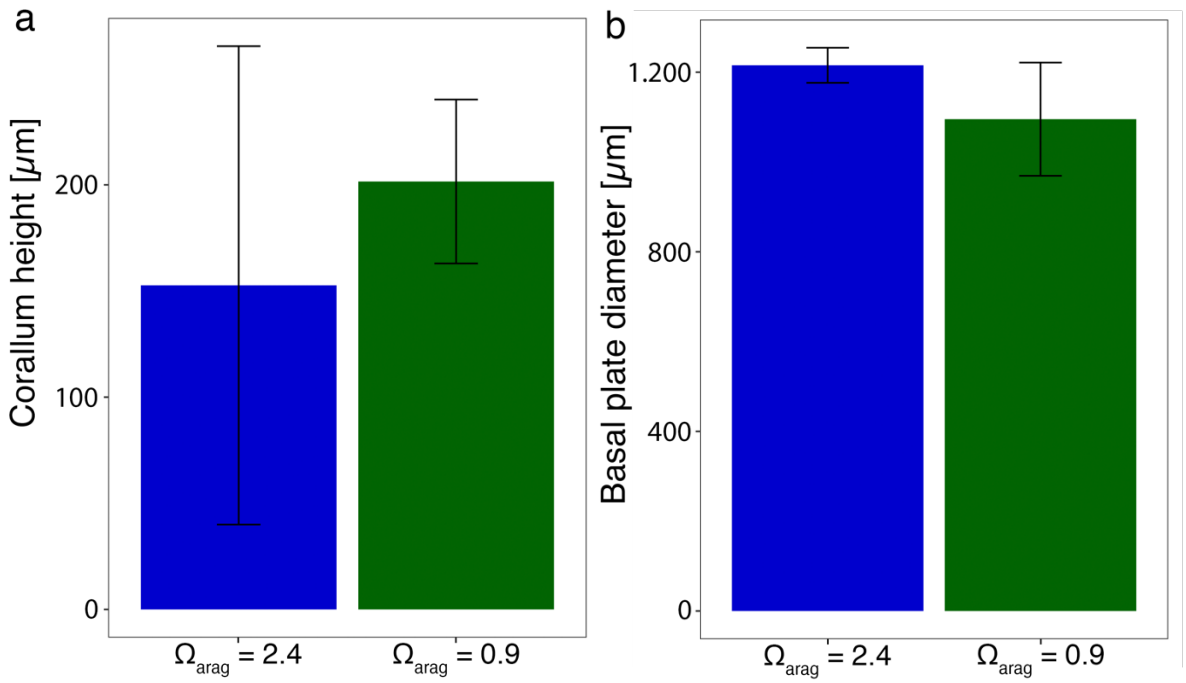

Figure 6: (a) Corallum height (n = 3 and n = 5 individuals in Ω_{arag} = 2.4 and Ω_{arag} = 0.9 conditions, respectively) and (b) BP diameter (n = 3 individuals per condition) measured from SEM images of recruits at Stage 3 under Ω_{arag} = 2.4 (blue) and Ω_{arag} = 0.9 (green) conditions (mean ± SE).

4.4 Discussion

The settlement and early life history stages of scleractinian corals are considered to be highly sensitive to OA (Cohen et al. 2009; Foster et al. 2016; Carbonne et al. 2022) and successful biomineralization during these stages is considered a bottleneck for survival (Vandermeulen 1975; Akiva et al. 2018). Therefore, it is crucial to understand the influence of OA on skeletal structure and growth. For the first time, we studied cold-water coral skeletal formation at the microstructure scale using newly settled recruits of *C. huinayensis* as our model. We have not only described early skeletal formation, but also, experimentally tested the influence of Ω_{arag} = 0.9 on the lowest and most fundamental level of skeletal organisation. Having successfully established suitable environmental conditions for scleractinian CWC reproduction, we have also developed a suitable small flow-through chamber system that allows rearing of CWC recruits and microscopic monitoring of *in vivo* skeletal development over the juvenile period.

Skeletogenesis of newly settled CWC *C. huinayensis* recruits revealed that ontogeny of the initial stages of skeletal formation follows a similar pattern to that of scleractinian WWCs (Vandermeulen and Watabe 1973; Le Tissier 1988; Gilis et al. 2014, 2015; Neder et al. 2019). As a common pattern, sequential skeletal development in scleractinian corals includes the formation of (i) FS and CP crystals, (ii) primary septa and wall, (iii) lateral fusion of platelets to form the BP, (iv) internal lateral extension of the BP, and (v) vertical extension of the septa, wall and columella. Our findings support the idea of a genetically encoded body plan encompassing defined biomineralization steps from micro- to macroscale in the early stages of development within the order scleractinia, as is observed in at least five species (Vandermeulen and Watabe 1973; Le Tissier 1988; Gilis et al. 2014, 2015; Neder et al. 2019), including this study.

Fastest growing skeletal regions (growing front of adult skeletal structures) are initiated by centres of calcification (CoC) (Ogilvie 1896), and other skeletal regions comprising the bulk of the skeleton are built by aragonite fibres (Cuif and Dauphin 1998; Cohen and McConnaughey 2003; Nothdurft and Webb 2007). Studies of adult

coral skeletons have described the formation of amorphous calcium carbonate (ACC) (Mass et al. 2017) as a precursor phase for aragonite crystals initiated in the CoC. ACC is a disordered phase of poorly oriented crystalline fibres containing high levels of magnesium (Mg) (Wainwright 1963; Vandermeulen and Watabe 1973; Gilis et al. 2014; Neder et al. 2019), which serves to stabilize this otherwise unstable phase of the ACC (Meibom et al. 2004). It is also possible that Mg-rich ACC transiently exists in the coral skeleton, creating a regulated environment for the formation and development of aragonite crystals within the CoC. While some studies have detected Mg-rich components during early stages of skeletogenesis of scleractinian WWCs (Shapiro et al. 2018; Neder et al. 2019), the crystal mineralogical analysis of *C. huinayensis* recruits shows pure aragonite (Suppl. Fig. 2). No trace of other mineral precursors was detected, consistent with some previous work (Cohen and Holcomb 2009; Clode et al. 2011; Foster and Clode 2016). Hence, it is possible that the presence or absence of Mg precursors in scleractinian corals is species-specific.

C. huinayensis initiated skeletogenesis with the transformation of FS crystals (Fig. 2a, f; Fig. 3e, j) via needle-shaped fibres into DS (Fig. 2b, g; Fig. 3d, i) and SSS (Fig. 2 c, h; Fig. 3 a–c, f–h), as described in the scleractinian WWC *Pocillopora damicornis* (Gilis et al. 2014, 2015). These crystals together with FBS and CP that form the BP, showed birefringence under PLM (Fig. 1a; Suppl. Fig. 3a). This indicates a spherulite arrangement (Bryan and Hill 1941), where crystallites are arranged radially, growing outward from a CoC (Cuif and Dauphin 1998; Brahmi et al. 2010; Reggi et al. 2014) in a plane fashion. The radial arrangement of spherulite crystals allows space for its elongation that is 10 times faster (Sun et al. 2017) than non-spherulite crystals. Consequently, this crystal type can rapidly occupy the crystal-free central region of the coral recruit (Fig. 5). The fast-growing crystals FS, FBS and CP have not been reported in adult scleractinian CWCs, suggesting a different interaction of the recruit's basal cell layer between the underlying substrate and the developed skeleton. This could rely in the recruit's requirement to settle fast in order to withstand, for example, the water current to not be washed away. The fast growth of basal crystals increases the anchorage area for the specialized cells known as desmocytes.

The growth rate of recruits and juveniles of CWCs has been demonstrated to exceed that of adult corals (Beck et al. 2023). Therefore, it is important to investigate

whether the potentially higher energy-demanding process of pH up-regulation at the calcification site under OA (Allemand et al. 2011) would persist in recruits and juvenile CWCs, given their potentially limited energy reserves to trade off.

Here, we demonstrated that *C. huinayensis* recruits maintain a remarkably unaltered skeletal formation in spite of Ω_{arag} = 0.9. Recruits were able to form a structurally indistinguishable aragonite skeleton at similar growth rates (Fig. 5), corallum height (Fig. 6a), BP diameter (Fig. 6b), and crystal composition and morphology under acidified conditions.

The growth mechanism of scleractinian CWCs recruits at Ω_{arag} = 0.9 may be related to a long-term evolutionary trait. These species may have developed adaptive strategies to counteract the effect of unfavourable Ω_{arag} = 0.9 environment, allowing them to thrive. Scleractinian CWCs are able to elevate their carbonate saturation state in the ECM by ~0.8–1.0 units (ΔpH) relative to the ambient seawater, although at a higher energy expenditure (Spalding et al. 2017). In contrast, warm-water aragonitic corals are able to elevate by ~0.4–0.5 units (McCulloch et al. 2012). This difference may explain the significant effect of Ω_{arag} = 0.9 on early skeletal development of scleractinian WWC recruits. Studies have reported an increase in skeletal porosity, a reduction in both BP diameter and coral height, the occurrence of wall fractures, and a reduction in the number of septa (Cohen et al. 2009; Foster et al. 2016; Carbonne et al. 2022).

Within the naturally acidified Comau Fjord (Fillinger and Richter 2013), *C. huinayensis* polyps are ubiquitous (Cairns et al. 2005; Wurz 2014), suggesting that the parental polyps collected may also be adapted to low seawater pH. While the exact mechanisms of adaptation remain to be elucidated, transgenerational plasticity, i.e., somatic adaptation passed on from one generation to the next, could play a role in the capacity of *in vitro C. huinayensis* recruits to counteract the Ω_{arag} = 0.9 on skeletal formation. Transgenerational plasticity has been demonstrated in a study of *P. damicornis* (Putnam and Gates 2015). The study found that the parental polyps exhibited negative effect when subjected to low seawater pH and high temperatures. However, upon subsequent exposure to the adverse conditions, the released larvae

displayed notable size differences and metabolic adaptations, contrasting with larvae originating from parental polyps exposed to ambient environmental conditions.

Whether the higher energy expenditure of *C. huinayensis* recruits in up-regulating their internal pH at low seawater pH is derived from an internal or external source, or both, remains to be elucidated. However, a recent study of the life cycle of *C. huinayensis* using histological sections showed that a mouth and a pharynx are already developed as part of the gastrovascular system in brooded larvae (Heran et al. 2023). This suggests that larvae are planktotrophic and may be able to maintain their internal energy levels during the planktonic stage or, more suitably, accumulating energy prior to settlement. This, combined with their potential adaptability to low seawater pH may offset metabolic energy requirements once skeletogenesis begins under Ω_{arag} = 0.9 condition.

We determine for the first-time that ontogeny of the initial stages of skeletal formation in the scleractinian CWC *C. huinayensis* follows a similar temporal and spatial pattern to that of scleractinian WWCs. Moreover, we demonstrate that Ω_{arag} = 0.9 has no effect on skeletal formation during early ontogeny of a CWC (Fig. 5). *C. huinayensis* recruits are able to build integral crystal morphologies and structural skeletal components under Ω_{arag} = 0.9 (Fig. 6). Although the mechanism used by CWC recruits to compensate for the low seawater pH and Ω_{arag} = 0.9 is not yet known, it seems that the early life stages of *C. huinayensis* are equipped to cope with the projected alteration of seawater Ω_{arag} by the end of the century. However, seawater aragonite saturation is not altered in isolation, and further studies should examine the effect of multiple stressors, including the synergy of Ω_{arag} = 0.9, elevated seawater temperature, and altered food supply on the early skeletal formation of newly settled scleractinian CWC recruits.

4.5 Materials and Methods

4.5.1 Coral collection and rearing

Adult polyps of the solitary scleractinian CWC *Caryophyllia huinayensis* Cairns et al. (2005) were collected in 2014, 2015, and 2019 by SCUBA diving between 20–30 m water depth in X-Huinay (42° 23.213' S; 72° 27.772' W), Comau Fjord, Chile. Comau Fjord exhibits a natural vertical gradient of Ω_{arag}, ranging from 0.86 ± 0.12 to 1.36 ± 0.14 (Beck et al. 2022) (Table 2). The horizontal Ω_{arag} ranges from 1.09 ± 0.34 at the head of the fjord (Beck et al. 2022), to 0.98 ± 0.05 at X-Huinay in the central part of the fjord (Rossbach et al. 2021) (Table 2), and 1.3 ± 0.07 at the mouth of the fjord (Table 2).

After collection, corals were transported alive to the Alfred Wegener Institute in Bremerhaven, Germany, in plastic aquarium bags filled one third in volume with seawater and two thirds with pure oxygen. On arrival, the polyps were glued (underwater glue, Preis Aquaristik KG, Bayerfeld, Germany) to plastic screws for handling and placed in a closed-circuit maintenance aquarium with artificial seawater (Dupla Marin Premium Reef Salt, Dohse Aquaristik, Grafschaft-Gelsdorf, Germany). The corals were kept in the aquarium at water conditions similar to those found in the mouth area of Comau Fjord in autumn until the start of the experiments in 2019. The UV-treated artificial seawater was maintained with a temperature of 11.5 ± 0.8 °C and salinity of 31.7 ± 0.6. Seawater carbonate chemistry was maintained at 7.9 ± 0.1 pH, adjusted by a pH-dependent feedback system that bubbled pure CO_2 into the seawater when the pH raised 0.1 pH units from the set value (Dupla pH-Control Delta, Dohse Aquaristik GmbH & Co. KG, Grafschaft, Germany), maintaining a pCO_2 value of 480 (Ω_{arag} = 2.4) (Table 2).

4.5.2 Larval collection and settling

Brooding *C. huinayensis* polyps were selected based on the visible larvae in the gastrovascular region and tentacles, as their tissue is translucent (Heran et al. 2023). Polyps were placed in individual plastic beakers with a hight of 7.2 cm and a diameter of 5.4 cm (125 ml sample beakers, Burkle Inc., New York, USA) with three 4.0 × 4.5 cm side windows, covered with a 100 μm nylon mesh screen to allow water exchange. The beakers were attached to a horizontal plastic support by screwing the coral's screw through the closed bottom centre of the beaker. This allowed the open top of the beaker to be positioned 1 cm above the water surface, allowing the retention and collection of released larvae. The released larvae were transferred to a closed flow-through cube (2 × 2 × 2 cm) consisting of four glass coverslips glued together with silicone (Silexo, Juwel Aquarium AG & Co. KG, Germany). A 100 μm nylon mesh screen was placed in front of and behind the cube to allow water exchange. Larval attachment to the coverslip was confirmed when the planula was kept in constant aboral contact with the substrate for 24 h, together with a change in body shape from elongated to flattened in an oral-aboral axis.

4.5.3 Experimental setup and design

Upon larvae attachment, the cube coverslip with the recruit was removed and placed with the oral side of the recruit facing upwards on the bottom of a polydimethylsiloxane (PDMS) flow-through chamber with a length of 72 mm, a width of 23 mm a height of 15 mm and an inlet and outlet on opposite sides of the chamber (Fig. 7). The PDMS chamber was set up on a microscope glass slide, allowing an aboral view of the recruit, while leaving an open space at the top of the chamber for access to microsensors (Fig. 7). Tubes with a diameter of 2.06 mm (TYGON®-Schlauch LMT-55 Peristaltic violet/violet, SAINT-GOBAIN, La Défence, Paris, France) were connected to the inlet and outlet and to a peristaltic pump (Watson-Marlow 205S, Falmouth, United Kingdom), which circulated the treated seawater from a 10-l glass bottle placed on a magnetic stirrer (700 rpm, Ikamag® Reo, Gemini b. v, Apeldoorn, Nederland) (Fig. 7). The seawater flow rate inside the chamber was maintained at 4.1

cm s^{-1}, so that the seawater volume of the chamber was exchange every 3 min. The seawater flow velocity corresponded to the current velocity recorded near the coral community in Comau Fjord (5 cm s^{-1}, maximum 15 cm s^{-1}) (Laudien et al. 2021).

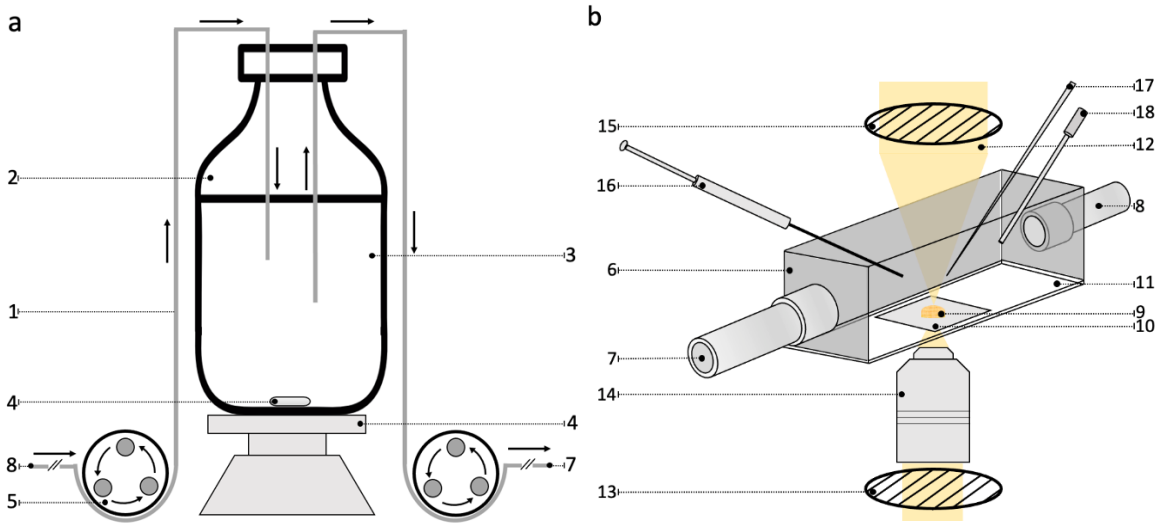

Figure 7: Schematic diagram of the closed seawater system (a) and the flow-through chamber (b). The plastic tubes (1) were placed in a 10-l glass bottle (2) containing the treated seawater (3) homogenized by a magnetic stirrer (4). A peristaltic pump (5) recirculated the seawater from the glass bottle to the PDMS chamber (6) through an inlet (7) and an outlet (8). The recruit (9), settled on a glass coverslip (10), was placed on a microscope glass slide (11) which formed the bottom of the chamber. Polarised images of the BP of the recruit were taken using light beam (12) passing through the analyser (13), a 5× objective (14), the coral recruit and a polariser (15). An optical oxygen meter (16), a pH micro-sensor (17) and a temperature sensor (18) were used to monitor the characteristics of the seawater inside the chamber. Figure not drawn to scale.

For both conditions, artificial seawater was obtained from the adult polyp maintenance aquarium. For the condition Ω_{arag} = 2.4, seawater from the maintenance aquarium (see text above for seawater parameters) was added directly to the 10-l glass bottle (Fig. 7). For the Ω_{arag} = 0.9 condition (Table 2), seawater from the maintenance aquarium was added to the 10-l glass bottle and CO_2 bubbled from a pre-mixed cylinder containing 1,200 ppm CO_2 (50 % synthetic O_2 and 45 % CO_2), calculated to keep the seawater constant at 7.6 ± 0.1 pH total scale (pH_T). For both conditions, the pH in the 10-l glass bottle was monitored daily using a WTW Multi 340i

pH meter equipped with a SenTix® 41-3 pH electrode, calibrated against a combination of WTW buffers (Ω_{arag} = 2.4: pH 7.01 and 10; Ω_{arag} = 0.9: pH 4 and 7.01). The pH within the chamber (Table 2) was monitored with a pH microelectrode Prosense (Unisense, Denmark) calibrated against a combination of WTW buffers (see above). Values were recorded using the SensorTrace-PRO software (Unisense, Denmark). Dissolved oxygen in seawater and its temperature in the chamber (Table 2) were monitored every 15 min using a microelectrode (Microx TX3, PreSens, Regensburg, Germany). Dissolved oxygen was 2-point calibrated in oxygen-free (bubbling nitrogen gas for 15 min) and air-saturated (bubbling oxygen gas for 15 min) conditions prior to each condition. Salinity in the 10-l glass bottle was checked daily using a WTW conductivity sensor (ProfiLine Cond 3110, Xylem Analytics, New York, USA). All experiments were conducted in a thermostatically controlled room where the seawater temperature was maintained at 12.5 ± 0.6 °C (mean ± SD). Salinity was kept at 31.8 ± 0.5 and oxygen concentration at > 80 % (Table 2). When the oxygen level dropped below 80 % and/or pH shifted by ± 0.1 units, seawater was exchanged. Immediately after each water exchange, TA was measured by Gran-titration (Smith and Kinsey 1978) using a sample exchanger in a titration unit (Titro-Line alpha plus, SI Analytics, Mainz, Germany, with A 157 1 M-DIN-ID pH electrode) (Table 2). Prior to each titration, the pH electrode was two-point calibrated using pH buffers 4.006 and 6.865 (WTW, Xylem Analytics, New York, USA). TA was calculated from linear Gran plots (Gran 1952) and corrected for seawater density using an in-house standard North Sea water (Table 2). In addition, DIC (4.5 ml) was measured from each water batch using sterile seawater filtered through GF/F polycarbonate membrane filters (0.2 μm pore size) and poisoned with 20 μl saturated $HgCl_2$ before storage at 4 °C until analysis. DIC was determined in two replicate samples, each measured twice, using a QuAAtro39 AutoAnalyser with a XY-2 autosampler (Seal Analytical GmbH, Norderstedt, Germany) and AACE software (version 7.09) (Table 2).

Aragonite saturation (Ω_{arag}) was calculated from DIC and pH_T using the program CO2SYS (Lewis et al. 1998) (Table 2). The dissociation constants of carbonic acid in seawater (K1, K2) were taken from Lueker et al. (2000), for hydrogen sulphate from Dickson (1990), for boric acid from Uppström (1974), and the pH was given on the total scale.

Table 2: Water parameters from both Ω_{arag} conditions and from X-Huinay, Comau Fjord. During the experiment, temperature, salinity, oxygen and pH on the total scale (pH_T) were measured daily, and dissolved inorganic carbon (DIC), dissolved organic carbon (DOC) and total alkalinity (TA) were measured after seawater exchange. Aragonite saturation state (Ω_{arag}) and atmospheric partial pressure of CO_2 (pCO_2) were calculated from dissolved inorganic carbon (DIC) and pH_T using the CO2Sys (Lewis et al. 1998) programme. X-Huinay 2014, 2015 data are from Rossbach et al. (2021) and X-Huinay 2019 data from Beck et al. (2022). All values are expressed as mean ± standard deviation (SD). n.d.= no data.

Condition	pCO_2 (ppm)	Temperature (°C)	O_2 (%)	Salinity	DIC (μmol kg^{-1})	pH_T	TA (μmol Kg^{-1})	Ω_{arag}
$\Omega_{arag} \geq 1$	481.5 ± 77.0	12.2 ± 0.4	93.8 ± 6.3	31.7 ± 0.5	2,439.2 ± 98.1	8.0 ± 0.1	2,788.2 ± 211.8	2.4 ± 0.3
$\Omega_{arag} < 1$	1,712.5 ± 76.8	13.1 ± 0.3	93.1 ± 4.9	31.9 ± 0.4	2,736.6 ± 65.6	7.6 ± 0.1	2,823.9 ± 57.6	0.9 ± 0.0
X-Huinay 2014	n.d.	11.5 ± 0.5	n.d.	32.5 ± 0.1	n.d.	7.63 ± 0.02	n.d.	n.d.
X-Huinay 2015	955 ± 42	11.5 ± 0.5	n.d.	32.7 ± 0.1	2,182 ± 32	7.7 ± 0.02	2,234 ± 36	0.98 ± 0.05
X-Huinay 2019	843.7 ± 297	12.5 ± 0.7	n.d.	31.9 ± 0.8	2,064 ± 43.7	7.7 ± 0.1	2,138.6 ± 34.2	1.1 ± 0.3

4.5.4 Polarized light microscopy (PLM)

A total of 14 coral recruits, seven under $\Omega_{arag} = 2.4$ and seven under $\Omega_{arag} = 0.9$ (Fig. 8), were reared *in vivo* in the PDMS chamber under an inverted polarized light microscope (PLM) (Zeiss Axiovert 200M, Carl Zeiss, Oberkochen, Germany). The PLM allowed to detect the occurrence of the first crystals deposited on the glass substrate on the aboral side of the recruit by the appearance of a typical cross-shaped conoscopic interference pattern (the determination of the onset of crystal formation with this method is described e.g., in Seepma et al. (2021)). This method allowed us to better define the onset of the calcification, together with the classification of three growth stages in each condition, based on the lateral extension of the coral skeletal structures (Fig. 1). See the results section for a description of the growth Stages 1–3.

During the development of the coral skeleton in both conditions, time-lapse photographs were taken through the PLM in both conditions to determine the basal plate crystals growth area (BPG) until its maximum diameter. BPG was calculated by measuring the lateral expansion of the BP from Stages 1–3 until it was completely closed. For both conditions, three coral recruits were used (Fig. 8).

For Stages 1–3, the microscopic integrity and mineral composition of the crystals were examined by scanning electron microscopy (SEM) and confocal Raman microscopy (CRM), respectively, for both conditions (Fig. 8). The SEM, CRM, and BPG procedures are described in detail below.

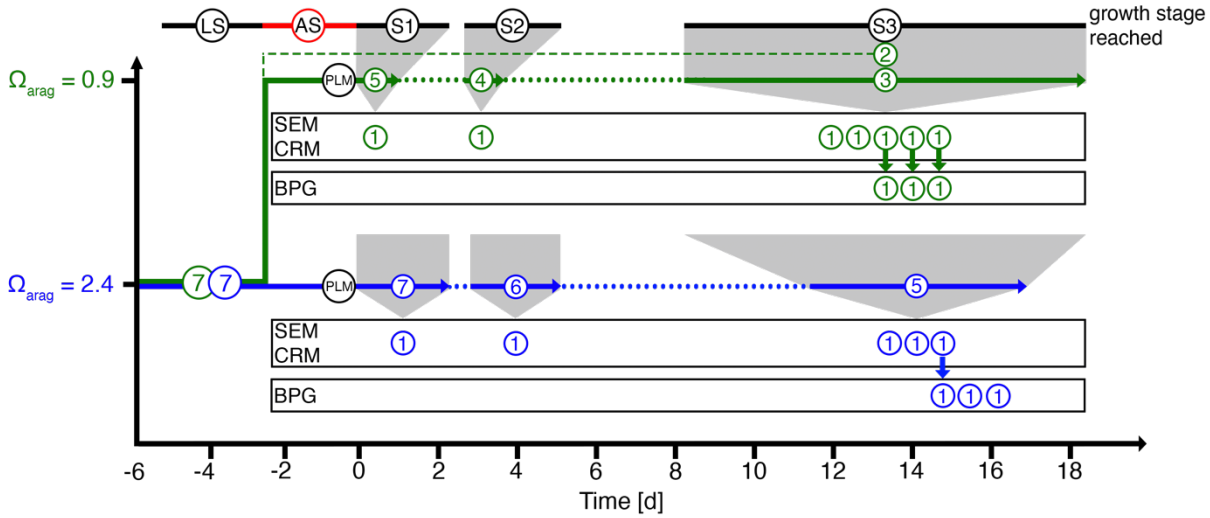

Figure 8: Experimental design showing interval time and number of *Caryophyllia huinayensis* specimens used in the larval stage (LS), attachment stage (AS, red line) and growth stages (1–3) per condition. The numbers in circles are the number of corals studied at each time step. See main text for description of Stages 1–3. In both conditions, the LS was maintained under Ω_{arag} = 2.4 (blue line) until larval attachment. Here, 14 recruits were immediately transferred to the PDMS chamber, where they settled and were reared *in vivo.* Seven recruits were reared under PLM under Ω_{arag} = 2.4. During the development of the recruits, one was collected at Stage 1, one at Stage 2 and five at Stage 3. Recruits in Stage 1 and 2 were used for SEM and CRM analysis. Of the five recruits collected in Stage 3, three were used for basal plate crystals growth area (BPG) measurements, and three for SEM and CRM analysis, where one of the recruits was used for both methods (blue arrow). In the Ω_{arag} = 0.9 condition (green line), seven recruits were reared under PLM. During their development, one recruit was collected at Stage 1, one at Stage 2 and five at Stage 3. Two additional recruits, who were not studied under PLM, settled on the same glass coverslip as a recruit that was continuously studied under the PLM (green dashed line). Of the five recruits collected in Stage 3, five were used for SEM and CRM analysis, and three were used for BPG measurements, where three of these recruits were used for both methods (green arrows).

4.5.5 Scanning electron Microscopy (SEM) procedure and settings

The skeletal microstructure of coral recruits from Stage 1 (n = 2, one recruit per condition), Stage 2 (n = 2, one recruit per condition), and Stage 3 (n = 8, three and

five recruits at Ω_{arag} = 2.4 and Ω_{arag} = 0.9, respectively, Fig. 8) was analysed using images taken under a JEOL SEM (JSM-IT100, New England, USA). Following Gilis et al. (2014), prior to SEM analysis, all organic material from the recruit attached to the coverslip was removed by immersion in 1 % sodium hypochlorite (NaClO) for 2 × 15 min, followed by 2 × 10 min in filtered (0.2 μm tap) reverse osmotic water (conductivity: 18.0 MΩcm; Sartorius Arium Pro, Sartorius Corporate Administration GmbH, Göttingen, Germany) for rinsing, and immersed in 99 % ethanol until analysis.

The coral recruits were left attached to the coverslip to maintain skeletal integrity while mounted on stubs with a carbon tab. A polyp was detached from the glass substrate by an external mechanical force and then placed directly onto a carbon tab (Suppl. Fig. 1a). The recruits were not coated with a conductive layer of gold, but surrounded with copper (Cu) tape, which was connected to the carbon tab and provided an exit path for the electrons. High-resolution images of the corallite, BP and primary septa of Stage 1–3 of each condition were taken at 10.0 kV, 1.7 μA filament current (Philips XL 30) in low-vacuum mode at 19–53 Pa.

4.5.6 Raman microscopy (CRM) and assessment of corallite height

After SEM imaging, the skeletal mineralogy of the coral recruits was analysed by means of CRM using a WITec alpha 300R (WITec GmbH, Germany) equipped with a 488 nm laser diode. The instrument configuration allowed measuring single skeletal elements with an aerial resolution of ~250 nm (25 μm confocal pinhole and 50× objective with an NA = 0.9). Spectral analysis and data processing were performed using the WITec Control Six software (version 6, WITec GmbH, Germany) (Suppl. Fig. 2). For details on CRM measurements on coral skeletons see Wall and Nehrke (2012).

The WITec Control Six software was also used to determine the mean corallite height at Stage 3 for three recruits from the Ω_{arag} = 2.4 and five recruits from Ω_{arag} = 0.9 conditions (Fig. 6a and Fig. 8). Mean corallite height was determined from the CRM Z-motor readings when the objective was focussed on the top of the calyx relative to the surface of the cover slip on which the coral grew.

4.5.7 Analysing the basal plate extension and diameter

Skeletal formation was assessed in recruits reared under Ω_{arag} = 2.4 and Ω_{arag} = 0.9 seawater conditions by analysing the extension of the mineralized BP. For this, time-lapse photographs were taken of the aboral side of the recruits using an AxioCam MRc camera attached to the PLM. Daily photographs were taken using the ZEN 2 pro software (©Carl Zeiss Microscopy, GmbH, 2011). Crystal measurements were started (time 0) when the first crystals deposited on the glass coverslip with a minimum length of 5.7 μm were detected at a 10× magnification, identified by their birefringence properties revealed by cross-polarised light. The daily changes in the cumulative cross-sectional area (μm^2) of individual crystals was used as the BP crystals growth area.

The software Adobe Photoshop® CC was used to process the PLM photos (Suppl. Fig. 3a) to determine the BP formation quantitatively for three recruits per condition (Fig. 8). This was done by scaling RGB photographs for calibration and converting them to high contrast black and white images using the "Threshold" filter (Suppl. Fig. 3b), which allowed automatic selection of crystals using the "Magic Wand" tool (Suppl. Fig. 3c). The automated selection was then manually checked for accuracy in each image, followed by the measurement of the crystal area (Suppl. Fig. 3d). To account for differences in the BP size of the recruits, we normalized by dividing the daily BP crystals area by the final BP crystals area within the corresponding recruit.

To compare the BP diameter at stage 3 (n = 6, three recruits per condition), based on the BP diameter of the recruits is not a circle, the BP diameter was approximated by the equivalent spherical diameter. The BP area (A) was measured using the "lasso tool" of the Photoshop software (summing up all the pixels within the contour of the BP) assuming an equivalent circle area:

$$BP\ diameter = \sqrt{\frac{4 \times A}{\pi}}$$

4.5.8 Statistical analysis

The RStudio software version 4.2.2 (2022.12.0+353) (RStudio 2022) was used for all statistical analyses. To test the effect of OA on the skeletal formation of CWC recruits under Ω_{arag} = 0.9, we evaluated the skeletal microstructures formation at the different stages (Suppl. Table 1), the BP crystal area and diameter, and corallum height using different models (Suppl. Table 2). In detail, we tested the Ω_{arag} = 0.9 effect on the size of the crystals CP, DS, FBS, and FS, and the corallum height and BP diameter using linear mixed models (LMM), and generalized linear models (GLM) depending on best data fit and model robustness. For further detail on the models build up and evaluated factors please refer to the Suppl. Table 1. The LMM, and GLM were fitted using the function *lmer* from the "lme4" package (Bates et al. 2014). Further, to test for differences in the normalized BP crystal area between conditions (Ω_{arag} > or < 1) and growth stages (Stages 1–3; n = 6, three recruits per condition) we used a generalized additive model (GAM). The GAM was fitted using the "mgcv" package (Wood 2011) and considering BP area and Ω_{arag} as fixed factors, and the variable time as a random factor (*s(time (d)), k=3;* see Suppl. Table 1). Model diagnosis was performed accordingly for each model type. Model comparisons were conducted, where relevant, through goodness of fit assessments, likelihood ratio tests, and the Akaike´s information criterion (AIC) for final model selection in each case. Statistical significance has been considered if the *p*-value were < 0.05.

4.6 Acknowledgments

We thank Esther Lüdtke and Mandy Kuck for their tireless assistance in the maintenance of the aquarium and corals and Susana Simancas for her statistical support. The research is part of the Ph.D. project of T.H. at the University of Bremen, carried out at the Alfred Wegener Institute Helmholtz-Zentrum für Polar- und Meeresforschung (AWI). T.H., J.L. and C.R. were supported by AWI (PACES II, and 'Changing Earth – Sustaining our Future', Topics 4.2 and 6.1). T.H. received additional financial support by Deutscher Akademischer Austauschdienst (DAAD) (grant-

91608520) and Agencia Nacional de Investigación y Desarrollo (ANID) (grant-62170011), Chile. Thanks are due to the Director and staff of San Ignacio del Huinay Foundation for contributing to the development of this research. The specimens were exported from Chile under CITES permits 14CL000003WS, 14CL000014WS, 15CL000004WS, 19CL000015WS, and imported to Germany under E00154/14, E00095/15, E00725/15, and E08854/1.

4.7 Supplementary figures

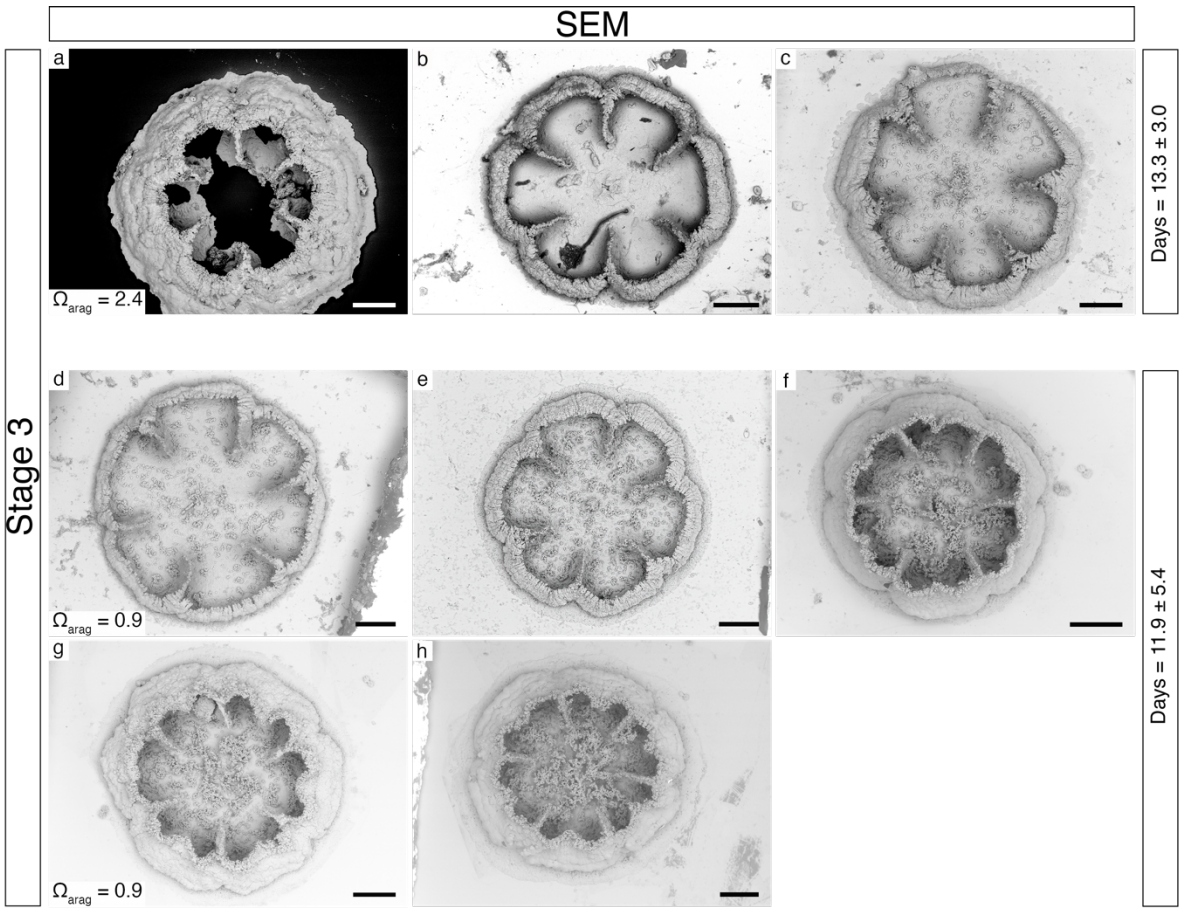

Supplementary Figure 1: SEM images of all *Caryophyllia huinayensis* recruits reaching Stage 3 under Ω_{arag} = 2.4 (a–c, n = 3) and Ω_{arag} = 0.9 (d–h, n = 5) conditions. Days (d, mean ± SD) represent the time from larval attachment until recruits reach growth Stage 3. Images “g” and “h” are the two additional recruits settled on the same glass coverslip as the recruit from image “f”. Note: The recruit in the image “a” has a broken BP because it was detached from the glass substrate by mechanical force and was then placed on a carbon tab. Scale bars: 200 *µ*m.

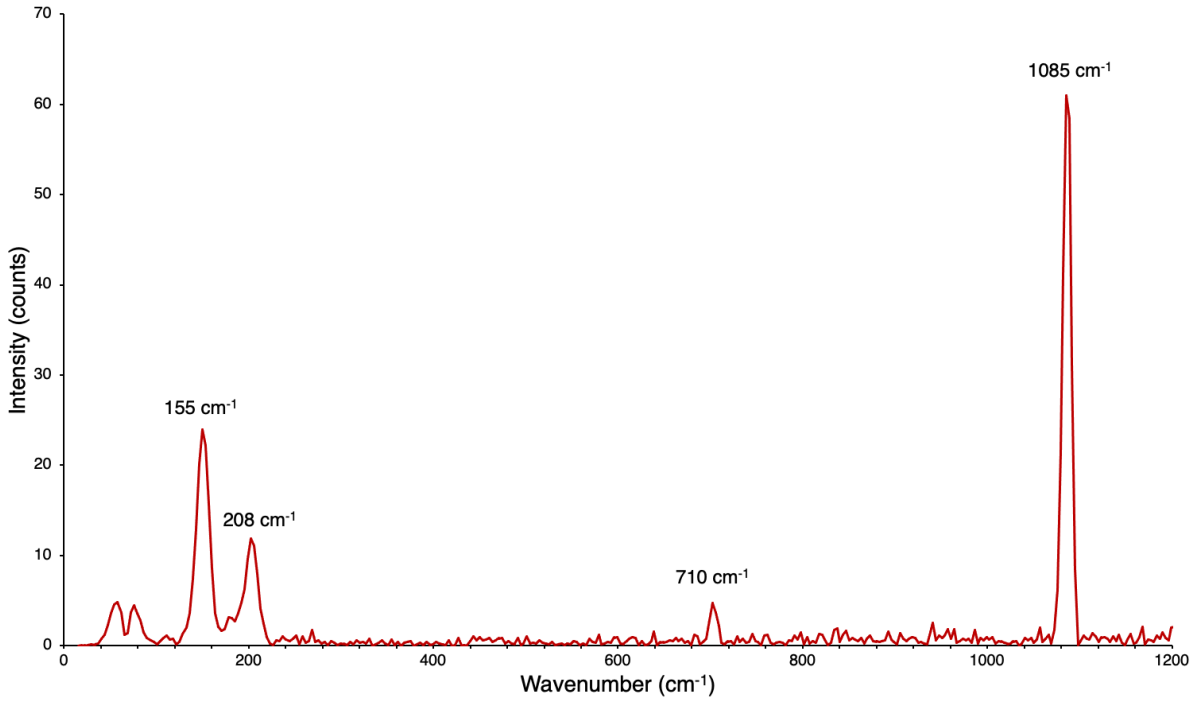

Supplementary Figure 2: Confocal Raman spectra obtained from aragonite extracted from a single crystal, which was considered representative of all crystal types observed during the recruits' growth from Stage 1–3 under Ω_{arag} = 2.4 and Ω_{arag} = 0.9 conditions.

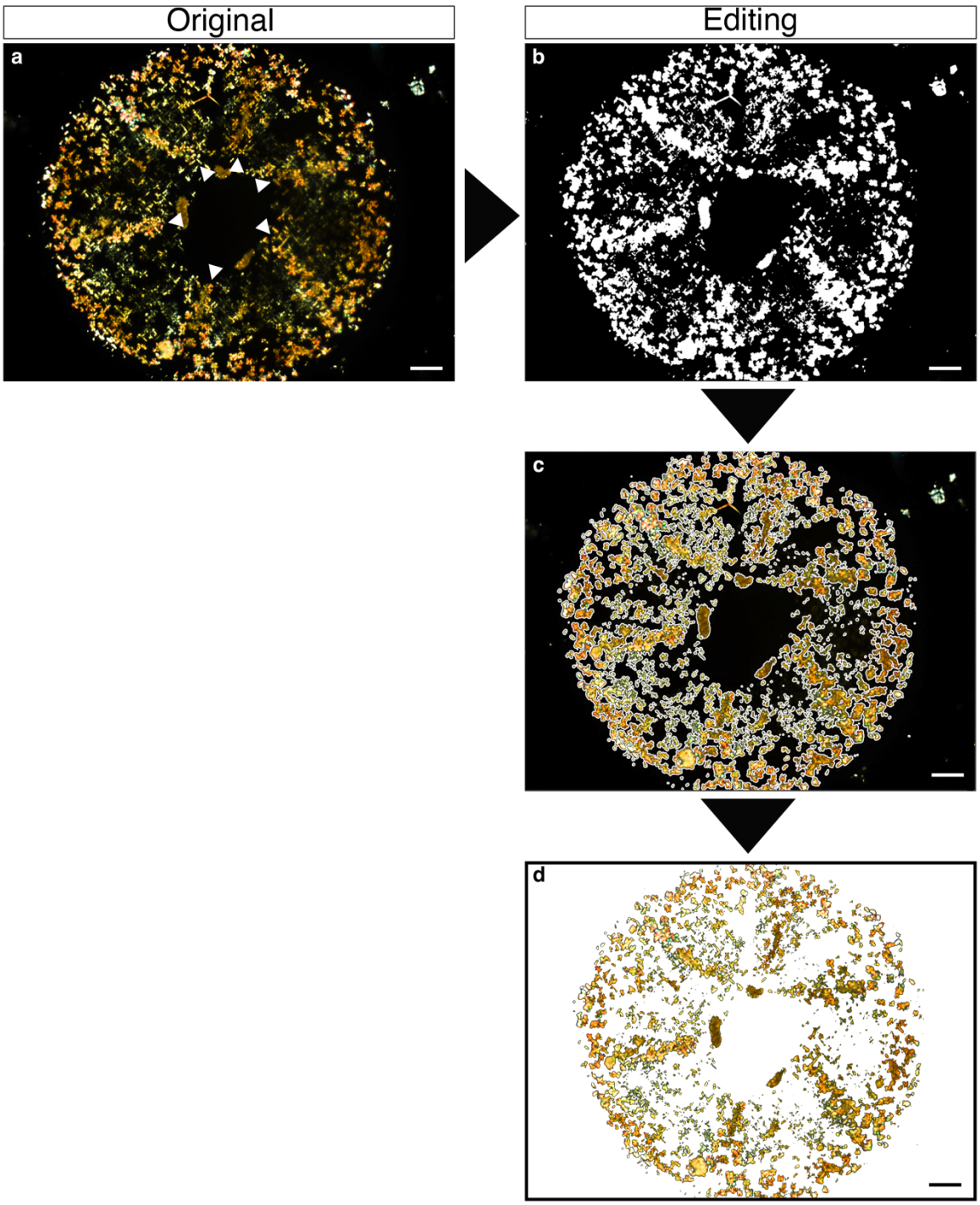

Supplementary Figure 3: Workflow from the original photo (left panel: a) obtained by the PLM to the editing process (right panels: b, c, d) in Adobe Photoshop® CC for measuring the BP area of *Caryophyllia huinayensis* recruits. (**a**) The RGB photo showing the first deposits of crystals forming the primary septa (white arrowheads) was (**b**) converted to high contrast black-and-white images using the "Threshold" filter. The "Magic Wand" tool was then used to automatically select the now white crystals (**c**). (**d**) The automatic crystal selection was manually corrected in case of inaccuracy. The measured crystal coverage area is expressed in μm^2 and the time-lapse image series is expressed as μm^2 day^{-1}. Scale bars 100 μm.

Supplementary Table 1: Linear mixed model (LMM), generalized linear model (GLM), and Generalized additive models (GAMs) results for the crystal size comparison between condition at each growth Stage (1–3) of the crystals circular platelet (CP), dumbbell-like shape (DS), flat basal shape (FBS), and fusiform-like shape (FS), and normalized basal plate area growth (BPA of *C. huinayensis* recruits.

Factor	**n**	**Model**	**F**	***df***	***p* value**
CP	50	LMM	1.975	48	0.166
DS	48	LMM	0.171	45	0.681
FBS	48	LMM	2.692	42	0.108
FS	50	GLM	–	48	0.063
BPA	6	GAMs	–	1	0.92

Note: LMM, type III analysis of variance with Satterthwaite`s approximation method of degrees of freedom.

Supplementary Table 2: Model equations for Generalized Additive Model (GAM), Linear Mixed Model (LMM), Generalized Linear Model (GLM), and Linear Model (LM) used for BP crystal growth area (BPA), crystal size, corallite height and BP diameter (ø). BP: basal plate, CP: circular platelet, DS: dumbbell-like structure, FBS: flat basal structure, and FS: fusiform-like structure. In the model equations, Condition denotes Ω_{arag} = 2.4 and Ω_{arag} = 0.9, s denotes the smoothing function, Cs denotes crystal size, Ch denotes corallite height, and CBP denotes corallite basal plate diameter.

	Basal plate area (BPA)	**Crystal size (Cs)**		**Corallite (C)**	
Model equation	gam(BPA ~ Condition + s(Time, k = 3) + s(Time, Condition, k = 3)	CP, DS, FBS lmer(Cs ~ Condition + (1Istage))	FS glm(Cs ~ Condition)	Height (h) lm(Ch ~ Condition)	BP ø lm(CBP ~ Condition)

5

Seasonal reproduction of a cold-water coral in a naturally acidified Chilean fjord

Thomas Heran[a,b,c], Rhian Waller[d], Claudio Richter[a,b], Verena Häussermann[e,f], Susana Simancas-Giraldo[a,b], Jürgen Laudien[a]

[a] Alfred-Wegener-Institut Helmholtz-Zentrum für Polar- und Meeresforschung, Am Alten Hafen 26, 27568 Bremerhaven, Germany.

[b] University of Bremen, Bibliothekstraße 1, 28359 Bremen, Germany.

[c] POETA Program (Programa de Observación de los Ecosistemas Terrestres y Acuáticos), Pontificia Universidad Católica de Valparaíso, Escuela de Ciencias del Mar, Avda. Brasil, 2950 Valparaíso, Chile.

[d] University of Gothenburg, Tjärnö Marine Laboratory, Strömstad, 452 96 Sweden.

[e] Fundación San Ignacio del Huinay, Casilla 462, Puerto Montt, Chile.

[f] Universidad San Sebastián, Escuela de Ingeniería en Gestión de Expediciones y Ecoturismo, Facultad de Ciencias de la Naturaleza, Lago Panguipulli, 1390 Puerto Montt, Chile.

Corresponding author
Thomas Heran
ORCID: 0000-0001-9970-9842
e-mail: thomas.heran@awi.de

Keywords: CWC, *Caryophyllia huinayensis*, gametogenesis, cyclical hermaphrodite, brooder, seawater pH

Prepared for ***Coral Reefs***, Springer

5.1 Abstract

Scleractinian cold-water corals (CWCs) are important habitat builders in the Chilean fjords, but their reproductive biology and sensitivity to ocean acidification in their natural environment is largely unknown. Here, we investigated the seasonal reproduction of the scleractinian CWC *Caryophyllia (Caryophyllia) huinayensis* along a natural seawater pH gradient in Comau Fjord, Chile. *C. huinayensis* proved to be an asynchronous cyclical hermaphrodite brooder, showing year-round occurrence of eggs and planula larvae. Most oocytes within an individual were at a similar stage, whereas asynchrony in oocyte development was observed among individuals collected in the same season and study site. While we found no seasonality in oocyte abundance, oocyte size was cyclical, with smallest vitellogenic (V) oocytes in austral winter, and largest V oocytes in the austral autumn. As brooded larvae were observed throughout the year, we conclude that V oocytes of all sizes were fertilized. Spatio-temporal variations in V oocyte size and abundance showed no consistent relation to corresponding variations in seawater pH, temperature, and oxygen, suggesting a mix of environmental and endogenous factors affecting *C. huinayensis* reproduction.

5.2 Introduction

Scleractinian cold-water corals (CWCs) are recognized as habitat builders for a rich associated fauna (Roberts et al. 2006; Braga-Henriques et al. 2013). In their shallower water depth range at the high latitude Chilean fjord region (Försterra 2009; Häussermann et al. 2021, 2024), they have also been described as habitat-forming species (Försterra et al. 2017; Häussermann et al. 2024). Despite their ecological importance in the benthic communities and the recent advances in knowledge of their biology and ecology, there is still too little information available for most CWC species compared to scleractinian warm-water corals (WWCs) (Roberts et al. 2009). The main reasons for this are the logistical challenges involved in studying these species, as their collection is complex and often results in small sample sizes without systematic seasonal sampling.

Sexual reproduction is essential for every species to successfully maintain and expand their populations. Among the over 3,000 known CWC species, reproductive biology information is available for less than 4 % (Waller et al. 2023). Of these, 23 species are scleractinian CWCs (Waller et al. 2023). Reproduction in scleractinian CWCs is predominantly characterized by gonochorism, where polyps are either male or female (Waller et al. 2008; Roberts et al. 2009; Mercier et al. 2011; Waller and Tyler 2011; Pires et al. 2014). In contrast, most scleractinian WWC species are hermaphroditic, with both sexes occurring in a single individual (Harrison 2011). Only three scleractinian CWC species have been identified as cyclic hermaphrodites, exhibiting mature gametes for a single sex at any given time, even though gametes of both sexes were found to be present within a single mesentery (Waller et al. 2005). Once the mature gametes are spawned, the gametes of the other sex continues to grow until mature, so that gametogenesis follows a continuous cycle (Waller et al. 2005, 2023). These species are described as broadcast spawners, releasing their gametes into the water column for external fertilization. This is in contrast to brooding species, where fertilisation and larval development occurs inside the polyp. Additionally, these hermaphrodite species are suggested to release their gametes quasi-continuously and asynchronously, meaning that gamete release occurs over an extended period rather than in a tightly coordinated event (Waller et al. 2005, 2023).

The oceans in the high latitudes are considered to be the most vulnerable to an increase in atmospheric CO_2, as cold water can store more dissolved gases (Gruber 2011). When CO_2 dissolves in seawater, carbonic acid is formed, which lowers the carbonate ion concentration and the seawater pH, a process known as ocean acidification (OA). Since pre-industrial times, the global sea surface pH has decreased by 0.1 units (Orr et al. 2005; Jiang et al. 2019), and is predicted to decrease by a further 0.3 units by the end of the century under a "business-as-usual" scenario (Pörtner et al. 2019; IPCC 2021). As OA limits the saturation state of aragonite, a crystalline form of calcium carbonate that is the building substance for coral skeletons (de Putron et al. 2011), scleractinian CWCs have long been considered especially vulnerable to OA (Guinotte et al. 2006; Turley et al. 2007; Guinotte and Fabry 2008).

Under the most conservative climate change scenarios, it is projected that between 28 % and 100 % of the CWC habitats will be located in aragonite-undersaturated waters by the end of the century (Hennige et al. 2015; Morato et al. 2020). Although scleractinian CWCs are thought to be sensitive to OA (Guinotte et al. 2006; Turley et al. 2007; Guinotte and Fabry 2008), they may be able to acclimatize (Leung et al. 2022) if they have sufficient energy reserves (Büscher et al. 2017; Maier et al. 2020; Martínez-Dios et al. 2020; Beck et al. 2022; Wall et al. 2023). For instance, the scleractinian CWCs *Desmophyllum dianthus* and *Caryophyllia huinayensis* occur in Comau Fjord, Chile, where low seawater pH occurs naturally (Fillinger and Richter 2013; Cairns, Häussermann & Försterra, 2005).The capacity of scleractinian CWCs to withstand low seawater pH depends on their ability to regulate the pH and dissolved organic carbon (DIC) (Venn et al. 2011) at the calcification site (Allemand et al. 2004). In acidified waters, calcification may become more energy-consuming, requiring the corals to modify their energy assimilation and prioritise its allocation by slowing down tissue growth and reproduction (Tsounis et al. 2012; Maier et al. 2020).

Several studies have shown that OA has a negative effect on the sexual reproduction of scleractinian WWCs, including reduced sperm motility and development (Morita et al. 2010; Marchini et al. 2021), and reduced fertilization (Albright and Mason 2013; Marchini et al. 2021). Although contrasting studies have shown no effect on gametogenesis and reproduction (Fine and Tchernov 2007; Gizzi et al. 2017; Caroselli et al. 2019; Rossin et al. 2019).

This study is the first to investigate the reproductive biology of the scleractinian CWC *C. (Caryophyllia) huinayensis* Cairns, Häussermann & Försterra, 2005. We described the sexuality, reproductive strategy, seasonal pattern of gametes development, fecundity, and potential relative fecundity (PRF; i.e., number of mature oocytes per polyp) using histological techniques. Moreover, we evaluated the effects of seasonal variability of seawater low pH on the reproduction of this species by assessing its effects on the oocyte size and PRF, by comparing naturally acidified sites in Comau Fjord in Chilean Patagonia.

5.3 Material and Methods

5.3.1 Organisms and study sites

The CWC *C. huinayensis* is a solitary, small (20 mm high, 7.6 mm ø) azooxanthellate coral (Cairns et al. 2005), which can reach high densities in some locations, up to 2,211 ± 180 ind. m^{-2}, Wurz (2014). It is a brooding species, and its larvae have been observed to be released throughout the year in specimens maintained in aquaria, albeit with a peak in austral winter (Heran et al. 2023). In Comau Fjord, located in the northernmost part of Chilean Patagonia (Fig. 1), this species was found from 11 to 265 m depth (Wurz 2014; Försterra et al. 2017). On the Chilean continental slope, it thrives between 740 and 870 m water depth (Sellanes et al. 2008).

Comau Fjord is 45 km long and 2–8.5 km wide (Häussermann et al. 2012) and has a tidal range of up to 7.5 m (Sobarzo 2009). Surface water temperature can reach 17 °C, although it ranges between 10.6 ± 0.2 °C and 12.6 ± 0.9 °C below the thermocline at 20–50 m water depth (Rossbach et al. 2021). The area receives high precipitation which, together with meltwater from a glacier, results in a brackish surface layer and a halocline between 7 and 15 m water depth, followed by fully marine conditions below the halocline (Sobarzo 2009; Fillinger and Richter 2013; Garcia-Herrera et al. 2022).

A total of 136 coral polyps were collected by scientific SCUBA diving between 23 and 30 m water depth at the three study sites Liliguapi, X-Telele and X-Huinay (Fig. 1c) in austral winter (July 2019), spring (November 2019), summer (February 2021), and autumn (April 2021) (Table 1).

Table 1 Study sites and their geographical coordinates, collection dates, season, and depth, and the total number of polyps collected per season.

Study site	Latitude Longitude	Date	Season	Depth (m)	N° of polyps collected
Liliguapi	42.162833°S 72.596467°W	26.07.2019	Winter	20–30	10
		08.11.2019	Spring		10
		24.02.2021	Summer		10
		20.04.2021	Autumn		9
X-Telele	42.279183°S 72.458683°W	27.07.2019	Winter	20–30	10
		07.11.2019	Spring		10
		19.02.2021	Summer		10
		13.04.2021	Autumn		10
X-Huinay	42.386883°S 72.462867°W	25.07.2019	Winter	20–30	10
		06.11.2019	Spring		10
		18.02.2021	Summer		9
		11.04.2021	Autumn		10

Zooplankton biomass in the water column of Comau Fjord is about three times higher in summer than in winter, where a peak in abundance occurs in spring, probably linked to the spring phytoplankton bloom (Garcia-Herrera et al. 2022). This high biomass combined with the influx of terrigenous organic matter, primarily from freshwater runoff, is degraded by bacteria in the water column, particularly in the deeper fjord. This aerobic degradation of organic matter entails both the consumption of oxygen, resulting in an oxygen-depleted water layer with a minimum value of 91 μmol O_2 l^{-1} below 300 m water depth (Fillinger and Richter 2013), and the production

of CO_2 (Thauer 2011). The latter, in combination with methane and sulphide seeping out of the cracks in the rock wall, which concentrates in the water column (Försterra et al. 2014), are responsible for the low seawater pH observed in the central (on an horizontal axis) area of the fjord (Fig. 1c), from the shallow water to the sea floor (Fillinger and Richter 2013).

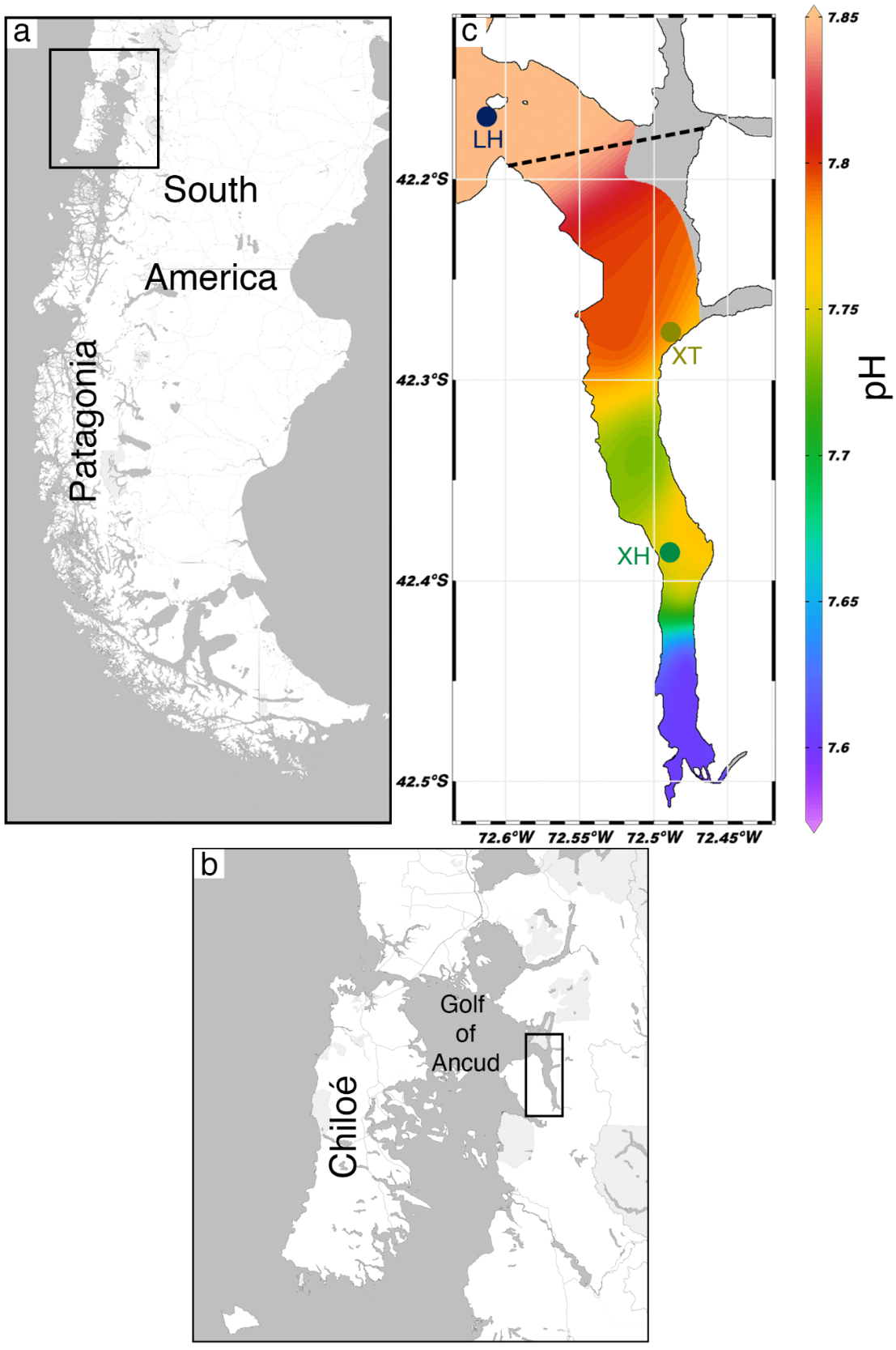

Fig. 1 Study area and collection sites of the scleractinian CWC *C. huinayensis*. (a) Overview of Patagonia. The black rectangle indicates the area of Chiloé Island and the Gulf of Ancud (b) connecting to Comau Fjord, denoted with the black rectangle. (c) Comau Fjord with annual mean seawater pH,

measured from discrete water samples taken at *ca.* 5 m distance from the coral wall at 23–30 m water depth between July 2019 and April 2021, and the study sites Liliguapi (LH: blue), X-Telele (XT: yellow) and X-Huinay (XH: green). The dashed line indicates the mouth of the fjord.

5.3.2 Environmental data

At each study site (Fig. 1c), all environmental data was obtained at 23–30 m water depth, accounting for the *ca.* 7 m tide (Försterra 2009; Sobarzo 2009), in close proximity to the sampled coral communities. Water temperature was recorded (Tidbit® v2 logger, Onset computers, Bourne, USA; 0.02 °C resolution, ±0.2 °C accuracy) at 30-min intervals throughout the study period (July 2019–April 2021) to quantify mean annual and seasonal temperature variability. A Conductivity Temperature Depth profiler (CTD) (AML PlusX, AML Oceanographic, Victoria, Canada) was used to measure salinity (PSU scale) and oxygen [μmol kg^{-1}] (Aanderaa 4831F, Xylem, Bergen, Norway; resolution < 0.032 [μmol kg^{-1}], < 0.256 [μmol kg ^{1}] accuracy) twice per season (July and November 2019, and February and April 2021). Discrete water samples for measuring seawater pH were taken three times per season at each study site using a Niskin bottle. Seawater pH measurements were carried out using a potentiometric method: A 25-ml seawater sample brought to 25.0 °C was measured with a Metrohm 713 pH meter (input resistance > 1,013 Ω, 0.1 mV sensitivity, and nominal resolution 0.001 pH units) with a glass combined-double junction Ag/AgCl electrode (Metrohm model 6.0219.100). Prior to each seawater pH measurement, the electrode was calibrated at 25 °C with an 8.089 Tris buffer.

5.3.3 Caryophyllia huinayensis *histology and sexuality*

Collected polyps were fixed in borax buffered 4 % formalin and decalcified in 100 % Rapid Bone Decalcifying Solution (Thermo Scientific™ Shandon™ TBD-1™, Tudor Road, UK) for 15–30 minutes. Decalcification was complete when CO_2 bubbles no longer formed as a result of dissolution of the calcium carbonate skeleton. For dehydration, the skeleton-free tissue was placed in 70 % ethanol and the concentration was successively increased in 10 % steps every 1 h up to 100 %

ethanol. The tissue was then immersed twice in xylene for 1 h and then transferred into paraffin wax (Polarit, Labortechnik Süsse, Hessen, Germany) at 60 °C (one polyp per wax block), where it underwent four wax changes over a period of 2.6 h (vacuum Tissue-Tek VIP® 6, Sakura Finetek Europe B.V., Netherlands). After cooling, the wax blocks were cut into 3 μm thick sections. A distance of 45 μm was maintained between each longitudinal section to prevent double counting or measurement of oocytes, given that the width of an oocyte nucleus ranged from 19.2 μm to 55.2 μm, with a mean of 45 μm ± 8.67 SD (based on measurements from 100 oocytes from two *C. huinayensis* individuals).

From the 136 collected polyps, 118 polyps were stained with haematoxylin-eosin (HE) and used for the reproductive cycle studies. The remaining 18 polyps were transversally sectioned and stained with Masson's trichrome to facilitate gamete identification and imaging (Fig. 2c, d, f). Masson's trichrome stain facilitates the identification of reproductive structures by colour differentiation of the nucleus, cytoplasm, fibres, and other cellular elements (Berzins et al. 2021). These polyps were not included in the quantitative analysis, since the 100 μm cutting method used for this stain was not comparable to the aforementioned 45 μm distance used for the HE stained ones.

Histological sections were examined under a Zeiss Axioscope microscope with an Olympus (DP70) camera mounted using a 40 × magnification. The oocytes and spermatocysts were classified according to maturity stage following Goffredo et al. (2010), and the sexuality (female, male, and hermaphrodite) of each polyp was determined (Fig. 2).

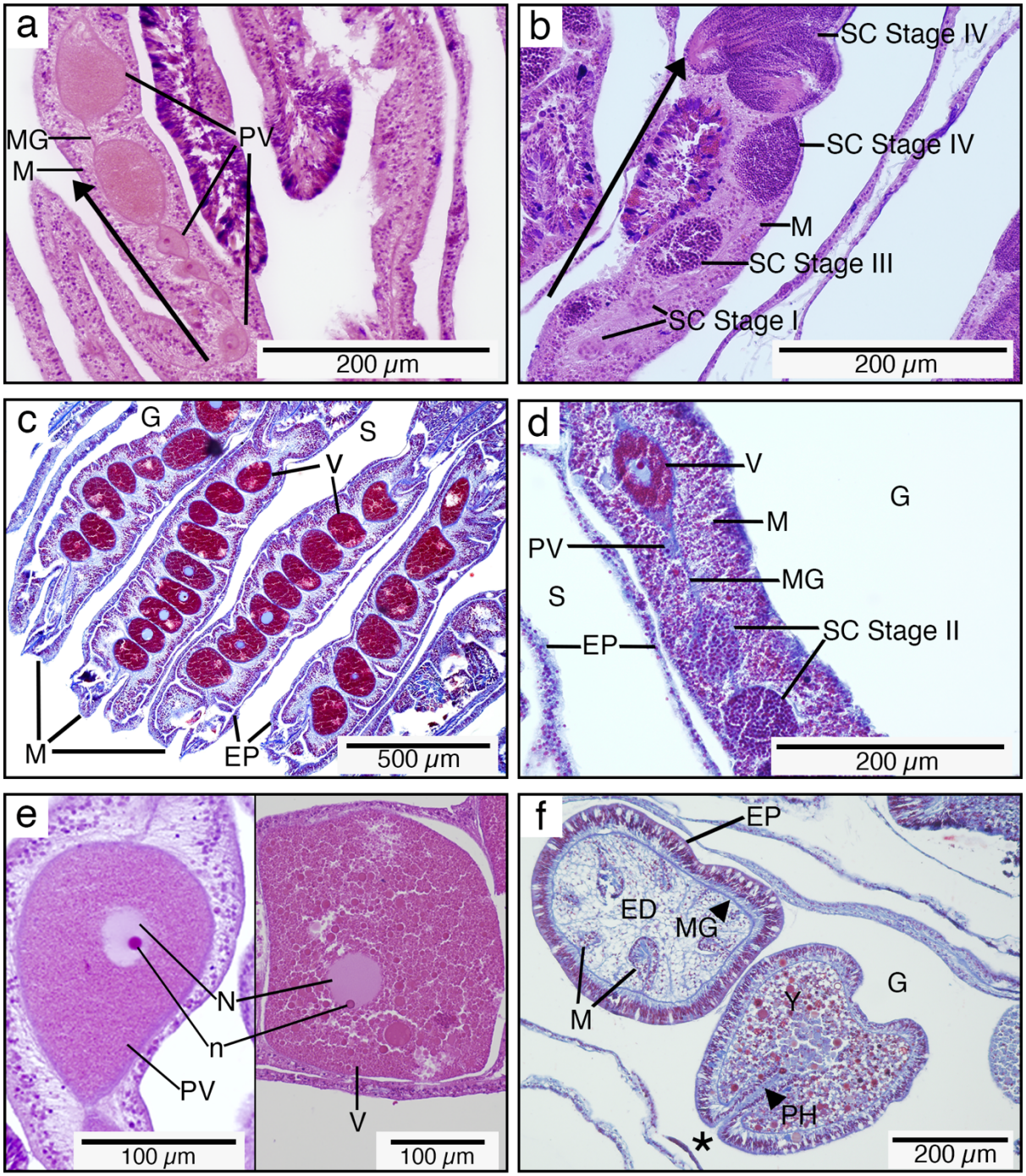

Fig. 2 Images of histological sections of the CWC *C. huinayensis*. Sections were stained with either haematoxylin-eosin (**a**, **b, e**) or Masson's trichrome (**c**, **d, f**). Sections **a**, **b**, **e**, **f** and **c**, **d** were cut longitudinally and transversally, respectively. **a** Section of female polyp with pre-vitellogenic (PV) oocytes developing in the mesoglea (MG) of a mesentery (M). **b** Section of a male polyp with spermatocyst (SC) with different stages of male gametes (Stage I: spermatogonia, [for SC Stage II see **c**], Stage III: elongated spermatids, Stage IV: spermatozoa). The maturity of gametes in sections **a** and **b** increases towards the apical side, denoted with the black arrows. **c** Section of the periphery of a female polyp showing vitellogenic (V) oocytes within the mesenteries. **d** Section of a hermaphrodite polyp showing a V and PV oocyte, and SC with spermatids (SC Stage II) can be seen in the mesentery.

e PV oocyte with a homogeneous content and a V oocyte with a heterogeneous content. Both oocytes show a nucleus (N) and a nucleolus (n). **f** Transverse and longitudinal section of two larvae inside a polyp with epidermis (EP), endodermis (ED; purple pigment surrounding the mesenteries), mesenteries (M), mesoglea, yolk (Y), and the pharynx (PH) connected to the blastopore/oral pore (*). G: gastrovascular cavity, S: septum.

Oocytes were classified into two developmental stages, pre-vitellogenic (PV) and vitellogenic (V), following previous studies on gametogenesis in scleractinians corals (Beauchamp 1993; Kramarsky-Winter and Loya 1998; Kruger and Schleyer 1998; Goffredo et al. 2005, 2010). The structural diagnostic to differentiate the development stages was based on the homogeneous and heterogeneous inner structure of PV and V oocytes, respectively (Fig. 2e). The oocyte size was measured for a maximum of 100 oocytes per polyp. To standardize the measurements and make them comparable with other studies (see for e.g., Flint et al. 2007; Brooke and Järnegren 2013), the diameter of each oocyte was calculated by first measuring its area using the "Lasso" tool of Adobe Photoshop® CC (San Jose, California, USA) and then adapted to a circle using the following formula: $D = 2\sqrt{A/\pi}$, where D is the diameter and A is the area of the oocyte.

Fecundity per polyp was assessed by counting all oocytes (PV and V) at each season and at each study site. Potential relative fecundity (PRF), as defined by Waller et al. (2023), is the total number of V oocytes per polyp, where the term "potential" refers to the maximum number of eggs that can possibly be fertilised and develop into larvae in this brooding species. Larval occurrence was determined by counting the polyps containing larvae.

Maturity stages of spermatocysts were classified into four stages (Stages I to IV), based on the sperm shape and distribution within the spermatocyst of at least 20 spermatocyst per polyp, following the classification from previous works (Goffredo et al. 2005, 2010). If more spermatocysts were present in the section, a maximum of 50 spermatocytes were classified.

In order to assess the relationship between PRF and polyp size, as well as the relationship between polyp corallum and V oocyte size, the morphometry of individual polyps was measured as follows: (1) The diameter of the calyx and the height (*h*) of

the polyp was measured using a caliper with an accuracy of 0.01 mm. (2) The volume (*Cv*) of the corallum was approximated by a cone and calculated using the formula: $Cv = \frac{1}{3} \pi r^2 h$.

5.3.4 Effect of seawater pH on the reproduction

To investigate the effect of the natural seasonal variability of seawater pH on the reproduction of *C. huinayensis*, polyps were collected each season from three study sites (Liliguapi, X-Telele, and X-Huinay) in Comau Fjord, where seawater pH ranged from 8 to as low as 7.7. The effect of the seawater pH was evaluated on V oocyte due to their potential to be fertilized, in contrast to PV, which may be reabsorbed during the vitellogenesis process (Rossin et al. 2019), and PRF. A total of 53 HE stained polyps containing female gametes were analysed, with 447 V oocytes used for the oocyte size assessment. From these V oocytes, 38 % were from Liliguapi, 38 % from X-Telele, and 25 % from X-Huinay.

5.3.5 Statistics

All statistical analyses and graphs in this study were performed using the software R, version 4.2.2 (RStudio 2022). Measures of central tendency and summary statistics including histograms were employed for descriptive analysis of the seasonal gametogenesis. Moreover, we evaluated the effects of seawater pH on the reproduction of *C. huinayensis*. The analysis were performed in two steps: First, we carried out a Principal Component Analysis (PCA) from the package *stats* R Core Team (2023) to assess the effect of seawater pH, temperature and oxygen on the V oocyte size. Second, we evaluated in further detail the effects of the seasonal variation in pH per study site and its interactions on the V oocyte size and PRF. We used Linear Mixed-effect Models (LMM) and Robust Linear Regression (LmRob) from the packages *lme4,* Bates et al. (2014) and *robustbase,* Maechler et al. (2024), respectively. The LMM models considered the seawater pH, the sites (Liliguapi, X-

Telele, and X-Huinay), the seasons, and the interaction between season and pH, and season and site as fixed factors. The corallum volume *Cv* and the polyp individual were included as random factors. The factor corallum volume did not contribute to the variance structure in any of the models, as it was not significant. Thus, it was dropped from the final selected model. To assess the effects of seasonal pH per site on the PRF, the factors pH, season, site and the interaction between pH and site were included in the model. Model diagnostics and fit were evaluated using residuals (Wood 2017) and Pearson correlation plots, together with data leverage (Online Resources 1–3). Model selection was done via model comparisons, using likelihood ratio tests and Akaike´s selection criteria (AIC). Statistically significant differences were determined using ANOVA type II (Zuur et al. 2009) and considered significant for *p*-value < 0.05. Whenever significant results were found, a corresponding posthoc Tukey test was performed using the R package “emmeans” ((Lenth et al. 2019); See Online resources 4–7)

5.4 Results

5.4.1 Environmental analysis

During the entire study period, the highest daily temperature fluctuations of up to 3.4 °C were observed in the austral summer, minimum and maximum temperatures were 9.5 °C and 16.3 °C, respectively (Fig. 3a–c, Table 2). The temperature records indicate a warm phase from November to July (temperature mostly above the average) and a cold phase from July to October (temperature mostly below the average) (Fig. 3a–c).

Measurements of water samples taken with the Niskin bottle and CTD showed that salinity was lowest in winter (31.4, Liliguapi, Fig. 3d, Table 2) and highest in spring (X-Huinay) and summer (Liliguapi) (32.4, Fig. 3d, Table 2). The minimum and maximum pH-values recorded in autumn were 7.6 pH and 8.1 pH, respectively (Fig.

3e, Table 2). For all and within sites, mean oxygen concentration varied less in winter and spring (221.3 ± 20.2 and 220.7 ± 26.1 μmol kg ^{1}) than in summer (210.6 ± 54.1 μmol kg^{-1}) (Fig. 3f, Table 2). At the local scale, these environmental parameters showed high variability between the three study sites.

Table 2 Seawater parameter values at the three study sites, Liliguapi, X-Telele, and X-Huinay, in Comau Fjord. The parameters include temperature, salinity, oxygen and pH and, range (mean). Salinity, and oxygen were measured twice, and pH three times per season, while temperature was measured continuously at a water depth of 23–30 m at each study site. The range pH values in some cases were identical to the mean and, therefore, are not presented. n.d.: no data.

Study sites and dates	Temperature (°C)	Salinity	Oxygen (μmol kg^{-1})	pH
Winter (July 2019)				
Liliguapi	9.5–12.2 (11.0)	31.4–32.3 (32.0)	231.1–256.3 (243.0)	(7.9)
X-Telele	10.1–12.1 (11.3)	31.7–32.3 (32.0)	199.7–253.0 (221.6)	(7.8)
X-Huinay	10.0–12.7 (11.2)	31.9–32.2 (32.1)	171.4–202.5 (189.1)	(7.7)
Spring (November 2019)				
Liliguapi	10.4–13.7 (11.2)	31.9–32.3 (32.2)	208.6–263.4 (230.1)	(7.9)
X-Telele	10.4–13.3 (11.1)	31.7–32.3 (32.1)	214.8–255.3 (239.3)	(7.9)
X-Huinay	10.5–13.7 (11.1)	32.3–32.4 (32.4)	194.8–218.3 (202.1)	(7.8)
Summer (February 2021)				
Liliguapi	11.0–15.7 (12.8)	32.2–32.4 (32.3)	164.8–234.0 (193.2)	(8.0)
X-Telele	10.8–14.7 (11.7)	32.1–32.3 (32.2)	210.7–337.7 (275.1)	7.9–8.0 (7.9)
X-Huinay	10.8–14.9 (12.3)	32.3–32.3 (32.3)	141.7–193.2 (158.7)	7.8–7.9 (7.9)
Autumn (April 2021)				
Liliguapi	11.8–15.4 (12.7)	n.d.	n.d.	7.9–8.0 (8.0)
X-Telele	11.4–14.8 (12.0)	n.d.	n.d.	(8.0)
X-Huinay	11.5–16.3 (12.5)	n.d.	n.d.	7.6–8.1 (7.8)
All seasons				
Liliguapi	(11.9)	(32.2)	(222.1)	(8.0)
X-Telele	(11.5)	(32.1)	(245.3)	(7.9)
X-Huinay	(11.8)	(32.3)	(183.3)	(7.8)

The mean annual seawater temperature at the three study sites are listed in Table 2 and plotted in Fig. 3a–c. With the exception of winter, the mean seawater temperature at Liliguapi was warmer than the other two study sites in all seasons (Table 2). In winter, the minimum temperature of 9.5 °C was recorded at Liliguapi,

while the maximum temperature of 16.3 °C was recorded in X-Huinay in autumn (Table 2). The mean seawater pH decreased from the mouth (Liliguapi) towards the head of the fjord in all seasons (Table 2, Fig. 3e). Oxygen levels at Liliguapi and X-Huinay showed a similar trend throughout the year, with low variability in winter and spring, followed by a marked decrease in summer (Table 2, Fig. 3f). In X-Telele, however, the oxygen concentration increased from the colder to warmer seasons (Table 2, Fig. 3f). The mean salinity at Liliguapi and X-Telele gradually increased from winter (mean 32.0) to summer 32.3 (Liliguapi) and 32.2 (X-Telele), respectively (Table 2, Fig. 3d). At X-Huinay, salinity increased from winter (32.1) to spring (32.4) and decreased in summer (32.3).

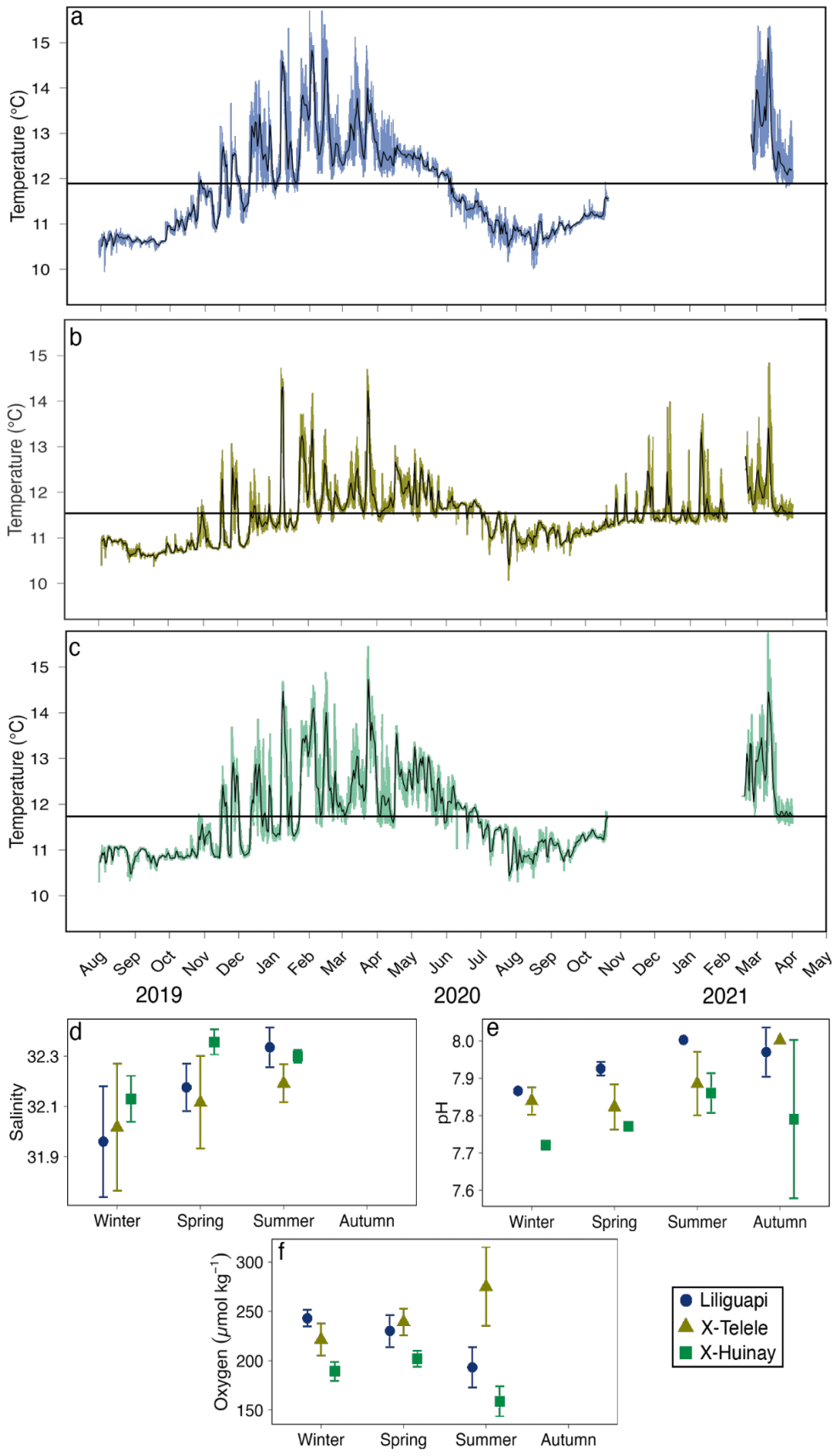

Fig. 3 Environmental parameters of Comau Fjord. **a**–**c** Means of seawater temperature obtained at 23–30 m water depth from the three study sites (Liliguapi (blue): **a**, X-Telele (yellow): **b**, X-Huinay (green):

c) between August 2019 and April 2021. In a, b, c, the translucent lines represent the raw temperature data, while the black lines indicate the daily mean temperature. The horizontal lines indicate the annual mean temperature. Gaps in the temperature curve, and in the records of salinity and oxygen in autumn are due to the lack of access to Comau Fjord during the SARS-CoV-2 pandemic. **d**–**f** Mean ± standard deviation at the three study sites (Liliguapi: blue circle, X-Telele: yellow triangle, X-Huinay: green square) in winter, spring, summer, and autumn (for autumn pH only).

5.4.2 Sexuality

Of the total 118 *C. huinayensis* polyps analysed, 28 % (33 polyps) were "exclusively female", 25 % (30 polyps) "predominantly male", 20 % (24 polyps) "exclusively male", 15 % (17 polyps) "equally female/male", 9 % (11 polyps) "predominantly female", 2 % (2 polyps) "brooding", and 1 % (1 polyp) "non reproductive" (see sexuality classification in Table 3). Throughout the seasons, the sexuality of the polyps varied with most being "exclusively male" in winter, "exclusively female" in spring, "predominantly male" in summer, and "predominantly female and male" in autumn (Table 3, Online Resource 8). Based on the aforementioned information and the pattern of reproduction based on the seasonal occurrence of larvae between polyps, as illustrated in Table 3 and Online Resource 9, it is suggested that *C. huinayensis* is an asynchronous cyclical hermaphrodite.

Table 3 Sexuality of *C. huinayensis* polyps. Percentage of polyps of the corresponding sexuality at the respective location and season. The percentage of these polyps with larvae is given in brackets. Individuals' sexuality were designated as "exclusively female", "exclusively male" if only a single gamete type was present, as "predominantly female" if oocytes were mature and abundant and male germ cells were immature and scarce, and vice versa as "predominantly male", and as "equally female/male" if both gametes were at a similar stage of development, as "non reproductive" if no gametes were detected, and as "brooding" if polyps brooded larvae but were sexually inactive.

	Winter			**Spring**			**Summer**			**Autumn**		
	Liliguapi	X-Telele	X-Huinay	Liliguapi	X-Telele	X-Huinay	Liliguapi	X-Telele	X-Huinay	Liliguapi	X-Telele	X-Huinay

"Exclusively female"	20 (0)	20 (0)	0 (0)	60 (0)	70 (0)	30 (0)	40 (0)	30 (0)	33 (33)	0 (0)	20 (0)	10 (0)
"Exclusively male"	40 (75)	40 (100)	40 (25)	30 (33)	20 (0)	30 (0)	10 (0)	0 (0)	11 (100)	0 (0)	0 (0)	20 (0)
"Predominantly female"	0 (0)	10 (0)	0 (0)	0 (0)	0 (0)	10 (0)	0 (0)	0 (0)	0 (0)	44 (0)	30 (0)	20 (50)
"Predominantly male"	10 (0)	0 (0)	10 (0)	10 (0)	10 (0)	30 (33)	30 (0)	60 (0)	56 (20)	22 (50)	40 (25)	30 (0)
"Equally female/male"	10 (0)	30 (0)	40 (0)	0 (0)	0 (0)	0 (0)	20 (0)	10 (100)	0 (0)	33 (0)	10 (0)	20 (0)
Non reproductive	0 (0)	0 (0)	10 (0)	0 (0)	0 (0)	0 (0)	0 (0)	0 (0)	0 (0)	0 (0)	0 (0)	0 (0)
Brooding	20 (100)	0 (0)	0 (0)	0 (0)	0 (0)	0 (0)	0 (0)	0 (0)	0 (0)	0 (0)	0 (0)	0 (0)
N° of polyps collected	10	10	10	10	10	10	10	10	9	9	10	10

The frequency of distinct sexuality relative to oocyte size indicates that polyps classified as "predominantly male" have the smaller percentage of larger oocytes (Online Resource 10, Fig. 4a) and a uniform representation of all spermatocyst at a similar developmental stage (Fig. 4b). Conversely, as the oocytes increase in size, the sexuality shifts from "equally female/male" to "exclusively-female" and "predominantly-female," with spermatocyst stages transitioning from stages III and IV to primarily stage I, respectively.

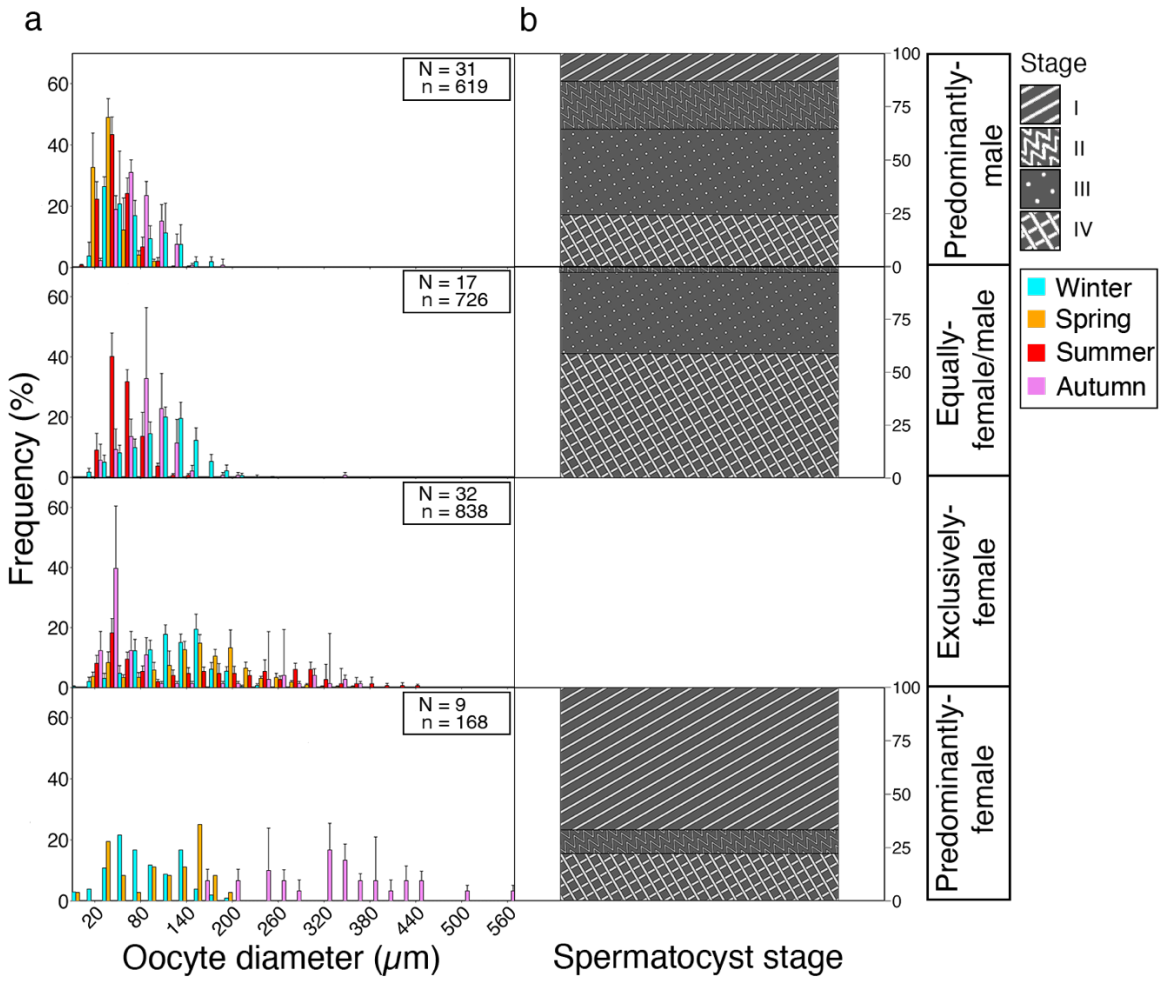

Fig. 4 Female and male gametes of *C. huinayensis* separated by sexuality ("predominantly male", "equally female/male", "exclusively female", and "predominantly female"). (a) Frequency (%) distribution of PV and V oocyte size (μm) plotted per season (winter: turquoise; spring: orange; summer: red; autumn: violet), and (b) frequency (%) distribution of the development stages of spermatocysts (Stage I–IV). In (a), vertical bars in each graph indicate the mean oocyte size and its corresponding error bars indicating the standard error. N: total number of polyps collected in all seasons; n: total number of oocytes. Note: the absence of the spermatocyst graph is a consequence of the lack of male gametes in "exclusively female" polyps.

The smallest sexually active polyp, based on the polyp volume, was observed at X-Huinay. The specimen, described as "predominantly male", had a height of 6.0 mm and a calyx diameter of 3.0 mm. It contained a total of four oocytes in the PV state and spermatocysts in Stages II and III.

5.4.3 From gametogenesis to larvae

The gametes of both sexes developed in the mesenteries (M; Fig. 2a–e). Both oocytes and spermatocysts often appeared in separate mesenteries with increasing abundance and maturity towards the apical side (Fig. 2a, b). More rarely, however, both gametes were observed in a single mesentery (Fig. 2d).

Oogenesis: we found that 81 % of the total oocytes measured, within all seasons, were PV (72 μm mean oocyte size), and 19 % were V oocytes (200 μm mean oocyte size) (Online Resource 3). The majority of the population (70 %) exhibited oocytes within an individual at a similar stage of development (Fig. 2c), whereas the remaining portion of the population displayed both PV and V oocytes, as illustrated in Fig. 2d. Individuals collected in the same season and at the same site exhibited asynchronous oocyte development as the size of V oocytes did not peak, especially in summer and autumn (Fig. 5b).

Spermatogenesis: four stages were found within spermatogenesis. In Stage I, spermatocyst were round and surrounded by mesoglea without being arranged in clusters. Spermatocytes within the spermatocyst were rather loosely and homogeneously distributed (Fig. 2b). In Stage II, spermatocysts showed a thicker border within which spermatocytes began to cluster (Fig. 2d). Stage III spermatocysts were frequently round, had a slender border and a hollow lumen in which the densely packed spermatids begin their tail formation. These tails exhibited a distinct light purple filamentous pattern (Fig. 2b). Stage IV spermatocysts were commonly oval, with densely packed spermatozoa and sperm tails that were unidirectionally oriented, generating “channels” towards the center of the spermatocyst (Fig. 2b). Stages III and IV were typically clustered within the mesoglea. Of the 80 polyps that showed spermatocysts (“exclusively-male”, “predominantly-male”, “predominantly-female”, and “equally”), 30 were observed to exhibit only one stage of spermatocyst development, ranging from Stage I–IV. The remaining polyps exhibited spermatocysts in at least two different developmental stages. Only four polyps showed all four stages in both spring and autumn.

Developing larvae were only observed in the coelenteron. Different stages of larval development were observed within a polyp, as some larvae already had

mesenteries (M) and a pharynx (PH) indicating an advance maturity stage (Fig. 2f), whereas others were observed at the onset of the formation of bilayered tissue. Of the 91 polyps containing oocytes ("brooding" polyps, defined as those that brooded larvae but did not currently have categorizable gametes, were not counted (n = 3)), 20 % (18 polyps) contained larvae. Of these, 7 % (six polyps) were observed in winter, 2 % (two polyps) in spring, 6 % (five polyps) in summer, and 6 % (four polyps) in autumn (Table 3).

5.4.4 Seasonal gametogenesis

During winter, PV oocytes were abundant (163, 362, and 208 for Liliguapi, X-Telele, and X-Huinay, respectively, Fig. 5a), while the opposite was true for V oocytes (51, 45, and 70 for Liliguapi, X-Telele, and X-Huinay, respectively, Fig. 5b). During this season, the oocyte's size ranged from 5 to 243 μm and the mean (± SD) for all three study sites was 93 ± 40 μm and 153 ± 27 μm for PV and V oocytes, respectively. X-Huinay had the largest V oocytes (243 μm) among the study sites. In spring, the mean size of PV oocytes for all three study sites was 91 ± 56 μm, while V oocytes were 193 ± 47 μm. Therefore, a second cohort of oocytes began to form at that time and its presence was evident in summer and autumn (Fig. 5a). During spring, the mean size of PV oocytes at Liliguapi and X-Huinay was 83 ± 64 μm and 72 ± 55 μm, respectively, while it was larger at X-Telele (102 ± 53 μm) (Fig. 5a). The mean size of V oocytes was larger than the one for the PV oocytes at all study sites (Liliguapi 196 ± 51 μm, X-Telele 197 ± 42 μm, and X-Huinay 167 ± 38 μm) (Fig. 5b). In summer, the mean size of PV oocytes for all three study sites was 42 ± 27 μm, while the mean size of V oocytes was 247 ± 74 μm. The V oocytes at Liliguapi had the highest mean size (285 ± 63 μm) compared to X-Telele and X-Huinay (240 ± 63 μm and 196 ±73 μm, respectively). In autumn, the mean size of V oocytes for all three study sites was the highest of all seasons (268 ± 102 μm), also for X-Telele and X-Huinay (290 ± 92 μm and 270 ± 96 μm, respectively), while Liliguapi exhibited an oocyte mean size of 225 ± 103 μm. The mean size of the PV oocytes (60 ± 27 μm) for all three study sites increased from the summer season onwards (Fig. 5a).

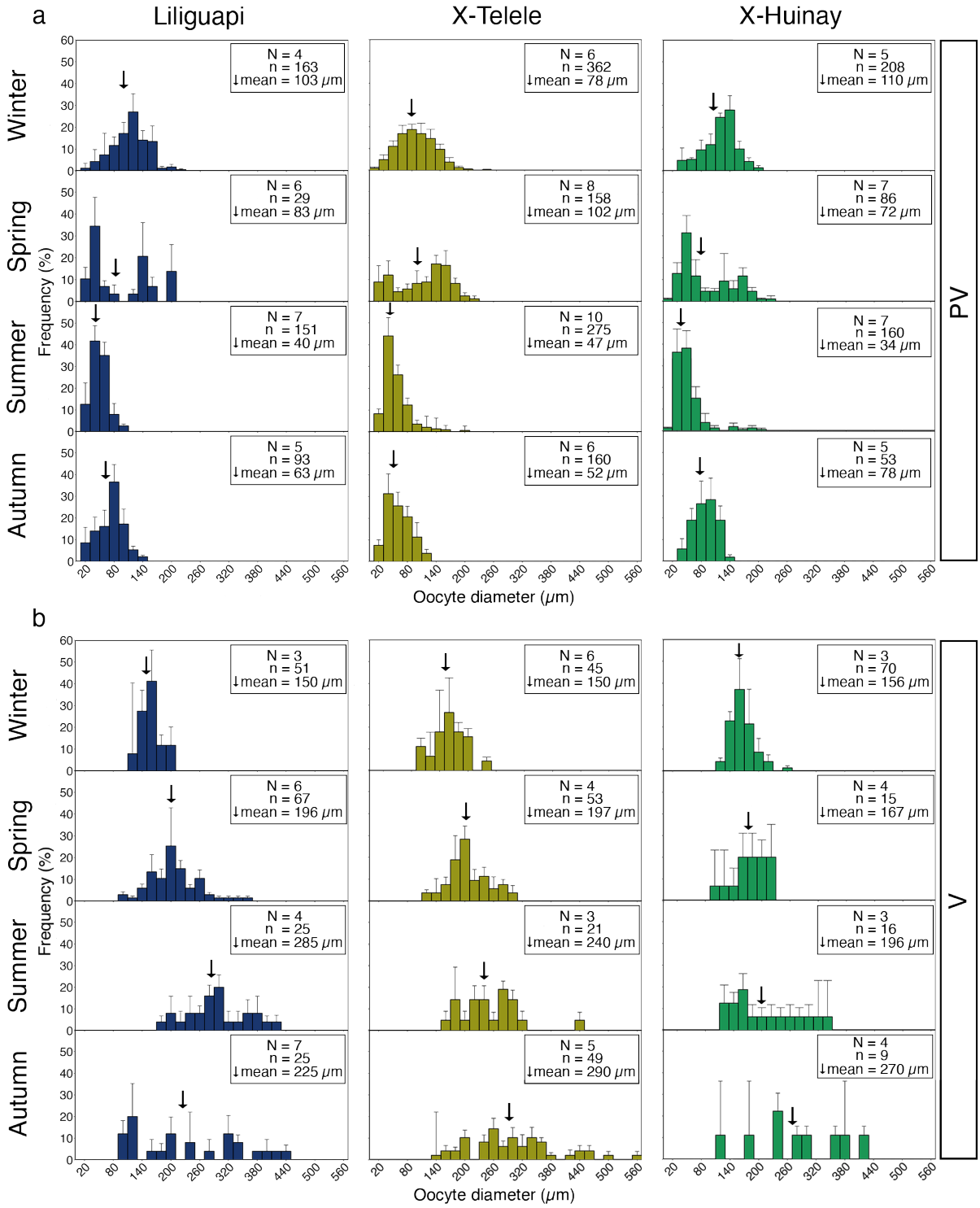

Fig. 5 Frequency distributions (%) of *C. huinayensis* oocyte size illustrated separately for site (Liliguapi: blue, X-Telele: yellow, and X-Huinay: green) and season (winter, spring, summer, and autumn). Vertical bars in each graph indicate the mean oocyte size (μm) for (a) PV and (b) V oocytes. Error bars indicate the standard error. N: total number of polyps analysed; n: total number of oocytes.

Seasonal differences were observed in the differently developed spermatocysts. In winter, Stage IV (spermatozoa) was the most frequent in all sites

(Liliguapi: 45 %, X-Telele: 44 %, X-Huinay: 67 %), and in spring Stage II (spermatids) dominated (Liliguapi: 46 %, X-Telele: 36 %, X-Huinay: 31 %). In both summer and autumn Stage III (spermatids) was the most frequent (with the exception of X-Huinay in autumn, where Stage IV was the most frequent at 36 %), with Liliguapi: 52 %, X-Telele: 62 %, X-Huinay: 44 %, and Liliguapi: 44 % and X-Telele: 40 %, respectively. The other developmental stages (I (spermatogonia), II, and IV) showed greater variability in these two seasons when compared across the study sites (Fig. 6).

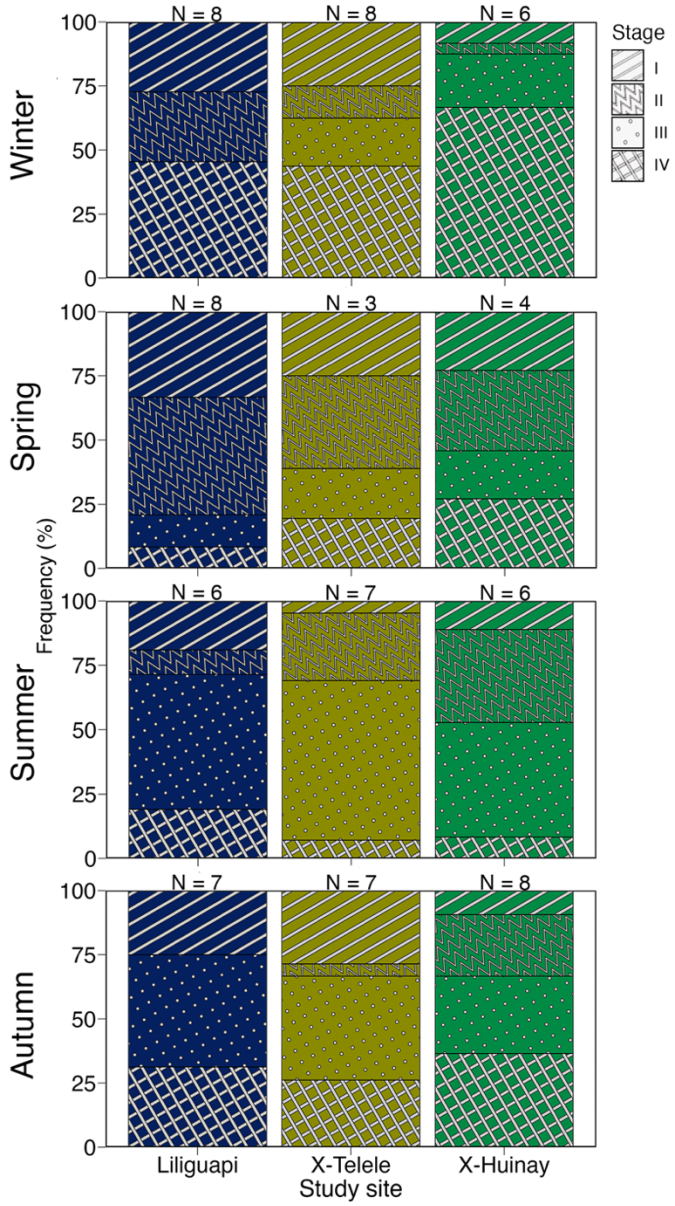

Fig. 6 Frequency (%) development stages of male gametes of *C. huinayensis* per site (Liliguapi: blue, X-Telele: yellow, and X-Huinay: green) and season (winter, spring, summer, and autumn). The

developmental stages of the male gametes were classified into Stage I to IV with increasing maturity. N: Total number of polyps examined per study site. Note: Stage II and III were not observed in autumn and winter at Liliguapi.

5.4.6 Effects of low seawater pH on the seasonal reproduction

The PCA analysis, used to evaluate the overall effect of seawater pH on the V oocyte size, considering the seawater temperature and oxygen revealed that all three variables had a significant effect on the V oocyte sizes observed with the total explained variance accumulated within the first three principal components (Table 4).

Table 4 Principal Component Analysis (PCA) of the effect of seawater pH, temperature, and oxygen on the V oocyte size (PC1–3).

Factor	Fixed Effect	PC1	PC2	PC3
V oocyte size	pH	0.77	-0.25	0.588
	Temperature	0.17	-0.80	-0.564
	Oxygen	0.62	0.53	-0.579
Proportion of explained variance (%)		48.39	46.35	5.26
Cumulative of explained proportion (%)		48.39	94.74	100
Standard deviation		1.205	1.179	0.397

The PC1 and PC2 accounted for 48.39 % and 46.35 % of the total explained variance (94.74 %), respectively (Table 4). Seawater pH had the largest contribution to the PC1, with a loading of 0.77, compared to its negative loading of -0.25 to the PC2. In contrast, temperature had the highest contribution to PC2, with a negative loading of -0.80, while oxygen contributed positively to both PC1 and PC2 with 0.62 and 0.53, respectively. The relevance and the nature (i.e., if the contribution is positive or negative) for each of the variables tested, is reflected in the vector's direction and the length of each of the environmental variable depicted in the PCA biplot (Online Recourse 11, Table 4). The seawater pH showed a strong effect on the V oocyte size given the length of its vector, and a correlation with temperature and oxygen given vector angles < 90° between them.

The natural seasonal variability of the seawater pH on the V oocyte size at all study sites can be observed in Fig. 7. The results obtained in the LMM model aligned

with the PCA results for seawater pH. These results support the significant effects of the pH parameter on the V oocyte size (LMM, $p < 0.05$, Table 5). Moreover, the analysis revealed that the factors of season, study site, and the seasonal variation of the natural seawater pH per site and season had a significant effect on the V oocyte size. Both the individual factors and their interactions remained statistically significant, as evidenced by the effect size presented in Fig. 8 (LMM, $p < 0.05$, Table 5).

Table 5 Linear models results for V oocyte size (LMM) and PRF (LmRob). Type II ANOVA with Chi-square tests. Significant *p*-values ($p \leq 0.05$) are highlighted in bold.

Factor	Fixed Effect	Chisq	*Df*	*p*-value
V oocyte size	pH	19.73	3	**0.0002*** **
	Site	13.55	2	**0.0011** **
	Season	33.83	3	**< 2.1e-07*** **
	pH × Season	24.58	2	**< 4.6e-06*** **
	Site × Season	3.98	1	**0.046***
PRF	pH	3.74	3	0.2907
	Site	5.01	2	0.0817
	Season	6.30	3	0.0977
	pH × Site	2.73	2	0.2559

In detail, seawater pH increased from winter to autumn in all study sites, though it was maintained during summer and autumn for Liliguapi (Fig. 7). The V oocytes were smallest in winter for all study sites, with an overall increase towards warmer seasons. At the study site level, at X-Telele, oocyte sizes increased from winter to autumn. At Liliguapi, on the other hand, oocyte size decreased in autumn, despite it showed the same trend as in X-Telele in winter, spring, and summer. The comparison of V oocyte size within the same study site across seasons showed significant differences in Liliguapi and X-Telele in winter compared to all other seasons, while X-Huinay on the other hand, follows similar trend as X-Telele and is not significantly from Liliguapi. Finally, summer and autumn showed significant differences of V oocyte size compared to winter and spring seasons for Liliguapi and X-Telele, respectively (Fig. 7, LMM, $p < 0.05$, Online Resource 4–7).

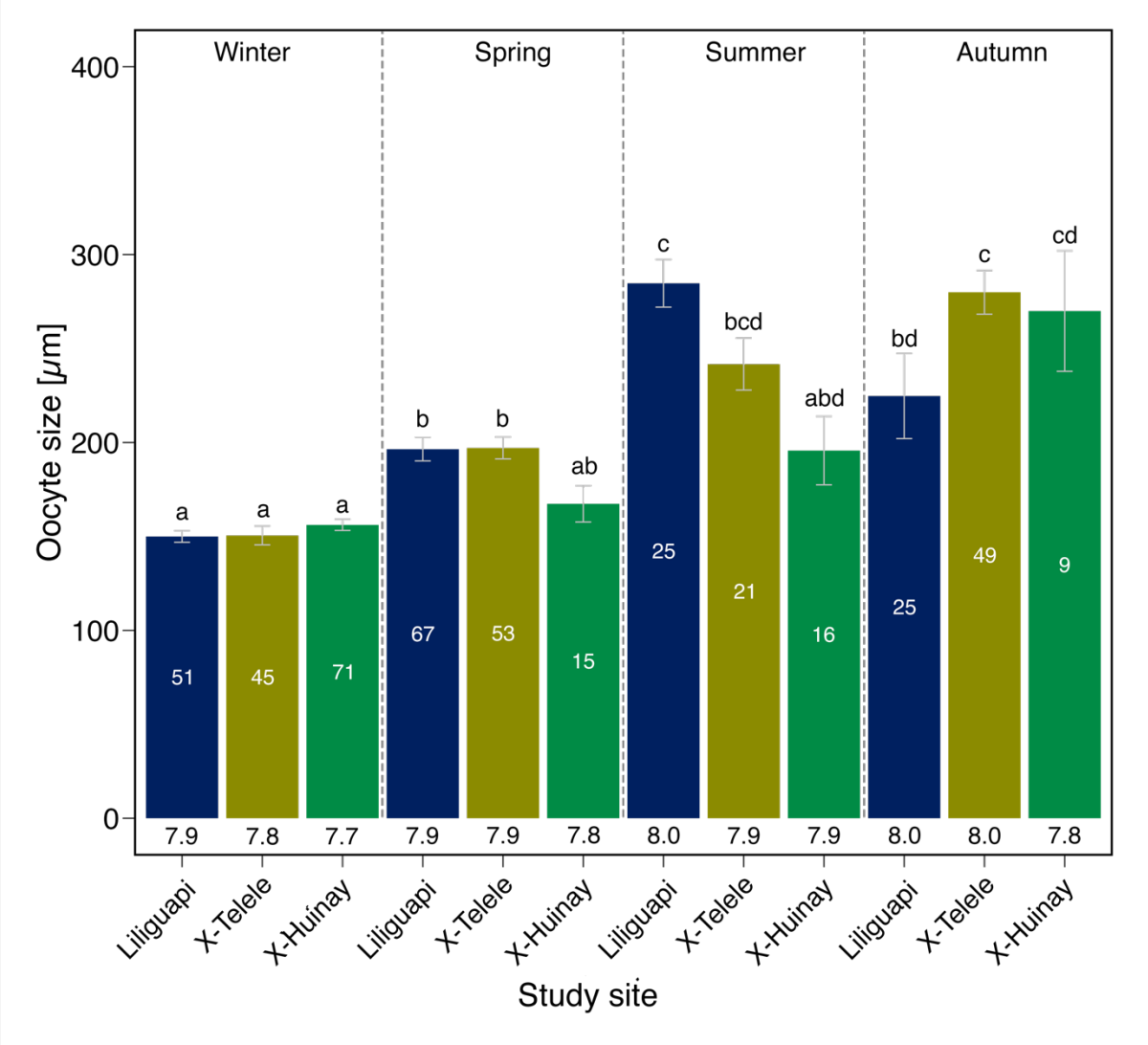

Fig. 7 Size (*µ*m) of examined V oocytes in *C. huinayensis* polyps for each season (winter, spring, summer, autumn) and each study site (Liliguapi: blue; X-Telele: yellow; X-Huinay: green). Bars sharing the same letter above are not statistically different (LMM, $p < 0.05$). The bar values indicate the mean ± SE, and the numbers within the bars indicate the total number of V oocytes measured at the respective study site and season (n = 447) within a total of 53 polyps. The respective mean seawater pH for each study site and season is shown below each bar.

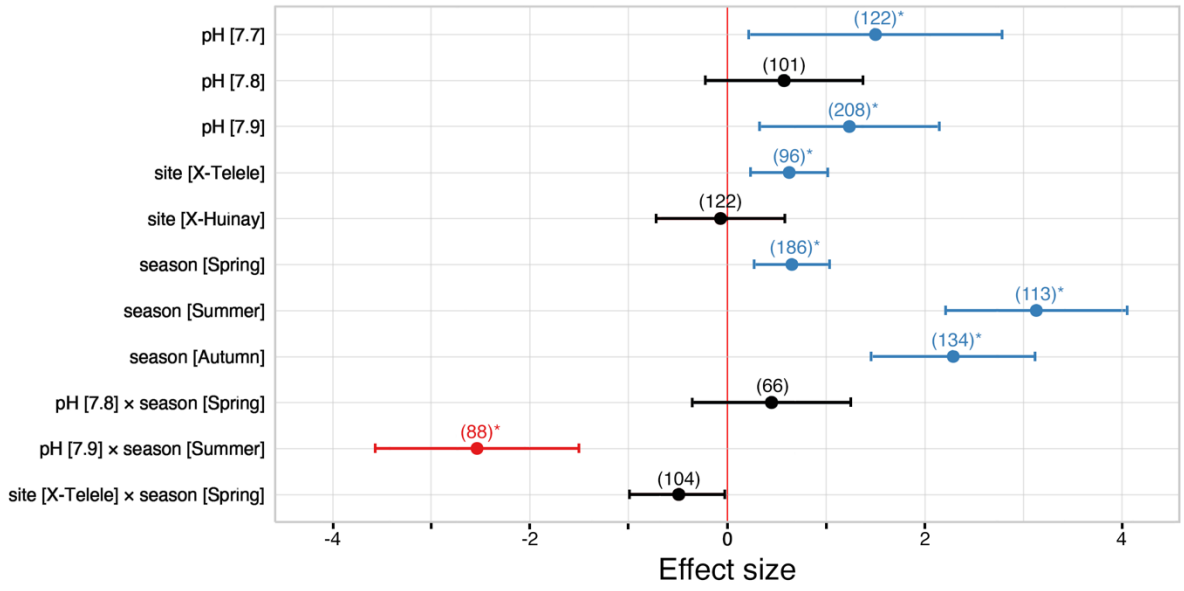

Fig. 8 Mean effect size of seawater pH seasonal variation and study sites on the V oocyte size. The calculated mean effect sizes (Cohen's *d* based) and 95 % confidence intervals (CI) are shown relative to the reference indicated by the red vertical line at zero. Whenever the effect sizes CI do not overlap zero, the mean effect sizes are considered significant as indicated by the asterisks (*). Negative effect sizes are depicted in red while positive effect sizes in blue. Non-significant effect sizes (which CI's do overlap with the zero-reference) are shown in black. The further a mean effect size is from the zero-reference line, the larger its effect. The number of observations used to calculate mean effectsizes are shown in parentheses.

The natural variability of seawater pH had no significant effect on the PRF across all study sites and seasons (Fig. 9, LmRob $p > 0.05$, Table 5). The overall mean PRF of the four seasons was higher at X-Telele (8.8 ± 1.8) and Liliguapi (8.4 ± 2.2) than in X-Huinay (7.9 ± 3.0), although no statistically significant differences were detected when comparing PRF across seasons and study sites (Fig. 9). Also, we did not observe correlations between polyp size and the seasonal PRF (Online Resource 12).

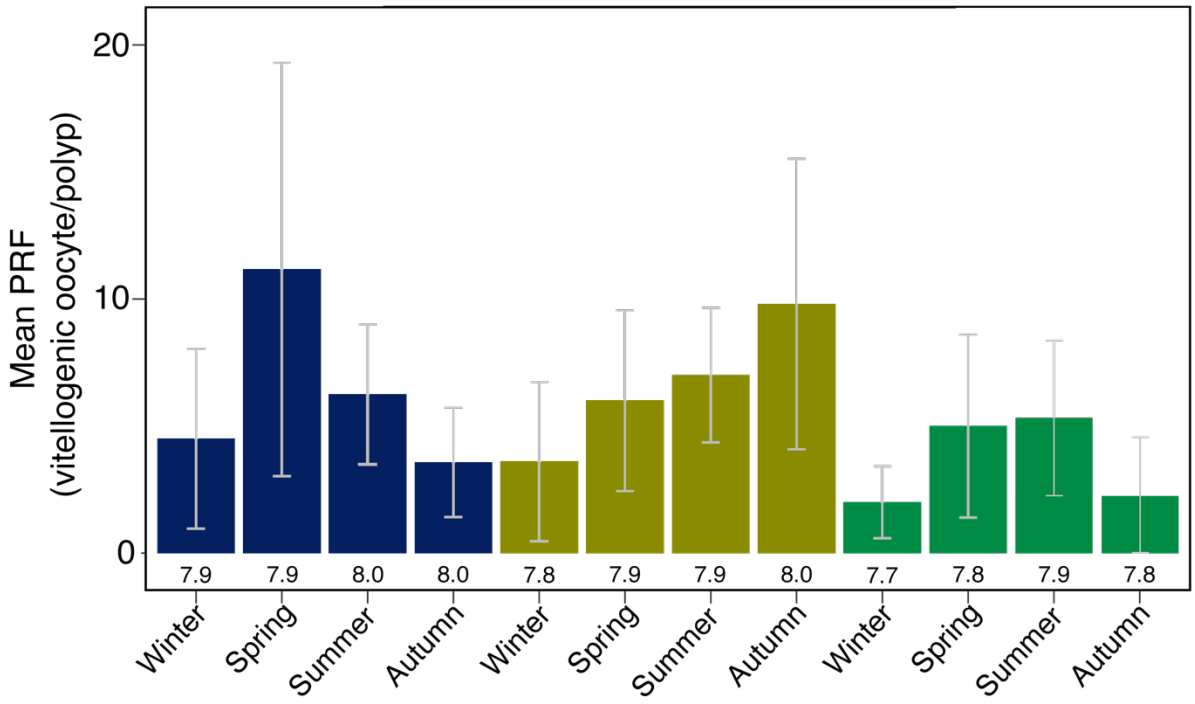

Fig. 9 Mean PRF of *C. huinayensis* by study site (Liliguapi: blue, X-Telele: yellow, and X-Huinay: green) and season (winter, spring, summer, and autumn). A total of 53 polyps were analysed across all study site resulting in an overall number of 447 V oocytes, all of which were analysed. The bar values indicate the mean value of all polyps of the respective study site and season, the error bars indicate the standard error (SE). The respective mean seawater pH for each study site and season is shown below each bar.

5.5 Discussion

Gametogenesis in corals is believed to be highly sensitive to OA, affecting several species (Rossin et al. 2019; Liberman et al. 2021; Marchini et al. 2021). Successful sexual reproduction is crucial for species persistence. Therefore, understanding the impact of OA on gametogenesis is essential. For the first time, we described the reproductive biology and assessed the effects of naturally occurring low seawater pH on the reproduction of the scleractinian CWC *C. huinayensis*. Our findings indicate that *C. huinayensis* is an asynchronous hermaphrodite that cycle its sexuality. Furthermore, our results indicate that seasonal fluctuation in seawater pH is one of the multiple factors driving the oocytes size, potentially affecting reproduction.

To date, *C. huinayensis* is the only scleractinian CWC described as an asynchronous (Online Resource 9), cyclic hermaphrodite (Fig. 4, Online Resource 8) that broods its larvae (Fig. 2f, Heran et al. 2023). Only three other scleractinian CWCs have been described as asynchronous cyclical hermaphrodites, all from the family Caryophylliidae, though they likely spawn their gametes as no larvae were observed within the polyps (Waller et al. 2005). All other scleractinian CWCs studied so far have exhibited gonochorism (Table 1 in Waller et al. 2023).

The observation of male and female gametes within the same mesentery, as well as their density and maturity increasing towards the apical side of the polyp, has also been identified in other Caryophylliidae CWCs (Waller et al. 2005). This disposition of gametes in hermaphroditic brooding polyps allows self-fertilization (Brazeau et al. 1998; Okubo et al. 2007). However, in *C. huinayensis*, which is suggested to be a cyclic hermaphrodite based on observed changes in sexuality during oocyte and spermatocysts development (occurring regardless of the season, Fig. 4, Online Resource 8), the gametes mature at different times (Fig. 2d), making self-fertilisation unlikely. This capacity, also described in three other solitary Caryophylliidae (Waller et al. 2005), may ensure that, regardless of polyp density, a proportion of the population will have mature gametes throughout the year, thereby facilitating cross-fertilization.

In *C. huinayensis*, as in all scleractinian CWCs studied so far, spermatogenesis takes place within spermatocysts contained within the mesenteries. These either rupture before spawning within the mesenteries and mature spermatozoa move into the gastrovascular cavity (e.g., *D. pertusum* (Larsson et al. 2014), Waller pers. obs.)) or spermatocysts are expelled into the gastrovascular cavity before leaving the polyp through the mouth into the surrounding water, where they rupture and release mature spermatozoa (e.g., *Pennatula aculeata* (Eckelbarger et al. 1998)) for external fertilization. Given that the aforementioned strategies of spermatozoa release occur within seconds and that the likelihood of release occurring during histological preparation is low, the mechanism by which *C. huinayensis* releases its spermatozoa remains unknown.

Regarding oogenesis, reproduction in *C. huinayensis* is characterized by the onset of this process primarily in winter, with a second cohort of PV oocytes initiated during spring, followed by late vitellogenesis during summer and autumn (Fig. 5). This continuous but unequal quantitative production of oocytes indicates presence of V oocytes throughout the year (see Fig. 5). Since oocyte nucleus grows during development, a 45 μm section width did not capture all oocyte sizes after analysing all polyps (n = 118), PV oocyte frequency in Fig. 5 may be underestimated. Although reducing section width could increase the frequency of smaller PV oocytes, it is unlikely to significantly alter the overall study results.

Stage IV spermatocytes were present in all seasons at each study site, with different seasonal frequencies (Fig. 6). Although the reason for the pre-production of mature spermatozoa in *C. huinayensis* is unknown, this is a common feature in invertebrates (Goffredo et al. 2002; Baillon et al. 2011). One possible explanation is that spermatogenesis is generally less energetically demanding than oogenesis, allowing a faster spermatogenesis than oogenesis (Goffredo et al. 2002; Baillon et al. 2011). In line, Waller et al. (2005) did not observe seasonal reproduction in the three spawning *Caryophyllia* species. This suggests that spawned sperm are near constant throughout the year, due to their asynchronous reproductive pattern. This indicate that all four *Caryophyllia* species (*C. ambrosia*, *C. cornuformis*, *C. sequenzae*, and *C. huinayensis*) produce ripe gametes all year-round, despite their contrasting reproductive modes. The reconstruction of the original mode of Scleractinia

reproduction may indicate that neither spawning nor brooding is an evolutionary advantage over time and therefore both modes of reproduction can occur simultaneously in related species (Kerr et al. 2011). Conversely, all four species, which inhabit distinct habitats (435–2000 m deep Atlantic ocean versus 11–265 m deep Patagonian fjord systems) are cyclical hermaphrodites, a phenomenon that is likely to be phylogenetically driven (Eckelbarger and Watling 1995; Kerr et al. 2011).

The low abundance and size of V oocytes observed in winter (Fig. 5b and Fig. 7), contrasted with the high abundance of polyps presenting developed larvae (Fig. 2f) during the austral winter and spring (Table 3), suggests that fertilisation primarily occur from spring to autumn. This increased number of brooding polyps during the winter and spring, is consistent with the results of the larval release observed during a study based on aquaria experiments with *C. huinayensis* (Heran et al. 2023). Although the peak of both brooding polyps in this study and the larval release in the aquaria study occurred during the same months of the year, though in different hemispheres, indicates that in the absence of external timing signals, such as changes in water temperature, food amount, frequency of food supply and quality, and others, the coral's internal clock is indeed maintained. This behaviour has been observed in the soft corals alcyonaceans (Sun et al. 2010a, b; Waller et al. 2023).

Environmental cues that allow scleractinian CWCs to synchronize the release of their gametes to enhance fertilization success are poorly understood compared to scleractinian WWCs (Babcock et al. 1986; Richmond and Hunter 1990; Mangubhai and Harrison 2008). This is due to the challenges of collection and monitoring their deep-sea environment over prolonged periods of time. Spawning has been observed in austral winter in the actinia *Corynactis* sp. (Häussermann and Försterra 2015) in Comau Fjord. Similarly, winter has been proposed as the spawning season for the shallow-water community of the scleractinian CWC *D. dianthus* (Feehan et al. 2019) and the octocoral *Primnoella chilensis* (Rossin et al. 2017). This period coincides with the seasonal minimum seawater temperature in the upper layer of Comau Fjord (Fig. 3a–c), and one of the seasons with the highest abundance of larvae observed in *C. huinayensis* polyps (Table 3). Hence, it is plausible that oogenesis (Fig. 5) starts shortly after the period of low seawater temperatures, leading to release of brooded larvae before spring. This is advantageous as predation in the water column is likely

to be lower at this time of year due to the lower abundance of predatory zooplankton that increases in spring (Garcia-Herrera et al. 2022). However, environmental disturbances such as that due to landslides (Sepúlveda et al. 2011), earthquakes (Försterra 2009), hypoxia (caused by terrestrial organic matter and phytoplankton bloom degradation (Breitburg 2002; Silva and Vargas 2014), and elevated levels of methane and sulphide (Försterra et al. 2014) can occur in the Patagonian fjord region. Consequently, the presence of *C. huinayensis* larvae and their potential release throughout the year, enhances the probability of rapid recolonisation after a disturbance, regardless of the season.

In a study of the broadcast spawning CWC *D. dianthus* at shallow waters from Comau Fjord, Feehan et al. (2019) observed that 70 % of the individuals were non-reproductive during the reproductive season, suggesting that unfavourable environmental conditions may downregulate reproduction. Given the naturally low seawater pH in the area (Fillinger and Richter 2013), Comau Fjord presents a unique opportunity to investigate how in-situ seasonal fluctuations in seawater pH could affect coral reproduction.

Our statistical results indicate that seawater pH has a significant effect on the oocyte size, and thus on reproduction (Table 4, Table 5). The overall effect of seawater pH was positive (Table 4; PC1, Fig. 8), as supported by e.g., the increased V oocyte size observed at pH 7.8 and 7.9 (Fig, 7). This finding contrast with the generally expected negative effects at lower pH levels on reproduction in WWCs (Morita et al. 2010; Albright and Mason 2013; Marchini et al. 2021). These results may suggest how *C. huinayensis* and other scleractinian CWCs from the same area (Försterra and Häussermann 2003; Rossbach et al. 2021) are capable of thriving in this naturally acidified fjord, indicating local adaptation to this environment.

Nevertheless, a significant negative effect of seawater pH was also observed (Table 4; PC2), especially when interacting with other abiotic environmental factors (Table 4, Fig. 8), were seawater pH and temperature, and pH and oxygen can act synergistically (Table 4, Fig. 8). For instance, during warmer seasons, when seawater temperature increases in combination with a pH of 7.9, negative effects on oocyte size were observed (Fig. 8). In a study on OA in scleractinian WWCs, where seawater pH was reduced to 7.8, it was observed that under low water flow conditions of 2 cm s^{-1}

(and thus lower oxygen concentration in the boundary layer), coral calcification rates decreased by 18 % (Martins et al. 2024). This suggest that reduced oxygen availability may exacerbate the negative effects of low pH by failing to meet metabolic oxygen demands under acidified conditions. Conversely, higher seawater oxygen levels can exert a positive influence, that may counteract the negative effects of pH (Table 4, Online Resource 11). However, in Comau Fjord, lowered oxygen concentrations occur more regularly (Silva 2008, 2014) and thus negative synergies may be prone to occur with higher frequencies. Interestingly, during a mass die-off event of *D. dianthus* in Comau Fjord in 2013, oxygen levels measured near the coral wall (> 50 cm) ranged from 154.1 to 163.9 μmol kg^{-1} (Försterra et al. 2014). These oxygen levels were at the lower range of measurements in our study (Table 2, Fig. 3f). It is therefore plausible that, in combinations with a mean current velocity of 5 cm s^{-1} recorded near the coral wall in Comau Fjord (Laudien et al. 2021) and the naturally low seawater pH of the area (Fillinger and Richter 2013), these factors may have contributed to the mass mortality event.

When considering seasonality and study site locations, the smallest V oocyte size were observed in winter for all study sites (Table 5, Fig. 7). This effect is likely driven by the seawater temperature, perhaps in negative synergy with lower pH values observed during that season (Table 4, 5; Fig. 8, Online Resource 11). A potential consequence of fertilizing smaller V oocytes is that they may contain lesser lipid reserves compared to larger V oocytes. During the vitellogenic process, lipids accumulate within the oocyte, leading to a roughly twofold increase in its size, thereby enhancing the energy reserves available for the future larva (Eckelbarger et al. 1998; Eckelbarger and Hodgson 2021). When smaller V oocytes are fertilized, their reduced lipid content could shorten larval duration, limiting dispersal potential (Levitan 2006), or result in earlier settlement in suboptimal environments to conserve energy for metamorphosis into a polyp (see Moran and McAlister 2009). Additionally, smaller V oocytes may become unfertilisable if the size discrepancy between oocytes becomes too pronounced (Levitan 2006; Waller et al. 2019; Johnstone et al. 2021). While the production of smaller V oocytes could theoretically be offset by an increase in V oocyte number, the high variability in PRF within and between study sites across seasons prevent us from drawing definitive conclusions (Fig. 9). In addition, our results showed

no significant effect of the seasonal fluctuations in seawater pH on PRF (Fig. 9, Table 5) and the number of V oocytes seemed to remain stable throughout the year (Fig. 9).

Moreover, we found site-season specific differences in the V oocyte size response to the seawater pH (Table 5, Fig. 7, Online Resources 4–7), e.g., the negative significant effects found when comparing X-Telele-spring with Liliguapi-winter (Fig. 8). Yet, the observed site-season effects can be of varying nature, i.e., positive or negative, depending on particular combinations (Fig. 8; Online Resources 4–7, 11). In the first case, the observed effects can be related to the influence of oxygenated subantarctic oceanic water entering the fjord. As this water moves towards the inner fjord, it may mix with water from the head of the fjord, which often has low oxygen levels, possibly due to spring algal blooms (Breitburg 2002), affecting negatively X-Telele. In the second case, the variability in the observed effects can be explained given the Comau Fjord landform and this species intrinsic sensitivity to lowered pH. Despite that the three study sites can be considered in a close distance from each other's (ca. 17 km), they showed significant variation in their environmental parameters across seasons, affecting reproduction. On the other hand, the OA effects on marine calcifiers biology including reproduction, as reviewed in Kroeker et al. (2013), suggests generally large and negative responses together with variations in sensitivity, having important implications for marine ecosystems. The fitness trade-off in response of environmental variability have been study on *D. dianthus* within the same fjord. Corals transplanted from an unstable, shallow water environment–with higher aragonite saturation ($\Omega_{arag} > 1$) and temperature (> 12 °C)–to a deeper fjord basin, where both aragonite saturation and temperature were lower but more stable, exhibited the fastest growth and the healthiest phenotypes (Beck et al. 2022).

In this study, the reproductive strategy of the solitary scleractinian CWC *C. huinayensis* is described as an asynchronous hermaphrodite with the ability to switch sexuality during gamete formation. This ability allows the coral to thrive even in isolated locations, as any individual can produce both male and female gametes regardless of the season, increasing the likelihood of cross-fertilization. *C. huinayensis* is capable of producing mature gametes and larvae year-round, a trait also observed in an aquaria study (Heran et al. 2023). In this controlled environment, the peak of larval production aligns with the observations from our study, even in the absence of

external timing signals, indicating the persistence of an internal biological clock. Regarding the effects of naturally low seawater pH on *C. huinayensis* reproduction, our results suggest that this parameter does not have an overall negative effect on V oocyte size. Instead, the effects of seawater pH can vary, with positive or negative outcomes depending on interactions with temperature, oxygen, season and study site–factors likely influenced by the fjord's landform. Thus, environmental factors can downregulate reproduction. Yet, biotic factors such as food availability, the coral's endogenous reproductive rhythm for oogenesis, and the polyp's energy budget, which balances resource allocation between metabolic processes, somatic growth and reproduction, must also be considered.

5.6 Acknowledgement

We would like to thank the director and staff of the San Ignacio del Huinay Foundation for their support during field work. We would like to considerably thank Petra Kohse-Kordes and her team, Institut für Pathologie, Gesundheit Nord gGmbH, Klinikverbund Bremen, and Annette Pintak and her team, Institut für Pathologie, Hannover for performing the histological sections and staining. We would also like to thank Andrea Gori for his valuable advice on conducting the multivariate analysis. The research is part of the Ph.D. project of T.H. at the University of Bremen, carried out at the Alfred-Wegener-Institut Helmholtz-Zentrum für Polar- und Meeresforschung (AWI). T.H., J.L. and C.R. were supported by the AWI (PACES II, and 'Changing Earth – Sustaining our Future', Topic 4.2). T.H. received additional financial support from the National Geographic Society (grant-EC-56391R-19), Deutscher Akademischer Austauschdienst (DAAD) (grant-91608520), and Agencia Nacional de Investigación y Desarrollo (ANID), Chile (grant-62170011). We acknowledge support by the Open Access Publication Funds of AWI. Specimens were exported from Chile under CITES permits 19CL000007WS, 19CL000015WS, 21CL000003WS, and 21CL000004WS and imported to Germany under permits E00711/19, E08854/19, E02410/21, and E02411/21.

5.7 Online supplementary material information

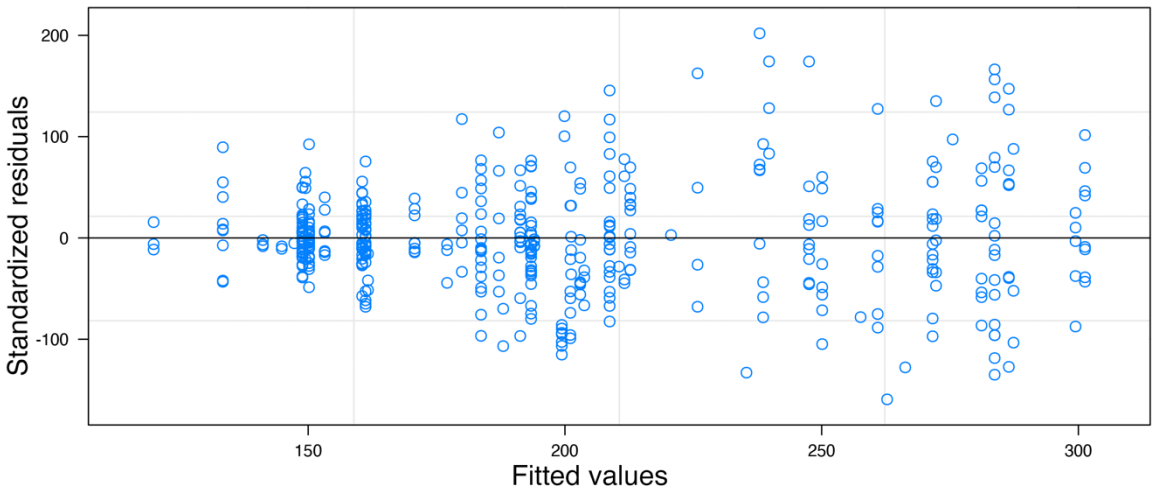

Fig. SM1 Pearson plot of the fitted model showing the heterogeneity of the residuals in the LMM model for V oocyte size, as indicated by their dispersion.

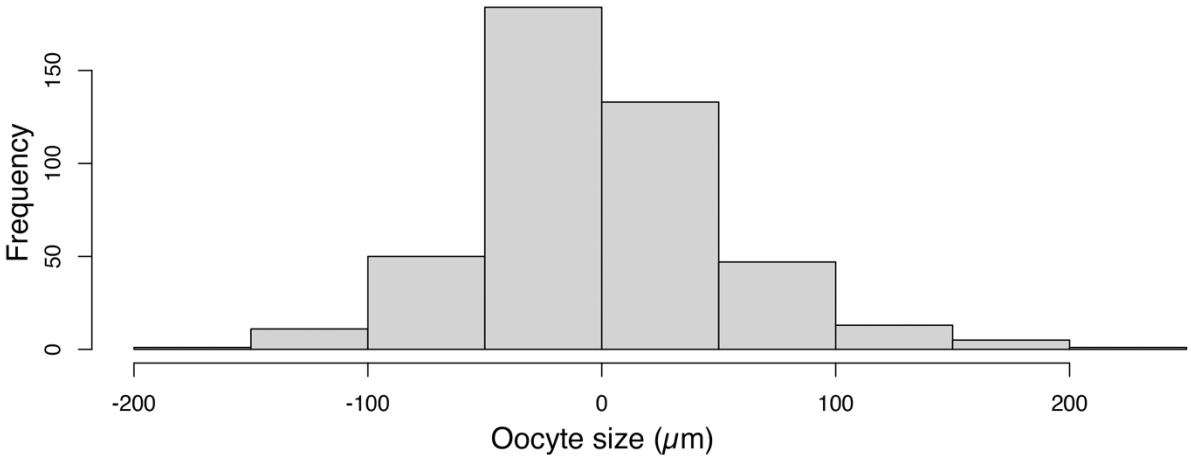

Fig. SM2 Histogram of the LMM model residuals from V oocyte size fitted data, showing a normal distribution.

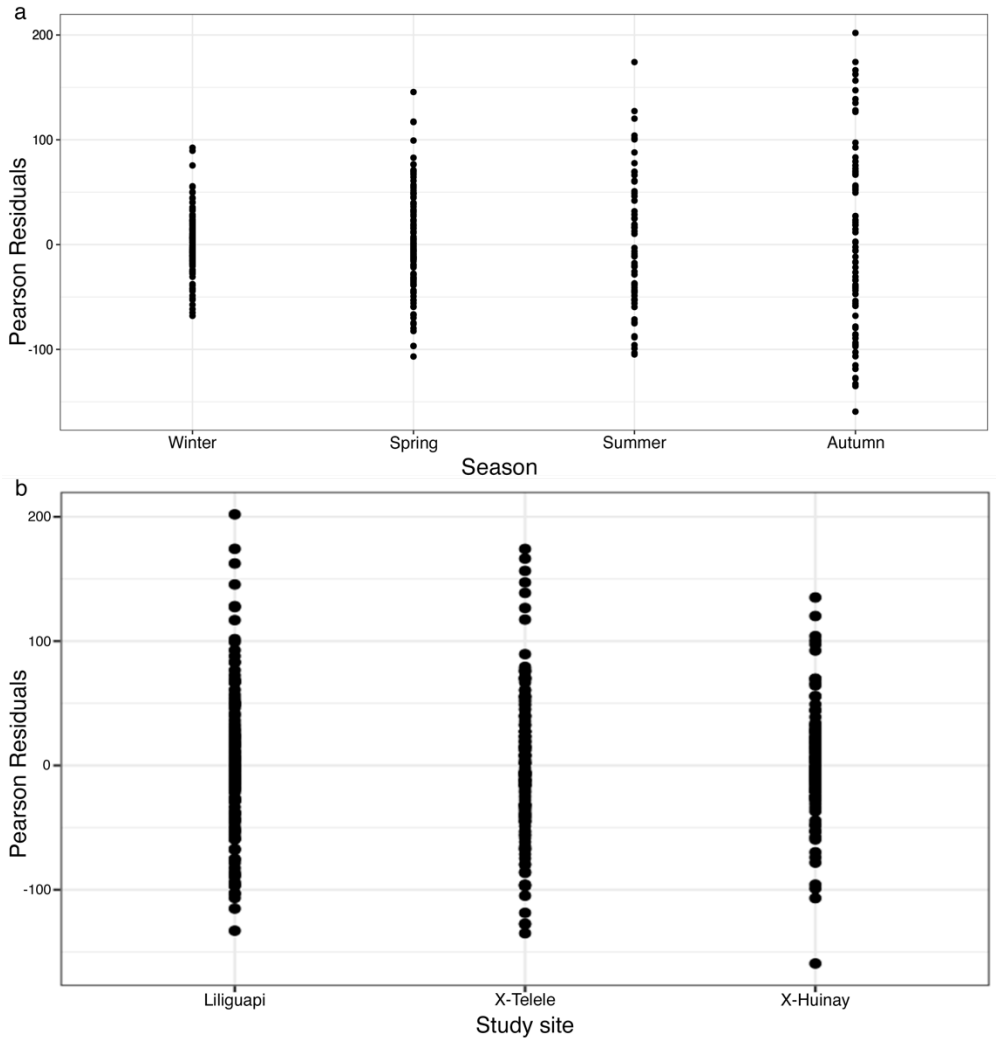

Fig. SM3 Diagnostic scatter-plots of Pearson residuals evaluating the seasons (**a**) and the site (**b**) factors linearity in the LMM model fitted for the response variable V oocyte size.

Table SM4 Tukey contrasts for site and seawater pH by season. The *p*-values defined as significant at a threshold of $p \leq 0.05$ are highlighted in bold.

Season	Contrast	Estimate	SE	*Df*	t.ratio	*p*-value
Winter	(X-Huinay – pH 7.7) - (X-Telele – pH 7.8)	16.79	13.6	142.6	1.235	0.4345
	(X-Huinay – pH 7.7) - (Liliguapi – pH 7.9)	14.25	15.2	65.4	0.936	0.6197
	(X-Telele – pH 7.8) - (Liliguapi – pH 7.9)	-2.53	15.7	93.7	-0.162	0.9857
Spring	(X-Huinay – pH 7.8) - (Liliguapi – pH 7.9)	-20.73	17.9	238.5	-1.159	0.6533
	(X-Huinay – pH 7.8) - (X-Telele – pH 7.9)	-30.48	17.9	295.8	-1.7	0.3256
	(Liliguapi – pH 7.9) - (X-Telele – pH 7.9)	-9.75	10.9	380.1	-0.894	0.808
Summer	(Liliguapi – pH 8.0) - (X-Telele – pH 7.9)	49.34	17.3	380.4	2.847	**0.024***
	(Liliguapi – pH 8.0) - (X-Huinay – pH 7.9)	100.23	18.1	427.9	5.547	**< 0.0001*****

	(X-Telele – pH 7.9) - (X-Huinay – pH 7.9)	50.89	20.2	313.7	2.515	0.0596
Autumn	(Liliguapi – pH 8.0) - (X-Telele – pH 8.0)	-45.78	14.2	406.7	-3.218	**0.0076****
	(Liliguapi – pH 8.0) - (X-Huinay – pH 7.8)	-36.92	22.4	408.9	-1.649	0.3523
	(X-Telele – pH 8.0) - (X-Huinay – pH 7.8)	8.86	20.7	424.2	0.429	0.9736

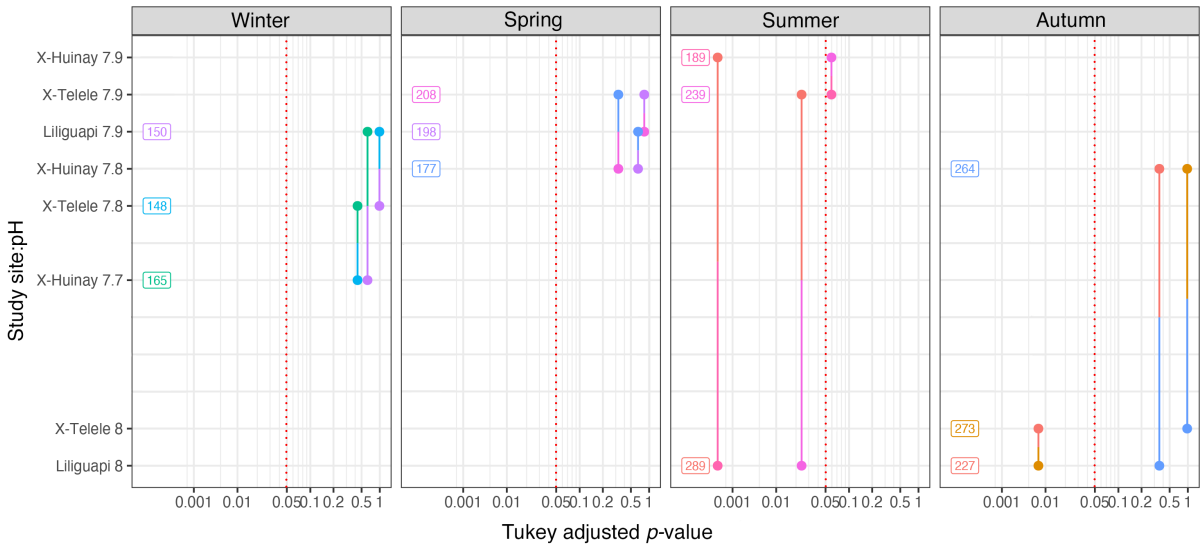

Fig. SM5 Pairwise emmeans comparisons plot. Tukey contrasts for site and seawater pH by season. The *p*-value is defined significant at a threshold of $\alpha = 0.05$, depicted with the red dotted line.

Table SM6 Tukey contrasts for season and seawater pH by site. The *p*-values defined as significant at a threshold of $p \leq 0.05$ are highlighted in bold.

Study site	Contrast	Estimate	SE	*Df*	t.ratio	*p*-value
Liliguapi	(Summer – pH 8.0) - (Autumn – pH 8)	61.5	15.6	433	3.941	**0.0005****
	(Summer – pH 8.0) - (Winter – pH 7.9)	138.5	15.9	230.1	8.737	**< 0.0001****
	(Summer – pH 8.0) - (Spring – pH 7.9)	90.7	14.4	278.1	6.297	**< 0.0001****
	(Autumn – pH 8.0) - (Winter – pH 7.9)	77	15.3	280.5	5.045	**< 0.0001****
	(Autumn – pH 8.0) - (Spring – pH 7.9)	29.2	14.1	284.9	2.069	0.1659
	(Winter – pH 7.9) - (Spring – pH 7.9)	-47.8	14.2	85.5	-3.358	**0.0063****
X-Telele	(Autumn – pH 8.0) - (Winter – pH 7.8)	125.3	13.3	248.2	9.424	**< 0.0001****
	(Autumn – pH 8.0) - (Spring – pH 7.9)	65.2	13.3	195	4.897	**< 0.0001****
	(Autumn – pH 8.0) - (Summer – pH 7.9)	33.6	14.9	427.9	2.26	0.1091
	(Winter – pH 7.8) - (Spring – pH 7.9)	-60	13.4	208.6	-4.493	**0.0001****
	(Winter – pH 7.8) - (Summer – pH 7.9)	-91.7	17	236.4	-5.389	**< 0.0001****
	(Spring – pH 7.9) - (Summer – pH 7.9)	-31.7	16.3	253.7	-1.945	0.2122
X-Huinay	(Winter – pH 7.7) - (Spring – pH 7.8)	-12.8	18.7	194.3	-0.685	0.9028

(Winter – pH 7.7) - (Autumn – pH 7.8)	-99.6	22.1	241.8	-4.502	**0.0001*** **
(Winter – pH 7.7) - (Summer – pH 7.9)	-24	18.1	182.7	-1.328	0.5465
(Spring – pH 7.8) - (Autumn – pH 7.8)	-86.9	25	347	-3.478	**0.0032** **
(Spring – pH 7.8) - (Summer – pH 7.9)	-11.2	22.2	257	-0.506	0.9576
(Autumn – pH 7.8) - (Summer – pH 7.9)	75.6	24.6	363.2	3.073	**0.0122***

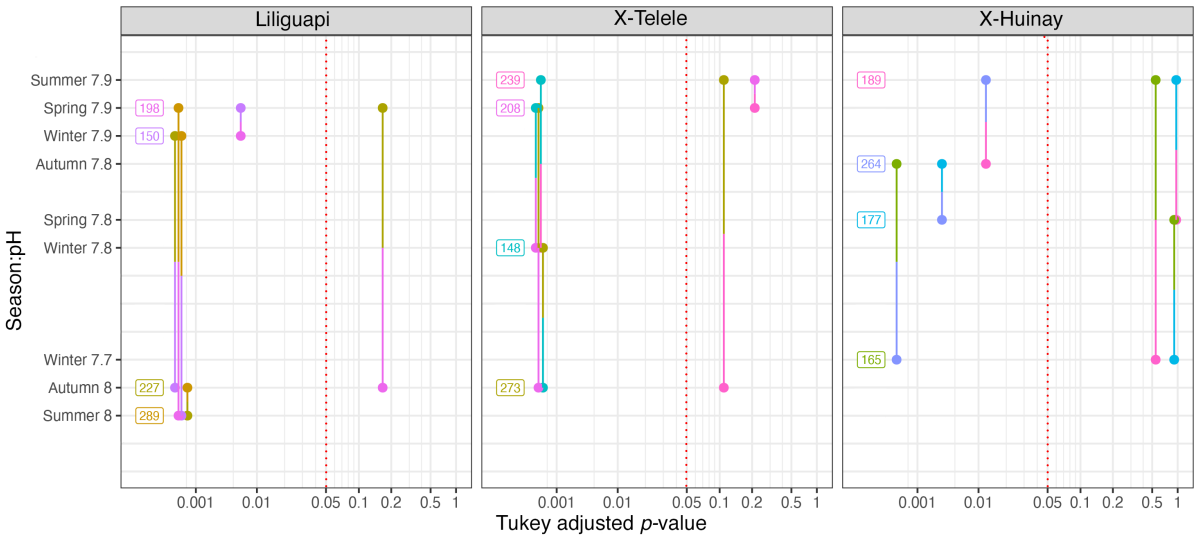

Fig. SM7 Pairwise emmeans comparisons plot. Tukey contrasts for season and seawater pH by site. The *p*-value is defined significant at a threshold of $\alpha = 0.05$, depicted with the red dotted line.

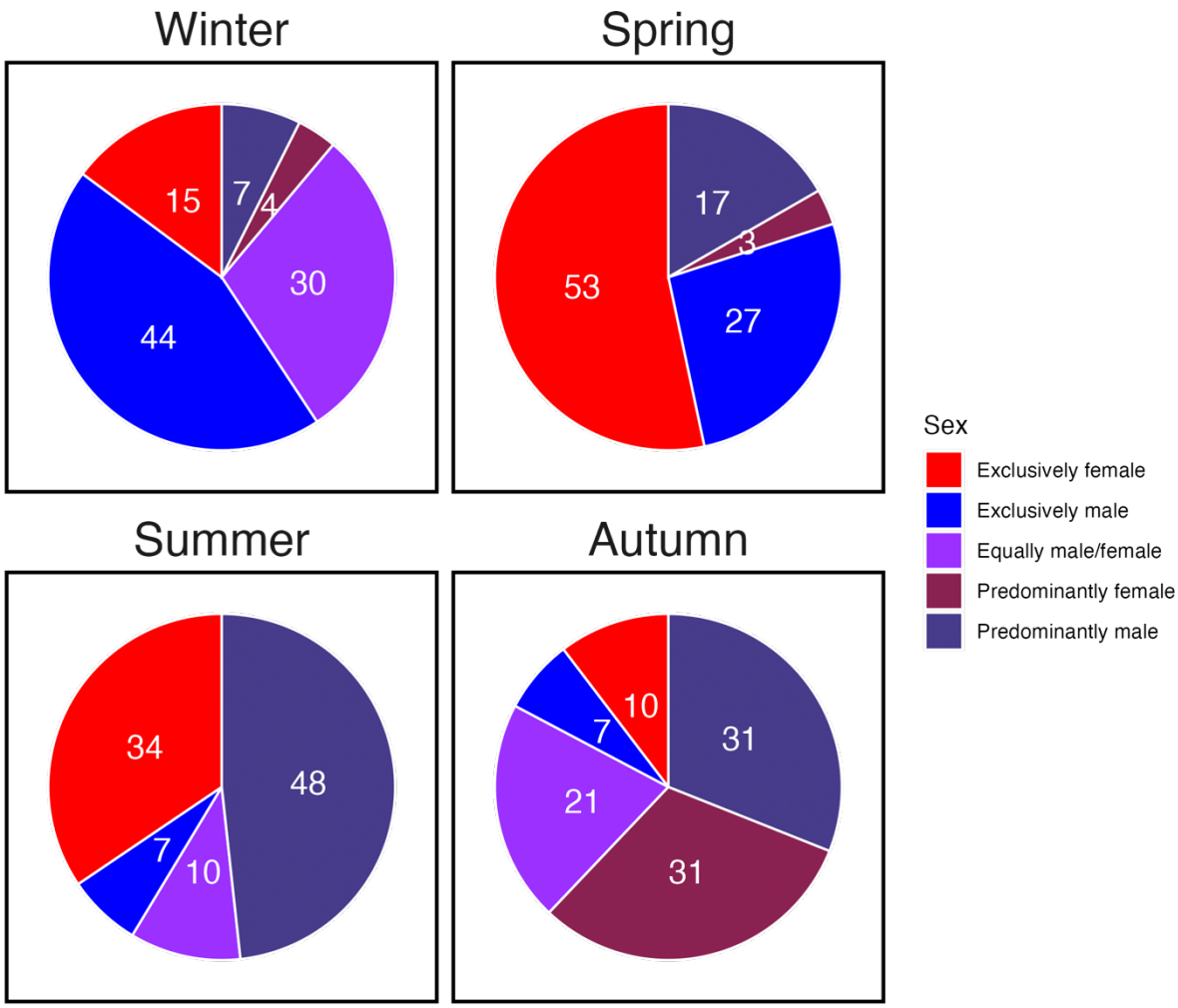

Fig. SM8 Percentage of polyps per respective sexuality (“exclusively female”, “exclusively male”, “equally female/male”, “predominantly female”, and “predominantly male”) from all three study sites (Liliguapi, X-Telele, X-Huinay) was plotted per season (winter, spring, summer, and autumn).

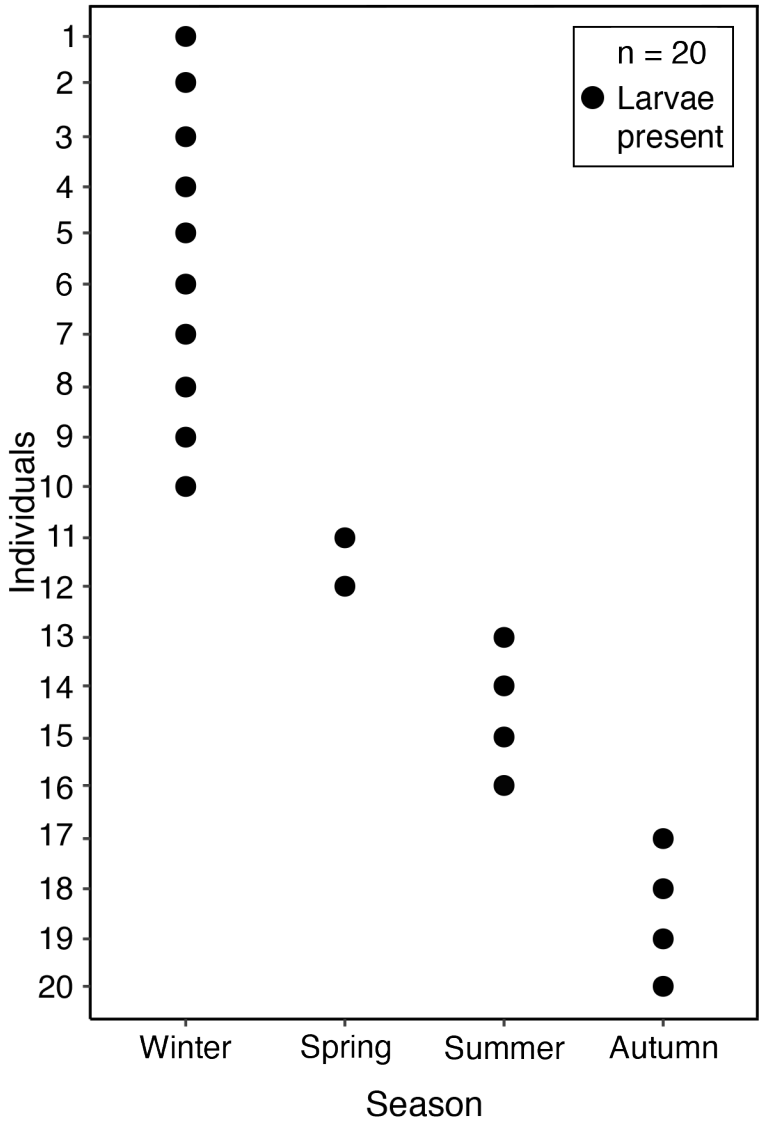

Fig. SM9 Larval presence during the seasonal reproductive periods of *C. huinayensis*. Each of the 20 black circles indicate an individual polyp containing larvae, out of a total of 118 polyps collected across winter, spring, summer, and autumn seasons, all stained with HE.

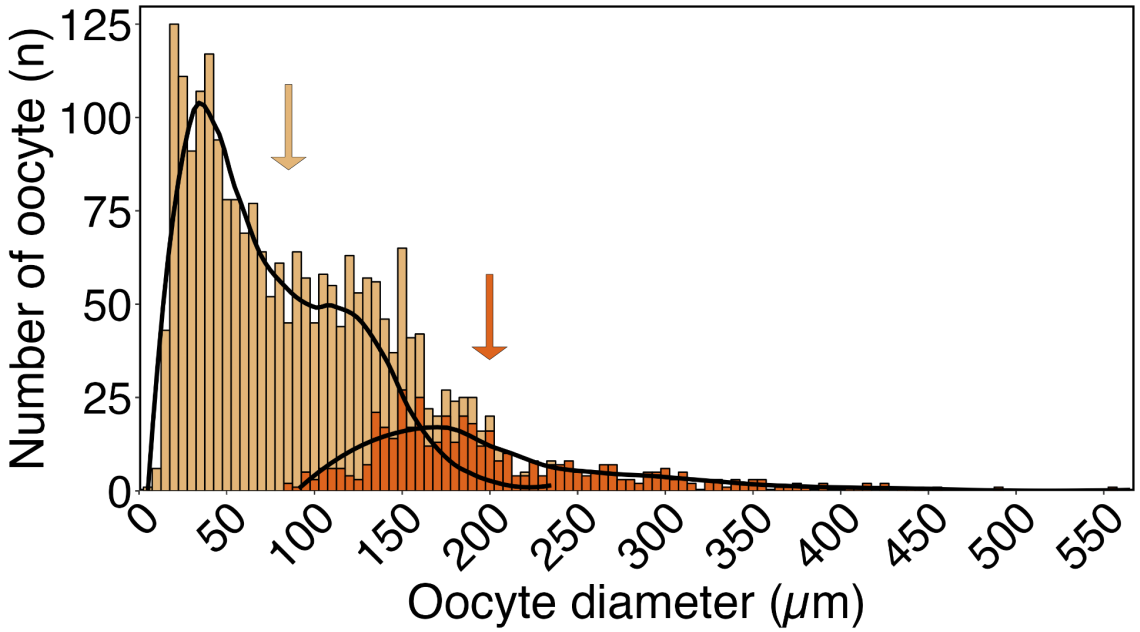

Fig. SM10 Number of PV (light-orange) and V (orange) oocytes of *C. huinayensis* distributed by size. Light-orange and orange arrows indicate the mean oocyte size (72 μm and 200 μm, respectively). The division of PV and V oocytes was based on the homogeneous and heterogeneous structural content, respectively (refer to Fig. 2e).

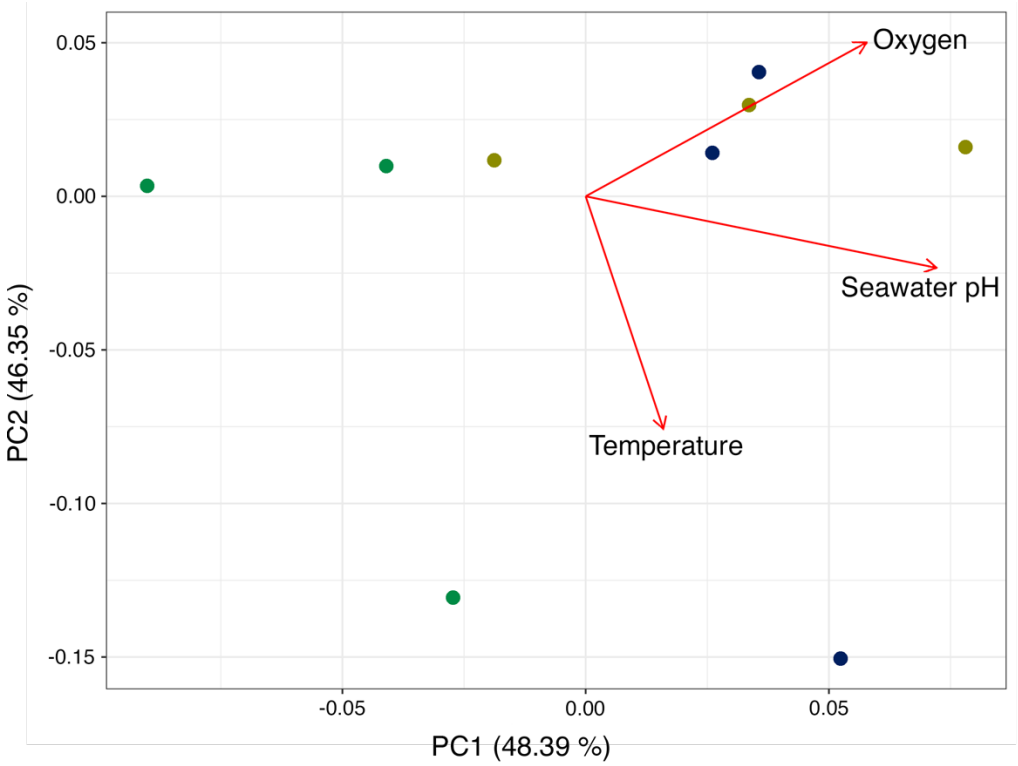

Fig. SM11 Principal Component Analysis (PCA) biplot representing the environmental variables seawater pH, temperature, and oxygen obtained at each study site (Liliguapi: blue; X-Telele: yellow; X-

Huinay: green). The vector's direction and length indicates the environmental variable's contribution to the first two components in the PCA. The angles between the vectors reflect correlation between the variables: i.e., pH and temperature, pH and oxygen. The black dots correspond the projected oocyte size data over the principal components PC1 and PC2.

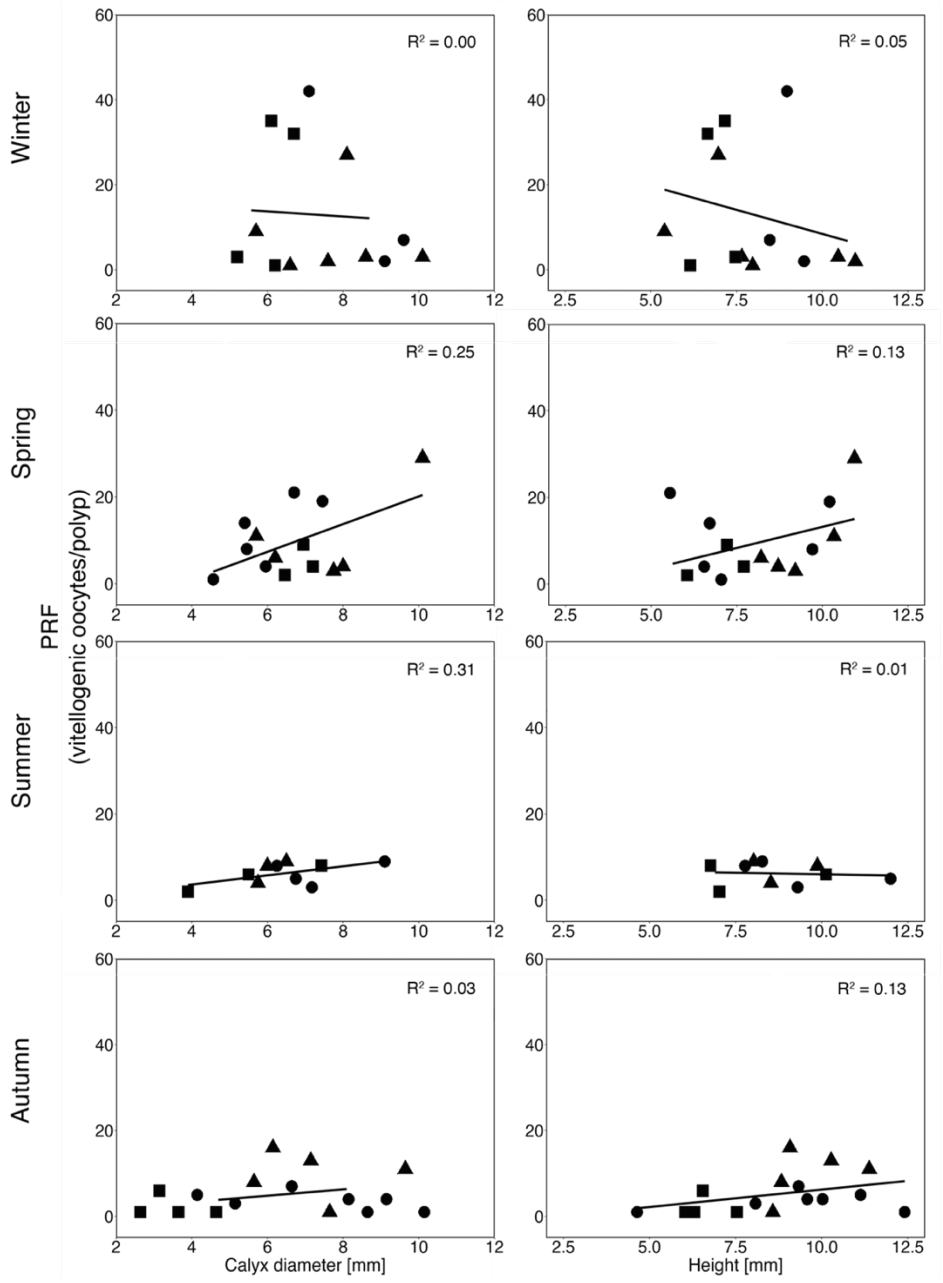

Fig. SM12 Seasonal potential relative fecundity (PRF: number of V oocytes per polyp) in relation to the corallum size (calyx diameter and height). Data points correspond to individual polyps collected at each study site (Liliguapi: circle, X-Telele: triangle, X-Huinay: square). The black solid line represents the linear model fitted to the data.

6

Discussion and Conclusions

Understanding the life cycle of species is fundamental to their conservation and management in the face of environmental change. While the number of studies on deep-sea and shallow-water scleractinian CWCs has increased rapidly in recent years, information on metamorphosis stages, reproductive biology and ecology remains limited. In particular, there is a lack of information on how early life stages will cope with the predicted (RCP 8.5, Meinshausen et al. (2011)) low seawater pH and the undersaturation of seawater with respect to aragonite ($\Omega_{arag} < 1$), compared to scleractinian WWCs. In this chapter, I discuss the findings of my research, which aimed to reveal and describe the early development of scleractinian CWCs from the larval to the polyp stage, highlight potential new dispersion pathways, and assess the effects of low seawater pH on gametogenesis, and $\Omega_{arag} < 1$ on skeletogenesis in newly recruited polyps. Here, for the first time in a scleractinian CWC, I have described the early stages of recruitment after metamorphosis. I also introduce a new type of a reverse development process that may have implications for polyp dispersal. Additionally, I have experimentally demonstrated that newly recruited *C. huinayensis* polyps are able to build integral skeletons under aragonite-undersaturated water. In line, *in situ* studies showed that the naturally low seawater pH in a Chilean fjord influences oogenesis.

6.1 Answers to the research questions

Q.1 What is the reproductive mode and strategy of the scleractinian CWC *C. huinayensis*? Has its reproduction seasonal peaks?

Brooding was identified as the reproductive mode of *C. huinayensis* (**Chapter 2**), with larvae being released in the aquaria throughout the year (**Chapter 2**), and based on histological analysis, brooding *in situ* throughout the year with a peak during austral winter (**Chapter 5**). This reproductive mode is however rather unexpected considering that other scleractinian CWC species from the same family Caryophylliidae are all broadcast spawners, e.g., *Caryophyllia ambrosia, C. seguenzae, Desmophyllum pertusum, Premocyathus cornuformis* (Waller and Tyler 2005), *D. dianthus* (Feehan et al. 2019) *C. smithii* (Tranter et al. 1982), as well as *Goniocorella dumosa* and *Solenosmilia variabilis* (Burgess and Babcock 2005). Thorson's rule (Thorson 1957; Mileikovsky 1971), which suggest that brooding is a characteristic of species living at higher latitudes while broadcast spawning is more common in species residing at mid- and lower-latitudes, may support this unexpected finding. Considering observations of six other species of the genus *Caryophyllia*, all of which are endemic to Antarctica, and the fact that *C. huinayensis* broods like high-latitude species (**Chapter 2**), it is plausible to suggest that its mid-latitudes distribution may be favoured by the cold Humboldt Current deriving from the Southern Ocean.

C. huinayensis exhibits cyclic hermaphroditism as a reproductive strategy (**Chapter 5**). It has also been demonstrated that the hermaphroditism observed in this species presents different combinations of sexuality, which vary within the same study site and season. Each season is characterized by sexual dominance as follows: “exclusively-male” in winter, “exclusively-female” in spring, “predominantly-male” in summer, and “equally-female/male” in autumn (**Chapter 5**). To date, this reproductive strategy has been observed in four scleractinian CWCs, all of which belong to the family Caryophylliidae (Waller et al. 2005).

Q.2 Can scleractinian CWCs undergo reverse development to disperse, similar to what has been observed in scleractinian WWCs?

Yes, for the first time, we provide evidence of a new form of reverse development in a scleractinian CWC based on aquarium and *in situ* observations: polyp dropout in *C. huinayensis* (**Chapter 3**). Reverse development has been observed under environmental stress through ontogenetic reversal and polyp detachment, expulsion, and bail-out (Sammarco 1982; Kramarsky-Winter et al. 1997; Piraino et al. 2004; Kružić 2007; Capel et al. 2014; Serrano et al. 2018), whereby in all cases the calcified sedentary polyp becomes mobile again and can be dispersed by currents to eventually settle. Polyp dropout in *C. huinayensis* (**Chapter 3**) differs from the aforementioned reverse development, as it was not triggered under stress. Here, the dropout polyps attached to the substrate with their tentacles, but settlement was not observed even after 8 months of the dropout. However, if we assume that reattachment is possible beyond our observation period, as has been demonstrated in the scleractinian WWC *Tubastraea coccinea* (Capel et al. 2014), we can assume that there is a potential for lateral dispersal for *in situ* of at least 3.7 km by the current (5 cm s^{-1}), which would then be followed by settlement and the onset of skeletogenesis to re-establish the life cycle. A process that may have occurred during the Permian-Triassic mass extinction that allowed scleractinian polyps to survive as “naked polyps” as hypothesized by Stanley Jr (2003) (**Chapter 3**).

Q.3 Do the distinct developmental stages from larvae to juvenile polyps of the scleractinian CWC *C. huinayensis* arise at a similar timing to that of zooxanthellate scleractinian WWCs, despite major environmental differences?

Yes, the present observations show similarities in both the timing and sequence of development of mesenteries and endotentacles (first set of six tentacles) between *C. huinayensis* and zooxanthellate scleractinian WWCs (**Chapter 2**). The development time of the exotentacles (second set of six tentacles), the formation of

the first crystals and the subsequent crystal structures of the basal plate and the septa also show similarities.

The metamorphosis towards an early juvenile in scleractinian corals is an energy intensive process due to the initiation of calcification (Allemand et al. 2011). Usually, this energy demand in recruits of scleractinian CWCs is supplemented by photosynthates such as glucose provided by endosymbionts. However, the larvae of *C. huinayensis* lack photosynthetic endosymbionts, suggesting that internal reserves, heterotrophic feeding, or a combination of both cover the energy requirements during early juvenile growth (**Chapter 2**). Nonetheless, the similarities in the early ontogenetic stages of *C. huinayensis* compared to scleractinian WWCs, such as *Galaxea fascicularis* and *Acropora brueggemanni* (Atoda 1951a, b), suggest a highly conserved, genetically encoded process that is not extended in time despite the major environmental differences (e.g., seawater temperature) (Kleypas et al. 1999; Riegl and Purkis 2012).

Q.4 Do early-life history stages of scleractinian CWCs during ontogenetic skeletal formation exhibit similar timing and crystal deposition patterns to those of scleractinian WWCs, despite significant environmental differences?

Yes, in a specially designed *in vitro* flow-through chamber, we documented for the first time *in vivo* under a polarized microscope the skeletal development of newly recruited scleractinian CWC *C. huinayensis* and revealed similarities in both timing and the micro- and macro skeletal formation and pattern to those observed in scleractinian WWCs (**Chapter 4**). Following the experimental run, we analysed the crystals that had developed to shape the skeleton using scanning electron microscopy and confocal Raman microscopy. Our observations revealed that this CWC species shares a similar composition (Cohen and Holcomb 2009; Clode et al. 2011; Foster and Clode 2016), shape, and timing of crystal precipitation, as well as the pattern of crystal formation for the basal plate and primary septa with some scleractinian WWC species (Vandermeulen and Watabe 1973; Le Tissier 1988; Gilis et al. 2014, 2015; Neder et al. 2019). Remarkably, despite differences in environmental conditions such

as water temperature and nutrition types (e.g., mixotrophy or heterotrophy), there were no temporal divergences.

Q.5 How does aragonite undersaturation of seawater affect early skeletogenesis of scleractinian CWCs?

No negative effect on the early skeletogenesis of scleractinian CWCs were observed, as scanning electron microscopy results reveal that *C. huinayensis* recruits are capable of forming an integral aragonite skeleton, maintaining remarkable consistency in their early biomineralization under Ω_{arag} = 0.9 (**Chapter 4**). In contrast, juveniles of scleractinian WWC species exhibit skeletal alterations, including changes in shape, size, reduction in their calcified attachment area, number of septa, and increased porosity (Cohen et al. 2009; Foster et al. 2016; Carbonne et al. 2022). One possible explanation for these different responses between the two groups of scleractinians may lie in the long-term evolutionary divergence in their traits. Scleractinian CWCs typically thrive in deep-sea environments where unfavourable conditions, such as low seawater saturation states with regard to aragonite can occur and persist (Thresher et al. 2011). This may have given them the ability to elevate their carbonate saturation state in the calcifying medium by ~0.8–1.0 units (ΔpH) relative to the ambient seawater, in contrast to scleractinian WWCs, which can elevate it by ~0.4–0.5 units (McCulloch et al. 2012). This ability may explain why scleractinian CWCs can counteract the effect of Ω_{arag} = 0.9 on calcification processes.

Q.6 Does the low seawater pH predicted under the "business-as-usual" scenario (Pörtner et al. 2019) affect the reproduction of scleractinian CWCs that thrive in naturally acidified waters?

We observed that seawater pH has variable effects on the V oocyte size. Spatio-temporal variations in V oocyte size and abundance showed no consistent relation to corresponding variations in seawater pH, temperature, salinity and oxygen,

suggesting a mix of environmental and endogenous factors affecting *C. huinayensis* reproduction (**Chapter 5**).

6.2 General discussion

This thesis broadens our knowledge and understanding of the life history of scleractinian CWCs and the effects of OA on their reproduction and early skeletal development. I have combined aquaria experiments and field observations to describe the reproductive strategy and mode, pelagic larval duration (PLD), and a novel potential dispersal mechanism on the scleractinian CWC *Caryophyllia huinayensis* (**Chapter 2**, **3**, **5**). Moreover, the early developmental stages from larvae to newly settled recruits were described for the first time in a scleractinian CWC (**Chapter 2**). Additionally, I investigated the effects of seawater pH on oogenesis and the effects of OA on early skeletogenesis in recruits, revealing that CWCs can cope with the current and potentially with future environmental changes (**Chapter 4** and **5**).

Scleractinian CWCs typically inhabit the deep-sea, often forming sparse populations. As a result, obtaining large sample sizes for conclusive studies requires significant sampling efforts and expenses. Due to limited funding, basic biological and ecological information remains scarce. This is why, among the more than 3,000 known CWC species, reproductive biological information is available for less than 4 % (Waller et al. 2023). Of these, 23 species belong to scleractinian CWCs (Waller et al. 2023). In **Chapter 2** and **5,** I contributed to this knowledge by describing *C. huinayensis* as the only scleractinian CWC identified to date as an asynchronous cyclic hermaphrodite that releases brooded larvae throughout the year.

The scleractinian CWC *D dianthus* can be ubiquitous in Comau Fjord (Fillinger and Richter 2013), forming pseudocolonies as an organizational structure. As this species is gonochoric and has the potential to broadcast spawn (Feehan et al. 2019), this organizational form increases the likelihood of cross-fertilization. Conversely, *C. huinayensis* is a solitary polyp, relatively small in size (20 mm high, 7.6 mm in diameter) (Cairns, Häussermann & Försterra, 2005), and has the potential to be

ubiquitous in Comau Fjord as well (Försterra et al. 2014). In **Chapter 5**, I described *C. huinayensis* as an asynchronous cyclic hermaphrodite. Based on its organizational structure and potential distribution, this reproductive strategy could enhance cross-fertilization assurance for this corals. Given that scleractinian CWC populations tend to scatter into deeper waters (Fillinger and Richter 2013), the capacity of *C. huinayensis* to undergo asynchronous sexual cycle changes, also observed in three other solitary Caryophylliidae (Waller et al. 2005), may ensure that a portion of the population has mature gametes year-round, facilitating cross-fertilization even at low polyp densities. This allows year-round production of larvae.

In situ studies of larval production and release would require continuous monitoring of selected polyps. While this approach is feasible, it is not particularly practical due to the extensive time require to accurately determine both the number and timing of larval releases. The distinctive culturing system at the Alfred Wegener Institute (AWI), designed to mimic the environmental parameters of the scleractinian CWC populations in Comau Fjord, successfully created the conditions necessary for reproduction in the maintained *C. huinayensis* population. Consequently, I took advantage of this unique opportunity and conducted a three-year experiment to determine the number and periodicity of larvae released. In **Chapter 2**, I described that the reproductive mode of *C. huinayensis* is brooding, with larvae been released throughout the year. This continuous larval production and released may allow this coral to rapidly colonize new available spaces created by biological events, such as mass mortalities (Försterra et al. 2014), or mechanical disturbances such as landslides (Sepúlveda et al. 2011). In this highly dynamic system and in aquaria, we observed that in the absence of any clear environmental trigger, *C. huinayensis* can detach from its skeleton and potentially drift with currents to new habitats (**Chapter 3**). This process, named as polyp dropout, may allow the freed polyp to resettle and continue its life cycle in a new location–a hypothesis that has yet to be proven.

Year-round brooding in *C. huinayensis* allows for efficient resource allocation, as investing energy fewer, well-protected, and well-developed larvae could enhance recruitment success and survival rates (Szmant 1986). Conversely, broadcast spawning is usually highly seasonal (see for example, Feehan et al. 2019; Maier et al. 2020), involving the release of larger number of gametes compared to brooders. The

higher gamete output may help offset the increased risk of predation associated with the prolonged exposure of gametes and larvae in the water column (Oliver and Babcock 1992). However, neither spawning nor brooding seems to confer a consistent evolutionary advantage over time, as these reproductive modes can occur within the same environment (Kerr et al. 2011). Differences between these reproductive modes my primarily influence their PLD, affecting dispersal and population connectivity (van der Ven et al. 2021).

In *C. huinayensis*, the PLD was found to be in the order of one week (**Chapter 2**), suggesting a relatively low dispersal potential compared to broadcast spawning species, which can have a PLD ranging from several weeks to a year (Brooke and Young 2003; Strömberg and Larsson 2017). This shorter PLD increases the likelihood of larvae settling near the parental community. As detailed in **Chapter 5**, histological samples indicate that gametes of one sex develop and mature at different times than those of the opposite sex, making self-fertilization unlikely. This suggest that sperms must be taken up from close conspecifics for oocytes fertilization, indicating that *C. huinayensis* population in Comau Fjord may exhibit panmictic, as is the case of *D. dianthus* in the same area (Addamo et al. 2021; Addamo et al. 2022). Moreover, the reduced dispersal potential may have implications for population connectivity and genetic exchange (van der Ven et al. 2021), potentially contributing to the endemic status of *C. huinayensis* in Chile.

Once the mobile larvae find a suitable substrate, they settle and begin the metamorphosis stage. At this stage of development, it is generally assumed that somatic growth (tissue and skeleton development) occurs faster in zooxanthellate scleractinian corals than in azooxanthellate corals (Schuhmacher and Zibrowius 1985). This assumption stems from the fact that symbiotic dinoflagellates transfer most of their photosynthates to the host, aiding with the energetic demands for metamorphosis into young polyps (Falkowski et al. 1984; Dubinsky and Falkowski 2011). However, experimental evidence supporting this assumption is scarce (Marshall 1996), primary due to the challenges of replicating appropriate environmental conditions for reproduction and settlement in aquaria settings. Consequently, both this hypothesis and the early developmental stages of scleractinian CWCs remain largely unverified. The only documented instance of larval

settlement in CWCs was described in *Oculina varicosa* by Brooke and Young (2003), though it lacks detailed characterization.

As previously mentioned, the experimental aquaria at AWI provided the first documented instance of polyp metamorphosis into newly recruited scleractinian CWCs (**Chapter 2**). This unique setup also enabled a comparison of the developmental rate and timing of early skeletal formation in *C. huinayensis* with other scleractinian CWCs through *in vivo* microscopic observations, utilizing a specialized flow-through chamber system (**Chapter 4**). Therefore, in these two chapter, I demonstrated that the newly recruited azooxanthellate *C. huinayensis* exhibits not only similar timing but also comparable sequential development of microstructural crystal elements forming the basal plate, septa, and columella to those observed in at least four newly recruited scleractinian WWCs species (Vandermeulen and Watabe 1973; Le Tissier 1988; Gilis et al. 2014; Gilis et al. 2015; Neder et al. 2019). The similarity in rapid skeletal growth between scleractinian WWCs and CWCs is a noteworthy finding. Several factors likely contribute to this phenomenon, with temperature, feeding (Freiwald 2002; White et al. 2005; Maier et al. 2020), and seawater aragonite saturation (Kroeker et al. 2013), suggested to be the most significant variables.

The successful reproduction of *C. huinayensis* in the aquarium suggest that the environmental conditions (see Laudien et al. 2021) were conducive to both reproduction and somatic growth. For *C. huinayensis* to sustain similar somatic growth to those of scleractinian WWCs (Atoda 1951a, b), its heterotrophic feeding and/or internal energy reserves must have been at least equal to those of mixotrophic coral species, as its energy uptake would have had meet the metabolic demands of metamorphosis in the recruits. This implies the presence of a highly conserved evolutionary ontogenetic mechanism in Hexacorallia that can be expressed under optimal environmental conditions. However, the rising atmospheric CO_2 levels and associated changes in seawater chemistry (Kleypas et al. 1999b; Feely et al. 2004; Orr et al. 2005) raise concerns about whether such optimal conditions still exist in the natural environment. This causes critical questions about the potential impacts of lowered seawater pH on the early development stages, which are often considered a bottleneck for species survival (Cohen et al. 2009; Foster et al. 2016; Carbonne et al. 2022).

To further investigate the effect of low seawater pH on early developmental stages, I collected *C. huinayensis* polyps from naturally acidified sites in Comau Fjord, Chile, across all seasons. These polyps were histologically analysed to assess the seasonal development of mature oocytes, i.e., vitellogenic (V) oocytes. Sampling was conducted at three study sites, each characterized by different seawater pH levels, ranging from 7.7 to 8.0 (**Chapter 5**). Our findings indicate that seawater pH does not have an overall negative effect on V oocyte size. Instead, its effects vary, with both positive or negative outcomes depending on interactions with environmental parameters such as seawater temperature and oxygen, seasonal variability and site location, likely influenced by the fjord's geography. Thus, environmental factors can affect reproductive processes (**Chapter 5**). However, while these results indicate seawater pH, in synergy with environmental variables, affects oocyte development, it remains unclear whether these effects extend to larval formation and subsequent metamorphosis into juvenile polyps under acidified water conditions.

Allemand et al. (2004) demonstrated that scleractinian CWCs can regulate their internal pH and DIC in the calcifying medium to compensate for external seawater pH changes. However, this process requires higher energy expenditure (Spalding et al. 2017), which, in larvae with limited energy reserves, may deplete these reserves, potentially altering the metamorphosis process from larva to juvenile polyps, particularly their early skeletal development. Such impacts has been observed in scleractinian WWCs recruits exposed to low seawater pH (Cohen et al. 2009; Foster et al. 2016; Carbonne et al. 2022).

To test this hypotheses, I employed a small flow-through chamber system, which allowed me for microscopic monitoring of early skeletal formation *in vivo* during the metamorphosis from larvae to a juvenile polyps, under conditions of low seawater pH and undersaturated aragonite concentration of seawater (**Chapter 4**). Here, I demonstrated that *C. huinayensis* recruits maintain remarkable skeletal formation under Ω_{arag} = 0.9, supporting the assumption of a long-term evolutionary trait in scleractinian CWCs that allows them to elevate their carbonate saturation state in the calcifying medium (McCulloch et al. 2012). This indicate that they have the mechanisms to cope with the projected reduction in seawater aragonite saturations by the end of the century (Meinshausen et al. 2011). However, current and projected

global changes do not affect seawater aragonite saturation in isolation. Further studies should examine the combined effects of multiple stressors, such as $\Omega_{arag} < 1$, elevated seawater temperatures, and changes in food supply on the early skeletal formation of newly settled scleractinian CWC recruits.

6.3 Concluding remarks

The life history of the CWC *Caryophyllia huinayensis*, thriving in a naturally acidified Chilean fjord, was previously unknown. My research has revealed that this solitary, azooxanthellate scleractinian polyp is a hermaphrodite, capable of brooding its larva and cycling its sexuality during gamete development. This ability is likely linked to its asynchronous gamete production, which supports continuous larval released throughout the year. Notably, this year-round larval production was observed even in aquaria settings located in different hemispheres, suggesting that in the absence of external timing signals such as water temperature fluctuations, food availability, and other environmental factors, the coral's internal reproductive clock remains active. Moreover, without clear signals, *C. huinayensis* can detach from its skeleton, potentially drifting with currents to alternative habitats. This polyp dropout mechanism may enable the coral to continue its life cycle if the organism successfully resettles in a new habitat (Fig. 5). Upon released, the larvae can remain in the plankton for about a week (Fig. 5), but they relatively short PLD suggests limited dispersal potential, which may contribute to the species' constrained distribution along the Chilean coast.

For the first time, the transition phase from larvae to juvenile polyps has been described in a scleractinian CWC. Over a three-year documentation period, we documented skeletal deposition occurring within a week, with recruits beginning to feed before the end of the first moth. However, it was noted that the polyps did not reach full tentacle development–most individuals had 24 tentacles, compared to the adult 48–and they not achieved reproductive maturity. Despite environmental conditions such as seawater temperature differing from those experienced by

zooxanthellate scleractinian WWCs, the early developmental stages of *C. huinayensis* exhibited remarkably similar timing and sequential development of soft tissue and microstructural crystal formation to certain zooxanthellate counterparts (Fig. 5). This suggest that the high energy demands for rapid somatic growth were sustain though heterotrophic feeding, and potentially due to optimal temperature and environmental conditions this coral was reared in the aquaria.

In contrast, in the naturally acidified Comau Fjord, we observed that low seawater pH had a variable effect on oogenesis, specifically on the V oocyte size. The effect of seawater pH was both positive and negative, depending on interactions with seawater temperature and oxygen, seasonality and site location. This indicate that, compared to aquaria settings, variability and combination of certain environmental parameters do affect reproduction (Fig. 5). Conversely, experimental tests low seawater pH and unsaturated aragonite of seawater revealed that newly recruits polyps are capable to form integral skeletal structures and exhibiting high growth rates. Since recruits are not mature enough to reproduce, this may support the notion that reproduction, particularly oogenesis, is a highly energetic process constrained by somatic growth (Fig. 5).

These findings raise important questions about the mechanisms of acclimatization and adaptation in response to anthropogenic climate change. Rapidly understanding of scleractinian CWC population responses at a larger scale often overlooks the early life stages, which are crucial for population survival. A comprehensive understanding of how scleractinian CWCs utilize various mechanisms to sustain gametogenesis and early biomineralization under changing environmental conditions is essential for predicting their responses to ongoing global anthropogenic changes. In this thesis, I developed a method to test different environmental scenarios on the early developmental stages of corals, providing foundational insights into the effects of OA and naturally low seawater pH on the early life cycle of scleractinian CWCs

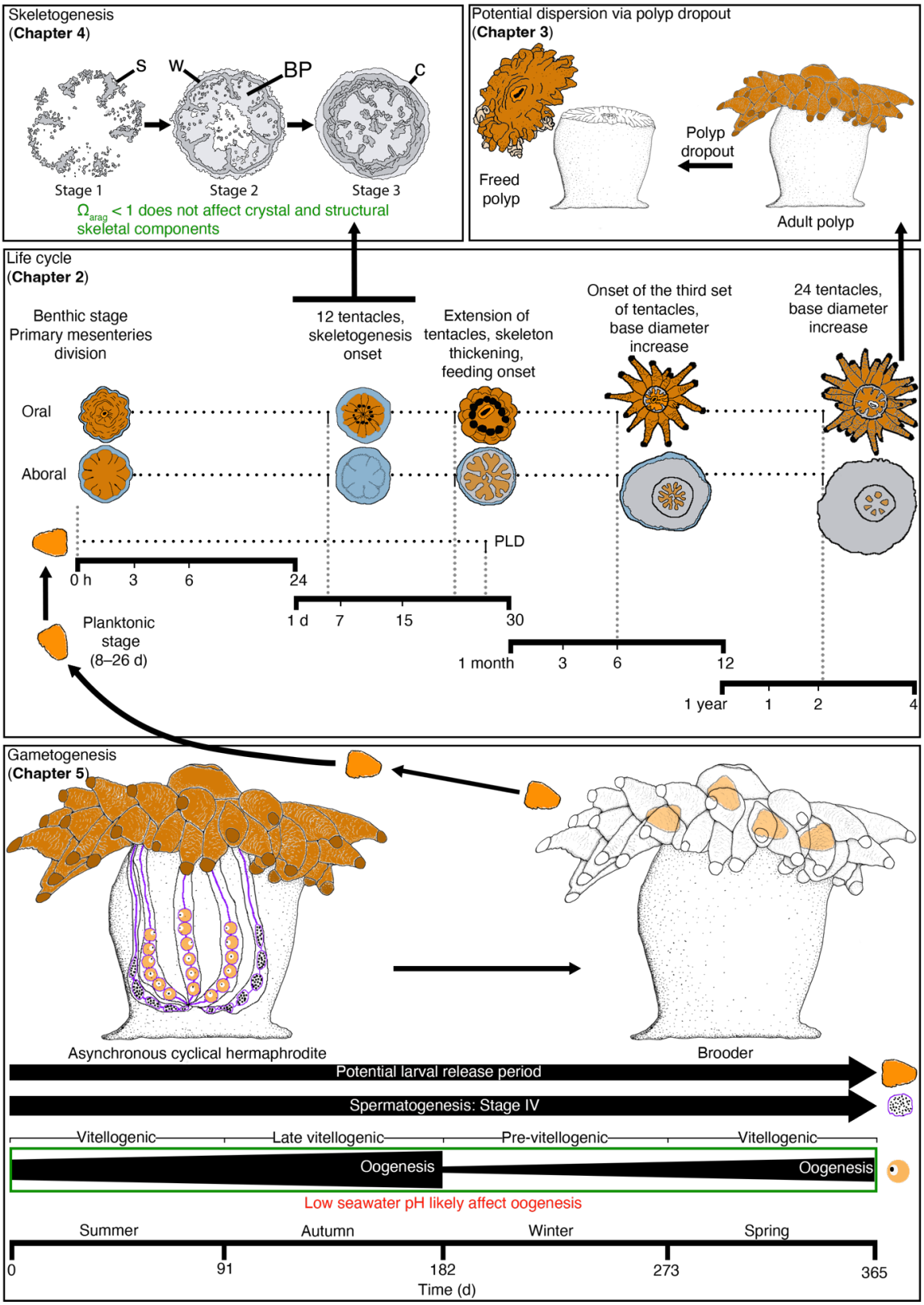

Figure 5: Summarized results of **Chapters 2–5** presented in this thesis. The scleractinian CWC *C. huinayensis* is an asynchronous cyclical hermaphrodite that initiates oogenesis in austral winter, with late vitellogenic oocytes occurring in autumn. Throughout oogenesis, mature Stage IV sperms and developed larvae indicate potential year-round release of both. Oocyte size (indicated in green letters, **Chapter 5**) was affected by low seawater pH (**Chapter 5**). When larvae were released, the potential

larval duration (PLD) was a maximum of 26 d before settling to begin their metamorphosis into young polyps (**Chapter 2**). As adults, they can detach from the skeleton by a process called polyp dropout, which is a possible dispersal mechanism (**Chapter 3**). Approximately two days after settlement, recruits initiate skeletogenesis and around 21 d after settlement feeding begins (**Chapter 2**). Three growth stages were defined on the basis of micro- and macrostructural aspects of the primary skeleton. The septa (s), wall (w), basal plate (BP), and columella (c) form spatially and temporally similar to tropical and temperate scleractinian corals. Furthermore, the low aragonite saturation of seawater (indicated in green letters, **Chapter 4**) has no adverse effect on the crystal type or skeletal structure of the three growth stages (**Chapter 4**).

Outlook

Between 34 % and 49 % of the population of two brooding hermaphroditic scleractinian WWCs self-fertilized the oocytes, indicating that self-fertilization may be an important mode of reproduction in WWCs (Brazeau et al. 1998). However, it remains unclear whether the brooded larvae (**Chapter 2**) of the asynchronous cyclical hermaphrodite *C. huinayensis* (**Chapter 5**) are the result of cross-fertilization, self-fertilization, or asexual reproduction. Due to the asynchronous hermaphroditism observed in *C. huinayensis*, whereby the development and maturation of gametes alternates between sexes, self-fertilization is considered unlikely. An alternative reproductive mechanism has been deducted in the scleractinian WWC *Pocillopora damicornis*. Genetic studies indicate that the larvae are produced asexually via budding or parthenogenesis (Stoddart 1983; Combosch and Vollmer 2013; Oury et al. 2019). Consequently, future studies should compare the genetics of the offspring with that of their parental polyps to elucidate whether the brooded larvae of *C. huinayensis* are produced sexually, asexually or by both.

Both *in vitro* and *in situ* studies of the shallow-water population of *C. huinayensis* in Comau Fjord revealed that oogenesis onset and the highest larval abundance occur in winter (**Chapter 2** and **5**). Additionally, the spawning event in the shallow-water population of *D. dianthus* (Feehan et al. 2019) and the octocoral *Primnoella chilensis* (Rossin et al. 2017) in Comau Fjord is expected to occur at the same time of the year. As the winter season coincides with the seasonal minimum of seawater temperature, it is plausible to assume that oogenesis and spawning of the aforementioned species are triggered by temperature fluctuations in the shallow-water community, in addition to other environmental factors. In the deep waters of Comau Fjord, however, deep mixing causes heat loss at the surface during autumn, driving the warm upper water to greater depths. This results in a significant temperature difference between the upper and deepest water layers during the same season (Fillinger and Richter 2013; Jantzen et al. 2013; Addamo et al. 2021). It would be of interest to ascertain whether the thermal differences in question may result in a discrepancy in the onset of oogenesis between the deep and shallow populations of the aforementioned corals.

This thesis demonstrated that Ω_{arag} = 0.9 has no adverse effect on the micro- and macrostructural skeletal components of newly settled recruits of *C. huinayensis* (**Chapter 4**). However, it is anticipated that OA and elevated seawater temperature will occur in conjunction. Consequently, the combined effects of these two stressors on skeletogenesis represent a significant constraint that needs to be taken into account. A number of studies have indicated that elevated seawater temperature may exacerbate the adverse effects of reduced seawater pH on calcification of scleractinian WWCs, suggesting a synergistic effect (Reynaud et al. 2003; Anthony et al. 2008; Rodolfo-Metalpa et al. 2011; Kroeker et al. 2013). To date, no study has quantified the impact of the combined effect of warming and OA on early skeletogenesis of scleractinian CWCs. Thus, the question of how synergistic multi-stressors affect early skeletogenesis remains unanswered and should be addressed by future studies.

Acknowledgements

I would like to thank everyone whose inspiration, encouragement and support gave me the determination and perseverance without which the realization of my study would have been much more difficult.

To the reviewers of this thesis, Prof. Claudio Richter and Dr. Covadonga Orejas, and the evaluation committee, chairperson (pending con confirmation) and reviewer (pending confirmation).

I also like to thanks PhD candidate (pending confirmation) and Patrik Beggel for being part of my evaluation committee.

Dear Natu, Baby and Tato, it is not easy to find the right words or just a few ones to express how important you have been to me during this process. Natu, thanks for your endless support, clever advises, and for those big decisions you took to always be together. Baby and Tato, without your life example, which is my biggest inspiration, I would have never considered to go through this process. You are my All.

Dear Jürgen Laudien, I will never forget that talk in Isla Jaime (Pitipalena, Chile) where you told me I could do a PhD project with you. And here I am, deeply grateful for your invaluable supervision and above all, your friendship! You managed to showed me that there is always a way-out through all possible struggles that can occur on the way, and the support you gave me was always with a smile and a hand on my shoulder. Thanks for showing me how to think out of the box and for your guidance at any moment…any moment!

Thank you, Claudio Richter, for structuring my scientific thinking and for teaching me to think rationally. A road that I will continue to traverse. Also, I thank you for the opportunity to immerse myself into the cold-water coral world, which fascinates me more than I originally thought.

I would also like to thank my PhD committee – Vreni Häussermann, Humberto González-Estay and Günter Försterra – for their great and clear advises during our meetings, and for their valuable comments on our manuscripts.

Special thanks to my co-authors, Marlene Wall, Gernot Nehrke, and Rhian Waller. Without your expertise, guidance, and support, I would not have gained the extensive knowledge I now have about biocalcification and reproduction in CWCs.

I also thank all members of the former section Bentho Pelagic Processes, now Benthic ecology at AWI for their administrative and scientific support, especially Ursula Liebert, Horst Bornemann, Henning Schröder, Steffi Meyer, and Moritz Holtappels. I would particularly like to thanks Nils Owsianowski for your ingenious advises and ideas, and for those great walks with an ice-cream.

Esther Lüdtke, Ulrike Holtz, Mandy Kuck, and Erika Allhusen, I would like to thank you not only for helping me with all those practical details in the laboratories, but also for your warm friendship and nice spontaneous talks.

To my fellows Cesar Pacherres, Elena Schall, Cote Diaz, Santiago Pineda-Metz, Nur Garcia, Mariano Martinez, Miriam Gerhard, Kristina Beck, Susana Simancas, Marwa Baloza, Luisa Federwisch, Felix Auer, Vincent Rigalleau, Nathan Beech, and Hameed Moqadam, thank you for always been there, during the good and bad times! For your friendship, unconditional support, and for all those times you made me smile, although it was not so hard. You truly enriched this process with your beautiful personalities.

Hermana doctoral, querida Susana Simancas, although you joined me at a late stage, your great personality, energy and willingness to help whenever I needed it made me feel like you were with me from the start. Thanks so much for your genuine friendship!

Querida Mamá, Papá, Irene, Ale, Cati, Cami, Dani, Mati, sin aun creyéndolo les estoy escribiendo estas líneas. Ustedes son los únicos que saben todo lo que he pasado en esta vida para lograr esta meta. Meta que sin su cariño, apoyo, y amor jamás hubiese

logrado. Los quiero muchísimo! A cada uno de ustedes les dedico esta tesis. Gracias por siempre estar ahí.

Quiero también expresar mis agradecimientos a Carlos Pozo, Vero Matthei, Tito Pozo, Vale Pozo, Flori Campos, Ale Montero, Lenja and Jonas Hagemann, cuyo apoyo y aliento han sido una fuente constante de energía y consuelo, los que han añadieron calor y fuerza en este largo proceso. Muchas gracias por su compañia!

Finally, I cannot close this section without mentioning the support and friendship of Fernando Cornejo, Verena Merk, Yéssica Sanhueza, Lene Sparwaater, Francisco Mayorga, Juan Pablo Espinoza, and Boris Hernández.

General references

Addamo AM, Zaccara S, Försterra G, Höfer J, García-Jiménez R, Crosa G, Machordom A (2021) Genetic conservation management of marine resources and ecosystems of Patagonian fjords. Frontiers in Marine Science 8:96

Addamo AM, Zaccara S, Häussermann V, Höfer J, Försterra G, García-Jiménez R, Crosa G, Machordom A (2022) The shrunk genetic diversity of coral populations in North-Central Patagonia calls for management and conservation plans for marine resources. Scientific Reports 12:1-11

Adkins JF, Boyle EA, Curry W, Lutringer A (2003) Stable isotopes in deep-sea corals and a new mechanism for "vital effects". Geochim Cosmochim Ac 67:1129-1143

Akiva A, Neder M, Kahil K, Gavriel R, Pinkas I, Goobes G, Mass T (2018) Minerals in the pre-settled coral *Stylophora pistillata* crystallize via protein and ion changes. Nature communications 9:1-9

Albright R, Mason B (2013) Projected near-future levels of temperature and pCO_2 reduce coral fertilization success. Plos One 8:e56468

Allemand D, Tambutté É, Zoccola D, Tambutté S (2011) Coral calcification, cells to reefs Coral Reefs: An Ecosystem in Transition, Dubinsky (ed) Coral Reefs Elsevier, Amsterdam, pp119-150

Allemand D, Ferrier-Pagès C, Furla P, Houlbrèque F, Puverel S, Reynaud S, Tambutté É, Tambutté S, Zoccola D (2004) Biomineralisation in reef-building corals: from molecular mechanisms to environmental control. Comptes Rendus Palevol 3:453-467

Altieri AH (2003) Settlement cues in the locally dispersing temperate cup coral *Balanophyllia elegans*. The Biological Bulletin 204:241-245

Anthony KR, Kline DI, Diaz-Pulido G, Dove S, Hoegh-Guldberg O (2008) Ocean acidification causes bleaching and productivity loss in coral reef builders. Proceedings of the National Academy of Sciences 105:17442-17446

Atoda K (1951a) The larva and postlarval development of the reef-building corals III. *Acropora brüggemanni* (Brook, 1893). Journal of Morphology 89:1-15

Atoda K (1951b) The larva and postlarval development of the reef-building corals IV. *Galaxea aspera* (Quelch, 1886). Journal of Morphology 89:17-35

Ayre D, Resing J (1986) Sexual and asexual production of planulae in reef corals. Marine Biology 90:187-190

Babcock R, Bull G, Harrison PL, Heyward A, Oliver J, Wallace C, Willis B (1986) Synchronous spawnings of 105 scleractinian coral species on the Great Barrier Reef. Marine Biology 90:379-394

Baco AR, Morgan N, Roark EB, Silva M, Shamberger KE, Miller K (2017) Defying dissolution: discovery of deep-sea scleractinian coral reefs in the North Pacific. Scientific Reports 7:5436

Baillon S, Hamel J-F, Mercier A (2011) Comparative study of reproductive synchrony at various scales in deep-sea echinoderms. Deep Sea Research Part I: Oceanographic Research Papers 58:260-272

Balogh V, Fragkopoulou E, Serrão EA, Assis J (2023) A dataset of cold-water coral distribution records. Data in Brief 48:109223

Bates D, Mächler M, Bolker B, Walker S (2014) Fitting linear mixed-effects models using lme4. Journal of Statistical Software

Beauchamp KA (1993) Gametogenesis, brooding and planulation in laboratory populations of a temperate scleractinian coral *Balanophyllia elegans* maintained under contrasting photoperiod regimes. Invertebrate Reproduction & Development 23:171-182

Beck KK, Schmidt-Grieb GM, Laudien J, Försterra G, Häussermann V, González HE, Espinoza JP, Richter C, Wall M (2022) Environmental stability and phenotypic plasticity benefit the cold-water coral *Desmophyllum dianthus* in an acidified fjord. Communications biology 5:1-12

Beck KK, Nierste J, Schmidt-Grieb GM, Lüdtke E, Naab C, Held C, Nehrke G, Steinhoefel G, Laudien J, Richter C (2023) Ontogenetic differences in the response of the cold-water coral *Caryophyllia huinayensis* to ocean acidification, warming and food availability. Science of The Total Environment:165565

Bedgood SA, Bracken ME, Ryan WH, Levell ST, Wulff J (2020) Nutritional drivers of adult locomotion and asexual reproduction in a symbiont-hosting sea anemone *Exaiptasia diaphana*. Marine Biology 167:1-12

Berzins IK, Yanong RP, LaDouceur EE, Peters EC (2021) Cnidaria. Invertebrate Histology:55-86

Borneman E (2008) Introduction to the husbandry of corals in aquariums: A review. Public Aquarium Husbandry Serries 2:3-14

Børsheim KY, Myklestad SM, Sneli J-A (1999) Monthly profiles of DOC, mono-and polysaccharides at two locations in the Trondheimsfjord (Norway) during two years. Marine Chemistry 63:255-272

Braga-Henriques A, Porteiro F, Ribeiro P, De Matos V, Sampaio Í, Ocaña O, Santos R (2013) Diversity, distribution and spatial structure of the cold-water coral fauna of the Azores (NE Atlantic). Biogeosciences 10:4009-4036

Brahmi C, Meibom A, Smith D, Stolarski J, Auzoux-Bordenave S, Nouet J, Doumenc D, Djediat C, Domart-Coulon I (2010) Skeletal growth, ultrastructure and composition of the azooxanthellate scleractinian coral *Balanophyllia regia*. Coral Reefs 29:175-189

Brazeau DA, Gleason DF, Morgan ME (1998) Self-fertilization in brooding hermaphroditic Caribbean corals: evidence from molecular markers. Journal of Experimental Marine Biology and Ecology 231:225-238

Breitburg D (2002) Effects of hypoxia, and the balance between hypoxia and enrichment, on coastal fishes and fisheries. Estuaries 25:767-781

Brooke S, Young CM (2003) Reproductive ecology of a deep-water scleractinian coral, *Oculina varicosa*, from the southeast Florida shelf. Continental Shelf Research 23:847-858

Brooke S, Young C (2005) Embryogenesis and larval biology of the ahermatypic scleractinian *Oculina varicosa*. Marine Biology 146:665-675

Brooke S, Young CM (2009) *In situ* measurement of survival and growth of *Lophelia pertusa* in the northern Gulf of Mexico. Marine Ecology Progress Series 397:153-161

Brooke S, Järnegren J (2012) Reproductive periodicity of the scleractinian coral *Lophelia pertusa* from the Trondheim Fjord, Norway. Marine Biology 160:139-153

Brooke S, Järnegren J (2013) Reproductive periodicity of the scleractinian coral *Lophelia pertusa* from the Trondheim Fjord, Norway. Marine biology 160:139-153

Bryan WH, Hill D (1941) Spherulitic crystallization as a mechanism of skeletal growth in the hexacorals. Proceedings of the Royal Society of Queensland LII:78-91

Buhl-Mortensen P, Buhl-Mortensen L, Purser A (2015) Trophic ecology and habitat provision in cold-water coral ecosystems. Marine Animal Forests: The Ecology of Benthic Biodiversity Hotspots:1-26

Burgess SN, Babcock RC (2005) Reproductive ecology of three reef-forming, deep-sea corals in the New Zealand region. Cold-water Corals and Ecosystems. Springer, pp701-713

Burt K, Hamoutene D, Mabrouk G, Lang C, Puestow T, Drover D, Losier R, Page F (2012) Environmental conditions and occurrence of hypoxia within production cages of Atlantic salmon on the south coast of Newfoundland. Aquaculture Research 43:607-620

Büscher JV, Form AU, Riebesell U (2017) Interactive effects of ocean acidification and warming on growth, fitness and survival of the cold-water coral *Lophelia pertusa* under different food availabilities. Frontiers in Marine Science 4:101

Buschmann AH, Cabello F, Young K, Carvajal J, Varela DA, Henríquez L (2009) Salmon aquaculture and coastal ecosystem health in Chile: Analysis of regulations, environmental impacts and bioremediation systems. Ocean & Coastal Management 52:243-249

Byrne M, Prowse T, Sewell M, Dworjanyn S, Williamson J, Vaïtilingon D (2008) Maternal provisioning for larvae and larval provisioning for juveniles in the toxopneustid sea urchin *Tripneustes gratilla*. Marine Biology 155:473-482

Cairns SD (1981) Marine flora and fauna of the northeastern United States Scleractinia. NOAA technical report NMFS Circular

Cairns SD (1982) Antarctic and subantarctic Scleractinia. Biology of the Antarctic Seas XI 34:1-74

Cairns SD (1988) Asexual reproduction in solitary Scleractinia. Proceedings of the 6th International Coral Reef Symposium, Townsville

Cairns SD (2007) Deep-water corals: an overview with special reference to diversity and distribution of deep-water scleractinian corals. Bulletin of Marine Science 81:311-322

Cairns SD, Stanley GD (1982) Ahermatypic coral banks: living and fossil counterparts. Proceedings of the 4th International Coral Reef Symposium 1:611-618

Cairns SD, Häussermann V, Försterra G (2005) A review of the Scleractinia (Cnidaria: Anthozoa) of Chile, with the description of two new species. Zootaxa 1018:15-46

Caldeira K, Wickett ME (2005) Ocean model predictions of chemistry changes from carbon dioxide emissions to the atmosphere and ocean. Journal of Geophysical Research: Oceans 110

Capel KCC, Migotto ÁE, Zilberberg C, Kitahara MV (2014) Another tool towards invasion? Polyp “bail-out” in *Tubastraea coccinea*. Coral Reefs 33:1165-1165

Carbonne C, Comeau S, Chan PT, Plichon K, Gattuso J-P, Teixidó N (2022) Early life stages of a Mediterranean coral are vulnerable to ocean warming and acidification. Biogeosciences 19:4767-4777

Caroselli E, Gizzi F, Prada F, Marchini C, Airi V, Kaandorp J, Falini G, Dubinsky Z, Goffredo S (2019) Low and variable pH decreases recruitment efficiency in populations of a temperate coral naturally present at a CO_2 vent. Limnology and Oceanography 64:1059-1069

Carreiro-Silva M, Cerqueira T, Godinho A, Caetano M, Santos R, Bettencourt R (2014) Molecular mechanisms underlying the physiological responses of the cold-water coral *Desmophyllum dianthus* to ocean acidification. Coral Reefs 33:465-476

Cathalot C, Van Oevelen D, Cox TJ, Kutti T, Lavaleye M, Duineveld G, Meysman FJ (2015) Cold-water coral reefs and adjacent sponge grounds: hotspots of benthic respiration and organic carbon cycling in the deep sea. Frontiers in Marine Science 2:37

Clode P, Lema K, Saunders M, Weiner S (2011) Skeletal mineralogy of newly settling *Acropora millepora* (Scleractinia) coral recruits. Coral Reefs 30:1-8

Cohen AL, McConnaughey TA (2003) Geochemical perspectives on coral mineralization. Reviews in Mineralogy and Geochemistry 54:151-187

Cohen AL, Holcomb M (2009) Why corals care about ocean acidification: uncovering the mechanism. Oceanography 22:118-127

Cohen AL, McCorkle DC, de Putron S, Gaetani GA, Rose KA (2009) Morphological and compositional changes in the skeletons of new coral recruits reared in acidified seawater: Insights into the biomineralization response to ocean acidification. Geochemistry, Geophysics, Geosystems 10

Combosch D, Vollmer S (2013) Mixed asexual and sexual reproduction in the Indo-Pacific reef coral *Pocillopora damicornis*. . Ecology and Evolution 3:3379-3387

Coppari M, Mestice F, Betti F, Bavestrello G, Castellano L, Bo M (2019) Fragmentation, re-attachment ability and growth rate of the Mediterranean black coral *Antipathella subpinnata*. Coral Reefs 38:1-14

Cubitt F, Butterworth K, McKinley RS (2008) A synopsis of environmental issues associated with salmon aquaculture in Canada. Aquaculture, Innovation and Social Transformation. Springer, pp123-162

Cuif J-P, Dauphin Y (1998) Microstructural and physico-chemical characterization of 'centers of calcification' in septa of some recent scleractinian corals. Paläontologische Zeitschrift 72:257-269

Dahl M, Pereyra R, Lundälv T, André C (2012) Fine-scale spatial genetic structure and clonal distribution of the cold-water coral *Lophelia pertusa*. Coral Reefs 31:1135-1148

de Putron SJ, McCorkle DC, Cohen AL, Dillon A (2011) The impact of seawater saturation state and bicarbonate ion concentration on calcification by new recruits of two Atlantic corals. Coral Reefs 30:321-328

Dickson AG (1990) Thermodynamics of the dissociation of boric acid in synthetic seawater from 273.15 to 318.15 K. Deep Sea Research Part A Oceanographic Research Papers 37:755-766

Dickson AG, Sabine CL, Christian JR (2007) SOP 3b — Total alkalinity (open cell). North Pacific Marine Science Organization

Drenkard EJ, Cohen AL, McCorkle DC, de Putron SJ, Starczak VR, Zicht A (2013) Calcification by juvenile corals under heterotrophy and elevated CO_2. Coral Reefs 32:727-735

Dubinsky Z, Falkowski P (2011) Light as a source of information and energy in zooxanthellate corals. Coral Reefs: An Ecosystem in Transition:107-118

Duerden JE (1904) The coral *Siderastrea radians* and its postlarval development. Carnegie Institution of Washington 20:1-129

Dullo W-C, Flögel S, Rüggeberg A (2008) Cold-water coral growth in relation to the hydrography of the Celtic and Nordic European continental margin. Marine Ecology Progress Series 371:165-176

Eckelbarger K, Tyler P, Langton R (1998) Gonadal morphology and gametogenesis in the sea pen *Pennatula aculeata* (Anthozoa: Pennatulacea) from the Gulf of Maine. Marine Biology 132:677-690

Eckelbarger KJ, Watling L (1995) Role of phylogenetic constraints in determining reproductive patterns in deep-sea invertebrates. Invertebrate Biology:256-269

Eckelbarger KJ, Hodgson AN (2021) Invertebrate oogenesis–a review and synthesis: comparative ovarian morphology, accessory cell function and the origins of yolk precursors. Invertebrate Reproduction & Development 65:71-140

Ellis VL, Ross D, Sutton L (1969) The pedal disc of the swimming sea anemone *Stomphia coccinea* during detachment, swimming, and resettlement. Canadian Journal of Zoology 47:333-342

Espinel-Velasco N, Hoffmann L, Agüera A, Byrne M, Dupont S, Uthicke S, Webster NS, Lamare M (2018) Effects of ocean acidification on the settlement and metamorphosis of marine invertebrate and fish larvae: a review. Marine Ecology Progress Series 606:237-257

Fadlallah Y (1985) Reproduction in the coral *Pocillopora verrucosa* on the reefs adjacent to the industrial city of Yanbu (Red Sea, Saudi Arabia). Proceedings of the 5th International Coral Reef Congress 4:313-318

Fadlallah Y, Pearse J (1982) Sexual reproduction in solitary corals: overlapping oogenic and brooding cycles, and benthic planulas in *Balanophyllia elegans*. Marine Biology 71:223-231

Fadlallah YH (1983) Sexual reproduction, development and larval biology in scleractinian corals. Coral Reefs 2:129-150

Falkowski PG, Dubinsky Z, Muscatine L, Porter JW (1984) Light and the bioenergetics of a symbiotic coral. Bioscience 34:705-709

Farrant P (1986) Gonad development and the planulae of the temperate Australian soft coral *Capnella gaboensis*. Marine Biology 92:381-392

Feehan KA, Waller RG, Häussermann V (2019) Highly seasonal reproduction in deep-water emergent *Desmophyllum dianthus* (Scleractinia: Caryophylliidae) from the Northern Patagonian Fjords. Marine Biology 166:52

Feely RA, Sabine CL, Lee K, Berelson W, Kleypas J, Fabry VJ, Millero FJ (2004) Impact of anthropogenic CO_2 on the $CaCO_3$ system in the oceans. Science 305:362-366

Fietzke J, Wall M (2022) Distinct fine-scale variations in calcification control revealed by high-resolution 2D boron laser images in the cold-water coral *Lophelia pertusa*. Science Advances 8:eabj4172

Fillinger L, Richter C (2013) Vertical and horizontal distribution of *Desmophyllum dianthus* in Comau Fjord, Chile: a cold-water coral thriving at low pH. PeerJ 1:e194

Fine M, Tchernov D (2007) Scleractinian coral species survive and recover from decalcification. Science 315:1811-1811

Flint HC, Waller RG, Tyler PA (2007) Reproductive ecology of *Fungiacyathus marenzelleri* from 4100 m depth in the northeast Pacific Ocean. Marine Biology 151:843-849

Fordyce AJ, Camp EF, Ainsworth TD (2017) Polyp bailout in *Pocillopora damicornis* following thermal stress. F1000Research 6

Form AU, Riebesell U (2012) Acclimation to ocean acidification during long-term CO_2 exposure in the cold-water coral *Lophelia pertusa*. Global Change Biol 18:843-853

Försterra G (2009) Ecological and biogeographical aspects of the Chilean fjord region. In: Häussermann V, Försterra G (eds) Marine benthic fauna of Chilean Patagonia. Nature in Focus, pp61-76

Försterra G, Häussermann V (2003) First report on large scleractinian (Cnidaria: Anthozoa) accumulations in cold-temperate shallow water of south Chilean fjords. Zoologische Verhandelingen 345:117-128

Försterra G, Häussermann V, Laudien J (2017) Animal Forests in the Chilean Fjords: Discoveries, Perspectives, and Threats in Shallow and Deep Waters Marine Animal Forests: The Ecology of Benthic Biodiversity Hotspots, pp277-313

Försterra G, Häussermann V, Laudien J, Jantzen C, Sellanes J, Muñoz P (2014) Mass die-off of the cold-water coral *Desmophyllum dianthus* in the Chilean Patagonian fjord region. Bulletin of Marine Science 90:895-899

Foster NL, Baums IB, Mumby PJ (2007) Sexual vs. asexual reproduction in an ecosystem engineer: the massive coral *Montastraea annularis*. Journal of Animal Ecology 76:384-391

Foster T, Clode PL (2016) Skeletal mineralogy of coral recruits under high temperature and pCO_2. Biogeosciences 13:1717-1722

Foster T, Falter JL, McCulloch MT, Clode PL (2016) Ocean acidification causes structural deformities in juvenile coral skeletons. Science Advances 2:e1501130

Foster T, Gilmour J, Chua C, Falter J, McCulloch M (2015) Effect of ocean warming and acidification on the early life stages of subtropical *Acropora spicifera*. Coral Reefs 34:1217-1226

Fox AD, Henry L-A, Corne DW, Roberts JM (2016) Sensitivity of marine protected area network connectivity to atmospheric variability. Royal Society open science 3:160494

Freiwald A (2002) Reef-forming cold-water corals Ocean Margin Systems. Springer, pp365-385

Freiwald A, Henrich R, Pätzold J (1997) Anatomy of a deep-water coral reef mound from Stjernsund, West Finnmark, northern Norway. Cool-Water Carbonatess, Society for Sedimentary Geology 56:141-162

Freiwald A, Fossâ JH, Grehan A, Koslow T, Roberts JM (2004) Cold-water coral reefs: out of sight-no longer out of mind. UNEP-WCMC

Gagnon AC, Adkins JF, Erez J (2012) Seawater transport during coral biomineralization. Earth and Planetary Science Letters 329:150-161

Galloway SB, Woodley C, McLaughlin S, Work T, Bochsler V, Meteyer C, Sileo L, Peters E, Kramarsky-Winters E, Morado J (2006) Coral disease and health workshop: coral histopathology II:84

Garcia-Herrera N, Cornils A, Laudien J, Niehoff B, Höfer J, Försterra G, González H, Richter C (2022) Seasonal and diel variations in the vertical distribution, composition, abundance and biomass of zooplankton in a deep Chilean Patagonian Fjord. PeerJ 10:e12823

Gattuso J, Magnan A, Billé R (2015) Contrasting futures for ocean and society from different anthropogenic CO_2 emissions scenarios. Science 349

Gerrodette T (1981) Dispersal of the solitary coral *Balanophyllia elegans* by demersal planular larvae. Ecology 62:611-619

Gilis M, Meibom A, Domart-Coulon I, Grauby O, Stolarski J, Baronnet A (2014) Biomineralization in newly settled recruits of the scleractinian coral *Pocillopora damicornis*. Journal of Morphology 275:1349-1365

Gilis M, Meibom A, Alexander D, Grauby O, Stolarski J, Baronnet A (2015) Morphology, microstructure, crystallography, and chemistry of distinct $CaCO_3$ deposits formed by early recruits of the scleractinian coral *Pocillopora damicornis*. Journal of Morphology 276:1146-1156

Gizzi F, de Mas L, Airi V, Caroselli E, Prada F, Falini G, Dubinsky Z, Goffredo S (2017) Reproduction of an azooxanthellate coral is unaffected by ocean acidification. Scientific Reports 7:1-8

Goffredo S, Arnone S, Zaccanti F (2002) Sexual reproduction in the Mediterranean solitary coral *Balanophyllia europaea* (Scleractinia, Dendrophylliidae). Marine Ecology Progress Series 229:83-94

Goffredo S, Radetić J, Airi V, Zaccanti F (2005) Sexual reproduction of the solitary sunset cup coral *Leptopsammia pruvoti* (Scleractinia: Dendrophylliidae) in the Mediterranean. 1. Morphological aspects of gametogenesis and ontogenesis. Marine Biology 147:485-495

Goffredo S, Gasparini G, Marconi G, Putignano MT, Pazzini C, Zaccanti F (2010) Gonochorism and planula brooding in the Mediterranean endemic orange coral *Astroides calycularis* (Scleractinia: Dendrophylliidae). Morphological aspects of gametogenesis and ontogenesis. Marine Biology Research 6:421-436

Goffredo S, Marchini C, Rocchi M, Airi V, Caroselli E, Falini G, Levy O, Dubinsky Z, Zaccanti F (2012) Unusual pattern of embryogenesis of *Caryophyllia inornata* (Scleractinia, Caryophylliidae) in the mediterranean sea: Maybe agamic reproduction? Journal of Morphology 273:943-956

Goreau TF, Goreau NI (1959) The physiology of skeleton formation in corals. II. Calcium deposition by hermatypic corals under various conditions in the reef. The Biological Bulletin 117:239-250

Goreau TF, Goreau NI, Yonge C (1971) Reef corals: autotrophs or heterotrophs? The Biological Bulletin 141:247-260

Gori A, Ferrier-Pages C, Hennige SJ, Murray F, Rottier C, Wicks LC, Roberts JM (2016) Physiological response of the cold-water coral *Desmophyllum dianthus* to thermal stress and ocean acidification. PeerJ 4:e1606

Gran G (1952) Determination of the equivalence point in potentiometric titrations. Part II. Analyst 77:661-671

Gruber N (2011) Warming up, turning sour, losing breath: ocean biogeochemistry under global change. Philosophical Transactions of the Royal Society A: Mathematical, Physical and Engineering Sciences 369:1980-1996

Guinotte JM, Fabry VJ (2008) Ocean acidification and its potential effects on marine ecosystems. Annals of the New York Academy of Sciences 1134:320-342

Guinotte JM, Orr J, Cairns S, Freiwald A, Morgan L, George R (2006) Will human-induced changes in seawater chemistry alter the distribution of deep-sea scleractinian corals? Frontiers in Ecology and the Environment 4:141-146

Harrison PL (2011) Sexual reproduction of scleractinian corals Coral Reefs: An Ecosystem in Transition. Springer, pp59-85

Harrison PL, Wallace C (1990) Reproduction, dispersal and recruitment of scleractinian corals. In: Dubinsky Z (ed) Ecosystems of the World. Elsevier, Amsterdam, New York, pp133-207

Häussermann V, Försterra G (2007) Large assemblages of cold-water corals in Chile: a summary of recent findings and potential impacts. Bulletin of Marine Science 81:195-207

Häussermann V, Försterra G (2015) *In situ* broadcast spawning of *Corynactis* sp. in Chilean Patagonia. Coral Reefs 34:119-119

Häussermann V, Försterra G, Plotnek E (2012) Sightings of marine mammals and birds in the Comau Fjord, Northern Patagonia, between 2003 and mid 2012. Spixiana 35:247-262

Häussermann V, Försterra G, Laudien J (2024) Hard Bottom Macrobenthos of Chilean Patagonia: Emphasis on Conservation of Sublitoral Invertebrate and Algal Forests. Conservation in Chilean Patagonia: Assessing the State of Knowledge, Opportunities, and Challenges:263-284

Häussermann V, Försterra G, Melzer RR, Meyer R (2013) Gradual changes of benthic biodiversity in Comau Fjord, Chilean Patagonia-Lateral observations over a decade of taxonomic research. Spixiana 36:161-171

Häussermann V, Ballyram SA, Försterra G, Cornejo C, Ibáñez CM, Sellanes J, Thomasberger A, Espinoza JP, Beaujot F (2021) Species That Fly at a Higher Game: Patterns of Deep–Water Emergence Along the Chilean Coast, Including a Global Review of the Phenomenon. Frontiers in Marine Science:1101

Heltzel P, Babcock R (2002) Sexual reproduction, larval development and benthic planulae of the solitary coral *Monomyces rubrum* (Scleractinia: Anthozoa). Marine Biology 140:659-667

Hennige S, Wicks L, Kamenos N, Perna G, Findlay H, Roberts J (2015) Hidden impacts of ocean acidification to live and dead coral framework. Proceedings of the Royal Society B: Biological Sciences 282:20150990

Hennige SJ, Wolfram U, Wickes L, Murray F, Roberts JM, Kamenos NA, Schofield S, Groetsch A, Spiesz EM, Aubin-Tam M-E (2020) Crumbling reefs and cold-water coral habitat loss in a future ocean: evidence of “Coralporosis” as an indicator of habitat integrity. Frontiers in Marine Science:668

Heran T, Laudien J, Waller RG, Häussermann V, Försterra G, González HE, Richter C (2023) Life cycle of the cold-water coral *Caryophyllia huinayensis*. Scientific Reports 13:2593

Hessler R (1970) High-latitude emergence of deep-sea isopods. United States Antarctic Research Journal 5:133-134

Hixon MA, Pacala SW, Sandin SA (2002) Population regulation: historical context and contemporary challenges of open vs. closed systems. Ecology 83:1490-1508
Hoegh-Guldberg O, Emlet R (1997) Energy use during the development of a lecithotrophic and a planktotrophic echinoid. The Biological Bulletin 192:27-40
Holcomb M, Cohen AL, Gabitov RI, Hutter JL (2009) Compositional and morphological features of aragonite precipitated experimentally from seawater and biogenically by corals. Geochim Cosmochim Ac 73:4166-4179
Honnay O, Bossuyt B (2005) Prolonged clonal growth: escape route or route to extinction? Oikos 108:427-432
Hughes TP, Kerry JT, Álvarez-Noriega M, Álvarez-Romero JG, Anderson KD, Baird AH, Babcock RC, Beger M, Bellwood DR, Berkelmans R (2017) Global warming and recurrent mass bleaching of corals. Nature 543:373-377
Hughes TP, Kerry JT, Baird AH, Connolly SR, Dietzel A, Eakin CM, Heron SF, Hoey AS, Hoogenboom MO, Liu G (2018) Global warming transforms coral reef assemblages. Nature 556:492-496
IPCC (2021) Climate Change 2021 – The Physical Science Basis
Jantzen C, Häussermann V, Försterra G, Laudien J, Ardelan M, Maier S, Richter C (2013a) Occurrence of a cold-water coral along natural pH gradients (Patagonia, Chile). Marine Biology 160:2597-2607
Jantzen C, Laudien J, Sokol S, Försterra G, Häussermann V, Kupprat F, Richter C (2013b) *In situ* short-term growth rates of a cold-water coral. Marine and Freshwater Research 64:631-641
Jiang L-Q, Carter BR, Feely RA, Lauvset SK, Olsen A (2019) Surface ocean pH and buffer capacity: past, present and future. Scientific Reports 9:1-11
Johnstone JW, Waller RG, Stone RP (2021) Shallow-emerged coral may warn of deep-sea coral response to thermal stress. Scientific Reports 11:22439
Jones CG, Lawton JH, Shachak M (1994) Organisms as ecosystem engineers. Oikos:373-386
Keller N, Os' kina N (2008) Habitat temperature ranges of azooxantellate scleractinian corals in the world ocean. Oceanology 48:77-84
Kerr AM, Baird AH, Hughes TP (2011) Correlated evolution of sex and reproductive mode in corals (Anthozoa: Scleractinia). Proceedings of the Royal Society B: Biological Sciences 278:75-81
Kiessling W, Flügel E, Golonka J (2002) Phanerozoic reef patterns. SEPM Society for Sedimentary Geology
Kinchington D (1982) Organic-matrix synthesis by scleractinian coral larval and post-larval stages during skeletogenesis. Proceedings of the 4th International Coral Reef Symposium 2:107-113
Kleypas JA, McManus JW, Meñez LA (1999a) Environmental limits to coral reef development: where do we draw the line? American zoologist 39:146-159
Kleypas JA, Buddemeier RW, Archer D, Gattuso J-P, Langdon C, Opdyke BN (1999b) Geochemical consequences of increased atmospheric carbon dioxide on coral reefs. Science 284:118-120
Knutson TR, McBride JL, Chan J, Emanuel K, Holland G, Landsea C, Held I, Kossin JP, Srivastava A, Sugi M (2010) Tropical cyclones and climate change. Nature Geoscience 3:157-163

Kramarsky-Winter E, Loya Y (1998) Reproductive strategies of two fungiid corals from the northern Red Sea: environmental constraints? Marine Ecology Progress Series 174:175-182

Kramarsky-Winter E, Fine M, Loya Y (1997) Coral polyp expulsion. Nature 387:137

Kroeker KJ, Kordas RL, Crim R, Hendriks IE, Ramajo L, Singh GS, Duarte CM, Gattuso JP (2013) Impacts of ocean acidification on marine organisms: quantifying sensitivities and interaction with warming. Global Change Biol 19:1884-1896

Kruger A, Schleyer M (1998) Sexual reproduction in the coral *Pocillopora verrucosa* (Cnidaria: Scleractinia) in KwaZulu-Natal, South Africa. Marine Biology 132:703-710

Kružić P (2007) Polyp expulsion of the coral *Cladocora caespitosa* (Anthozoa, Scleractinia) in extreme sea temperature conditions. Natura Croatica 16:211

Kvitt H, Kramarsky-Winter E, Maor-Landaw K, Zandbank K, Kushmaro A, Rosenfeld H, Fine M, Tchernov D (2015) Breakdown of coral colonial form under reduced pH conditions is initiated in polyps and mediated through apoptosis. Proceedings of the National Academy of Sciences 112:2082-2086

Larsson AI, Järnegren J, Strömberg SM, Dahl MP, Lundälv T, Brooke S (2014) Embryogenesis and larval biology of the cold-water coral *Lophelia pertusa*. Plos One 9:e102222

Laudien J, Holtz U, Heran T, Richter C (2018) Water parameters of the cold-water experimental aquarium system at AWI in 2017/2018, Pangaea

Laudien J, Heran T, Häussermann V, Försterra G, Schmidt-Grieb GM, Richter C (2021) Polyp dropout in a solitary cold-water coral. Coral Reefs:1-9

Laudien J, Heran T, Hartig A, Bartsch J, Kuwerr P, Häussermann V, Försterra G, Schmidt-Grieb G, Richter C (2019) Photographs of cold-water scleractinian corals maintained in the AWI experimental aquarium system, Pangaea

Le Goff-Vitry M, Pybus O, Rogers A (2004) Genetic structure of the deep-sea coral *Lophelia pertusa* in the northeast Atlantic revealed by microsatellites and internal transcribed spacer sequences. Molecular Ecology 13:537-549

Le Tissier M (1988) Patterns of formation and the ultrastructure of the larval skeleton of *Pocillopora damicornis*. Marine Biology 98:493-501

Lee CS, Walford J, Goh BPL (2012) The effect of benthic macroalgae on coral settlement. In: Siang T (ed) Contributions to Marine Science: a commemorative volume celebrating 10 years of research on St John's Island, National University of Singapore, pp89–93

Lenth R, Singmann H, Love J, Buerkner P, Herve M (2019) emmeans: Estimated marginal means, aka least-squares means.

Leung JY, Zhang S, Connell SD (2022) Is ocean acidification really a threat to marine calcifiers? A systematic review and meta-analysis of 980+ studies spanning two decades. Small 18:2107407

Levitan DR (2006) The relationship between egg size and fertilization success in broadcast-spawning marine invertebrates. Integrative and Comparative Biology 46:298-311

Lewis E, Wallace D, Allison L (1998) Program developed for CO_2 system calculations, carbon dioxide information analysis center Oak Ridge National Laboratory, Oak Ridge, Tenn

Liberman R, Fine M, Benayahu Y (2021) Simulated climate change scenarios impact the reproduction and early life stages of a soft coral. Marine Environmental Research 163:105215
Liu C, Cheng SH, Lin S (2020) Illuminating the dark depths inside coral. Cellular Microbiology 22:e13122
Lueker TJ, Dickson AG, Keeling CD (2000) Ocean pCO_2 calculated from dissolved inorganic carbon, alkalinity, and equations for K_1 and K_2: validation based on laboratory measurements of CO_2 in gas and seawater at equilibrium. Marine Chemistry 70:105-119
Maechler M, Rousseeuw P, Croux C, Todorov V, Ruckstuhl A, Salibian-Barrera M, Verbeke T, Koller M, Conceicao EL, di Palma MA (2024) Package 'robustbase' Basic Robust Statistics
Magalon H, Adjeroud M, Veuille M (2005) Patterns of genetic variation do not correlate with geographical distance in the reef-building coral *Pocillopora meandrina* in the South Pacific. Molecular Ecology 14:1861-1868
Maier C, Hegeman J, Weinbauer M, Gattuso J-P (2009) Calcification of the cold-water coral *Lophelia pertusa*, under ambient and reduced pH. Biogeosciences 6:1671-1680
Maier C, Schubert A, Berzunza Sànchez MM, Weinbauer MG, Watremez P, Gattuso J-P (2013) End of the century pCO_2 levels do not impact calcification in Mediterranean cold-water corals. Plos One 8:e62655
Maier C, Popp P, Sollfrank N, Weinbauer MG, Wild C, Gattuso J-P (2016) Effects of elevated pCO_2 and feeding on net calcification and energy budget of the Mediterranean cold-water coral *Madrepora oculata*. Journal of Experimental Biology 219:3208-3217
Maier SR, Bannister RJ, van Oevelen D, Kutti T (2020) Seasonal controls on the diet, metabolic activity, tissue reserves and growth of the cold-water coral *Lophelia pertusa*. Coral Reefs 39:173-187
Mangubhai S, Harrison PL (2008) Asynchronous coral spawning patterns on equatorial reefs in Kenya. Marine Ecology Progress Series 360:85-96
Manuel R (1988) British Athozoa (revised)
Marchini C, Gizzi F, Pondrelli T, Moreddu L, Marisaldi L, Montori F, Lazzari V, Airi V, Caroselli E, Prada F (2021) Decreasing pH impairs sexual reproduction in a Mediterranean coral transplanted at a CO_2 vent. Limnology and Oceanography 66:3990-4000
Marshall A (1996) Calcification in hermatypic and ahermatypic corals. Science 271:637-639
Martínez-Dios A, Pelejero C, López-Sanz À, Sherrell RM, Ko S, Häussermann V, Försterra G, Calvo E (2020) Effects of low pH and feeding on calcification rates of the cold-water coral *Desmophyllum dianthus*. PeerJ 8:e8236
Martins CP, Simancas-Giraldo SM, Schubert P, Wall M, Wild C, Wilke T, Ziegler M (2024) Short periods of decreased water flow may modulate long-term ocean acidification in reef-building corals. bioRxiv:2024.2002. 2023.581783
Mass T, Giuffre AJ, Sun C-Y, Stifler CA, Frazier MJ, Neder M, Tamura N, Stan CV, Marcus MA, Gilbert PU (2017) Amorphous calcium carbonate particles form coral skeletons. Proceedings of the National Academy of Sciences 114:E7670-E7678

Masson-Delmotte V, P. Zhai, A. Pirani, S.L. Connors, C. Péan, S. Berger, N. Caud, Y. Chen, L. Goldfarb, M.I. Gomis, M. Huang, K. Leitzell, E. Lonnoy, J.B.R. Matthews, T.K. Maycock, T. Waterfield, O. Yelekçi, R. Yu, Zhou B, (eds.) (2021) IPCC, 2021: Summary for Policymakers. In: Climate Change 2021: The Physical Science Basis. Contribution of Working Group I to the Sixth Assessment Report of the Intergovernmental Panel on Climate Change

McCulloch M, Trotter J, Montagna P, Falter J, Dunbar R, Freiwald A, Försterra G, Correa ML, Maier C, Rüggeberg A (2012) Resilience of cold-water scleractinian corals to ocean acidification: Boron isotopic systematics of pH and saturation state up-regulation. Geochim Cosmochim Ac 87:21-34

Meibom A, Cuif JP, Hillion F, Constantz BR, Juillet-Leclerc A, Dauphin Y, Watanabe T, Dunbar RB (2004) Distribution of magnesium in coral skeleton. Geophysical Research Letters 31

Meinshausen M, Smith SJ, Calvin K, Daniel JS, Kainuma ML, Lamarque J-F, Matsumoto K, Montzka SA, Raper SC, Riahi K (2011) The RCP greenhouse gas concentrations and their extensions from 1765 to 2300. Climatic change 109:213-241

Mercier A, Sun Z, Hamel J-F (2011) Reproductive periodicity, spawning and development of the deep-sea scleractinian coral *Flabellum angulare*. Marine Biology 158:371-380

Mileikovsky S (1971) Types of larval development in marine bottom invertebrates, their distribution and ecological significance: a re-evaluation. Marine Biology 10:193-213

Miller K, Ayre D (2004) The role of sexual and asexual reproduction in structuring high latitude populations of the reef coral *Pocillopora damicornis*. Heredity 92:557-568

Miller KJ, Gunasekera RM (2017) A comparison of genetic connectivity in two deep sea corals to examine whether seamounts are isolated islands or stepping stones for dispersal. Scientific Reports 7:46103

Moran A, Manahan D (2004) Physiological recovery from prolonged 'starvation' in larvae of the Pacific oyster *Crassostrea gigas*. Journal of Experimental Marine Biology and Ecology 306:17-36

Moran AL, McAlister JS (2009) Egg size as a life history character of marine invertebrates: is it all it's cracked up to be? The Biological Bulletin 216:226-242

Morato T, González-Irusta JM, Dominguez-Carrió C, Wei CL, Davies A, Sweetman AK, Taranto GH, Beazley L, García-Alegre A, Grehan A (2020) Climate-induced changes in the suitable habitat of cold-water corals and commercially important deep-sea fishes in the North Atlantic. Global Change Biol 26:2181-2202

Morita M, Suwa R, Iguchi A, Nakamura M, Shimada K, Sakai K, Suzuki A (2010) Ocean acidification reduces sperm flagellar motility in broadcast spawning reef invertebrates. Zygote 18:103-107

Morrison CL, Ross SW, Nizinski MS, Brooke S, Järnegren J, Waller RG, Johnson RL, King TL (2011) Genetic discontinuity among regional populations of *Lophelia pertusa* in the North Atlantic Ocean. Conservation Genetics 12:713-729

Mortensen PB, Buhl-Mortensen L (2005) Deep-water corals and their habitats in The Gully, a submarine canyon off Atlantic Canada Cold-water Corals and Ecosystems. Springer, pp247-277

Movilla J, Orejas C, Calvo E, Gori A, López-Sanz À, Grinyó J, Domínguez-Carrió C, Pelejero C (2014) Differential response of two Mediterranean cold-water coral species to ocean acidification. Coral Reefs 33:675-686

Neder M, Laissue PP, Akiva A, Akkaynak D, Albéric M, Spaeker O, Politi Y, Pinkas I, Mass T (2019) Mineral formation in the primary polyps of pocilloporoid corals. Acta biomaterialia 96:631-645

Nothdurft LD, Webb GE (2007) Microstructure of common reef-building coral genera *Acropora*, *Pocillopora*, *Goniastrea* and *Porites*: constraints on spatial resolution in geochemical sampling. Facies 53:1-26

Ogilvie MM (1896) III. Microscopic and systematic study of madreporarian types of corals. Philosophical Transactions of the Royal Society of London Series B, Containing Papers of a Biological Character:83-345

Okubo N, Isomura N, Motokawa T, Hidaka M (2007) Possible self-fertilization in the brooding coral *Acropora* (Isopora) *brueggemanni*. Zoological Science 24:277-280

Oliver J, Babcock R (1992) Aspects of the fertilization ecology of broadcast spawning corals: sperm dilution effects and *in situ* measurements of fertilization. The Biological Bulletin 183:409-417

Orejas C, Ferrier-Pagès C, Reynaud S, Tsounis G, Allemand D, Gili JM (2011) Experimental comparison of skeletal growth rates in the cold-water coral *Madrepora oculata* Linnaeus, 1758 and three tropical scleractinian corals. Journal of Experimental Marine Biology and Ecology 405:1-5

Orr JC, Fabry VJ, Aumont O, Bopp L, Doney SC, Feely RA, Gnanadesikan A, Gruber N, Ishida A, Joos F (2005) Anthropogenic ocean acidification over the twenty-first century and its impact on calcifying organisms. Nature 437:681-686

Oury N, Gélin P, Massé L, Magalon H (2019) First study of asexual planulae in the coral *Pocillopora damicornis* type *β* SSH05c from the southwestern Indian Ocean. Coral Reefs 38:499-503

Palomares MLD, Pauly D (2022) SeaLifeBase, World Wide Web electronic publication.

Pechenik JA (1990) Delayed metamorphosis by larvae of benthic marine invertebrates: does it occur? Is there a price to pay? Ophelia 32:63-94

Pendleton A, Hartill E, Waller R (2021) Notes on reproduction in the deep-sea cup coral *Balanophyllia malouinensis* (Squires 1961) from the Southern Ocean. Polar Biology 44:977-986

Petit J-R, Jouzel J, Raynaud D, Barkov NI, Barnola J-M, Basile I, Bender M, Chappellaz J, Davis M, Delaygue G (1999) Climate and atmospheric history of the past 420,000 years from the Vostok ice core, Antarctica. Nature 399:429-436

Piraino S, Boero F, Aeschbach B, Schmid V (1996) Reversing the life cycle: medusae transforming into polyps and cell transdifferentiation in *Turritopsis nutricula* (Cnidaria, Hydrozoa). The Biological Bulletin 190:302-312

Piraino S, De Vito D, Schmich J, Bouillon J, Boero F (2004) Reverse development in Cnidaria. Canadian Journal of Zoology 82:1748-1754

Pires D, Silva J, Bastos N (2014) Reproduction of deep-sea reef-building corals from the southwestern Atlantic. Deep-Sea Research Part II: Topical Studies in Oceanography 99:51-63

Porter JW (1976) Autotrophy, heterotrophy, and resource partitioning in Caribbean reef-building corals. The American Naturalist 110:731-742

Pörtner H-O, Roberts DC, Masson-Delmotte V, Zhai P, Tignor M, Poloczanska E, Weyer N (2019) The ocean and cryosphere in a changing climate. Geneva: Intergovernmental Panel on Climate Change

Putnam HM, Gates RD (2015) Preconditioning in the reef-building coral *Pocillopora damicornis* and the potential for trans-generational acclimatization in coral larvae under future climate change conditions. Journal of Experimental Biology 218:2365-2372

Rakka M, Bilan M, Godinho A, Movilla J, Orejas C, Carreiro-Silva M (2019) First description of polyp bailout in cold-water octocorals under aquaria maintenance. Coral Reefs 38:15-20

Reed JK (1981) *In situ* growth rates of the scleractinian coral *Oculina varicosa* occurring with zooxanthellae on 6-m reefs and without on 80-m banks. Proceedings of the 4th International Coral Reef Symposium 2:201-206

Reggi M, Fermani S, Landi V, Sparla F, Caroselli E, Gizzi F, Dubinsky Z, Levy O, Cuif J-P, Dauphin Y (2014) Biomineralization in Mediterranean corals: the role of the intraskeletal organic matrix. Crystal Growth & Design 14:4310-4320

Reynaud S, Leclercq N, Romaine-Lioud S, Ferrier-Pagés C, Jaubert J, Gattuso JP (2003) Interacting effects of CO_2 partial pressure and temperature on photosynthesis and calcification in a scleractinian coral. Global Change Biol 9:1660-1668

Richmond RH (1985) Reversible metamorphosis in coral planula larvae. Marine Ecololgy Progress Series 22:181-185

Richmond RH, Hunter CL (1990) Reproduction and recruitment of corals: comparisons among the Caribbean, the Tropical Pacific, and the Red Sea. Marine Ecology Progress Series 60:185-203

Riegl BM, Purkis SJ (2012) Coral reefs of the Gulf: adaptation to climatic extremes in the world's hottest sea Coral reefs of the Gulf: Adaptation to climatic extremes. Springer, pp1-4

Riemann-Zürneck K, Griffiths CL (1999) *Korsaranthus natalensis* (Carlgren, 1938) nov. comb.(Cnidaria: Actiniaria) a mobile sea anemone attacking octocorals. African Zoology 34:190-196

Riemann-Zürneck K (1998) How sessile are sea anemones? A review of free-living forms in the Actiniaria Cnidaria: Anthozoa. Marine Ecology 19:247-261

Rinkevich B, Loya Y (1979) The reproduction of the Red Sea coral *Stylophora pistillata*. I. Gonads and planulae. Marine Ecology Progress Series 1:133-144

Roberts JM, Cairns SD (2014) Cold-water corals in a changing ocean. Current Opinion in Environmental Sustainability 7:118-126

Roberts JM, Wheeler AJ, Freiwald A (2006) Reefs of the deep: the biology and geology of cold-water coral ecosystems. Science 312:543-547

Roberts JM, Wheeler A, Freiwald A, Cairns S (2009) Habitats and ecology Cold-water corals: the biology and geology of deep-sea coral habitats. Cambridge University Press, pp324

Roberts JM, Murray F, Anagnostou E, Hennige S, Gori A, Henry L-A, Fox A, Kamenos N, Foster GL (2016) Cold-Water Corals in an Era of Rapid Global Change: Are These the Deep Ocean's Most Vulnerable Ecosystems? The Cnidaria, Past, Present and Future. Springer, pp593-606

Robson EA (1961) The swimming response and its pacemaker system in the anemone *Stomphia coccinea*. Journal of Experimental biology 38:685-694

Rodolfo-Metalpa R, Houlbrèque F, Tambutté É, Boisson F, Baggini C, Patti FP, Jeffree R, Fine M, Foggo A, Gattuso J (2011) Coral and mollusc resistance to ocean acidification adversely affected by warming. Nature Climate Change 1:308-312

Rodriguez SR, Ojeda FP, Inestrosa NC (1993) Settlement of benthic marine invertebrates. Marine Ecology Progress Series 97:193-207

Rossbach S, Rossbach FI, Häussermann V, Försterra G, Laudien J (2021) *In situ* skeletal growth rates of the solitary cold-water coral *Tethocyathus endesa* from the Chilean Fjord region. Frontiers in Marine Science 8

Rossi S, Bramanti L, Gori A, Orejas Saco del Valle C (2017) Marine animal forests: the ecology of benthic biodiversity hotspots. Springer

Rossin AM, Waller RG, Försterra G (2017) Reproduction of the cold-water coral *Primnoella chilensis* (Philippi, 1894). Continental Shelf Research 144:31-37

Rossin AM, Waller RG, Stone RP (2019) The effects of in-vitro pH decrease on the gametogenesis of the red tree coral, *Primnoa pacifica*. Plos One 14:e0203976

RStudio T (2022) RStudio: Integrated Development Environment for R. RStudio, PBC, Boston, MA

Sammarco PW (1982) Polyp bail-out: an escape response to environmental stress and a new means of reproduction in corals. Marine Ecology Progress Series 10:57-65

Schuhmacher H, Zibrowius H (1985) What is hermatypic? A redefinition of ecological groups in corals and other organisms. Coral Reefs 4:1-9

Seepma SjY, Ruiz-Hernandez SE, Nehrke G, Soetaert K, Philipse AP, Kuipers BW, Wolthers M (2021) Controlling $CaCO_3$ Particle Size with $\{Ca^{2+}\}$:$\{CO_3^{2-}\}$ Ratios in Aqueous Environments. Crystal Growth & Design 21:1576-1590

Seifert M, Rost B, Trimborn S, Hauck J (2020) Meta-analysis of multiple driver effects on marine phytoplankton highlights modulating role of pCO_2. Global Change Biol 26:6787-6804

Sellanes J, Quiroga E, Neira C (2008) Megafauna community structure and trophic relationships at the recently discovered Concepción Methane Seep Area, Chile, ~ 36° S. ICES Journal of Marine Science 65:1102-1111

Sepúlveda SA, Náquira V, Arenas M (2011) Susceptibility of coastal landslides and related hazards in the Chilean Patagonia: The case of Hornopirén area (42°S). Investigaciones Geográficas 43:35-46

Serrano E, Coma R, Inostroza K, Serrano O (2018) Polyp bail-out by the coral *Astroides calycularis* (Scleractinia, Dendrophylliidae). Marine Biodiversity 48:1661-1665

Sevilgen DS, Venn AA, Hu MY, Tambutté E, de Beer D, Planas-Bielsa V, Tambutté S (2019) Full *in vivo* characterization of carbonate chemistry at the site of calcification in corals. Science Advances 5:eaau7447

Sewell M, Manahan D (2001) Echinoderm eggs: biochemistry and larval biology. Echinoderms 2000: proceedings of the 10th international conference:55-58

Shapiro OH, Kartvelishvily E, Kramarsky-Winter E, Vardi A (2018) Magnesium-rich nanometric layer in the skeleton of *Pocillopora damicornis* with possible involvement in fibrous aragonite deposition. Frontiers in Marine Science 5:246

Shapiro OH, Kramarsky-Winter E, Gavish AR, Stocker R, Vardi A (2016) A coral-on-a-chip microfluidic platform enabling live-imaging microscopy of reef-building corals. Nature communications 7:10860

Sherman C, Ayre DJ, Miller K (2006) Asexual reproduction does not produce clonal populations of the brooding coral *Pocillopora damicornis* on the Great Barrier Reef, Australia. Coral Reefs 25:7-18

Silva N (2008) Dissolved oxygen, ph, and nutrients in the austral chilean channels and fjords. Progress in the oceanographic knowledge of Chilean interior waters, from Puerto Montt to Cape Horn:37

Silva N, Vargas CA (2014) Hypoxia in Chilean patagonian fjords. Progress in Oceanography 129:62-74

Siringoringo RM, Putra RD, Abrar M, Sari NW (2021) Coral reef damage and recovery related to a massive earthquake (March 2005) in Nias Island, Indonesia. Aquaculture, Aquarium, Conservation & Legislation 14:3391-3402

Smith S, Kinsey D (1978) Calcification and organic carbon metabolism as indicated by carbon dioxide. Coral reefs: research methods:469-484

Sobarzo M (2009) The Southern Chilean Fjord Region: oceanographic aspects. In: Häussermann V, Försterra G (eds) Marine benthic fauna of Chilean Patagonia. Santiago: Nature In Focus, Santiago, pp58-60

Solomon S (2007) IPCC (2007): Climate Change The Physical Science Basis. AGU Fall Meeting Abstracts 9:01

Spalding C, Finnegan S, Fischer WW (2017) Energetic costs of calcification under ocean acidification. Global Biogeochemical Cycles 31:866-877

Stanley Jr GD (2003) The evolution of modern corals and their early history. Earth-Science Reviews 60:195-225

Stoddart J (1983) Asexual production of planulae in the coral *Pocillopora damicornis*. Marine Biology 76:279-284

Strömberg SM, Larsson AI (2017) Larval behaviour and longevity in the cold-water coral *Lophelia pertusa* indicate potential for long distance dispersal. Frontiers in Marine Science 4:411

Strömberg SM, Östman C, Larsson AI (2019) The cnidome and ultrastructural morphology of late planulae in *Lophelia pertusa* (Linnaeus, 1758)—With implications for settling competency. Acta Zoologica 100:431-450

Sun C-Y, Marcus MA, Frazier MJ, Giuffre AJ, Mass T, Gilbert PU (2017) Spherulitic growth of coral skeletons and synthetic aragonite: nature's three-dimensional printing. ACS nano 11:6612-6622

Sun Z, Hamel J-F, Mercier A (2010a) Planulation periodicity, settlement preferences and growth of two deep-sea octocorals from the northwest Atlantic. Marine Ecology Progress Series 410:71-87

Sun Z, Hamel J-F, Edinger E, Mercier A (2010b) Reproductive biology of the deep-sea octocoral *Drifa glomerata* in the Northwest Atlantic. Marine biology 157:863-873

Szmant AM (1986) Reproductive ecology of Caribbean reef corals. Coral Reefs 5:43-53

Szmant-Froelich A, Yevich P, Pilson ME (1980) Gametogenesis and early development of the temperate coral *Astrangia danae* (Anthozoa: Scleractinia). The Biological Bulletin 158:257-269

Szmant-Froelich A, Reutter M, Riggs L (1985) Sexual reproduction of *Favia fragum* (Esper): lunar patterns of gametogenesis, embryogenesis and planulation in Puerto Rico. Bulletin of Marine Science 37:880-892

Tebben J, Motti C, Siboni N, Tapiolas D, Negri A, Schupp P, Kitamura M, Hatta M, Steinberg PD, Harder T (2015) Chemical mediation of coral larval settlement by crustose coralline algae. Scientific Reports 5:1-11

Thauer RK (2011) Anaerobic oxidation of methane with sulfate: on the reversibility of the reactions that are catalyzed by enzymes also involved in methanogenesis from CO_2. Current Opinion in Microbiology 14:292-299

Thorson G (1957) Bottom communities (sublittoral or shallow shelf) Treatise on Marine Ecology and Paleoecology. Geological Society of America, pp461-534

Thresher RE, Tilbrook B, Fallon S, Wilson NC, Adkins J (2011) Effects of chronic low carbonate saturation levels on the distribution, growth and skeletal chemistry of deep-sea corals and other seamount megabenthos. Marine Ecology Progress Series 442:87-99

Tokuda Y, Haraguchi H, Ezaki Y (2017) First real-time observation of transverse division in azooxanthellate scleractinian corals. Scientific Reports 7:41762

Tracey D, Goode S, Waller R, Marriott P, Beaumont J, Moss G, Cummings V, Mobilia V (2021) Protected coral reproduction. Literature review, recommended study species, and description of spawning event for *Goniocorella dumosa*, Final report prepared by NIWA for the Conservation Services Programme 63 p

Tranter P, Nicholson D, Kinchington D (1982) A description of spawning and post-gastrula development of the cool temperate coral, *Caryophyllia smithii*. Journal of the Marine Biological Association of the United Kingdom 62:845-854

Treml EA, Ford JR, Black KP, Swearer SE (2015) Identifying the key biophysical drivers, connectivity outcomes, and metapopulation consequences of larval dispersal in the sea. Movement Ecology 3:17

Tsounis G, Martinez L, Bramanti L, Viladrich N, Gili J-M, Martinez Á, Rossi S (2012) Anthropogenic effects on reproductive effort and allocation of energy reserves in the Mediterranean octocoral *Paramuricea clavata*. Marine Ecology Progress Series 449:161-172

Turley C, Roberts J, Guinotte J (2007) Corals in deep-water: will the unseen hand of ocean acidification destroy cold-water ecosystems? Coral Reefs 26:445-448

Uppström L (1974) The Boron/Chlorinity Ratio of Deep-sea Water from the Pacific Ocean. Deep-Sea Research and Oceanographic Abstracts 21:161-162

van der Ven RM, Heynderickx H, Kochzius M (2021) Differences in genetic diversity and divergence between brooding and broadcast spawning corals across two spatial scales in the Coral Triangle region. Marine Biology 168:17

Van Moorsel GW (1983) Reproductive strategies in two closely related stony corals (*Agaricia*, Scleractinia). Marine Ecology Progress Series:273-283

Vandermeulen J (1974) Studies on reef corals. II. Fine structure of planktonic planula larva of *Pocillopora damicornis*, with emphasis on the aboral epidermis. Marine Biology 27:239-249

Vandermeulen J (1975) Studies on reef corals. III. Fine structural changes of calicoblast cells in *Pocillopora damicornis* during settling and calcification. Marine Biology 31:69-77

Vandermeulen J, Watabe N (1973) Studies on reef corals. I. Skeleton formation by newly settled planula larva of *Pocillopora damicornis*. Marine Biology 23:47-57

Venn A, Tambutté E, Holcomb M, Allemand D, Tambutté S (2011) Live tissue imaging shows reef corals elevate pH under their calcifying tissue relative to seawater. Plos One 6:e20013

Venn AA, Tambutté E, Holcomb M, Laurent J, Allemand D, Tambutté S (2013) Impact of seawater acidification on pH at the tissue–skeleton interface and calcification in reef corals. Proceedings of the National Academy of Sciences 110:1634-1639

Wainwright SA (1963) Skeletal organization in the coral, *Pocillopora damicornis*. Journal of Cell Science 3:169-183

Wall M, Nehrke G (2012) Reconstructing skeletal fiber arrangement and growth mode in the coral *Porites lutea* (Cnidaria, Scleractinia): a confocal Raman microscopy study. Biogeosciences 9:4885-4895

Wall M, Beck KK, Garcia-Herrera N, Schmidt-Grieb GM, Laudien J, Höfer J, Försterra G, Held C, Nehrke G, Espinoza JP (2023) Lipid biomarkers reveal trophic relationships and energetic trade-offs in contrasting phenotypes of the cold-water coral *Desmophyllum dianthus* in Comau Fjord, Chile. Functional Ecology 38:126-142

Wallace RA, Selman K (1985) Major protein changes during vitellogenesis and maturation of *Fundulus* oocytes. Developmental Biology 110:492-498

Waller R, Tyler P, Gage J (2002) Reproductive ecology of the deep-sea scleractinian coral *Fungiacyathus marenzelleri* (Vaughan, 1906) in the northeast Atlantic Ocean. Coral Reefs 21:325-331

Waller RG, Tyler PA (2005) The reproductive biology of two deep-water, reef-building scleractinians from the NE Atlantic Ocean. Coral Reefs 24:514

Waller RG, Tyler PA (2011) Reproductive patterns in two deep-water solitary corals from the north-east Atlantic—*Flabellum alabastrum* and *F. angulare* (Cnidaria: Anthozoa: Scleractinia). Journal of the Marine Biological Association of the United Kingdom 91:669-675

Waller RG, Feehan KA (2013) Reproductive ecology of a polar deep-sea scleractinian, *Fungiacyathus marenzelleri* (Vaughan, 1906). Deep Sea Research Part II: Topical Studies in Oceanography 92:201-206

Waller RG, Tyler PA, Gage JD (2005) Sexual reproduction in three hermaphroditic deep-sea *Caryophyllia* species (Anthozoa: Scleractinia) from the NE Atlantic Ocean. Coral Reefs 24:594

Waller RG, Tyler PA, Smith CR (2008) Fecundity and embryo development of three Antarctic deep-water scleractinians: *Flabellum thouarsii*, *F. curvatum* and *F. impensum*. Deep-Sea Research Part II: Topical Studies in Oceanography 55:2527-2534

Waller RG, Goode S, Tracey D, Johnstone J, Mercier A (2023) A review of current knowledge on reproductive and larval processes of deep-sea corals. Marine Biology 170:58

Waller RG, Stone RP, Rice LN, Johnstone J, Rossin AM, Hartill E, Feehan K, Morrison CL (2019) Phenotypic plasticity or a reproductive dead end? *Primnoa pacifica* (Cnidaria: Alcyonacea) in the southeastern Alaska region. Frontiers in Marine Science 6:709

Walther G-R, Post E, Convey P, Menzel A, Parmesan C, Beebee TJ, Fromentin J-M, Hoegh-Guldberg O, Bairlein F (2002) Ecological responses to recent climate change. Nature 416:389-395

Warner RR, Chesson PL (1985) Coexistence mediated by recruitment fluctuations: a field guide to the storage effect. The American Naturalist 125:769-787

Webster NS, Smith LD, Heyward AJ, Watts JE, Webb RI, Blackall LL, Negri AP (2004) Metamorphosis of a scleractinian coral in response to microbial biofilms. Applied and Environmental Microbiology 70:1213-1221

Wecker P, Lecellier G, Guibert I, Zhou Y, Bonnard I, Berteaux-Lecellier V (2018) Exposure to the environmentally-persistent insecticide chlordecone induces detoxification genes and causes polyp bail-out in the coral *P. damicornis*. Chemosphere 195:190-200

Wells CD, Tonra KJ (2021) Polyp bailout and reattachment of the abundant Caribbean octocoral *Eunicea flexuosa*. Coral Reefs 40:27-30

White M, Mohn C, de Stigter H, Mottram G (2005) Deep-water coral development as a function of hydrodynamics and surface productivity around the submarine banks of the Rockall Trough, NE Atlantic Cold-water corals and ecosystems. Springer, pp503-514

Wilson J (1979) 'Patch' development of the deep-water coral *Lophelia pertusa* (L.) on Rockall Bank. Journal of the Marine Biological Association of the United Kingdom 59:165-177

Wood SN (2011) Fast stable restricted maximum likelihood and marginal likelihood estimation of semiparametric generalized linear models. Journal of the Royal Statistical Society: Series B (Statistical Methodology) 73:3-36

Wood SN (2017) Generalized additive models: an introduction with R. CRC press

Wurz E (2014) Autökologie der Kaltwassersteinkoralle *Caryophyllia huinayensis* aus der patagonischen Fjordregion. Universität Rostock

Young CM (1995) Behavior and locomotion during the dispersal phase of larval life. In: McEdward L (ed) Ecology of Marine Invertebrate Larvae, pp29

Yuyama I, Ito Y, Watanabe T, Hidaka M, Suzuki Y, Nishida M (2012) Differential gene expression in juvenile polyps of the coral *Acropora tenuis* exposed to thermal and chemical stresses. Journal of Experimental Marine Biology and Ecology 430:17-24

Zuur AF, Ieno EN, Walker NJ, Saveliev AA, Smith GM (2009) Mixed effects models and extensions in ecology with R. Springer

Versicherung an Eides Statt

Ich, Thomas Heran Arce,

versichere an Eides Statt durch meine Unterschrift, dass ich die vorstehende Arbeit selbständig und ohne fremde Hilfe angefertigt und alle Stellen, die ich wörtlich dem Sinne nach aus Veröffentlichungen entnommen habe, als solche kenntlich gemacht habe, mich auch keiner anderen als der angegebenen Literatur oder sonstiger Hilfsmittel bedient habe. Ich versichere an Eides Statt, dass ich die vorgenannten Angaben nach bestem Wissen und Gewissen gemacht habe und dass die Angaben der Wahrheit entsprechen und ich nichts verschwiegen habe.

Die Strafbarkeit einer falschen eidesstattlichen Versicherung ist mir bekannt, namentlich die Strafandrohung gemäß § 156 StGB bis zu drei Jahren Freiheitsstrafe oder Geldstrafe bei vorsätzlicher Begehung der Tat bzw. gemäß § 161 Abs. 1 StGB bis zu einem Jahr Freiheitsstrafe oder Geldstrafe bei fahrlässiger Begehung.

Ort, Datum

Unterschrift

ALFRED-WEGENER-INSTITUT
HELMHOLTZ-ZENTRUM FÜR POLAR- UND MEERESFORSCHUNG

Early life history of the scleractinian cold-water coral Caryophyllia huinayensis *from a naturally acidified Chilean fjord*

Dr. Thesis

Author: Thomas Heran Arce

1st Examiner: Prof. Dr. Claudio Richter
Benthic Ecology, Alfred-Wegener-Institut,
Bremerhaven, Germany

2nd Examiner: Dr. Covadonga Orejas Saco del Valle
Instituto Español de Oceanografía, Gijón, Spain

The present study was carried out from January 2018 to August 2024 at the Alfred-Wegener-Institut, Helmholtz-Zentrum für Polar- und Meeresforschung (AWI), Bremerhaven, Germany. It was financed by the AWI, ANID (Agencia Nacional de Investigación y Desarrollo, Chile), DAAD (Deutscher Akademischer Austaushdienst), including DAAD/BECAS Chile and STIBET Doktoranden (Stipendien- und Betreuungsmaßnahmen für internationale Studierende), and NGS (National Geographic Society).

Date Doctoral colloquium: 18.12.2024